Ontogeny and Adaptation: A Cross-Sectional Study of Primate Limb Elements

NADELL, JASON,ALEXANDER

Ontogeny and Adaptation:
A Cross-Sectional Study of Primate Limb Elements

Jason Alexander Nadell

A thesis submitted in fulfilment of the requirements for the degree of Doctor of Philosophy

Department of Anthropology

Durham University

September 2017

Ontogeny and Adaptation:
A Cross-Sectional Study of Primate Limb Elements

Jason Alexander Nadell

Abstract

How primates achieve their adult skeletal form can be ascribed to two broad biological mechanisms: genetic inheritance, where morphological characters are regulated by an individual's phenotype over development; and plastic adaptation, where morphology responds to extrinsic factors engendered by the physical environment. While skeletal morphology should reflect an individual's ecological demands throughout its life, only a limited amount of published research has considered how ontogeny and locomotor behaviour influence limb element form together. This thesis presents an investigation of long bone cross-sectional shape, size and strength, to inform how five catarrhine taxa adapt their limbs over development, and further, evaluate which limb regions more readily emit signals of plasticity or constraint along them. The sample includes *Pan*, *Gorilla*, *Pongo*, Hylobatidae and *Macaca*, subdivided into three developmental stages: infancy, juvenility and adulthood. Three-dimensional models of four upper (humerus and ulna) and lower (femur and tibia) limb elements were generated using a laser scanner and sectioned at proximal, midshaft and distal locations along each diaphysis. Three methods were used to compare geometry across the sample: 1) principal and anatomical axis ratios served as indices of section circularity, 2) polar section moduli evaluated relative strength between limb sections and 3) a geometric morphometric approach was developed to define section form. The results demonstrated that irrespective of taxonomic affinity, forelimb elements serve as strong indicators of posture and locomotor ontogenetic transitions, while hindlimb form is more reflective of body size and developmental shifts in body mass. Moreover, geometric variation at specific regions like the mid-humerus was indistinguishable across all infant taxa in the sample, only exhibiting posture-specific signals among mature groups, while sections like the distal ulna exhibited little or no intraspecific variation over development. Identifying patterns of plasticity and constraint across taxonomic and developmental groups informs how limb cross-sections either allometrically or isometrically scale their form as they grow. These findings have direct implications to extant and extinct primate research pertaining to body mass estimation, functional morphology and behavioural ecology.

Table of Contents

List of Figures

List of Tables

List of Abbreviations

AIM – Anthropological Institute and Museum, Zurich, CH

AMNH – American Museum of Natural History, New York, USA

ANOVA – Analysis of Variance

ANCOVA – Analysis of Covariance

AP – Anteroposterior

CS – Centroid Size

CV% – Coefficient of Variation

CV – Canonical Variate

CVA – Canonical Variate Analysis

df – Degree of Freedom

DL – Duckworth Laboratory, Cambridge, UK

F – Variance of group means ÷ mean of within group variances

F/H – Bending strength of the femoral relative to humeral midshaft

GM – Geometric Morphometrics

GPA – Generalised Procrustes Analysis

I – Second moment of area

I_{max} – Maximum second moment of area

I_{min} – Minimum second moment of area

I_{max}/I_{min} – Circularity about the principal axes

I_x – Second moment of area about the mediolateral axis

I_y – Second moment of area about the anteroposterior axis

I_x/I_y – Circularity about the anatomical axes

J – Polar second moment of area

K-S – Kolmogorov-Smirnov nonparametric test of probability

Ln – Natural logarithm

MCZ – Museum of Comparative Zoology, Cambridge, MA, USA

ML – Mediolateral

M-W – Mann-Whitney U nonparametric test of independent sample distribution

N and n – Total and sub-sample size, respectively.

η_p^2 – Partial eta squared

NMS – National Museum of Scotland, Edinburgh, UK

P – Calculated probability

PC – Principal Component

PCA – Principal Components Analysis

P-CM – Powell-Cotton Museum, Quex Park, UK

R – Coefficient of reliability

R^2 – Coefficient of determination

SD – Standard Deviation

SNMNH – Smithsonian National Museum of Natural History

SS – Sum of Squares

T50/T20 – Strength of the tibial midshaft relative to the distal tibia

TEM – Technical Error of Measurement

U50/U20 – Strength of the ulnar midshaft relative to the distal ulna

Z_p – Polar section modulus

Acknowledgements

It takes the support of others to achieve any form of worthwhile success. The individuals and institutions that made this thesis possible are too numerous to name, but there are some that I would like to give special thanks to.

My greatest debt is to my supervisors and mentors, Dr. Kris Kovarovic and Prof. Sarah Elton. Their unyielding guidance and patience were principal components to this project, second only to their confidence in allowing me to develop it from our first meetings together in 2013.

This thesis would not have been possible without the generous financial support of several institutions and organisations, including the Wenner-Gren Foundation, the British Association of Biological Anthropology and Osteoarchaeology, the Royal Anthropological Institute and University College, Durham University.

Many thanks are owed to Ms. Eileen Westwig and staff at the American Museum of Natural History, Dr. Marcia Ponce de León, Prof. Christoph Zollikofer and the staff and students at the Anthropological Institute and Museum, Ms. Inbal Livne and staff at the Powell-Cotton Museum, Dr. Katrina Jones at the Museum of Comparative Zoology, Ms. Emma Devereux and Prof. Marta Mirazon Lahr at the Duckworth Laboratory, the staff at the Smithsonian National Museum of Natural History and Dr. Andrew Kitchener and Ms. Zena Timmons at the National Museum of Scotland. A special thank you goes to Robert and Wendy Teale for offering their home and hospitality to me during my data collection trips to Birchington.

In addition to those named above, the following individuals provided me with invaluable advice and assistance over the years: Dr. Colin Shaw, for

introducing me to the field of biomechanics and painstakingly helping me become a better writer and researcher. Dr. Tom Davies, for taking the time to explain the nuts and bolts of AsciiSection and always being a call away for any technical help. To Dr. Damiano Marchi, Dr. Jay Stock, Dr. Charlotte King, Dr. Kimberly Plomp, Dr. Adam Gordon, Dr. Laura Buck, Dr. Gabrielle Russo and Dr. Mike Berthaume, for sharing their knowledge and personal experience with me throughout the course of this project.

I cannot give enough thanks to the staff and faculty of Durham University's Department of Anthropology, especially John Forster, Judith Manghan and Kate Payne, for rescuing me from several administrative nightmares and always being a pleasure to interact with around the office. I am also grateful to the Primatology and Palaeo-Morpho research groups at Durham University, for taking the time to review several chapters of this thesis and for offering helpful suggestions to improve it along the way.

Whether in the form of research advice or emotional support, the following colleagues, friends and family were crucial to keeping my feet on the ground over the years, including Brian Aufiero, Sownak Bose, Andrew Farrer, Mike Fusco, Josh Jowitt, Marino Krstolović, Liina Mansukoski, Stephanie Morris, Jordan Nadell, Amelia Sturm-Parry, Lauren Powell, Janelle Wagnild, Ryan Wieczkowksi, Manuel Will and my dear friends from Castle. My deepest gratitude goes to Simone Lemmers, without whom I would have lost my sanity a long time ago, and to Kayla Crowder, for always standing by my side in the most stressful moments, and making sure I was fed along the way.

And to my parents, who have stood in my corner at every stage of my locomotor development with love, support and encouragement.

This thesis is dedicated to my grandmother, Millie Nadell,
for babysitting me in the garden instead of the playpen, teaching me the importance of appreciating the natural world over the material and for always reminding me never to stop learning.

Chapter One:
Introduction

1.1 Thesis overview and aims

Understanding an animal's behaviour is fundamental to appreciating its biology as a "whole organism" (Begun, 2004a). The inference of functional morphology among extant and fossil primates is a central component to the study of their behavioural ecology, but the numerous intrinsic and extrinsic factors that govern skeletal shape and size (form) make it difficult to explain variation among and between taxa (Kivell, 2016a). Researchers attempt to define the proximate sources of limb morphological variation by comparing differences between primate skeletons at discrete levels (i.e., between taxa, developmental stages, individual elements and specific element regions). However, the interaction of these components are infrequently considered together, despite their interrelation.

To attain a better understanding of the ways long bones achieve their adult form, this thesis examines the influence of development and behaviour along the fore- and hindlimb elements of five hominoid and cercopithecoid taxa, including *Pan*, *Gorilla*, *Pongo*, Hylobatidae and *Macaca*. The unique phylogenies, ecologies, life histories and body sizes of these groups make them model candidates for investigating relationships between their morphological form and function. Specifically, geometric properties proportional to cross-sectional shape and strength are considered among infant, juvenile and adult individuals, to determine whether these properties vary both inter- and intragenerically over development. Because long bone cross-sectional geometry is closely linked to biological and behavioural phenomena like body size and locomotor profile (Demes and Jungers, 1993), an ontogenetic series is used to inform whether important developmental events, such as increases in body mass or locomotor transitions, can be established as physical signals along the diaphyses. To determine how different aspects of the diaphyses develop, (i.e., adaptively plastic and constrained bone sections) (Ruff and Runestad, 1992), geometry is measured proximally and distally to the mid-diaphysis, as well as at the midshaft itself. Accounting for variation at multiple regions along each diaphysis will further illuminate whether limb segments and sections develop independently of each other or as single functional units.

Understanding the ways in which extant primates grow and adapt their skeletons in accordance with their environment has direct application to the study of their recent ancestors, especially in a primate fossil record composed of fragmentary material and limited ontogenetic diversity.

1.2 Bone cross-sectional geometry and the principles of beam theory

Bone and muscle are metabolically active tissues susceptible to apposition and deposition upon their use and disuse. Both form a dependent relationship in their development, where an increase in muscle mass as a result of physical strain (loading), should prompt an increase in bone mass and strength to support it (Burr, 1997; Frost and Schönau, 2000; Flück, 2006). This concept of functional equivalence between different sized animals and their skeletal form has been contemplated by naturalists since at least the 17th century (Galilei, 1638), though the phenomenon was first described comprehensively by anatomists in the 19th century (Pearson and Lieberman, 2004), eventually being coined the "Law of Bone Transformation", or simply, "Wolff's Law", by German orthopaedist and surgeon, Julius Wolff (Wolff, 1892; Turner and Pavalko, 1998). Contemporary research on skeletal biomechanics has since built upon Wolff's observations to more accurately quantify the form-function relationship between bone and its loading environment (Trinkaus et al., 1994; Hsieh et al., 2001; Pearson and Lieberman, 2004; Barak et al., 2011; Shaw et al., 2014; Wallace et al., 2014; Auerbach et al., 2017; Tsegai et al., 2017).

Research has since improved our understanding of skeletal biology, allowing for more nuanced analyses and interpretations of cross-sectional form. One of the most common approaches to cross-sectional analysis for the past several decades has been the modelling of weight-bearing bones after simple engineering beams, after the principles of classical beam theory. The mechanical forces experienced by long bones and engineering beams are analogous, and so the same conventions employed by civil engineers to evaluate beam structural integrity can be applied to evaluate the geometric properties of diaphyseal cross-sections (Huiskes, 1982; Daegling, 2002; Marchi and Shaw, 2011; Trinkaus and Ruff., 2012; Weatherholt and Warden, 2017). Using a beam theory approach, geometric properties proportional to the forces that act on a given section (called second moments of area), are calculated at discrete sections along the diaphyses. While cross-sectional properties like cortical bone area can inform about a section's ability to resist

compressive and tensile loads (Skedros et al., 2003), the dynamic nature of limb movement during locomotion make forces like pure compression and tension uncommon. Instead, forces like torsion and bending (Figure 1.1) are more typical during human and non-human primate locomotion (Ruff, 2008), and so, are the central focus of the studies herein. In this thesis, four long bones from the forelimb (humerus and ulna) and hindlimb (femur and tibia) are considered. By incorporating elements from the proximal and distal segments, the limbs can be studied both as whole functional units and separately as individual components. Moreover, the generally robust proximal aspects of the limb are not expected to be constrained by tissue economy to the same extent as distal elements (Stock, 2006), allowing development to be studied in light of limb tapering (Alexander, 1998). The decision to omit the radius and fibula from analysis was made on two grounds: first, developmental changes along the distal segments can be studied effectively using single elements. Though mechanical forces are transferred and deflected between the two bones of the forearm and lower leg (Birkbeck et al., 1997; Marchi and Shaw, 2011), accounting for the ulna and tibia alone still provides adequate information on variation between groups, as well as changes between developmental stages related to growth and behaviour (Ruff et al., 2013), relative to the radius and fibula. Second, omitting the radius and fibula made it possible to increase the total size of the sample, allowing data to be collected from more individuals for robust statistical analyses.

The geometric properties chosen for analysis typically complement an investigation's specific research questions. For example, studying a femoral midshaft's ability to resist torsional and shearing forces would better benefit from calculating its polar second moment of area (J) as opposed to its maximum section modulus (Z_{max}), as J is proportional to the section's torsional rigidity, whereas Z_{max} acts as better indicator of its maximum bending strength. While there are numerous software packages capable of rapidly measuring geometric properties automatically, the determining factor of how they are calculated is dependent on the second moment of area itself. For measures of bending strength or rigidity, second moments of area are always measured through the diameter of a section and can be calculated along any axis (though measurement along the anatomical or principal axes are most common). In this thesis, measures of circularity derived from ratios of the maximum and minimum second moments of area (I_{max}/I_{min}) and second moments of area in the anatomical planes (I_x/I_y), are used to infer cross-sectional shape. Comparatively, measures of torsional rigidity and strength are calculated about a section's centre (centroid) (e.g.,

distance from the centroid to the outermost fibre of a section). Regardless of the type of load, a given cross-section's ability to resist deformation before mechanical failure (fracture) is defined as rigidity, and a section's ability to resist fracturing itself denotes its strength (Ruff, 2008). More simply, a section's rigidity describes its ability to elastically return to its normal state after it is unloaded while its strength is a measure of the stress it can resist before yielding to permanent deformation, or in a material like bone, breaking. In this thesis, the polar section modulus (Z_p) is considered in each limb to compare measures of diaphyseal strength.

While certain aspects of the appendicular skeleton, like long bone linear dimensions (lengths, articular surfaces, etc.), are more closely associated with innate developmental mechanisms (Schultz, 1973; Biewener and Bertram, 1994; Ruff, 2003), midshaft cross-sectional dimensions are understood to economically adapt to the habitual loading behaviours imposed on them, especially prior to adulthood (Connour et al., 2000; Carter and Beaupre', 2007). This adaptive configuration makes it possible to infer broad locomotor behaviours in most tetrapod skeletons (Rubin and Lanyon, 1984; Nicholson et al., 2010), including members of the primate order (Sarringhaus et al., 2005; Carlson et al., 2014). Midshafts are of key importance to researchers interested in long bone cross-sectional properties because they are typically the points of peak bending during locomotor-related loading (Biewener, 1982; Biewener and Taylor, 1986). As such, midshafts must adapt their form in accordance with the forces they regularly experience to avert the risk of fracture. This phenomenon has been demonstrated experimentally in adult and subadult modern humans, where tibial midshaft geometry successfully discriminated exercise from control groups (Macdonald et al., 2009; Ireland et al., 2011; Weatherholt and Warden, 2017) and even distinguished athletic groups by the sport (Shaw and Stock, 2009a). Long bone epiphyses may be more adaptively constrained due to their proximity to neighbouring joints, by comparison. Unlike midshafts, epiphyses and metaphyses transfer loads between elements via trabecular tissue, rather than relying on the cortex to deflect loads directly (Ruff and Runestad, 1992; Currey, 2002). It follows that bone regions adjoining articular surfaces should not have to adapt to the same capacity as midshafts, as a dramatic change in form could negatively impact their primary function of enabling and inhibiting a set range of limb movement. Differences in cortical area and rigidity have been shown to vary significantly between locomotor-variable groups at midshaft, while remaining virtually indistinguishable at their epiphyses, for instance (Nadell and Shaw, 2016).

Despite their constrained nature, regions proximal and distal to midshaft should be of interest in studies that compare cross-sectional variation, if only as points of comparison to the more plastic midshaft. Unfortunately, non-midshaft sections are continually overlooked in long bone biomechanical studies, likely because the stresses, and subsequent strains placed on these regions, are not as well understood.

1.2.1 Estimating cross-sectional geometry using the periosteal contour

Through the measure of external maximum and minimum diameters, diaphyseal circumferences and total areas, a long bone's cross-sectional properties can be estimated accurately without analysing its internal architecture directly (Figure 1.2) (Stock and Shaw, 2007; Sparacello and Pearson, 2010; Macintosh et al., 2013). The quantity, density and distribution of cortical bone about a cross-section are all important components to understanding diaphyseal structure (Lovejoy et al., 1976). The role of skeletal tissue to resist torsion and bending loads increases with distance from the section centroid (Bertram and Swartz, 1992), making the external dimensions of a cross-section a critical component for gauging its structural integrity (Stock and Shaw, 2007). A study by Davies et al. (2012) found that the diaphyseal contours of virtual bone models can be used to accurately estimate second moments of area about a cross-section. In fact, their analysis suggested that cross-sectional properties estimated from virtual models are more accurate than those derived from techniques like periosteal moulding in some cases, where orientation observation errors are more likely to produce inexact results (Davies et al., 2012). More traditional methods such as computed tomography (CT) and biplanar radiography (BR) are used to determine biomechanical properties by taking both the periosteal and endosteal surfaces into account. As such, CT and BR are advantageous for returning data on trabecular and cortical area as well as geometry within the medullary cavity. However, medical and micro-CT or BR technology can be difficult to access in certain areas and when they are available, often require fragile skeletal specimens to be transported offsite for data collection.

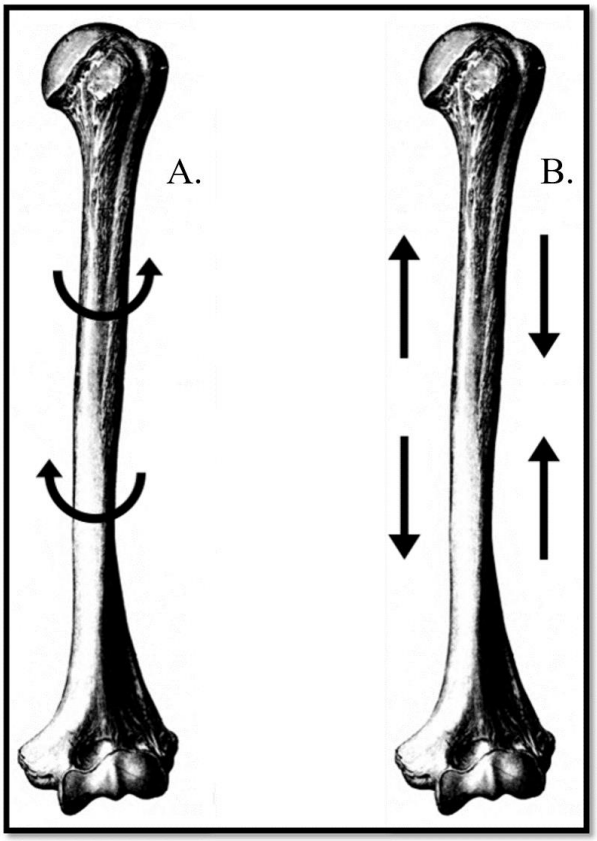

Fig. 1.1. Humeral model depicting the most common forces that act on long bones during mechanical loading. **A.** Torsion, brought on by twisting about the long axis of a diaphysis. **B.** Bending, brought on by compression and tension acting together on opposing sides of a diaphysis.

1.3 Catarrhines as a study sample

Table 1.1 gives general size and locomotor information of the five catarrhine taxa studied in this thesis. The decision to study the living apes and macaques was made on several grounds pertaining to their body sizes and the markedly different locomotor behaviours they exhibit (Napier and Walker, 1967; Smith and Jungers, 1997; Dunbar and Badam, 1998). Fossil and molecular evidence suggests that the first catarrhines emerged in what is modern day Africa and Arabia as early as 40 – 44 million years ago (Chatterjee et al., 2009) and as late as 29 – 32 million years ago (Harrison, 2005, 2013) (Figure 1.2). Among the crown catarrhines studied here, hominoid postcranial morphology is typically characterised by a relatively large body, a mobile shoulder due

to dorsally placed scapulae, a high intermembral index, lack of a tail and a broad ribcage and trunk, culminating in an orthograde plan (Fleagle, 1976; Thorpe and Crompton, 2006, Young et al., 2010b; Nakatsukasa et al., 2016). Macaques are comparatively smaller than apes, comprising an extended vertebral column ending with a tail, a relatively low intermembral index, a stabilized wrist and a deep, long, slender ribcage and pelvis, that enables their pronograde postures (Fleagle, 1999; Young et al., 2010b; Hunt, 2016). The catarrhines each exhibit unique ontogenies, social behaviours, ecologies and evolutionary histories from one another, which contribute to their locomotor behaviour, and subsequently, their limb morphology (Figure 1.3). To address how limb form varies across the sampled taxonomic groups, an understanding of these ecological variables must first be established.

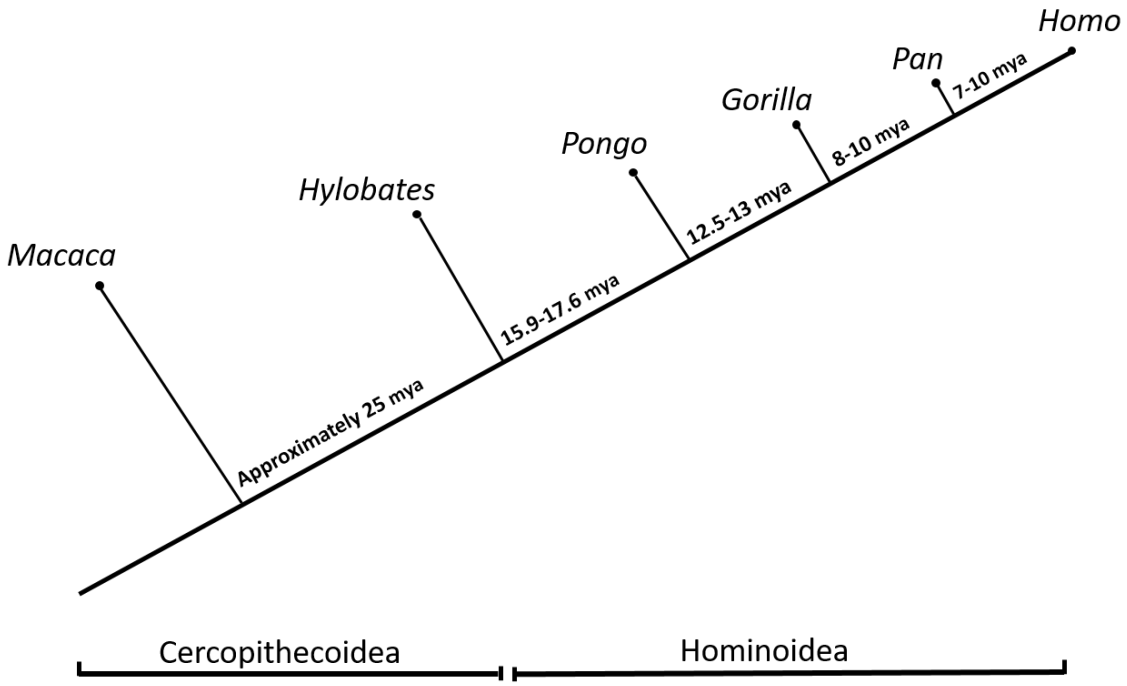

Fig. 1.2. Cladogram of the crown catarrhines examined in this thesis relative to *Homo*, along with their approximate divergence dates in millions of years. Sources of divergence: Moyà-Solà,, 2004; Gibbs, 2007; White et al., 2009; Scally et al., 2012; Carbone et al., 2014.

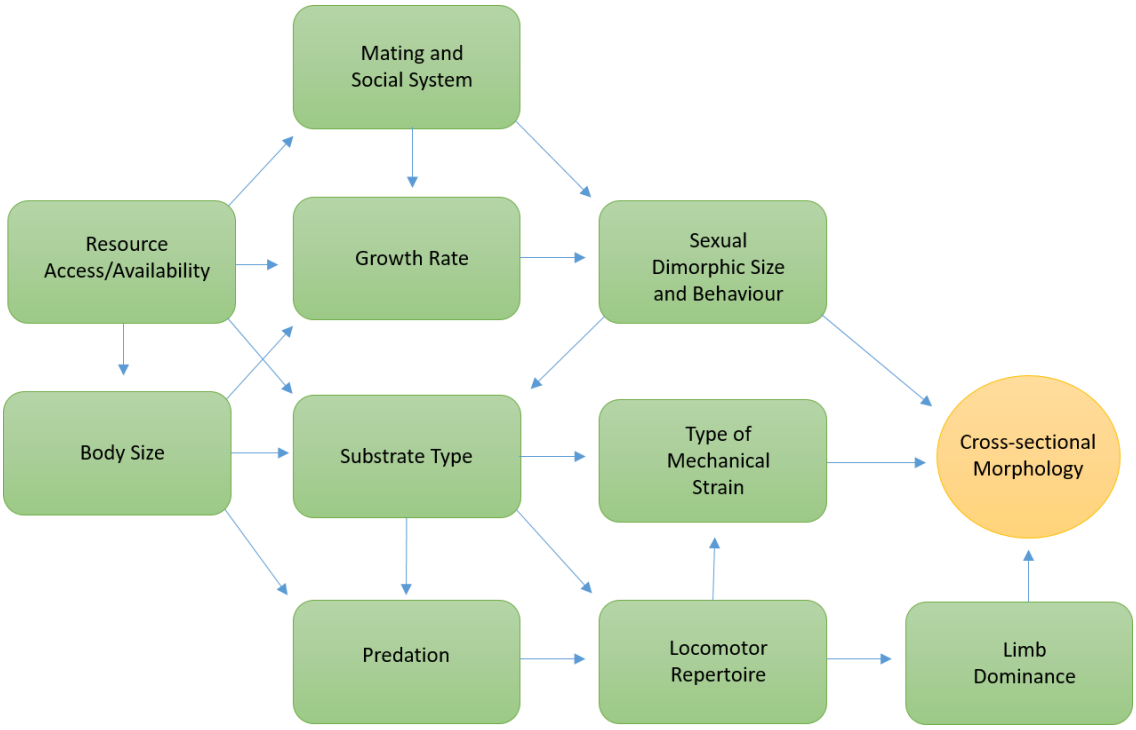

Fig. 1.3. Path diagram of several proximate and ancillary factors understood to influence primate limb morphology.

1.3.1 The African apes

Despite the relatively recent molecular divergence of *Pan* and *Gorilla* (approximately 8 – 10 million years ago) (Langergraber et al., 2012), along with the similar environments they exploit (Tutin et al., 1991), both African ape genera have adapted their form, and consequently, their behaviour, in fundamentally different ways. Over the course of their development, chimpanzees and gorillas grow at different rates and durations of time, where gorillas grow faster than chimpanzees (both *P. troglodytes* and *P. paniscus*), but growth ceases earlier among females and later in males, relative to *Pan* (Leigh, 1992; Leigh and Shea, 1996). As a result, gorillas reach the same developmental junctures as chimpanzees at larger sizes (Shea, 1983). African ape comparative ontogeny highlights this growth disparity well, by drawing parallels between chimpanzee and gorilla size and behaviour over their development. Doran's (1997) research revealed that from six months of age, the larger gorilla infants adopt a quadrupedal-dominant gait,

while climbing and suspensory behaviour continue to dominate the chimpanzee locomotor repertoire. Of the five genera studied in this thesis, gorillas engage in terrestrial positional behaviours most frequently (Remis, 1994; Doran and Mcneilage, 1998; Larson, 1998).

Both male and female mountain gorillas (*G. berengei berengei*) are already competent quadrupeds (both palmigrade and knuckle-walking) by 6 – 23 months of age, becoming incrementally more terrestrial across juvenility and into adulthood, when terrestrial locomotion accounts for up to 86% of total locomotor time (Doran, 1997). That said, sexual differences (the smaller females tend to be more arboreal than males, overall) and species differences (western lowland gorillas exhibit arboreal locomotor behaviours more regularly) are notable within the genus (Remis, 1999; Masi, 2004; Doran-Sheehy et al., 2009; but see Neufuss et al. 2017). Interspecific variation has also been identified in *Pan*, as common adult chimpanzees (*P. troglodytes*) engage in less suspensory and other arboreal behaviours than adult bonobos (*P. paniscus*) (Doran, 1992a,b; Doran and Hunt, 1994). Doran and Hunt (1994; pp. 103-106) also identified locomotor and positional behaviour differences among chimpanzee sub-species; (*P. t. troglodytes, P. t. schweinfurthii*, and *P. t. verus*) though these differences were largely driven by environmental variation and were trivial compared to those made with *P. paniscus*. Both African ape genera are also sexually dimorphic in adulthood, though sexual characteristics are considerably more pronounced among gorilla than chimpanzee species (Leigh and Shea, 1995, 1996), including sexual bimaturism, which is exaggerated in *Gorilla* and virtually indiscernible in *P. troglodytes* (Leigh, 1992).

The broader differences between African ape genera appear greater than the differences within them, however. For instance, male gorillas are typically 3 – 4 times larger than female chimpanzees, while they are only about twice the size of female gorillas (Jungers and Sussman, 1984). Placing their size differences into a finer context, a four-year-old gorilla at the onset of juvenility is approximately the same weight as an adult female chimpanzee, with each exhibiting similar locomotor profiles despite their age difference (Leigh, unpublished data, reported in Doran, 1997). Thus, while both African ape genera adopt a more quadrupedal gait as they mature, the smaller size and mass of chimpanzees enables their comparatively arboreal lifestyle into adulthood. Unlike the largely terrestrial lifestyle of the mountain gorillas or the predominantly suspensory Asian apes, the mosaic positional behaviour and postcranial morphology of

chimpanzees (Rose, 1991) could place them into the category of locomotor generalists, at least in regard to the other extant hominoids. From terrestrial knuckle-walking to a suite of suspensory postures (e.g., arm-hanging, arm-swinging, brachiation) (Hunt, 1992; Hunt et al., 1996), the chimpanzee locomotor profile is adapted to negotiate a variety of environments as their size changes over development (Sarringhaus et al., 2014). While chimpanzees primarily rely on knuckle-walking for terrestrial locomotion (Hunt, 1992), one bioenergetic study found that upwards of ten times as much energy is expended during knuckle-walking compared to vertical climbing (Pontzer and Wrangham, 2004). Even with the decline of chimpanzee suspensory and climbing behaviours in adulthood, their frequency in juvenility and adolescence are reflected by shifts in limb strength proportions among adults (Sarringhaus et al., 2016). The mechanics that govern African ape knuckle-walking likely evolved to support their distinct ecological differences, from interspecific growth and size to the locomotor environments they exploit (Inouye, 1994; Kivell and Schmitt, 2009). It follows that these locomotor and size differences should further influence their limb cross-sectional morphology as a means of accounting for the unique loads they experience with maturity. Both genera indeed exhibit distinct shifts in midshaft bone strength from the fore- to hindlimb as they develop, in correspondence with changes in locomotor behaviour (Ruff et al., 2013; Sarringhaus et al., 2016). While intraspecific differences in behaviour and form help elucidate variation within populations and between subspecies, an interspecific and ontogenetic comparison will establish whether such differences are innate among the African apes, or if morphology can discriminate the genera at discrete stages of their development. Therefore, the limb morphology from a combined sample of gorilla (including *G. beringei* and *G. g. gorilla*) and common chimpanzee species (*P. t. schweinfurthii, troglodytes* and *verus*) are considered together in the studies ahead, taking a broad perspective on African ape development.

1.3.2 The Asian apes

Compared to the more recent divergence between African apes, the living orangutans and hylobatids shared a common ancestor some 14 – 18 million years ago (Young and MacLatchy, 2004). In spite of their relatively distant evolutionary history and differences in their mating systems and body sizes, both Asian apes are characterised by prolonged life histories. Orangutans delay their age at first reproduction until 15.7 years of age on average (Knott et al., 2009), about

5.6 years later than gorillas and 1.4 years later than chimpanzees (Watts, 1991; Boesch and Boesch-Achermann, 2000). Moreover, immature orangutans do not achieve full ecological independence (defined as no longer associating with daily maternal contact) until approximately three years of age and as late as six (van Adrichem et al., 2006). This extended investment into offspring development also helps explain why the orangutan interbirth interval exceeds that of all other living apes, including humans (Kelley and Schwartz, 2010; Schuppli et al., 2016). Compared to the two species (and subspecies therein) of *Pongo* (*P. abelii* and *P. pygmaeus*), the Hylobatidae family consists of four separate genera, including *Hylobates, Hoolock, Nomascus* and *Symphalangus* (Chatterjee et al., 2009). All four genera are understood to be monophyletic (Hall et al.,1998; Chatterjee, 2006; Chatterjee et al., 2009), and while they exhibit a range of sizes – from the seven dwarf gibbon species (*Hylobates*) to the larger-bodied siamang (*Symphalangus*) – the hylobatids each share similar ecologies (i.e., diet, habitat, serial monogamous reproduction, minimal sexual body size dimorphism (Palombit, 1994; Leigh and Shea, 1995; Asensio et al., 2017), musculoskeletal anatomy (Channon et al., 2010a; Vereecke and Channon, 2013) and locomotor profiles (Fleagle, 1974; Andrews and Groves, 1975; Michilsens et al., 2009). These relatively homogeneous characteristics allow for the pooling of species in samples interested in broad form-function relationships among multiple taxonomic groups (Bartlett, 2007; Buck et al., 2010), including the studies presented in this thesis. Even with respect to the slow-developing extant hominids, the hylobatids are exemplified by their prolonged life histories compared to other small-bodied primates (Reichard and Barelli, 2008; Reichard et al., 2012). It is probable that the hylobatids inherited their life histories from an earlier stem hominoid prior to their reduction in size, however (Begun, 2004b; Ward et al., 2004). Among extant siamangs, locomotor and nutritional independence is not achieved until approximately two years of age (Lappan, 2009), though recent observations report infant-mother nipple contact through the first three years of life (Morino and Borries, 2016), extending the infant period closer to that of gorillas (Watts and Pusey, 1993).

The Asian apes display forelimb suspensory behaviours like brachiation and arm-hanging more frequently than any other catarrhine taxon (Hunt, 2016), reflected by their high intermembral indices (Young et al., 2010a). Though orangutans and hylobatids both exploit similar locomotor environments, their variable body sizes require them to do so in fundamentally different ways. For

one, the larger orangutans are highly sexually dimorphic, where adult males weigh nearly twice as much as females (Cant, 1987) and exhibit greater body size dimorphism than adult gorillas in some cases (Leigh, 1992). Unlike the significant sexual differences identified among gorillas, however, orangutans do not appear to exhibit pronounced positional or postural variation among age-sex categories (Sugardjito and van Hooff, 1986; Thorpe and Crompton, 2006; but see Cant, 1987 for a study on sexual locomotor differences among a small sample of adult *P. pygmaeus*). Orangutans are not known to transition between postures as dramatically as the African apes as they mature either (Thorpe and Crompton, 2006). Instead, the majority of gap-crossing manoeuvers are learned early in life and simply executed at different frequencies over development (Chappell et al., 2015). The orangutan locomotor profile has traditionally been described as dominated by torso-orthograde suspension (Cant, 1987), but Thorpe and Crompton (2006) found that forelimb-hindlimb and pronograde suspensory locomotion distinguish the orangutans among the extant hominoids, and that the frequency of other locomotor behaviours are similar to those found in the African apes. Compared to the above-branch and pronograde suspension characteristics of the orangutans, the smaller hylobatids exhibit forelimb-driven brachiation more regularly. While brachiation frequency varies by species, wild focal research suggests that the forelimb-driven manoeuver encompasses anywhere between 67% (in gibbons) and 59% (in siamangs) of total locomotor time (Fleagle, 1980; Hunt, 2004), though others have reported frequencies as high as 80% (Fleagle, 1974; Michilsens et al., 2009). To place this disparity in perspective, the other extant hominoids brachiate less than 15% of their respective total locomotor times (Remis, 1995; Doran, 1996; Thorpe and Crompton, 2006). Bipedal locomotion is also an important component to the Asian ape locomotor profile, with bipedal walking (both hand-assisted and free) comprising over 7% of orangutan locomotion (Thorpe and Crompton, 2006; Thorpe et al., 2007) and between 4 – 12% in gibbons and siamangs (Whitmoor, 1975). The hylobatids (and especially gibbons) are also accomplished leapers (Fleagle, 1976; Channon et al., 2010b), executing leaping behaviour at a similar rate to some colobine and arboreal cercopithecine species (Hunt, 2016). With increased size in species like the siamang though, leaping frequency is diminished, giving way to a locomotor profile convergent with that of orangutans, and further suggesting that the locomotor strategies adopted by the Asian apes are a solution to their variable body masses (Collis et al., 1999). Accounting for differences in *Pongo* and hylobatid limb form will provide insight into the

influence that these biological and behavioural differences place on their skeletons as they grow, as well as their relation to their African counterparts.

1.3.3 Cercopithecoidea – the macaques

Like their hominoid relatives, the cercopithecoids vary in their ecology, morphology, size and behaviour (Strasser, 1992). While ape locomotor profiles are centred around a torso-orthograde posture, Old World monkeys are defined by pronogrady, enabling nimble and efficient quadrupedal movement through arboreal and terrestrial contexts. Macaque (genus *Macaca*) ecology and ontogeny is especially variable, where species have been classified as primarily terrestrial, semi-terrestrial and arboreal (Chatani, 2003). The macaques are small- to medium-bodied monkeys that inhabit a vast range of environments across Asia (with Barbary macaques (*Macaca sylvanus*) serving as the sole African exception), from montane forest to densely populated cities (Ciani, 1986). Concerning their ontogeny, the genus has not evolved a single developmental pathway to adulthood, but several, where sexual bimaturism ranges from virtually non-existent in species like the Celebes crested macaque (*Macaca nigra*), to extreme in species like the rhesus macaque (*Macaca mulatta*) (approximately four years difference between males and females), even when compared among other anthropoids (Leigh, 1992). Of the two macaque species studied in this project, sexual dimorphism is more pronounced in the rhesus compared to the smaller long-tailed species (*Macaca fascicularis*) (Leigh, 1992). In spite of their developmental differences, rhesus and long-tailed macaques descended from a common *fascicularis*-like ancestor that lived in Southeast Asia around 2.5 million years ago (Tosi et al., 2003). The two sister species also exhibit geographically widespread and long-established Y DNA haplotypes (Tosi and Coke, 2007; Klegarth et al., 2017). Both employ quadrupedal walking, running, galloping, and clambering: modes of locomotion which may influence the morphology of the appendicular skeleton to a different extent than the predominantly arboreal and suspensory primates (Cant, 1988; Demes et al., 2001; Patel, 2009; Patel and Polk, 2010). While rhesus macaques are on average larger, and as might be implied, possess shorter tails than their long-tailed relatives, interspecific variation cannot entirely be attributed to ecogeographical clinal differences (i.e., Allen's and Bergmann's rules) or parapatric hybridisation over their evolutionary history and in the present (Kanthaswamy et al., 2008; Osada et al., 2010; Hamada et al., 2016). Accordingly,

their broad morphological similarities make it possible to pool the taxa in comparative studies of body proportion and ontogeny (Cheng and Scott, 2000).

The locomotor behaviour and musculoskeletal form of rhesus macaques are closely correlated over development, where positional and postural changes in growing infants are reflected by shifts in mass cranially to caudally along the axial skeleton (Turnquist and Wells, 1994). In the appendicular skeleton, a disproportionate increase in mass is shifted to the hindlimb relative to the forelimb in early infancy (approximately 4 – 6 months of age) (Turnquist and Kessler, 1989; Schneider and Zernicke, 1992), which corresponds to a transition into hind-limb driven propulsion and locomotor independence (Turnquist and Wells, 1994). Compared to the slower life histories of the hominoids, the macaques achieve ecological independence earlier in life (Leigh and Blomquist, 2011). Further, changes in habitat also factor into rhesus macaque ontogeny, where arboreal activity increases among individuals as they enter juvenility, and then declines into adulthood (Wells and Turnquist, 2001). That said, terrestrial locomotion is dominant among all age groups of rhesus macaques compared to the more arboreal long-tailed taxon, which spend around 2% of their time on the forest floor (Wheatley, 1980). Unfortunately, there is a lack of published research on long-tailed macaque locomotor ontogeny compared to that available on rhesus macaques, though studying the cross-sectional morphology of their limbs across development could provide context to their behaviour, especially when compared at the generic level. Morphological and positional differences identified between macaque species are thought to result from foraging strategies, helping to explain the smaller bodies and longer tails associated with arboreal taxa (Rodman, 1979). Even so, a quadrupedal locomotor profile is common to the genus and dominant in both terrestrial and arboreal taxa (Burr et al., 1989), making macaques ideal study candidates for inter- and intragroup comparisons.

TABLE 1.1. Size and locomotor information of the five catarrhine taxa studied in this thesis

Property	*Pan*	*Gorilla*	*Pongo*	Hylobatidae[a]	*Macaca*[b]
Body Mass kg (Male/Female)[1]	59.7/45.8	170.4/71.5	77.9/35.6	5.9/5.34; 11.9/10.7	5.36 – 11.9/3.59 – 8.8
Sexual Dimorphism[2]	1.3	2.38	2.19	1.1	1.47
Intermembral Index[3]	106	116	139	131-145	93
Dominant Position[4]	Mixed (travel: 99% terrestrial, feeding: 85% arboreal)	Terrestrial 80-97%	Arboreal > 90%	Arboreal approx. 99%	Mixed *M. mulatta*: 50% terrestrial; *M. fascicularis*: 98% arboreal
Primary Locomotor Mode[4]	Knuckle-walking, Vertical Climbing, Arm-hanging	Knuckle-walking, Vertical Climbing	Orthograde clambering/transferring, Forelimb-hindlimb Suspension	Brachiation, Orthograde forelimb suspension, Leaping	Quadrupedal Walking/Running/Galloping, Vertical Climbing, Leaping

[a] Value ranges represent the smaller *H. lar* (left) and larger-bodied *S. syndactylus* (right).
[b] Value ranges represent the smaller *M. fascicularis* (left) and the larger-bodied *M. mulatta* (right).
[1] Adult mean body masses of males and females from Smith and Jungers, 1997.
[2] Male divided by female mean body mass
[3] Values from Young et al., 2010a, supplementary information.
[4] *Pan*: Hunt, 1992; *Gorilla*: Tuttle and Watts, 1985; Remis, 1998; *Pongo*: Cant, 1987; Thorpe and Crompton, 2006; Hylobatidae: Sati and Alfred, 2002; Vereecke et al., 2006a,b, Hunt, 2016; *Macaca*: Rodman, 1979; Wheatley, 1980; Wells and Turnquist, 2001.

1.4 Thesis structure

This dissertation is divided into six chapters. The present chapter introduced the broad aims of the thesis while providing a framework for the research conducted ahead. Chapter 2 defines the data collection protocol used in each study, including information on the catarrhine skeletal sample, the approach used to collect cross-sectional data from virtual long bone models and an overview of the geometric analyses used to interpret variation among and between taxa. Chapters 3, 4 and 5 encompass the three primary research sections of the thesis and act as independent studies, including their own introductions, methods, results, discussions and summaries (Table 1.2). Each of the three research chapters employ a unique analytical approach, either by building upon traditional cross-sectional analyses or developing novel techniques in order to answer specific research questions pertaining to the thesis's aims. First, Chapter 3 investigates long bone cross-sectional circularity (as a proxy for shape), using principal and anatomical second moment of area ratios along the humerus, ulna, femur and tibia. The research objective of the study seeks to determine whether changes in shape over development, as well as shape variation between taxa, can be attributed to biological or behavioural phenomena. Rather than focusing on discrete sections along the diaphyses, Chapter 4 compares the relative strength between limbs, as well as along individual elements therein. In doing so, an examination of the ways primates invest in skeletal 'tissue economy' by modelling specific elements and sections along them is addressed, with reference to their unique locomotor repertoires and body sizes. Chapter 5 investigates the cross-sectional shape of each long bone, but unlike Chapter 3, a geometric morphometric approach to cross-section form is implemented to obtain an accurate impression of each contour's shape rather than through means of their relative dimensions. Allometric comparisons and growth trajectories of each element are then used to study how form changes among and between taxonomic groups as they mature. Finally, Chapter 6 synthesises the findings of all three research chapters, with a brief review of their results and implications, followed by their potential application to future research on extant and extinct primate limb form and function.

TABLE 1.2. Research objectives for the three primary research chapters presented in this thesis

Chapter	Method	Research Question(s)	Predictions
Three	Principal and second moment of area ratios are generated as estimates of cross-sectional circularity along the diaphyses.	1) How does diaphyseal shape vary between taxa over development? 2) Does shape change between developmental stage within taxa?	Section circularity is expected to correspond to locomotor behaviour and body size contingent on diaphyseal location. Specifically, midshafts are expected to emit stronger signals than proximal and distal sections. Moreover, intraspecific changes in shape should reflect locomotor transitions or increases in size.
Four	Cross-sectional strength is compared between limb midshafts as well as between mid- and distal sections along elements.	1) How does limb strength change over development and do said changes reflect ecological signals?	Inter-limb strength ratios should reflect broad changes in limb dominance over ontogeny (i.e., fore- to hindlimb propulsion) while intra-limb ratios are expected to reflect more specific differences between taxa, like locomotor behaviour or body size.
Five	Geometric morphometric (GM) analyses are implemented to preserve the effects of size when making comparisons of midshaft shape in each element.	1) Can section shape be measured taking a GM approach, and if so, does variation appear to be an effect of biology or behaviour? 2) Can ontogenetic trajectories of section shape (principal component vectors) discriminate taxa?	A GM landmarking approach is expected to further clarify differences in shape by considering the effects of allometry, across development, as well as between taxonomic groups. Measuring the entire curve of the periosteal contour should inform about subtle differences in shape undetectable by area ratios alone.

Chapter Two:
General Materials and Methods

2.1 The sample

The sample comprises five extant catarrhine taxa, including *Pan* (*N* = 54), *Gorilla* (*N* = 52), *Pongo* (*N* = 54), Hylobatidae (*N* = 55) and *Macaca* (*N* = 56). Specimens were procured from seven collections across Europe and the United States, including the American Museum of Natural History (AMNH), New York, USA; the Anthropological Institute and Museum (AIM), Zurich, CH; the Duckworth Laboratory (DL), Cambridge, UK; the Museum of Comparative Zoology (MCZ), Cambridge, M.A, USA; the National Museum of Scotland (NMS), Edinburgh, UK; the Powell-Cotton Museum (P-CM), Quex Park, UK; and the Smithsonian National Museum of Natural History (SNMNH), Washington D.C, USA. The humerus, ulna, femur and tibia (the four long bones of focus in this thesis) were present in the majority of the skeletal specimens but were omitted when missing from an individual. Each of the five taxonomic groups consisted of multiple genera, species and sub-species (Table 2.1). Ideally, only wild-caught specimens would be included in the sample, but this was not always possible given the availability of certain collections. The majority of the total sample was wild-caught (94%), though three infants and one juvenile *M. fascicularis*, and 10 infants, 11 juveniles and six adult *M. mulatta* were included from the captive Mildred Trotter collection at SNMNH. Unfortunately, the housing conditions and locomotor activity of the Trotter macaques could not be verified due to their procurement from various biomedical facilities and institutions over several years (Trotter et al., 1975). Although some studies have identified significant differences in cross-sectional geometry between wild and captive specimens (Canington et al., 2017), others have found few or no differences (Morimoto et al., 2011). To determine whether the captive specimens could be included in the total sample, the circularity (I_{max}/I_{min}) dispersion of the wild and captive macaques was compared in the fore- (humerus) and hindlimb (femur) midshafts, due to the locomotor adaptive propensity of these sections. Midshaft circularity was deemed non-significant between age-sex pooled wild and captive groups in either bone following a Kolmogorov–Smirnov test of independent samples (Mid-humeral $P = 0.061$; Mid-femoral $P = 0.425$). Because greater overall shape variation was evident in the humerus among all of the sampled primates, a separate K–S test and a Mann–Whitney U

test was conducted on the wild and captive adult macaques, as fully developed midshafts were expected to exhibit the greatest adaptive morphological differences. The adult samples did not vary significantly in either comparison, however (K–S: $P = 0.356$; M–W: $P = 0.409$), so the Trotter macaques were incorporated into the general macaque sample.

TABLE 2.1. Sampled catarrhines by taxonomy and developmental stage[1,2]

Taxon and sample size	**Infant (*n*)**	**Juvenile (*n*)**	**Adult (*n*)**
P. t. troglodytes	M (3), F (1), U (1)	M (3), F (1)	M (5), F (5)
P. t. schweinfurthii	M (2), F (7), U (1)	M (5), F (5)	M (5), F (2)
P. t. verus	M (1), F (1), U (1)	F (1), U (1)	M (1), F (2)
Total *Pan* (*N* = 54)	***n = 18***	***n = 16***	***n = 20***
G. g. gorilla	M (9), F (3), U (2)	M (5), F (9), U (1)	M (12), F (9)
G. beringei spp.	-	-	F (2)
Total *Gorilla* (*N* = 52)	***n = 14***	***n = 15***	***n = 23***
P. pygmaeus spp.	M (3), F (6), U (3)	M (6), F (5), U (2)	M (10), F (11)
P. abelii	F (2)	M (1), F (2), U (1)	M (1), F (1)
Total *Pongo* (*N* = 54)	***n = 14***	***n = 17***	***n = 23***
Hy. agilis	-	F (1)	-
Hy. concolor	-	-	M (2)
Hy. lar spp.	M (3), F (9)	M (4), F (5)	M (4), F (5)
Hy. muelleri	M (1)	M (1)	M (1)
Ho. hoolock	U (1)	M (2), F (1), U (2)	M (2), F (3)
S. syndactylus	F (1), U (1)	F (1), U (1)	M (1), F (3)
Total Hylobatidae (*N* = 55)	***n = 16***	***n = 18***	***n = 21***
M. fascicularis	M (5)	M (2)	M (5), F (4)
M. mulatta	M (6), F (6), U (1)	M (5), F (10)	M (6), F (6)
Total *Macaca* (*N* = 56)	***n = 18***	***n = 17***	***n = 21***

[1] Subspecies unknown or unspecified by collection denoted by 'spp.'.
[2] Males = 'M', females = 'F', sex undetermined = 'U'.

Developmental subgroups were designated by chronological age when it was made available by the collections. In instances when age was unknown, developmental stage was scored dentally. Smith et al. (1994) assembled a compendium of the minimum and maximum dates of dental eruption of the taxa analysed here which was consulted for each individual. Because life history and tooth emergence vary between taxa and sex, age was estimated using separate crown eruption criteria for each genus or species, and where possible, subspecies (Table 2.2) (Wintheiser et al., 1977; Smith et al., 1994; Dirks, 1997; Dirks and Bowman, 2007; Breuer et al., 2009; Smith and Boesch, 2011; Smith et al., 2013). Though some primate taxa experience a short adolescence stage following juvenility (Sarringhaus et al., 2014), adolescents and subadults were ultimately grouped with adults. This decision was made with consideration to the rapidly declining rate of activity-induced loading adaptation following juvenility (Lieberman et al., 2003), and because an intermediate group would not necessarily clarify any developmental variation but potentially convolute it. Any individual that did not clearly exhibit all permanent teeth were scored on site and photographed so that they could be reassessed later, if needed. Figure 2.1 gives an example from a juvenile chimpanzee. Infant and juvenile comparisons were pooled by sex unless otherwise noted, while adult comparisons were both sex-pooled and discriminated in separate analyses.

TABLE 2.2. Developmental stage classification and tooth eruption estimates in years

Development	*Pan*[1]	*Gorilla*[2]	*Pongo*[3]	Hylobatidae[4]	*Macaca*[5]
Infant	0 – 5	0 – 4	0 – 6	0 – 2	0 – 0.10
Juvenile	5.1 – 10	4.1 – 8	6.1 – 13	2.1 – 6	0.11 – 1.5
Adult	10.1 +	8.1 +	13.1 +	6.1 +	1.51 +
Deciduous[6] Emergence	0.25 – 1.12	0.11 – 0.99	0.35 – 1.04	0 – 0.5	0.043 – 0.437
Permanent[6] Emergence	3.26 – 12.4	3.5 – 10.3	3 – 10	1.75 – 6.1	1.35 – 5.81

[1] Doran, 1997; Sarringhaus et al., 2014.
[2] Watts, 1991; Watts and Pusey, 1993; Doran, 1997; Breuer et al., 2009.
[3] Kelley and Schwartz, 2010; Schuppli et al., 2016.
[4] Burns and Judge, 2016; Morino and Borries, 2016.
[5] Cheverud, 1981; Turnquist, J E, Wells, 1994; Wells and Turnquist, 2001.
[6] Tooth emergence data taken from Smith et al., 1994; Dirks and Bowman, 2007; Breuer et al., 2009.

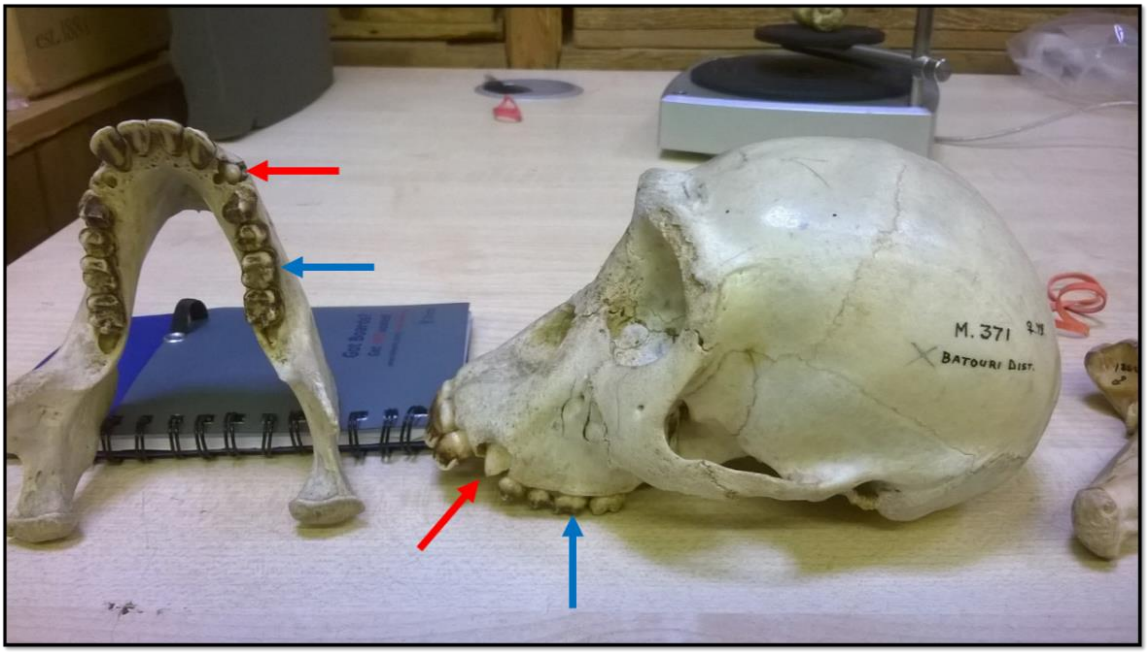

Fig. 2.1. This female juvenile chimpanzee (M371) was age-scored at the P-CM following the methods of H.B Smith et al. (1994) and T.M Smith et al. (2013). The first permanent molars had completely erupted (blue arrows), signaling the end of infancy, while second permanent molar emergence approached completion. The deciduous canines had also shed and were in the process of being replaced by the permanent canines at death (red arrows).

2.2 Data Collection

Linear measurements of the humerus, ulna, femur and tibia were taken from each individual, using an osteometric board (Paleo-Tech) and a pair of digital calipers (Mitutoyo IP67). Total element length was measured after the methods of Martin and Saller (1957) as follows: along the humerus, the proximal-most point of the surface of the humeral head to the distal-most point of the medial trochlear crest; along the ulna, the proximal-most point of the olecranon surface to the distal-most point of the styloid process; along the femur, the proximal-most point of the femoral head to the distal-most point of the medial condyle; and for the tibia, the proximal-most point of the medial or lateral tibial plateau (dependent on the individual) to the distal tip of the medial malleolus. In addition to measures of length, midshaft breadth (defined as maximum breadth at 50% of total element length) (Ruff, 2002), and where applicable, articular surface dimensions including condylar and epicondylar breadth, (surgical) neck width, maximum head breadth, and

length of the trochlear notch. The sample comprises a roughly equal amount of left and right bones, following Carlson (2005).

2.2.1 Laser scanning and three-dimensional model generation

A total of 1,098 three-dimensional (3D) models of the four elements were generated using a NextEngine laser scanner (NextEngine Inc.). The NextEngine consists of three pieces of equipment: the 3D HD scanner responsible for collecting surface data, a turntable used to rotate the target object, and a support pole for adjusting object size and keeping the target object stable during scanning. Each long bone was firmly fastened to the turntable facing anteriorly and bordered by foam insulators to prevent damage in the event of displacement during rotation. The software package 'ScanStudio HD' was used to operate the scanner and process the models after they were generated. A single scan family composed of 10-12 scan 'divisions' (i.e., instances by which the laser captures surface data in a single pass) was recorded for each bone at the highest possible definition (360K points per inch^2). For example, a scan family of 10 divisions implies that the object is rotated and scanned at 10 different angles before completing a full 360° rotation. Thus, the more scan divisions, the higher the model detail, but longer the total scan time. High definition scans ensure that the surface contours are recorded accurately, and that edge artefacts and undesirable model noise are minimised. While the NextEngine can be calibrated to scan different types of objects in multiple resolutions, the optimal settings for this project were established after the methodology of a prior study, which tested the accuracy of cross-sectional dimensions derived from NextEngine scans (Davies et al., 2012; Davies, personal communication, 2014).

For purposes of consistency, the upper and lower limbs of each individual were scanned unilaterally (e.g., right humerus, right ulna) where possible, to capture the potential effects of loading along each limb. In instances where a diaphysis was damaged, exhibited surface pathologies or was missing from the skeleton altogether, the most complete bone was chosen for scanning regardless of laterality. Lighting conditions were controlled using a black felt backdrop mounted behind each bone. A distance of 43 – 51cm was designated between the scanner and turntable, using the "wide-frame capture" setting in ScanStudio. If a bone was too thin or small to accurately record the contour using the wide-frame range, a macro-frame was selected to record

finer details at a closer distance (roughly 16–22cm). The macro option was primarily used to generate infant element models. In instances when individual bones were too large to fit in the scanning field (e.g., adult gorilla humeri or adult orangutan ulnae), the proximal half of the bone was first scanned in 360° and then flipped to record the distal end. After each diaphysis was scanned in 360°, the bone was reoriented superoinferiorly so that both epiphyses could be scanned in succession and attached to the primary long-axis model. While epiphyseal cross-sections were not of interest to the study's central questions, the articular surfaces of each bone had to be digitally fused to the diaphysis in order to accurately calculate total length, and thus, determine which sections of the shaft would be sequenced during analysis. Following these settings, each scan took approximately 17 – 21 minutes to complete. However, some scan families were duplicated to generate higher quality models, taking as long as 45 minutes per bone.

After scanning was completed, the scan families from each element were fused in ScanStudio HD, using identifiable features like nutrient foramina as markers for accuracy. The virtual models were then trimmed and polished so that no extraneous digital mesh projected from the diaphysis (Figure 2.2a). Each model was then aligned in three dimensions (X, Y, and Z axes), facing posteriorly, also in ScanStudio HD. The guidelines described by Ruff (2002; Appendix B) for long bone CT scanning were used to ensure orientation was consistent between individual bones before sectioning (Davies et al., 2012). An example of a fully refined and oriented femur ready for cross-section extraction is given in Figure 2.2b. Additional figures of each limb element at infant and adult stages are given in the Appendix (Figures A2.1a – A2.4b).

2.2.2 Cross-section extraction

Each polished long bone model was exported as a 'xyz' file to the freeware program, AsciiSection (Davies et al. 2012). Using AsciiSection, the virtual models were sliced into cross-sections at pre-determined increments along the diaphysis. A study by Macintosh et al. (2013) found that cross-sectional (or solid-sectional, as no information on cortical or medullary area is available) geometric properties derived from laser-scanned models could be accurately estimated approximately between 20% – 80% of total bone length. Accordingly, cross-sectional values were derived at 20% distal, 50% midshaft and 80% proximal length along each element and for their equidistance proximally and distally from the middiaphysis.

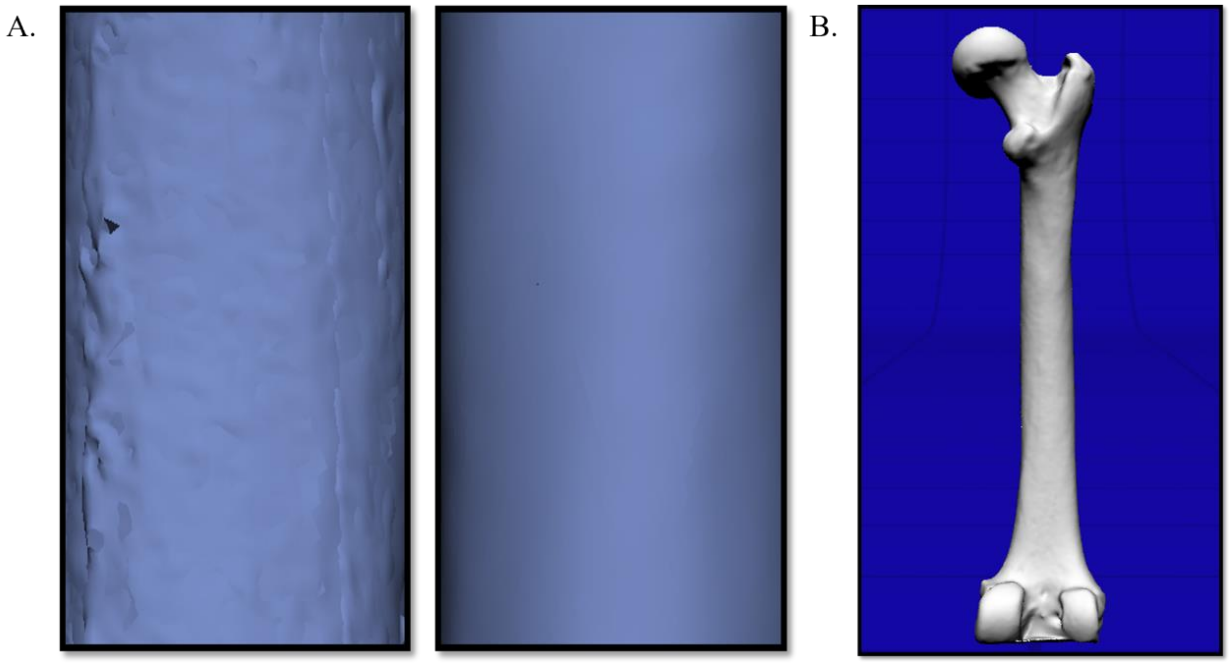

Fig. 2.2.A. Side-by-side close-up comparison of an untouched adult orangutan mid-femur (left) and the same area following trimming and polishing in ScanStudio HD (right). After editing, the digital contour more accurately resembles the true contour and can be accurately measured without obstruction from edge artefacts. **B.** The same finished model oriented posteriorly in preparation for extraction.

The cross-section data were generated by compressing the X, Y and Z coordinates of a given slice from a 3D cylinder into a series of 2D coordinates. The sectioning process itself is fully automated, allowing for the rapid translation of each image from its digital model without the risk of observer bias. A line-command graphing program called gnuplot was used to illustrate 2D solid-section images based on the coordinate data extracted by AsciiSection (Figure 2.3). After the models were sectioned at the proximal, midshaft and distal locations along the diaphyses, AsciiSection calculated four second moments of area about each section, including maximum bending rigidity (I_{max}), minimum bending rigidity (I_{min}), bending rigidity along the AP axis (I_x) and bending rigidity along the ML axis (I_y). More informative geometric properties – circularity ratios about the principal (I_{max}/I_{min}) and anatomical (I_x/I_y) axes, and the polar section modulus (Z_p), proportional to torsional strength and calculated as the polar second moment of area (J) raised to 0.73 (Ruff, 1995, 2002) – were then calculated manually. Because J is proportional to a section's overall torsional rigidity and two times its average bending rigidity, it can be calculated by adding

any two second moments of area about the same axis (e.g., I_{max} + I_{min}; or I_x + I_y both yield a section's *J*) (Ruff, 2008). Table 2.3 gives the eight geometric properties used for analysis in this thesis, along with their definitions and symbols. Unlike the second moments of area considered in Chapters 3 and 4, the third study of this thesis (Chapter 5) took a geometric morphometric approach to studying cross-sectional shape, using the 2D solid-section images generated by gnuplot. The images were converted from 'txt' to 'TIF' files and landmarked using the TPS software series (Rohlf, 2015) (comprehensive information on the landmark and analytical procedures are given in Chapter 5). An in-depth background on the development, error testing and second moment of area calculations of AsciiSection and gnuplot are given in greater detail by Davies and colleagues (2012).

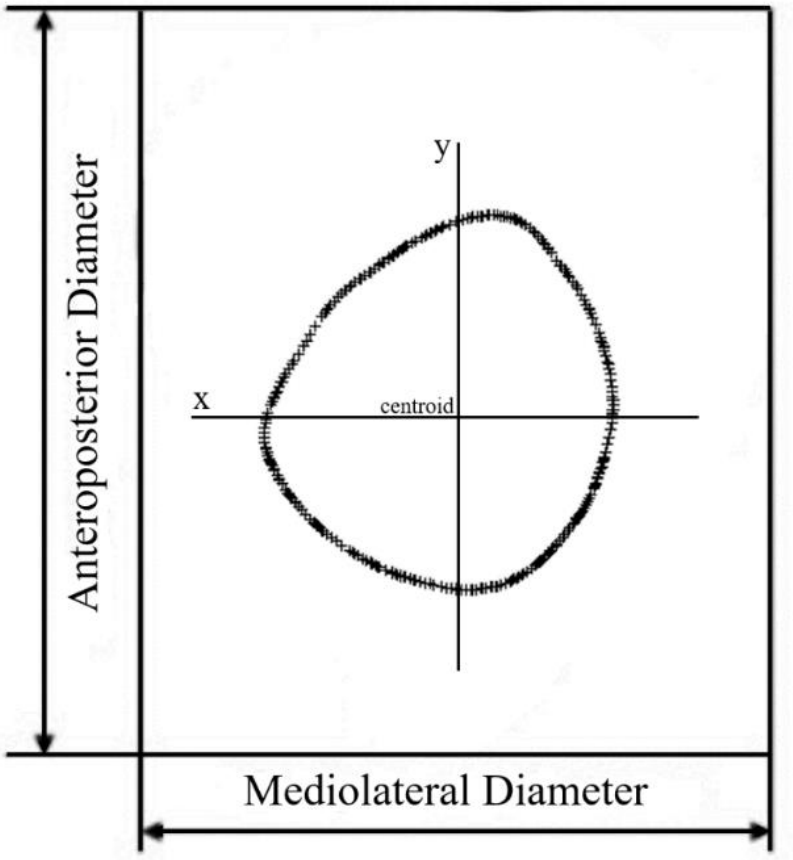

Fig. 2.3. Example of an adult chimpanzee mid-humeral solid-section (not to scale) generated using gnuplot from the coordinate data created by AsciiSection. The periosteal contour and anatomical diameters of a section can accurately predict geometric properties proportional to bending and torsional rigidity, strength or circularity without any information about the endosteal envelope (Stock and Shaw, 2007).

Prior research on long bone cross-sectional geometry has controlled for the influence of muscle attachment sites, like the humeral deltoid tuberosity, by making comparisons at locations distal to midshaft (typically at 40% of total length) (Ruff, 2002; Alba et al., 2011). However, the effects of behaviour on muscle attachment site morphology are questionable (Cunha and Umbelino, 1995; Marriotti et al., 2004). For instance, strength variation between the 40% and 50% humeral section in chimpanzees was found to be negligible (Sarringhaus et al., 2016), while interspecific studies of shape suggest that a sexual dimorphic signal caused by the deltoid tuberosity may be present in species like baboons but absent in vervet monkeys (Burgess et al., 2016). Due to the broad morphological differences between taxa in the following studies, true-midshaft (50% length of total length) was considered in analysis for all inter- and intraspecific comparisons. The proximal humeral retroflexion present in Old World monkeys (Hunt, 2016), was also included at the proximal (80% of total length) humeral section of the macaque sample.

TABLE 2.3. Geometric cross-sectional properties considered in this thesis

Property	**Symbol**	**Measure**	**Description**
Second Moment of Area about the mediolateral (ML) Axis	I_x	mm^4	Bending rigidity along the anteroposterior axis.
Second Moment of Area about the anteroposterior (AP) Axis	I_y	mm^4	Bending rigidity along the mediolateral axis.
Maximum Second Moment of Area	I_{max}	mm^4	Maximum bending rigidity about a section.
Minimum Second Moment of Area	I_{min}	mm^4	Minimum bending rigidity about a section.
Principal Moment of Area Ratio	I_{max} / I_{min}	mm^4	Ratio expressing deviation from section circularity relative to the principal axis.
Second Moment of Area Ratio	I_x / I_y	mm^4	Ratio expressing deviation from section circularity relative to the anatomical axis.
Polar Second Moment of Area[1]	J	mm^4	Sum of bending rigidity in two perpendicular planes; indicative of a section's torsional rigidity and (twice) bending rigidity.
Polar Section Modulus	Z_p	mm^3	Sum of bending strength in two perpendicular planes; indicative of a section's torsional strength and (twice) bending strength.

[1] The polar second moment of area was not directly considered for analysis but used to estimate the polar section modulus (Z_p).

2.2.3 Error testing and general analysis

AsciiSection is an effective alternative to cross-sectional extraction methods like CT or biplanar radiography and has been shown to be equally or more accurate than methods like periosteal moulding (Davies et al., 2012). While the accuracy of AsciiSection in predicting long bone cross-sectional geometry has been demonstrated among modern humans by the authors of the program (Davies et al., 2012; Macintosh et al., 2013), this thesis marks its first application to non-human primate long bones, to my knowledge. A recent study on humeral and femoral cross-sectional geometry in an industrial Finnish population verified AsciiSection's error of measurement using cross-sectional total area, by reorienting the elements in ScanStudio prior to sectioning (Mansukoski and Sparacello, in press). To test for orientation-related variation in the present sample, a similar approach was taken by offsetting the position of each bone in the X, Y and Z planes outside of their defined parameters of orientation, sectioning the augmented models and comparing differences in their geometry. An anatomical second moment of area (I_x) was chosen for comparison over a principal second moment of area because of the anatomical axes' reliance on orientation for accuracy (Carlson, 2005). A mixed taxonomic sample of 20 adult individuals (four from each taxon) was selected to determine if either of the four elements were particularly sensitive to intra-observer orientation errors. The technical error of measurement (TEM) and coefficient of reliability (R) were calculated to determine the variance between measures of long bone orientation (Lewis, 1999). First, TEM was calculated by summing the squared difference of I_x between the correct and augmented models, and dividing it by the product of total observations, multiplied by 2. Next, R was calculated as the standard deviation of the correct and augmented model I_x values squared, divided by the squared TEM and then subtracted from 1 for expression as a percentage. Of all four long bones, the ulna exhibited the greatest variance between correct and augmented models, where 96.2% variance was deemed unrelated to orientation-related error, while the femur exhibited the least unrelated variance (R = 98.1%; mean difference of 185.6 mm^2) (Appendix; Table A2.1). A second intra-observer test was conducted using TEM and R, where the same models were oriented for extraction from a neutral position on two different days; this time without intentionally augmenting the models out of the correct orientation parameters. Reliability was considerably higher in this test, where variance was virtually unrelated to measurement error (Femoral R = 99.8%).

Formula for TEM:

$$TEM = \sqrt{\Sigma D^2 / 2n}$$

Formula for R:

$$R = 1 - \{(TEM)^2 / SD^2\}$$

The three studies in this thesis used different statistical approaches to compare geometric variation within and between taxa, all of which are given in greater detail in their respective research chapters. Generally, statistical analyses in Chapters 3 and 4 were centred on pairwise multiple comparison tests of circularity and relative strength among the sample, and primarily conducted using SPSS v.21 (2012) and Microsoft Excel (2013). Chapter 5 took a geometric morphometric approach to quantify shape along the periosteal contour of each section, making comparisons of form and vector angle size using MorphoJ (Klingenberg, 2011) and the TPS software series (Rohlf, 2015). Figure 2.4 gives the three methods used compare cross-sectional variation in the sample.

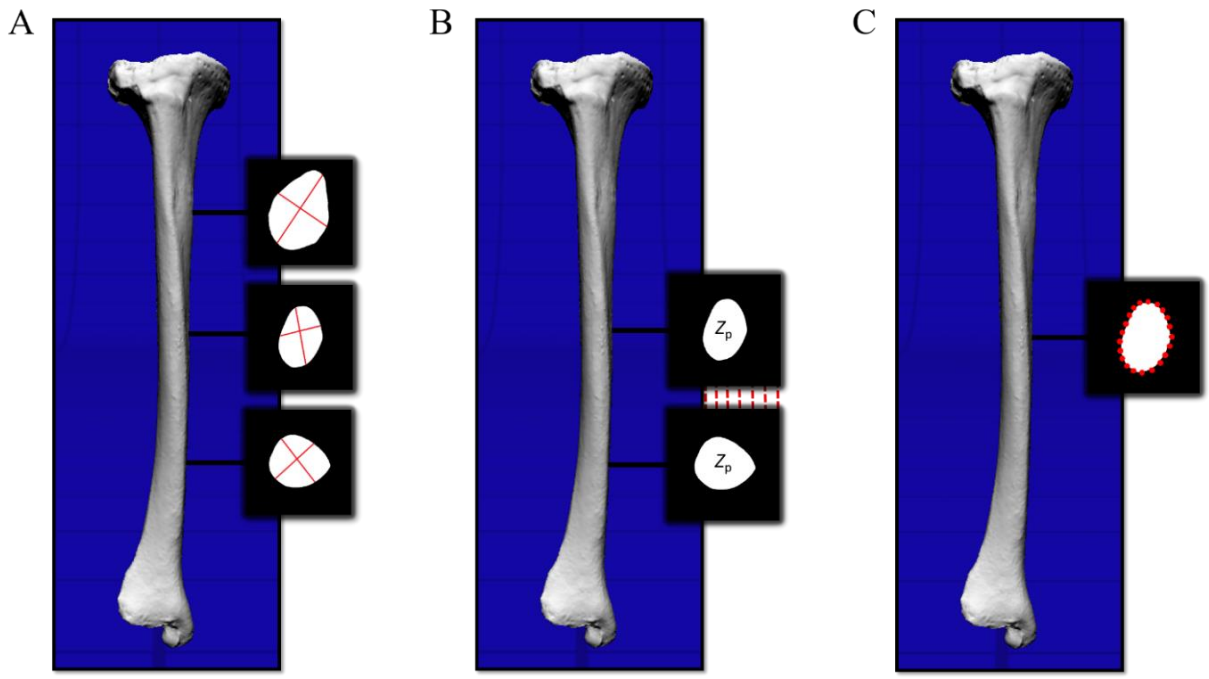

Fig. 2.4. The three primary techniques used in Chapter's 3, 4 and 5 (**A**, **B** and **C**) demonstrated on an adult male chimpanzee tibia. **A.** Principal and anatomical circularity ratios taken at three sections (20%, 50% and 80% length) along the diaphysis. **B**. Strength proportions expressed as ratios of polar section moduli between mid- and distal cross-sections. **C.** Semilandmarks placed along the periosteal contour to quantify section shape for geometric morphometric analyses.

Chapter Three:
Cross-sectional Circularity Along the Limbs

3.1 Introduction

The fore- and hindlimb are employed by all non-human primates during locomotion in a variety of ways. The processes that govern long bone form are multi-faceted however, being largely driven by an individual's phenotype (Lovejoy et al., 2003), along with the diaphyses propensity to adapt their form in response to habitual loading patterns (Robling et al., 2006). By modelling limb diaphyses as structural beams (Huiskes, 1982), it becomes possible to study a long bone's cross-sectional geometry (Biewener, 1982; Lanyon, 1987), granting insight into primate limb form and function at several critical developmental and behavioural junctures.

One method for interpretting an individual's locomotor behaviour is through measures of cross-sectional circularity of their long bone diaphyses. Measuring circularity about the periosteal contour informs about a section's overall shape, and in turn, can act as a general proxy for limb function between locomotor-variable groups (Stock and Pfeiffer, 2001). Because circularity is derived from a section's second moment of area (I), the distribution of tissue about the section is important for understanding its overall ability to deflect the mechanical loads placed on it. Specfically, I is used to estimate section circularity by calculating ratios between any two perpendicular axes of bending, effectively describing the degree by which they conform or vary. Typically, ratios are generated from the principal axes (maximum bending rigidity, I_{max}; minimum bending rigidity, I_{min}) or the anatomical axes (anteroposterior bending rigidity, I_x; mediolateral bending rigidity, I_y) of a given section (Schaffler et al., 1985; Ohman, 1993). The maximum and minimum bending rigidity of a cross-section is proportional to the planes of the greatest and least amount of bone distribution about the section. Therefore, the principal axes of a cross-section are absolute, regardless of the bone's orientation. By contrast, the anatomical axes are fixed in place and can only offer information about bone distribution in the mediolateral (ML) and anteroposterior (AP) axes (Figure 3.1). Interpretations of section circularity in relation to the anatomical axes are therefore sensitive to the bone's orientation. The primary function of I_{max}/I_{min} and I_x/I_y ratios is to describe how a section deviates from circularity relative to their respective

axes. In essence, both ratios act as indices of shape, where values closer to 1.0 represent axial symmetry (Daegling, 2002). When interpreting I_{max}/I_{min} ratios in particular, the greater a value is above 1.0, the more elliptical the cross-sectional shape. The closer the value is to 1.0, the more circular the section is (I_{max}/I_{min} values cannot fall below 1.0, however, as a section's maximum bending rigidity will always be greater or equal to its minimum bending rigidity). In contrast, I_x/I_y ratios describe bending rigidity in an anatomical plane and can be distributed above, as well as below 1.0. For example, an I_x/I_y value greater than 1.0 describes a section with more bone deposited in the AP axis. A number below 1.0, on the other hand, is representative of greater bone distribution in the ML axis. Both I_{max}/I_{min} and I_x/I_y ratios have their own advantages and disadvantages when used to describe cross-sectional shape. For one, I_{max}/I_{min} is a useful index of shape when anatomical orientation is uncertain (e.g., analyzing a bone fragment), as the ratio is extrapolated from the absolute maximum and minimum bending rigidity of the section. However, I_{max}/I_{min} values do not offer any information pertaining to the dimensions of which the bone is distributed. The use of I_x/I_y ratios resolves this problem by describing the way bone is distributed about the anatomical axes, but require accurate bone orientation to do so effectively. That said, I_x/I_y ratios are considered a less accurate estimator of circularity due to their fixed positional nature (Carlson, 2002), preventing them from describing shape beyond the anatomical axes. When used in tandem, however, both I_{max}/I_{min} and I_x/I_y values have the potential to serve as effective tools for estimating cross-sectional shape, as well as describing how bone is distributed throughout a section.

3.2 Research context and objectives

3.2.1 Shape variation along the diaphyses

The fore- and hindlimb elements of terrestrial mammals parallel each other morphologically (Owen, 1849), where robust stylopodial bones (humerus and femur) articulate with gracile zeugopodial bones (radius and ulna; tibia and fibula), forming a tapered configuration along the fore- and hindlimb (Smith and Savage, 1956; Hildebrand, 1985; Alexander, 1996). Concentrating greater muscle and bone mass proximally along the limbs conserves angular momentum during gait swing, decreasing energy expenditure during locomotion (Myers and

Steudel, 1985). A study conducted by Dellanini et al. (2003) demonstrated that adding mass to the distal limb causes runners to expend more energy (by increasing oscillations) in order to match the speeds of runners with greater mass situated proximally.

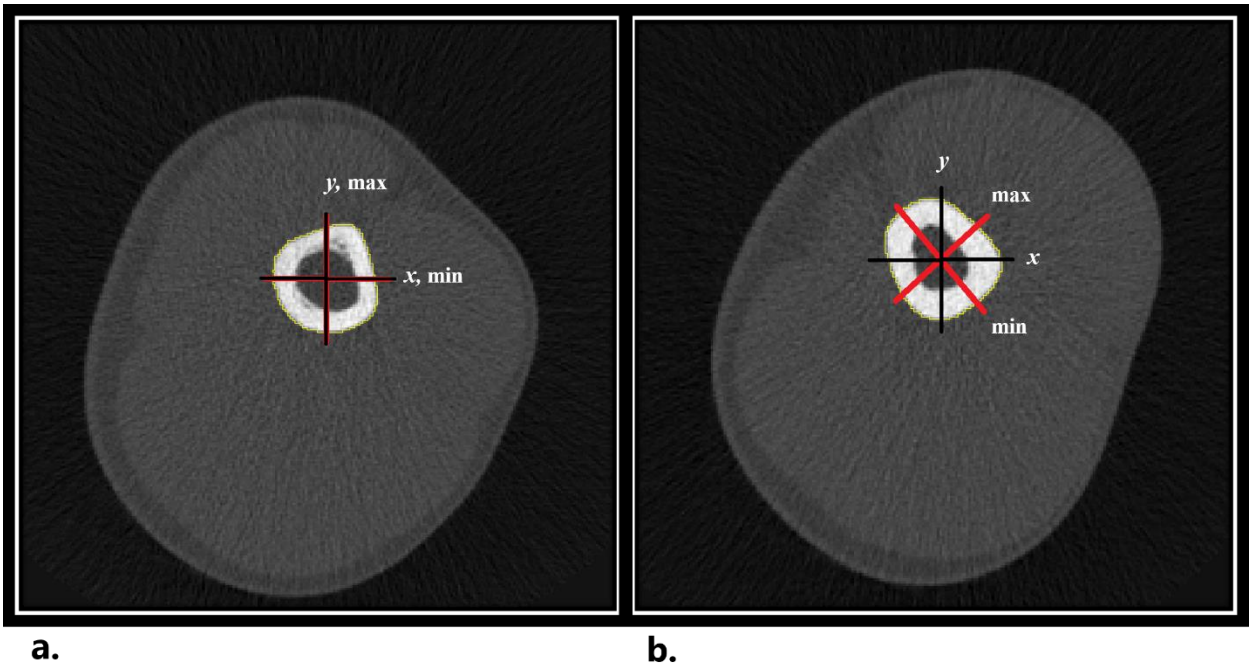

Fig. 3.1. pQCT scans of two human mid-humeri (50% of total length) sections illustrating the principal (red line) and anatomical (black line) axes in each cross-section. Image **a.** illustrates how bone distribution can overlap both axes while image **b.** demonstrates how bone distribution can vary considerably about both axes. Cortical bone is shown in (white), muscle (light grey), adipose tissue (dark grey), and air (black). Cross-sectional images courtesy of C.N. Shaw.

Further, maintaining mass closer to the core grants an advantage in locomotor dexterity by maximising limb velocity (Raichlen, 2006; Plochocki et al., 2008). The wide variation in size and mass between proximal and distal elements is responsible for the tapered limb configuration found in most terrestrial tetrapods, and likely contributes to the cross-sectional morphology of the long bones therein. For instance, the proximal elements of limbs have been shown to produce a greater anabolic response for new bone formation (periosteal modelling) compared to distal elements, when mechanically loaded (Matsuda et al., 1986; O'Neill and Ruff, 2004; Plochocki et al., 2008). It is therefore expected that proximal limb segment circularity should be more variable among taxa

that assume markedly different postures, as well as between developmental stages where locomotor transitions transpire.

Distal limb elements also model themselves in response to dynamic loading events, though it is apparent that the osteogenic response for bone formation is unequal to that of proximal segments, otherwise bone distribution would be comparable along the entirety of the limb (Lieberman et al., 2003). Instead, distal limb segments exhibit greater instances of Haversian remodelling, where osteoclasts first resorb damaged packets of bone, and are in turn, replaced via secondary osteons (Robling et al., 2006; White et al., 2012). The disposition of distal limb segments to remodel more often than model is likely due to their greater constraint of mass compared to more proximal segments (Drapeau and Streeter, 2006). The relative proximity of distal segments to ground vectors may promote remodelling as well, as surface impact forces are capable of microdamaging bone, necessitating their more frequent maintenance (Lieberman and Crompton, 1998). Lieberman and coworkers (2003) found that following a treadmill loading regime, the distal limb segments of sheep exhibited remodelling episodes at a greater rate than proximal segments, especially among adults. Moreover, loading the proximal segments engendered more frequent modelling instances (Lieberman et al., 2003). Given the variable responses that different limb segments display, it is anticipated that distal limb element shape should be constrained relative to proximal segments across development.

Like limb segments, the regional morphology of a long bone is not static either, in that shape and structure vary along the diaphyses and epiphyses contingent on their functional roles. Mid-diaphyses typically bear peak bending forces during loading (Biewener and Taylor, 1986) and therefore, must be strong enough to withstand mechanical failure during locomotion while also being as light as possible to conserve energy. Consequently, midshafts plastically adapt to the loads placed on them by economically resorbing and depositing cortical bone in order to mitigate fatigue damage (Woo et al., 1981; Turner, 1998; Frost, 2003). The structure and shape of articular surfaces are understood to be physiologically constrained compared to midshafts (Currey, 2002). For one, their endosteal architecture comprises a comparatively thin cortical envelope, limiting the potential for modelling to the same extent of the relatively thick midshaft cortex. Instead of relying solely on cortical distribution to resist loads, trabecular networks act to absorb and relieve articular surface stress beneath the cortical envelope (Ruff, 1988) (though trabecular bone also conforms

its shape and structure in response to loading stress) (Lanyon, 1982; Radin et al., 1982; Barak et al., 2011; Tsegai et al., 2013; Kivell, 2016a). The external dimensions of epiphyses and metaphyses are further constrained by their functional roles (i.e., limiting or permitting range of movement and supporting the diaphysis) (Jenkins and Camazine, 1977; Currey, 1984), where any substantial change in form could impact the joint's mechanical performance (Pauwels, 1976). The inherent functionality of primate epiphyses is further supported by the locomotor-specialised characters that constitute them (e.g., retroflexed epicondyles, spool-shaped trochleae, beveled or rounded radial heads). Several studies have since investigated the ontogeny of locomotor morphology in primates, offering insight into limb allometry between infancy and adulthood (Young et al., 2010a), as well as the correspondence between loading behaviour and plastic adaptation (Sarringhuas et al., 2016). However, these studies focused exclusively on the midshaft sections of each limb element. Taking a broader perspective, the plastic-constrained duality of long bones should be reflected in the relative shape along primate diaphyses as well, with sections farthest from midshaft expected to be more adaptively constrained, while midshafts are expected to display a greater degree of shape variation between taxonomic and developmental groups (Waddington, 1942; Ruff and Runestad, 1992; Siegal and Bergman, 2002; Young et al., 2006).

Previous investigations focused on long bone form and function have demonstrated that there is a close correspondence between a section's structure and the bone's loading regime (Hsieh et al., 2001; Carlson, 2005; Nicholson and Firth, 2010; Barak et al., 2011). For example, uniform or unidirectional loading patterns restricted to movement in the saggital plane correlate with a more elliptical cross-sectional shape (Carlson, 2002, 2005). Variable or multidirectional loading patterns are more closely associated with more circular sections (Carlson, 2002, 2005), a result of bone deposition reinforcing the section in multiple planes. Indeed, Shaw and Stock (2009b) demonstrated how repetitive multidirectional loading patterns like field hockey drive bone distribution more equally about the tibial midshaft, yielding a cross-sectional shape similar to that of an equilateral triangle. By comparison, unidirectional loading patterns, like distance running, were found to distribute more bone along the AP plane, yielding a section more closely resembling an isosceles triangle (Shaw and Stock, 2009b). Locomotor patterns associated with turning and multidirectional loading result in greater bone deposition along the ML axis compared to the AP axis, along the femoral diaphyses of mice as well (Carlson and Judex, 2007). Cross-sectional shape analyses of non-human primates have not been as candid, however. Carlson (2005) determined

that principal moment of area ratios (I_{max}/I_{min}) along African ape humeri and femora were capable of distinguishing between genera but were incapable of discriminating between the specific locomotor strategies they employ (e.g., quadrumanous climbing, arboreal quadrupedalism, arboreal scrambling). A more recent study by Patel et al. (2013) centred on humeral shape among primates and sloths similarly concluded that generalised locomotor profiles (suspension, quadrupedalism, etc.) could be distinguished based on cross-sectional shape, but finer taxonomic and functional groupings offered contradictory or overlapping results. That said, these studies primarily focused on overall deviation from circularity, rather than incorporating second moment of area ratios (about the anatomical axes) to complement their findings. Similarly, a recent study by Burgess et al. (2016) on vervet monkey and baboon limbs incorporated anatomical area ratios to better understand which axes bone is distrbitued across species, but excluded principal area ratios.

While research surrounding cross-sectional circularity and mechanical loading in non-human primates is limited, similar patterns to those found in humans have been recorded in rhesus macaques (*Macaca mulatta*) by Demes and coworkers (1998, 2001). In their *in vivo* strain gauge experiments, terrestrial quadrupedal locomotor bouts resulted in greater strain oriented along the AP axis of the tibial midshaft (Demes et al., 2001). Quadrupedal loading of the ulna, on the other hand, appeared to result in greater ML bending strain despite a lack of reinforcement in the plane of bending (Demes et al., 1998), emphasising a somewhat unpredictable relationship between loading and section distribution in the two monkeys they studied. A similar strain guage experiment conducted on exercised and sedentary sheep also found that load-induced modelling does not always reflect a predictable relationship between shape and load-directionality, likely due to the range of forces and biophysical signals that act on bone (Wallace et al., 2014). Instead of a straightforward relationship demonstrating structural reinforcement in the direction of bending (Main, 2007; Shaw and Stock, 2009b) or about the axis of bending (Lanyon and Rubin, 1985; Judex et al., 1997), the authors suggest that load-induced bone deposition may better reflect a compromise between the two, as a means of maintaining safety factors as well as balancing strain levels equally about a given section (Wallace at al., 2014). Aside from a limited amount of *in vivo* data on gibbons (Swartz et al., 1989) and rhesus macaques (Demes et al., 1998, 2001), a lack of strain gauge research makes it difficult to fully appreciate the loading history of the catarrhines of interest in the present study. That said, physical signals should still be discernable within the

sample if the effects of broad locomotor patterns (e.g., suspension or quadrupedalism) load the diaphyses in roughly similar ways.

Growth trajectories in human and non-human primates are also capable of shedding light on transitions between mobility patterns as individuals mature. For instance, both chimpanzees and gorillas display changes in locomotor behaviour throughout their development, favouring particular limbs, postures, and substrates during different stages of life (Doran, 1997; Sarringhaus et al., 2014). In terms of postnatal development as it pertains to body size, apes also experience considerably different growth trajectories, as the duration of growth in gorillas tends to be shorter than in chimpanzees (both *Pan troglodytes* and *P. paniscus*) (Leigh and Shea, 1996). Similarly, the transition from crawling to a bipedal gait in humans is thought to influence the strength and length proportions of the humerus and femur (Ruff, 2003a). Thus, changes in cross-sectional shape and structure are expected to arise as individuals grow and transition between locomotor positions and behaviours.

3.2.2 Research questions

The central aim of this chapter is to determine how long bone cross-sectional shape changes across five Old World primate taxa over the course of their development. The following analysis also seeks to advance the current understanding of site-specific bone adaptation in relation to distinctly different forms of locomotion. Two research questions are addressed: 1) how does long bone cross-sectional circularity vary between catarrhines at different stages of development? If circularity does correlate with locomotor position, it should be reflected by the positional behaviour assumed by each taxonomic group at a given stage of their development. Further, section shape and bone distribution is expected to correspond to load directionality (i.e., relative circularity with variable loading patterns; relative ellipticity with uniform patterns). 2) Does cross-sectional shape change between developmental stage within each taxonomic group? Because distal and proximal sections of long bones are understood to be more adaptively consrtrained than midshafts, it is anticipated that differences in shape will be more apparent at midshaft sections between developmental stages. It is also expected that section shape at the distal, midshaft and proximal aspects of each element will vary based on their functional role along the limb, where midshafts should adapt their shape to support increasing body mass or changes in locomotor

behaviour, while proximal and distal section shape should remain relatively static to transfer loads and support joint functionality. As primates increase in size, they are also more inclined to change their locomotor and postural behaviour to accommodate their mass (Doran, 1992b, 1997; Ruff, 2003a). Thus, it is expected that intraspecific shape comparisons will expose differences between developmental groups, as infants, juveniles and adults should reinforce their diaphyses to reflect the specific loads placed on them. Furthermore, it is expected that midshaft shape among adult taxa will more accurately reflect locomotor profile while distal and proximal section shape should exhibit the least change from infancy. Finally, the humerus and femur are predicted to reveal greater variation in midshaft shape between infancy and adulthood while the ulna and tibia should be more constrained.

3.3 Methods

Details of the primate skeletal sample, scanning method and cross-section extraction used for the long bone shape analysis ahead are reviewed in Chapter 2. Cross-sectional circularity was calculated from the maximum and minimum moments of area of each cross-section. Bone distribution about the anatomical axes was evaluated by generating ratios from second moments of area about the ML and AP axes. Principal and second moments of area were obtained from three cross-sectional locations along each diaphysis: distal (20% of total bone length), midshaft (50%) and proximal (80%). Once values for I were obtained, ratios were generated for both the principal and anatomical axes and expressed as (I_{max}/I_{min}) and (I_x/I_y), respectively.

For all intraspecific developmental comparisons, chimpanzee, gorilla, orangutan and macaque shape data were pooled by sex except among adults, as circularity was found to be significantly different between males and females along the four elements, following multiple-comparison tests. The one exception was the hylobatid group, where no significant shape differences were identified between males or females at any stage of development along each element. All interspecific comparisons were pooled by sex, as the primary interest of those analyses was to identify the broader locomotor differences between taxonomic groups (Patel et al., 2013).

After circularity ratios were created from principal and second moments of area, univariate analysis of variance (ANOVA) was used to compare shape variation between cross-section locations along each diaphysis for each developmental and taxonomic group. A Shapiro-Wilk test of normality was conducted on circularity at each diaphyseal section to determine whether the data was normally distributed (Shapiro and Wilk, 1965). When differences were identified among the means, *post hoc* tests were used to interpret variance between groups. Levene's test was consulted to evaluate the equality of variance in each of the developmental subgroups. When equal variance was assumed, corrections from the Tukey HSD test were used to interpret variation. When homogeneity of variance was violated, the Games-Howell test was used (Sokal and Rohlf, 1995). In two instances (infant distal humerus; infant tibial midshaft), the subgroup samples were deemed not normally distributed following a Brown-Forsythe and a Welch test. To control for variance in group size in those situations, shape comparisons were assessed with a Kruskal-Wallis H test. Coefficients of variation (CV%) were calculated to better illustrate intragroup shape variation among each developmental subgroup. Significance was recognised at $P < 0.05$ in all comparisons.

3.4 Results and preliminary discussion

The following section presents the study's findings in two subsections: the forelimb and the hindlimb. Shape comparisons along the diaphyses of each taxon and their respective developmental subgroups are reviewed in each. Table 3.9 (a-e) outlines the overall results for each taxon, including the predictions and observations found along the four limb elements.

3.4.1 The forelimb

Descriptive statistics for the infant humerus are given in Table 3.1a. Midshaft I_{max}/I_{min} ratios among infants revealed that no significant variation existed among the taxa (Table 3.2). Bone distribution in the anatomical axes did reveal that the Asian apes and chimpanzees each distributed more tissue in the AP axis while gorilla and macaque bone distribution was more concentrated along the ML axis during infancy. Unlike the midshaft, the proximal (80% of total length) and distal (20%) sections of the infant subgroups both revealed significant deviations from circularity among all five taxonomic groups. The entire infant subsample exhibited relatively small I_x/I_y ratios

at the distal diaphysis in particular, indicative of greater bone distribution along the ML axis. The minor interspecific variation observed across infant taxa at midshaft conforms to the prediction that young individuals' bones will not be as morphologically specialised to their locomotor environments until they achieve locomotor independence.

Humeral shape was more variable between juvenile taxa than it was among infants at midshaft (Table 3.1b). Juvenile hylobatid midshafts were significantly more circular compared to the juvenile gorilla subgroup, in support of the correspondence between elliptical proximal midshaft segments and uniform loading patterns. Midshaft shape did not differ between juvenile orangutans and chimpanzees, or gorillas and macaques, but was significantly more elliptical among these taxa than the more circular configuration of the juvenile hylobatid subgroup. Compared to the proximal humerus and humeral midshaft, the distal diaphyses of the juveniles showed little variation in shape compared to their infant counterparts. In fact, no significant shape differences were identified between the juveniles or infants of any taxon.

Compared to the infant and juvenile subgroups, adults displayed the greatest interspecific circularity variation at the humeral midshaft (Table 3.1c). Macaque mid-humeral I_{max}/I_{min} was significantly more ML elliptical compared to each of the adult hominoid taxa. This transition in section shape conformed to the predictions made at the humeral midshaft (Table 3.9), where infant macaques showed no shape differences with other taxa. Ultimately, the greatest deviation from circularity was observed in gorillas and macaques, while hylobatids, orangutans, and the semi-arboreal chimpanzees displayed the most circular section shape at midshaft. The distal humerus discriminated the large-bodied great apes from the hylobatids, as it did in both the infant and juvenile samples. However, due to an increase in distal circularity in the adult macaque sample compared to the juvenile sample, no significant differences were identified between the great apes and macaques at the distal humerus. Moreover, no intraspecific developmental shape differences were identified among the taxa at the distal humerus (Figures 3.2a,c,e,g,i).

TABLE 3.1a. Infant Humeral Circularity: Mean, Standard Deviation and Coefficient of Variation

	20% Length		50% Length		80% Length	
Taxon (*n*)	I_{max}/I_{min}	CV%	I_{max}/I_{min}	CV%	I_{max}/I_{min}	CV%
Pan (17)	2.30 ± 0.46	19.9	1.25 ± 0.17	15.1	1.85 ± 0.35	19.2
Gorilla (14)	2.39 ± 0.43	17.8	1.18 ± 0.1	9.2	1.54 ± 0.22	16.5
Pongo (14)	2.27 ± 0.48	21.1	1.34 ± 0.2	15.7	1.51 ± 0.19	13
Hylobatidae (16)	1.26 ± 0.16	12.9	1.26 ± 0.11	9.9	1.39 ± 0.17	12.8
Macaca (17)	2.97 ± 0.49	16.5	1.27 ± 0.16	13.7	1.86 ± 0.37	20.3
Taxon (*n*)	I_x/I_y	CV%	I_x/I_y	CV%	I_x/I_y	CV%
Pan (17)	0.46 ± 0.07	16.7	1.18 ± 0.2	17	1.12 ± 0.28	25.6
Gorilla (14)	0.44 ± 0.07	17.4	0.93 ± 0.09	9.7	0.84 ± 0.14	17.3
Pongo (14)	0.49 ± 0.09	19.1	1.29 ± 0.19	14.6	0.93 ± 0.13	14.8
Hylobatidae (16)	0.98 ± 0.17	17.5	1.21 ± 0.09	7.8	1.23 ± 0.21	17.6
Macaca (17)	0.42 ± 0.07	16.6	0.96 ± 0.12	12.9	1.23 ± 0.26	21.6

TABLE 3.1b. Juvenile Humeral Circularity: Mean, Standard Deviation and Coefficient of Variation

	20% Length		50% Length		80% Length	
Taxon (*n*)	I_{max}/I_{min}	CV%	I_{max}/I_{min}	CV%	I_{max}/I_{min}	CV%
Pan (16)	2.49 ± 0.41	16.8	1.29 ± 0.13	10.2	1.54 ± 0.15	10.2
Gorilla (15)	2.54 ± 0.34	13.7	1.3 ± 0.05	4.46	1.44 ± 0.19	13.1
Pongo (17)	2.42 ± 0.55	23	1.31 ± 0.13	10.3	1.39 ± 0.21	15.1
Hylobatidae (18)	1.17 ± 0.11	9.4	1.19 ± 0.09	7.73	1.34 ± 0.19	14.6
Macaca (16)	3.05 ± 0.67	21.9	1.31 ± 0.15	12.1	1.67 ± 0.17	10.5
Taxon (*n*)	I_x/I_y	CV%	I_x/I_y	CV%	I_x/I_y	CV%
Pan (16)	0.44 ± 0.06	13.6	1.23 ± 0.14	11.8	0.96 ± 0.16	17.1
Gorilla (15)	0.41 ± 0.05	12.1	0.89 ± 0.09	10.5	0.79 ±0.12	16
Pongo (17)	0.48 ± 0.11	22.6	1.26 ± 0.15	12.4	0.86 ± 0.15	18
Hylobatidae (18)	0.98 ± 0.11	11.2	1.04 ± 0.13	13.3	1.24 ± 0.18	15.1
Macaca (16)	0.41 ± 0.08	20.8	0.94 ± 0.1	11.4	1.27 ± 0.19	15.4

TABLE 3.1c. Adult Humeral Circularity: Mean, Standard Deviation and Coefficient of Variation

	20% Length		50% Length		80% Length	
Taxon (*n*)	I_{max}/I_{min}	CV%	I_{max}/I_{min}	CV%	I_{max}/I_{min}	CV%
Pan (20)	2.41 ± 0.48	20.1	1.23 ± 0.11	9.1	1.31 ± 0.15	11.6
Gorilla (23)	2.49 ± 0.56	22.5	1.31 ± 0.12	9.8	1.23 ± 0.1	8.7
Pongo (23)	2.11 ± 0.58	27.5	1.27 ± 0.12	10	1.23 ± 0.12	10.1
Hylobatidae (21)	1.24 ± 0.11	9.5	1.17 ± 0.09	8	1.26 ± 0.19	15.3
Macaca (20)	2.55 ± 0.49	19.5	1.59 ± 0.19	12.4	1.53 ± 0.26	17.1
Taxon (*n*)	I_x/I_y	CV%	I_x/I_y	CV%	I_x/I_y	CV%
Pan (20)	0.45 ± 0.07	16.4	1.17 ± 0.11	9.4	0.89 ± 0.11	13.1
Gorilla (23)	0.43 ± 0.08	20.4	0.87 ± 0.09	11.1	0.85 ± 0.07	8.5
Pongo (23)	0.56 ± 0.15	27.4	1.23 ± 0.13	10.4	0.99 ± 0.17	17.7
Hylobatidae (21)	0.87 ± 0.08	9.2	0.98 ± 0.12	12.7	1.14 ± 0.23	20
Macaca (20)	0.5 ± 0.11	22.2	0.82 ± 0.1	12.1	1.14 ± 0.19	16.9

TABLE 3.2 Interspecific ANOVA comparisons along the humerus

Diaphyseal Location by Development	**Area Ratio**	***F***	***P***	**Significantly different shape groupings (*Post hoc* – Tukey HSD or Games-Howell)**
Infant – 20% length	*Imax/Imin*	-	0.001	*Pan* – Hylobatidae, *Macaca* *Gorilla* – Hylobatidae, *Macaca* *Macaca* – Hylobatidae, *Pongo*
	Ix/Iy	-	0.001	Hylobatidae – *Pan, Gorilla, Pongo, Macaca*
Infant – 50% length	*Imax/Imin*	1.8	0.128	NS
	Ix/Iy	17.3	0.001	*Pan* – *Gorilla, Macaca* *Gorilla* – *Pan, Pongo,* Hylobatidae *Pongo* – *Gorilla, Macaca* Hylobatidae – *Gorilla, Macaca*
Infant – 80% Length	*Imax/Imin*	9.5	0.001	*Pongo* – *Pan, Macaca* Hylobatidae – *Pan, Macaca*
	Ix/Iy	9.4	0.001	*Gorilla* – *Pan,* Hylobatidae, *Macaca* *Pongo* – Hylobatidae, *Macaca*
Juvenile – 20% Length	*Imax/Imin*	48.2	0.001	*Pongo* – *Macaca* Hylobatidae – *Pan, Gorilla, Pongo, Macaca*
	Ix/Iy	140.4	0.001	Hylobatidae – *Pan, Gorilla, Pongo, Macaca*
Juvenile – 50% Length	*Imax/Imin*	3.7	0.007	Hylobatidae – *Gorilla, Pongo*
	Ix/Iy	24.8	0.001	Hylobatidae – *Pan, Gorilla, Pongo, Macaca* *Gorilla* – *Pan, Pongo,* Hylobatidae *Macaca* – *Pan, Pongo*
Juvenile – 80% length	*Imax/Imin*	8.9	0.001	*Pan* – Hylobatidae *Macaca* – *Gorilla, Pongo,* Hylobatidae
	Ix/Iy	28.6	0.001	*Pan* – Hylobatidae, *Macaca* *Gorilla* – Hylobatidae, *Macaca* *Pongo* – Hylobatidae, *Macaca*
Adult – 20% length	*Imax/Imin*	27.2	0.001	Hylobatidae – *Pan, Gorilla, Pongo, Macaca*
	Ix/Iy	62.1	0.001	Hylobatidae – *Pan, Gorilla, Pongo, Macaca* *Pan* – *Pongo,* Hylobatidae *Gorilla* – *Pongo,* Hylobatidae
Adult – 50% length	*Imax/Imin*	30.1	0.001	Hylobatidae – *Gorilla, Pongo* *Macaca* – *Pan, Gorilla, Pongo,* Hylobatidae
	Ix/Iy	56	0.001	*Pan* – *Gorilla* *Pongo* – *Gorilla, Macaca* Hylobatidae – *Pan, Gorilla, Pongo, Macaca*
Adult – 80% length	*Imax/Imin*	10.6	0.001	*Macaca* – *Pan, Gorilla, Pongo,* Hylobatidae
	Ix/Iy	15.1	0.001	*Pan* – Hylobatidae, *Macaca* *Gorilla* – *Pongo,* Hylobatidae, *Macaca*

Descriptive statistics and coefficients of variation for the infant ulna are given in Table 3.3a. Of the entire sample, infant chimpanzees displayed the most circular midshafts with virtually equal bone distribution about the anatomical axes. Gorillas and orangutans, on the other hand, displayed the most elliptical ulnar midshaft cross-sections (Table 3.4). Overall, shape variation along the proximal ulna deviated from circularity to a greater extent than the proximal humerus. The distal infant ulna was comparatively circular among all five taxa. Both infant and juvenile mid-ulnar shape (I_{max}/I_{min}) did not differ between the African apes. Compared to the infant gorilla sample, juvenile gorillas exhibited more circular midshafts (Table 3.3b), though the predominant bone distribution along the ML axis did not differ between either infant or juvenile groups. Juvenile hylobatids and macaques – the two smallest bodied genera in the sample – both displayed significantly more elliptical proximal ulnae compared to the great ape subgroups. The distal ulna showed little variation between taxa about either axis, by comparison. Compared to both the proximal ulna and ulnar midshaft, distal cross-sectional shape also tended closer to circularity (1.0) about the principal and anatomical axes.

Table 3.3c displays the descriptive statistics of the adult ulnar group. Adult chimpanzee and gorilla shape did not differ from one another about the principal axes of the ulnar midshaft as in the infant and juvenile subgroups (Table 3.4). Like the juvenile sample, adult gorillas were the only taxonomic subgroup to distribute more bone in the ML than the AP axis. Among the Asian apes, adult orangutan mid-ulnae were more circular than their juvenile counterparts but ultimately, exhibited the most elliptical sections of the sampled adult taxa. Furthermore, adult orangutans distributed more bone about the AP axis compared to both African ape genera, in contrast with earlier predictions (Table 3.9). Unlike at midshaft, adult African ape circularity about the principal axes was significantly different from one another at the proximal ulna but no different at the distal section. Ultimately, the proximal and midshaft sections of the ulna displayed more interspecific and developmental shape variation than the distal section, which did not change between developmental groups among any taxon, in agreement with the predictions made.

TABLE 3.3a. Infant Ulna Circularity: Mean, Standard Deviation and Coefficient of Variation

	20% Length		50% Length		80% Length	
Taxon (*n*)	I_{max}/I_{min}	CV%	I_{max}/I_{min}	CV%	I_{max}/I_{min}	CV%
Pan (18)	1.21 ± 0.97	8.01	1.34 ± 0.29	15.1	1.52 ± 0.24	15.8
Gorilla (14)	1.31 ± 0.16	12.2	1.79 ± 0.23	9.2	1.37 ± 0.14	10.3
Pongo (14)	1.36 ± 0.16	12	1.76 ± 0.27	15.7	1.5 ± 0.19	12.7
Hylobatidae (16)	1.36 ± 0.15	11.5	1.61 ± 0.22	9.9	2.31 ± 0.62	27
Macaca (16)	1.44 ± 0.34	23.8	1.73 ± 0.34	13.7	2.81 ± 0.4	14.3
Taxon (*n*)	I_x/I_y	CV%	I_x/I_y	CV%	I_x/I_y	CV%
Pan (18)	0.96 ± 0.16	16.6	1.02 ± 0.16	15.6	1.44 ± 0.26	18
Gorilla (14)	0.95 ± 0.16	16.8	0.82 ± 0.15	18.2	1.32 ± 0.14	10.6
Pongo (14)	0.86 ± 0.11	12.8	1.00 ± 0.22	22	1.35 ± 0.15	11.1
Hylobatidae (16)	1.28 ± 0.16	12.5	1.33 ± 0.38	28.5	2.14 ± 0.64	29.9
Macaca (16)	1.05 ± 0.31	29.5	1.61 ± 0.32	19.9	2.64 ± 0.33	12.5

TABLE 3.3b. Juvenile Ulna Circularity: Mean, Standard Deviation and Coefficient of Variation

	20% Length		50% Length		80% Length	
Taxon (*n*)	I_{max}/I_{min}	CV%	I_{max}/I_{min}	CV%	I_{max}/I_{min}	CV%
Pan (15)	1.15 ± 0.12	10.8	1.32 ± 0.2	15.4	1.78 ± 0.28	16.1
Gorilla (14)	1.21 ± 0.13	10.7	1.47 ± 0.2	13.7	1.45 ± 0.2	14
Pongo (17)	1.27 ± 0.13	10.6	2.03 ± 0.38	18.8	1.5 ± 0.26	16.7
Hylobatidae (18)	1.27 ± 0.12	10	1.49 ± 0.29	19.7	2.72 ± 0.74	27.3
Macaca (17)	1.34 ± 0.21	16.2	1.76 ± 0.37	21.3	2.95 ± 0.81	27.4
Taxon (*n*)	I_x/I_y	CV%	I_x/I_y	CV%	I_x/I_y	CV%
Pan (15)	0.99 ± 0.09	9.1	1.06 ± 0.15	14.2	1.69 ± 0.31	18.3
Gorilla (14)	0.93 ± 0.17	18.3	0.82 ± 0.12	14.6	1.36 ± 0.22	16.1
Pongo (17)	0.97 ± 0.15	15.4	1.33 ± 0.51	38.3	1.43 ± 0.21	14.6
Hylobatidae (18)	1.11 ± 0.19	17.1	1.17 ± 0.34	29	1.85 ± 0.75	40.5
Macaca (17)	1.0 ± 0.21	21	1.67 ± 0.34	20.3	2.80 ± 0.78	27.8

TABLE 3.3c. Adult Ulna Circularity: Mean, Standard Deviation and Coefficient of Variation

	20% Length		50% Length		80% Length	
Taxon (*n*)	I_{max}/I_{min}	CV%	I_{max}/I_{min}	CV%	I_{max}/I_{min}	CV%
Pan (20)	1.19 ± 0.14	12.1	1.27 ± 0.13	10.8	1.86 ± 0.63	33.9
Gorilla (23)	1.26 ± 0.14	11.6	1.42 ± 0.21	15.3	1.41 ± 0.2	14.4
Pongo (23)	1.31 ± 0.26	20.2	1.84 ± 0.53	29.2	1.63 ± 0.23	14.1
Hylobatidae (21)	1.32 ± 0.18	13.6	1.6 ± 0.37	23.5	2.44 ± 0.51	21.1
Macaca (18)	1.36 ± 0.2	14.8	1.61 ± 0.44	27.8	3.08 ± 0.75	24.4
Taxon (*n*)	I_x/I_y	CV%	I_x/I_y	CV%	I_x/I_y	CV%
Pan (20)	1.02 ± 0.17	16.6	1.01 ± 0.17	16.8	1.79 ± 0.63	35.2
Gorilla (23)	0.92 ± 0.13	14.1	0.89 ± 0.16	17.9	1.26 ± 0.17	13.5
Pongo (23)	1.07 ± 0.20	18.7	1.50 ± 0.43	28.6	1.51 ± 0.31	20.5
Hylobatidae (21)	1.05 ± 0.19	18.1	1.17 ± 0.37	31.6	1.81 ± 0.53	29.3
Macaca (18)	0.88 ± 0.14	15.9	1.39 ± 0.38	27.3	2.62 ± 0.73	27.9

TABLE 3.4. Interspecific ANOVA comparisons along the ulna

Diaphyseal Location by Development	**Area Ratio**	***F***	***P***	**Significantly different shape groupings (*Post hoc* – Tukey HSD or Games-Howell)**
Infant – 20% length	*Imax/Imin*	2.9	0.024	*Pan* – *Pongo,* Hylobatidae
	Ix/Iy	13.7	0.001	Hylobatidae – *Pan, Gorilla* *Macaca* – *Gorilla, Pongo*
Infant – 50% length	*Imax/Imin*	7.2	0.001	*Pan* – *Gorilla, Pongo,* Hylobatidae, *Macaca*
	Ix/Iy	20.5	0.001	Hylobatidae – *Pan, Gorilla* *Macaca* – *Pan, Gorilla, Pongo*
Infant – 80% Length	*Imax/Imin*	44.2	0.001	*Pan* – Hylobatidae, *Macaca* *Gorilla* – Hylobatidae, *Macaca* *Pongo* – Hylobatidae, *Macaca*
	Ix/Iy	39.5	0.001	*Pan* – Hylobatidae, *Macaca* *Gorilla* – Hylobatidae, *Macaca* *Pongo* – Hylobatidae, *Macaca*
Juvenile – 20% Length	*Imax/Imin*	3.7	0.007	*Pan* – *Macaca*
	Ix/Iy	2.7	0.032	*Gorilla* – Hylobatidae
Juvenile – 50% Length	*Imax/Imin*	14.8	0.001	*Pan* – *Macaca, Pongo* *Pongo* – *Pan, Gorilla*, Hylobatidae
	Ix/Iy	13.1	0.001	*Gorilla* – *Pan, Pongo,* Hylobatidae, *Macaca* *Macaca* – *Pan, Gorilla*, Hylobatidae
Juvenile – 80% length	*Imax/Imin*	27.8	0.001	*Pan* – *Gorilla*, Hylobatidae, *Macaca* *Gorilla* – *Pan,* Hylobatidae, *Macaca* *Pongo* – Hylobatidae, *Macaca*
	Ix/Iy	18.8	0.001	*Macaca* – *Pan, Gorilla, Pongo,* Hylobatidae *Pan* – *Gorilla, Pongo*
Adult – 20% length	*Imax/Imin*	2.1	0.084	NS
	Ix/Iy	4.9	0.001	*Macaca* – *Pongo*, Hylobatidae *Gorilla* – *Pongo*
Adult – 50% length	*Imax/Imin*	7.4	0.001	*Pan* – *Pongo,* Hylobatidae, *Macaca* *Gorilla* – *Pongo,* Hylobatidae, *Macaca*
	Ix/Iy	13.9	0.001	*Pan* – *Pongo, Macaca* *Gorilla* – *Pongo,* Hylobatidae, *Macaca*
Adult – 80% length	*Imax/Imin*	37.5	0.001	*Gorilla* – *Pan, Pongo,* Hylobatidae, *Macaca* Hylobatidae – *Pan, Gorilla, Pongo, Macaca* *Macaca* – *Pan, Gorilla, Pongo,* Hylobatidae
	Ix/Iy	20.8	0.001	*Gorilla* – *Pan, Pongo,* Hylobatidae, *Macaca* *Macaca* – *Pan, Gorilla, Pongo,* Hylobatidae

3.4.2 The hindlimb

Descriptive statistics and coefficients of variation for shape along the infant femur are given in Table 3.5a. Infant chimpanzees and hylobatids exhibited significantly more circular femoral midshafts compared to gorillas and orangutans but could not be discriminated from each other about either the principal or anatomical axes. Like the African apes, orangutan and hylobatid midshaft morphology differed from one another about the principal axes, where the hylobatids exhibited more circular midshafts. Proximally, infant macaques were found to have the most circular femoral sections about the principal axes, distinguishing them from all hominoids apart from the hylobatids (Table 3.6). Overall, distal femoral circularity was most effective at differentiating the infant sample, as the taxonomic groups displayed a greater range of shape variation from each other at 20% length. Indeed, all five infant groups displayed a greater deviation from circularity at the distal femur than at the proximal or midshaft sections, while also distributing more bone in the ML compared to AP axis, distally. Like the infant sample, the juvenile gorilla and orangutan groups displayed the most elliptical (AP) midshaft sections, while the hylobatids and macaques exhibited the most circular midshafts about both axes (Table 3.5b). At the proximal femur, the macaque sample displayed the most circular femora, and additionally, were the only juvenile taxonomic group to distribute more bone in the AP than ML axis.

Deviation from circularity at the femoral midshaft was most apparent among adult taxa than at any other stage of development, particularly among the great apes (Table 3.5c). In fact, midshaft shape among all three great ape genera was significantly different from their respective infant counter parts (Figures 3.2b,d,f,h,j). No discernible shape change was identified between juvenile and adult macaques, counter to the developmental predictions found in (Table 3.9). Macaques were again, the only taxon to distribute more bone along the AP axis at the proximal femur in adulthood, while the other adult taxa reinforced the ML axis. Shape at the midshaft and distal cross-sections (about both axes) appeared to correspond to the general body size of each taxon. For instance, the adult gorillas displayed the most elliptical distal femora in the ML plane, followed by orangutans, and chimpanzees, in that order. The adult hylobatids and macaques followed next, with the most circular cross-sections, though their I_{max}/I_{min} and I_x/I_y values were virtually identical.

TABLE 3.5a. Infant Femur Circularity: Mean, Standard Deviation and Coefficient of Variation

	20% Length		50% Length		80% Length	
Taxon (*n*)	I_{max}/I_{min}	CV%	I_{max}/I_{min}	CV%	I_{max}/I_{min}	CV%
Pan (17)	1.73 ± 0.26	15.4	1.11 ± 0.06	5.7	1.35 ± 0.2	14.8
Gorilla (14)	3.09 ± 0.67	21.8	1.29 ± 0.11	9.1	1.44 ± 0.26	18.2
Pongo (14)	2.33 ± 0.51	22.2	1.25 ± 0.13	10.9	1.59 ± 0.29	18.7
Hylobatidae (16)	1.62 ± 0.31	19.6	1.13 ± 0.07	6.6	1.25 ± 0.18	14.9
Macaca (18)	1.4 ± 0.21	15.4	1.22 ± 0.08	6.8	1.18 ± 0.08	7.2
Taxon (*n*)	I_x/I_y	CV%	I_x/I_y	CV%	I_x/I_y	CV%
Pan (17)	0.61 ± 0.08	17.2	1.05 ± 0.09	9.4	0.9 ± 0.1	11.1
Gorilla (14)	0.34 ± 0.07	14.3	0.81 ± 0.09	11.3	0.75 ± 0.14	18.5
Pongo (14)	0.46 ± 0.11	18.8	0.9 ± 0.18	19.2	0.77 ± 0.18	24.4
Hylobatidae (16)	0.65 ± 0.13	18.9	1.05 ± 0.07	7.4	1.01 ± 0.22	21.9
Macaca (18)	0.75 ± 0.11	15.7	0.97 ± 0.1	11.2	1.1 ± 0.12	11.1

TABLE 3.5b. Juvenile Femur Circularity: Mean, Standard Deviation and Coefficient of Variation

	20% Length		50% Length		80% Length	
Taxon (*n*)	I_{max}/I_{min}	CV%	I_{max}/I_{min}	CV%	I_{max}/I_{min}	CV%
Pan (16)	1.64 ± 0.29	17.9	1.19 ± 0.1	9	1.52 ± 0.25	16.9
Gorilla (14)	3.23 ± 0.45	14	1.54 ± 0.2	13.5	1.59 ± 0.35	22
Pongo (17)	2.42 ± 0.45	18.6	1.34 ± 0.15	11.5	1.85 ± 0.36	19.8
Hylobatidae (17)	1.57 ± 0.28	18	1.12 ± 0.08	7.8	1.32 ± 0.21	15.9
Macaca (17)	1.2 ± 0.12	10.5	1.14 ± 0.08	7.2	1.23 ± 0.11	9.6
Taxon (*n*)	I_x/I_y	CV%	I_x/I_y	CV%	I_x/I_y	CV%
Pan (16)	0.63 ± 0.1	16.5	0.92 ± 0.11	12.8	1.0 ± 0.15	15.1
Gorilla (14)	0.31 ± 0.04	13.8	0.67 ± 0.11	17.3	0.76 ± 0.12	15.9
Pongo (17)	0.43 ± 0.08	18.7	0.79 ± 0.1	13	0.66 ± 0.16	24.5
Hylobatidae (17)	0.68 ± 0.12	17.9	0.99 ± 0.08	8.78	0.9 ± 0.12	13.4
Macaca (17)	0.86 ± 0.1	12.3	0.92 ± 0.08	9.21	1.07 ± 0.12	11.4

TABLE 3.5c. Adult Femur Circularity: Mean, Standard Deviation and Coefficient of Variation

	20% Length		50% Length		80% Length	
Taxon (*n*)	I_{max}/I_{min}	CV%	I_{max}/I_{min}	CV%	I_{max}/I_{min}	CV%
Pan (20)	1.64 ± 0.17	10.9	1.36 ± 0.15	11.5	1.81 ± 0.59	32.6
Gorilla (23)	3.0 ± 0.53	17.6	1.78 ± 0.27	15.3	1.95 ± 0.31	15.9
Pongo (23)	2.3 ± 0.64	27.9	1.57 ± 0.2	12.7	2.27 ± 0.6	26.8
Hylobatidae (21)	1.34 ± 0.17	13.1	1.17 ± 0.08	6.9	1.53 ± 0.32	21
Macaca (21)	1.35 ± 0.18	14	1.16 ± 0.08	7.1	1.41 ± 0.52	37.3
Taxon (*n*)	I_x/I_y	CV%	I_x/I_y	CV%	I_x/I_y	CV%
Pan (20)	0.62 ± 0.07	11.5	0.75 ± 0.08	10.5	0.96 ± 0.22	23.2
Gorilla (23)	0.34 ± 0.05	17	0.58 ± 0.08	14.4	0.85 ± 0.19	23.1
Pongo (23)	0.46 ± 0.2	20	0.65 ± 0.07	11.9	0.8 ± 0.26	33.5
Hylobatidae (21)	0.77 ± 0.1	13.1	0.97 ± 0.08	8.9	0.93 ± 0.2	21.6
Macaca (21)	0.75 ± 0.11	14.7	0.93 ± 0.11	12	1.07 ± 0.17	15.8

TABLE 3.6. Interspecific ANOVA comparisons along the femur

Diaphyseal Location by Development	Area Ratio	*F*	*P*	Significantly different shape groupings (*Post hoc* – Tukey HSD or Games-Howell)
Infant – 20% length	*Imax/Imin*	42.8	0.001	*Pan* – *Gorilla*, *Pongo*, *Macaca* *Gorilla* – *Pan*, *Pongo*, Hylobatidae, *Macaca* *Pongo* – *Pan*, *Gorilla*, Hylobatidae, *Macaca*
	Ix/Iy	37.6	0.001	*Pan* – *Gorilla*, *Pongo*, *Macaca* *Gorilla* – *Pan*, *Pongo*, Hylobatidae, *Macaca* *Pongo* – *Pan*, *Gorilla*, Hylobatidae, *Macaca*
Infant – 50% length	*Imax/Imin*	10.5	0.001	*Pan* – *Gorilla*, *Pongo*, *Macaca* Hylobatidae – *Gorilla*, *Pongo*
	Ix/Iy	11.7	0.001	*Gorilla* – *Pan*, Hylobatidae, *Macaca*
Infant – 80% Length	*Imax/Imin*	9.1	0.001	*Macaca* – *Pan*, *Gorilla*, *Pongo* *Pongo* – Hylobatidae
	Ix/Iy	14.4	0.001	*Macaca* – *Pan*, *Gorilla*, *Pongo* *Gorilla* – Hylobatidae *Pongo* – Hylobatidae
Juvenile – 20% Length	*Imax/Imin*	89.5	0.001	*Gorilla* – *Pan*, *Pongo*, Hylobatidae, *Macaca* *Pongo* – *Pan*, *Gorilla*, Hylobatidae, *Macaca* *Macaca* – *Pan*, *Gorilla*, *Pongo*, Hylobatidae
	Ix/Iy	77.6	0.001	*Gorilla* – *Pan*, *Pongo*, Hylobatidae, *Macaca* *Pongo* – *Pan*, *Gorilla*, Hylobatidae, *Macaca* *Macaca* – *Pan*, *Gorilla*, *Pongo*, Hylobatidae
Juvenile – 50% Length	*Imax/Imin*	27.6	0.001	*Gorilla* – *Pan*, *Pongo*, Hylobatidae, *Macaca* *Pongo* – *Pan*, *Gorilla*, Hylobatidae, *Macaca*
	Ix/Iy	25.7	0.001	*Gorilla* – *Pan*, *Pongo*, Hylobatidae, *Macaca* *Pongo* – *Pan*, *Gorilla*, Hylobatidae, *Macaca*
Juvenile – 80% length	*Imax/Imin*	14.9	0.001	*Pongo* – *Pan*, Hylobatidae, *Macaca* *Macaca* – *Pan*, *Gorilla*, *Pongo*
	Ix/Iy	25.8	0.001	*Gorilla* – *Pan*, Hylobatidae, *Macaca* *Pongo* – *Pan*, Hylobatidae, *Macaca* Hylobatidae – *Macaca*
Adult – 20% length	*Imax/Imin*	66.2	0.001	*Pan* – *Gorilla*, *Pongo*, Hylobatidae, *Macaca* *Gorilla* – *Pan*, *Pongo*, Hylobatidae, *Macaca* *Pongo* – *Pan*, *Gorilla*, Hylobatidae, *Macaca*
	Ix/Iy	98.7	0.001	*Pan* – *Gorilla*, *Pongo*, Hylobatidae, *Macaca* *Gorilla* – *Pan*, *Pongo*, Hylobatidae, *Macaca* *Pongo* – *Pan*, *Gorilla*, Hylobatidae, *Macaca*
Adult – 50% length	*Imax/Imin*	49.6	0.001	*Pan* – *Gorilla*, *Pongo*, Hylobatidae, *Macaca* *Gorilla* – *Pan*, *Pongo*, Hylobatidae, *Macaca* *Pongo* – *Pan*, *Gorilla*, Hylobatidae, *Macaca*
	Ix/Iy	79.4	0.001	*Pan* – *Gorilla*, *Pongo*, Hylobatidae, *Macaca* Hylobatidae – *Gorilla*, *Pongo*, *Macaca* *Macaca* – *Pan*, *Gorilla*, *Pongo*, Hylobatidae
Adult – 80% length	*Imax/Imin*	11.1	0.001	*Gorilla* – Hylobatidae, *Macaca* *Pongo* – Hylobatidae, *Macaca*
	Ix/Iy	5	0.001	*Macaca* – *Gorilla*, *Pongo*

The infant tibial midshaft was relatively circular among the five taxa compared to their juvenile and adult counterparts, though more bone was distributed in the AP than ML axis at all three stages of development. Both infant chimpanzees and gorillas displayed identical I_{max}/I_{min} ratios at midshaft, while the orangutan and hylobatid samples displayed more circular midshafts (Table 3.7a). Infant macaques displayed the greatest deviation from circularity at midshaft, exhibiting significantly more elliptical sections than both chimpanzees and orangutans (Table 3.8). Similarly, the proximal tibia was AP elliptical among all five taxa. In fact, the African apes displayed similar I_{max}/I_{min} ratios proximally as they did at midshaft, despite differing significantly from one another about the anatomical axes. The distal tibia was the only section along the diaphysis where more bone was distributed distally in the ML than AP plane, resulting in I_x/I_y scores below 1.0, among all infant taxa. Descriptive statistics of the juvenile tibia are given in Table 3.7b. The juvenile mid-tibia exhibited a greater departure from circularity among chimpanzees, gorillas and hylobatids compared to their infant subgroups (while significance was approached in macaques: $P < 0.06$). Further, bone was disproportionately distributed along the AP axis at midshaft and proximal sections. The juvenile hylobatid group displayed the greatest shape change between infancy and juvenility as well, displaying the most elliptical midshaft and proximal sections compared to all other taxa. Like the infant sample, the juvenile distal tibia displayed a contrasting pattern compared to the midshaft and proximal section, where more bone was placed in the ML than AP plane. The juvenile great apes in particular displayed more ML reinforcement while the smaller hylobatids and macaques revealed virtually circular distal tibial sections.

The adult mid- and proximal tibia exhibited the greatest departure from circularity of any other ontogenetic group, indicating an incrementally more elliptical (AP distribution) shape with development, irrespective of taxon (Table 3.7c). At midshaft, hylobatid shape was found to be significantly more elliptical than all other taxa apart from the chimpanzees, while the adult orangutan group displayed the most circular midshafts of all taxa about the principal axes. The distal tibia once again exhibited greater bone distribution in the ML plane among the larger-bodied great apes, while hylobatids and macaques displayed relatively circular distal tibiae.

TABLE 3.7a. Infant Tibia Circularity: Mean, Standard Deviation and Coefficient of Variation

	20% Length		50% Length		80% Length	
Taxon (*n*)	I_{max}/I_{min}	CV%	I_{max}/I_{min}	CV%	I_{max}/I_{min}	CV%
Pan (16)	1.38 ± 0.16	12.1	1.35 ± 0.17	12.5	2.03 ± 0.19	9.7
Gorilla (14)	1.83 ± 0.23	12.5	1.35 ± 0.11	8.2	2.06 ± 0.23	11.5
Pongo (14)	1.89 ± 0.38	20.5	1.26 ± 0.16	13.1	1.39 ± 0.18	13.3
Hylobatidae (16)	1.22 ± 0.15	12.7	1.31 ± 0.12	9.5	1.84 ± 0.28	15.4
Macaca (16)	1.23 ± 0.11	9.3	1.41 ± 0.17	12.6	1.92 ± 0.25	13.4
Taxon (*n*)	I_x/I_y	CV%	I_x/I_y	CV%	I_x/I_y	CV%
Pan (16)	0.74 ± 0.09	13.1	1.17 ± 0.15	13.4	1.61 ± 0.23	14.3
Gorilla (14)	0.6 ± 0.1	17	1.06 ± 0.11	11.1	1.21 ± 0.27	22.4
Pongo (14)	0.6 ± 0.13	23.1	1.04 ± 0.17	16.3	1.31 ± 0.25	19.3
Hylobatidae (16)	0.91 ± 0.15	17.1	1.23 ± 0.16	13.3	1.73 ± 0.35	20.5
Macaca (16)	0.86 ± 0.07	8.6	1.35 ± 0.18	13.3	1.88 ± 0.25	13.6

TABLE 3.7b. Juvenile Tibia Circularity: Mean, Standard Deviation and Coefficient of Variation

	20% Length		50% Length		80% Length	
Taxon (*n*)	I_{max}/I_{min}	CV%	I_{max}/I_{min}	CV%	I_{max}/I_{min}	CV%
Pan (16)	1.4 ± 0.17	12.5	1.79 ± 0.26	14.5	2.19 ± 0.31	14.2
Gorilla (13)	1.74 ± 0.3	17.6	1.65 ± 0.19	11.5	2.19 ± 0.22	10.1
Pongo (17)	1.84 ± 0.28	15.4	1.34 ± 0.2	15.3	1.45 ± 0.22	15.7
Hylobatidae (18)	1.26 ± 0.15	12.5	2.0 ± 0.28	14	2.52 ± 0.51	20.2
Macaca (17)	1.17 ± 0.09	8.2	1.59 ± 0.18	11.6	2.35 ± 0.36	15.7
Taxon (*n*)	I_x/I_y	CV%	I_x/I_y	CV%	I_x/I_y	CV%
Pan (16)	0.78 ± 0.1	13.4	1.5 ± 0.24	16.4	1.48 ± 0.39	26.6
Gorilla (13)	0.66 ± 0.16	24.6	1.22 ± 0.18	15	0.88 ± 0.16	18.4
Pongo (17)	0.6 ± 0.12	19.9	1.26 ± 0.24	19.2	1.26 ± 0.27	21.9
Hylobatidae (18)	1.04 ± 0.16	15.7	1.86 ± 0.28	15.5	2.36 ± 0.51	21.8
Macaca (17)	0.96 ± 0.1	11.2	1.55 ± 0.17	11.2	2.21 ± 0.33	15.1

TABLE 3.7c. Adult Tibia Circularity: Mean, Standard Deviation and Coefficient of Variation

	20% Length		50% Length		80% Length	
Taxon (*n*)	I_{max}/I_{min}	CV%	I_{max}/I_{min}	CV%	I_{max}/I_{min}	CV%
Pan (20)	1.35 ± 0.18	13.6	2.27 ± 0.47	20.7	2.48 ± 0.44	18
Gorilla (23)	1.81 ± 0.29	16.2	1.96 ± 0.3	15.6	2.61 ± 0.34	13.1
Pongo (23)	1.67 ± 0.29	17.7	1.73 ± 0.22	12.7	1.85 ± 0.26	14.1
Hylobatidae (21)	1.08 ± 0.29	26.9	2.43 ± 0.56	23.2	2.87 ± 0.56	19.5
Macaca (21)	1.21 ± 0.15	13.1	1.91 ± 0.25	13.3	2.6 ± 0.44	17
Taxon (*n*)	I_x/I_y	CV%	I_x/I_y	CV%	I_x/I_y	CV%
Pan (20)	0.8 ± 0.11	14.2	1.99 ± 0.34	17.1	1.67 ± 0.26	16.1
Gorilla (23)	0.64 ± 0.11	17.6	1.51 ± 0.21	14.3	1.24 ± 0.15	12.7
Pongo (23)	0.7 ± 0.12	17.2	1.67 ± 0.24	14.4	1.6 ± 0.28	17.5
Hylobatidae (21)	1.08 ± 0.29	26.9	2.16 ± 0.4	18.6	2.57 ± 0.58	22.8
Macaca (21)	1.01 ± 0.13	13.7	1.86 ± 0.28	15.2	2.48 ± 0.41	16.8

TABLE 3.8. Interspecific ANOVA comparisons along the tibia

Diaphyseal Location by Development	**Area Ratio**	***F***	***P***	**Significantly different shape groupings (*Post hoc* – Tukey HSD or Games-Howell)**
Infant – 20% length	*Imax/Imin*	31.1	0.001	*Pan* – *Gorilla, Pongo, Macaca* *Gorilla* – *Pan*, Hylobatidae, *Macaca* *Pongo* – *Pan*, Hylobatidae, *Macaca*
	Ix/Iy	22.6	0.001	*Pan* – *Gorilla, Pongo*, Hylobatidae Hylobatidae – *Pan, Gorilla, Pongo* *Macaca* – *Gorilla, Pongo*
Infant – 50% length	*Imax/Imin*	-	0.106	*Gorilla* – *Pongo*
	Ix/Iy	9.8	0.001	*Macaca* – *Pan, Gorilla, Pongo* Hylobatidae – *Gorilla, Pongo*
Infant – 80% Length	*Imax/Imin*	18.4	0.001	*Pongo* – *Pan, Gorilla*, Hylobatidae, *Macaca*
	Ix/Iy	15.8	0.001	*Gorilla* – *Pan*, Hylobatidae, *Macaca* *Pongo* – *Pan*, Hylobatidae, *Macaca*
Juvenile – 20% Length	*Imax/Imin*	35	0.001	*Pan* – *Macaca* *Gorilla* – *Pan*, Hylobatidae, *Macaca* *Pongo* – *Pan*, Hylobatidae, *Macaca*
	Ix/Iy	37	0.001	*Pan* – *Pongo*, Hylobatidae, *Macaca* *Gorilla* – Hylobatidae, *Macaca* *Pongo* – Hylobatidae, *Macaca*
Juvenile – 50% Length	*Imax/Imin*	21.9	0.001	*Pongo* – *Pan, Gorilla*, Hylobatidae, *Macaca* Hylobatidae – *Gorilla, Pongo, Macaca*
	Ix/Iy	21.6	0.001	Hylobatidae – *Pan, Gorilla, Pongo, Macaca* *Gorilla* – *Pan, Macaca* *Pongo* – *Macaca*
Juvenile – 80% length	*Imax/Imin*	25.7	0.001	*Pongo* – *Pan, Gorilla*, Hylobatidae, *Macaca*
	Ix/Iy	49.9	0.001	*Pan* – *Gorilla*, Hylobatidae, *Macaca* *Gorilla* – *Pan, Pongo*, Hylobatidae, *Macaca* *Pongo* – *Gorilla*, Hylobatidae, *Macaca*
Adult – 20% length	*Imax/Imin*	20	0.001	*Pan* – *Gorilla, Pongo* Hylobatidae – *Gorilla, Pongo, Macaca* *Macaca* – *Gorilla, Pongo, Macaca*
	Ix/Iy	28.9	0.001	*Gorilla* – *Pan*, Hylobatidae, *Macaca* *Pongo* – Hylobatidae, *Macaca*
Adult – 50% length	*Imax/Imin*	12.8	0.001	*Pan* – *Pongo, Macaca* *Gorilla* – *Pongo*, Hylobatidae Hylobatidae – *Gorilla, Pongo, Macaca*
	Ix/Iy	16.7	0.001	Hylobatidae – *Gorilla, Pongo, Macaca* *Gorilla* – *Pan*, Hylobatidae, *Macaca* *Pan* – *Gorilla, Pongo*
Adult – 80% length	*Imax/Imin*	20.5	0.001	*Pongo* – *Pan, Gorilla*, Hylobatidae, *Macaca* *Pan* – Hylobatidae
	Ix/Iy	54.4	0.001	*Pan* – *Gorilla*, Hylobatidae, *Macaca* *Gorilla* – *Pan, Pongo*, Hylobatidae, *Macaca* *Pongo* – *Gorilla*, Hylobatidae, *Macaca*

TABLE 3.9a. Predictions for *Pan* developmental shape variation by long bone element and cross-section site.

Element	Section	Predicted shape change	Rationale	Prediction met?	Observation
Humerus	Distal	Shape will remain elliptical, with distribution in the ML across development.	The distal humerus is exposed to less bending and more compression strain compared to midshaft. Thus, it should scale with general isometry to accommodate increased size rather than conform its shape to bending loads[1].	Yes	The distal humerus was elliptical (ML) in each subgroup, no significant differences were identified between any stage of development.
	Midshaft	Increased distribution in the ML plane between infant and adult subgroups.	The humeral midshaft experiences peak bending loads during locomotion[2]. As chimpanzees transition from a more arboreal to terrestrial posture, it should be reflected at midshaft.	No	The section was circular in each subgroup, no significant differences were identified between any stage of development.
	Proximal	Shape will remain relatively circular across development subgroups.	The proximal humerus is exposed to less bending compared to midshaft[1]. Proximity to the glenohumeral socket joint should grant more mobility than the distal section, however, resulting in a more circular shape[3].	No	While developmental group shape varied, the section was more circular among adult males and females compared to infants.
Ulna	Distal	Shape will remain relatively circular between developmental groups.	Proximity to the radioulnar articulation grants the wrist multi-directional rotation, and thus, equal bone distribution to accommodate movement, irrespective of locomotor profile[4].	Yes	The section was circular in each subgroup, no significant differences were identified at any stage of development.
	Midshaft	More elliptical distribution in the AP as gait changes to more terrestrial posture.	While it should be more constrained than the humerus[5], the ulnar midshaft should experience peak bending along the diaphysis and conform to the knuckle-walking and suspensory bending loads placed on it[2].	No	The section was circular in each subgroup, no significant differences in shape were identified at any stage of development.
	Proximal	Shape will remain elliptical (AP) across development.	Proximity to the elbow joint inhibits bending loads compared to midshaft. Further, the elbow is a hinge joint, limiting variable bending loads[6].	Somewhat	The section was elliptical (AP) from infancy but became significantly more elliptical with development.
Femur	Distal	Shape will remain elliptical, with distribution in the ML across development.	The distal femur should experience less bending and greater compression/tension during locomotion[1]. Thus, it is expected to scale with general isometry to accommodate an individual's size rather than conform its shape to bending loads.	Yes	The section was elliptical (ML) in each group. No significant differences in shape were identified at any stage of development.
	Midshaft	More elliptical distribution in the ML	The femoral midshaft experiences peak bending loads during locomotion[2]. Further, bending loads should vary	Yes	Each developmental group incrementally revealed a more elliptical cross-sectional

	Midshaft	plane between infant and adult groups.	between development, as chimpanzees transition to a hindlimb dominant posture by juvenility[8].		shape between infancy and adulthood, though infant shape was relatively circular.
	Proximal	Elliptical shape with distribution in the ML plane across development.	The proximal femur should have more mobility than the distal section due to its proximity to the hip[7]. It should also experience less bending compared to the midshaft.	No	Shape was more elliptical (ML) among adult males compared to infants and juveniles. Adult females were more circular than males but not sub-adults.
Tibia	Distal	Elliptical shape, with distribution in the ML plane across development.	Distal tibial shape is constrained by safety factors and its proximity to the ankle[9]. Further, bending loads should not be as great distally compared to at midshaft[1].	Yes	The section was elliptical (ML) in each group, no significant differences were identified at any stage of development.
	Midshaft	More elliptical distribution in the AP plane as gait transitions to more terrestrial posture.	The transition to hindlimb-dominant terrestrial locomotion should influence bending loads at midshaft[8], influencing section shape. Further, the midshaft experiences peak bending loads along the diaphysis[2].	Yes	Shape was significantly more elliptical (AP) in all groups compared to the relatively circular infants. Adult male and female shape did not differ.
	Proximal	Elliptical shape, with distribution in the AP plane across development.	Proximal tibial bending should be constrained by its proximity to the adjacent knee joint[1]. Thus, shape should scale relatively isometrically through development.	Somewhat	Shape was significantly more elliptical (AP) among adult males compared to infants but juveniles and adult females overlapped with infants.

[1] Ruff and Runestad, 1992; Currey, 1984, 2002.
[2] Biewener and Taylor, 1986.
[3] Larson, 2015.
[4] Sarmineto, 1988.
[5] Lieberman et al., 2003.
[6] Rose, 1988.
[7] San Millán et al., 2015.
[8] Kimura et al., 1979; Demes et al., 1994.
[9] Currey and Alexander, 1985; Skedros et al., 2003; Nadell and Shaw, 2016.

TABLE 3.9b. Predictions for *Gorilla* developmental shape variation by long bone element and cross-section site.

Element	Section	Predicted shape change	Rationale	Prediction met?	Observation
Humerus	Distal	Shape will remain elliptical, with distribution in the ML across development.	The distal humerus is exposed to less bending but more compression compared to midshaft. Thus, it should scale with general isometry to accommodate increased size rather than conform its shape to bending loads[1].	Yes	The distal humerus was elliptical (ML) in each developmental subgroup.
	Midshaft	Increasing elliptical distribution in the ML plane between infant and adult groups.	The humeral midshaft experiences peak bending loads during locomotion[2]. As gorillas transition from a more arboreal to terrestrial posture, it should be reflected at midshaft.	Yes	In response to greater bending loads, more bone was distributed in the (ML) plane of adult males, but not females, compared to the infant group.
	Proximal	Shape will remain relatively circular across development groups.	The proximal humerus is exposed to less bending compared to midshaft. Proximity to the glenohumeral socket joint should grant more mobility than the distal section, however, resulting in a more circular shape[3].	No	While developmental group shape varied, the section was more circular among adult males and females compared to infants and juveniles.
Ulna	Distal	Shape will remain relatively circular between developmental groups.	Proximity to the radioulnar articulation grants the wrist multi-directional rotation, and thus, equal bone distribution to accommodate bending loads, irrespective of locomotor profile[4].	Yes	The section was circular in each subgroup, no significant differences were identified at any stage of development.
	Midshaft	More elliptical distribution in the AP as gait changes to more terrestrial posture.	While it should be more constrained than the humerus[5], the ulnar midshaft should experience peak bending along the diaphysis[2].	No	Shape did vary significantly but was more circular among juveniles and adult males and females, rather than elliptical.
	Proximal	Shape will remain elliptical across development.	Proximity to the elbow joint inhibits bending loads compared to midshaft. Further, the elbow is a hinge joint, limiting variable bending loads[6].	Yes	The section was elliptical (ML) in each group, no significant differences were identified at any stage of development.
Femur	Distal	Shape will remain elliptical, with distribution in the ML across development.	The distal femur experiences less bending and greater compression. Thus, it should scale with general isometry to accommodate size rather than conform its shape to bending loads[1].	Yes	The section was elliptical (ML) in each group. No significant differences were identified at any stage of development.
	Midshaft	More elliptical distribution in the ML plane between infant and adult groups.	The femoral midshaft experiences peak bending loads during locomotion[2]. Further, bending loads should change with development, as gorillas transition to a hindlimb dominant posture by juvenility[8].	Yes	Each developmental group incrementally revealed a more elliptical cross-sectional shape between infancy and adulthood.

	Proximal	Elliptical shape with distribution in the ML across development.	The proximal femur should have more mobility than the distal section due to its proximity to the hip[7]. It should also experience less bending compared to the midshaft[1].	No	Shape was more elliptical (ML) among adult males and more circular in females, compared to infants and juveniles.
Tibia	Distal	Elliptical shape, with distribution in the ML plane across development.	Distal tibial shape is constrained by safety factors and its proximity to the ankle[9]. Further, bending loads are not as great distally compared to at midshaft[1].	Yes	The section was elliptical (ML) in each group, no significant differences in shape were identified at any stage of development.
	Midshaft	More elliptical distribution in the AP plane as gait changes to more terrestrial posture.	The transition to hindlimb-dominant locomotion should influence bending loads at midshaft, dictating section shape[8]. Further, the midshaft should experience peak bending loads along the diaphysis[2].	Yes	Shape was significantly more elliptical (AP) in all groups compared to the relatively circular infants.
	Proximal	Elliptical shape, with distribution in the AP plane across development.	Proximal tibial bending should be constrained by its proximity to the adjacent knee joint[1]. Thus, shape should be relatively static through development.	No	Shape was significantly more elliptical among adult males and females compared to infants.

[1] Ruff and Runestad, 1992; Currey, 1984, 2002.
[2] Biewener and Taylor, 1986.
[3] Larson, 2015.
[4] Sarmineto, 1988.
[5] Lieberman et al., 2003.
[6] Rose, 1988.
[7] San Millán et al., 2015.
[8] Kimura et al., 1979; Demes et al., 1994.
[9] Currey and Alexander, 1985; Skedros et al., 2003; Nadell and Shaw, 2016.

TABLE 3.9c. Predictions for *Pongo* developmental shape variation by long bone element and cross-section site.

Element	Section	Predicted shape change	Rationale	Prediction met?	Observation
Humerus	Distal	Shape will remain elliptical, with distribution in the ML across development.	The distal humerus is exposed to less bending and more compression compared to the midshaft. Thus, it should scale with general isometry to accommodate increased size rather than conform its shape to bending loads[1].	Yes	The section was elliptical (ML) in each subgroup, no significant developmental differences were identified at any stage of development.
	Midshaft	Circularity will increase incrementally or remain circular across developmental subgroups.	The humeral midshaft experiences peak bending loads. Infant orangutans exhibit circular humeral midshafts which should become more circular or maintain their shape as they load their bones in multiple planes in the canopy[10].	Yes	The midshaft section was circular in each group across development. No significant differences were identified between any developmental subgroups.
	Proximal	Shape will remain relatively circular across development groups.	The proximal humerus is exposed to less bending compared to midshaft. Proximity to the glenohumeral socket joint should grant more mobility than the distal section, however, resulting in a more circular shape[3].	No	Unlike the midshaft, the proximal section was significantly more circular among adult males and females compared to infants.
Ulna	Distal	Shape will remain relatively circular between developmental groups.	Proximity to the radioulnar articulation grants the wrist multi-directional rotation[6], and thus, equal bone distribution to accommodate bending loads, irrespective of locomotor profile or developmental stage[4].	Yes	The midshaft section was circular in each group across development. No significant differences were identified between any developmental subgroups.
	Midshaft	More circular bone distribution after locomotor independence is achieved.	The ulnar midshaft should experience peak bending along the diaphysis and conform its shape to the multidirectional bending loads placed on it through suspensory behaviour[2].	No	The ulnar midshaft was elliptical (AP) in each developmental subgroup. Infants did not exhibit more AP plane distribution compared to juveniles and adults, however.
	Proximal	Shape will remain elliptical (AP) across development.	Proximity to the elbow joint inhibits bending loads compared to midshaft. Further, the elbow is a hinge joint, limiting variable bending loads[6].	Yes	The section was elliptical (AP) in each developmental subgroup, including adult males and females.
Femur	Distal	Shape will remain elliptical, with distribution in the ML across development.	The distal femur experiences less bending and greater compression during locomotion[1]. Thus, it should scale with general isometry to accommodate an individual's size rather than conform its shape to bending loads.	Yes	The section was elliptical (ML) in each developmental subgroup.
	Midshaft	Circularity will increase incrementally or remain	The femoral midshaft experiences peak bending during locomotion[2]. Further, multidirectional bending loads	No	Each developmental group incrementally revealed a more elliptical (ML) cross-

	Midshaft	circular across development.	during suspensory locomotion should distribute bone relatively evenly at the midshaft[10].		sectional shape over development. Infant and juvenile midshaft shape was circular.
	Proximal	Elliptical shape with distribution in the ML plane across development.	The proximal femur should provide greater mobility than the distal section due to its proximity to the hip, especially under multidirectional suspensory loading[7,10]. It should also experience less bending compared to the midshaft[1].	Yes	Shape was more elliptical (ML) among adult males and females compared to infants.
Tibia	Distal	Elliptical shape, with distribution in the ML plane across development.	Bending loads are not as great at the distal tibia compared to midshaft[1]. Further, distal tibial structure is constrained by tissue economy and safety factors near the ankle[9].	Somewhat	The distal tibia was elliptical (ML) in each group, though adult females exhibited significantly more circular sections compared to infants.
	Midshaft	More elliptical distribution in the AP over the course of development.	Because the knee-joint acts as a hinge, bending at the midshaft should be relatively uniform in the AP plane. The transition to hindlimb-dominant suspensory locomotion should further influence shape at midshaft as subadults achieve locomotor independence[8].	Yes	Shape was significantly more elliptical (AP) in all groups compared to the relatively circular infants. Adult male and female shape did not differ.
	Proximal	Elliptical shape, with distribution in the AP plane across development.	Proximal tibial bending should be constrained by its proximity to the adjacent knee joint. Thus, shape should be relatively static through development[1].	Somewhat	Shape was significantly more elliptical (AP) among adult males and females compared to the more circular infant and juvenile proximal shape.

[1] Ruff and Runestad, 1992; Currey, 1984, 2002.
[2] Biewener and Taylor, 1986.
[3] Larson, 2015.
[4] Sarmineto, 1988.
[5] Lieberman et al., 2003.
[6] Rose, 1988.
[7] San Millán et al., 2015.
[8] Kimura et al., 1979; Demes et al., 1994.
[9] Currey and Alexander, 1985; Skedros et al., 2003; Nadell and Shaw, 2016.
[10] Swartz et al., 1989; Patel et al., 2013.

TABLE 3.9d. Predictions for Hylobatidae developmental shape variation by long bone element and cross-section site.

Element	Section	Predicted shape change	Rationale	Prediction met?	Observation
Humerus	Distal	Shape will remain relatively circular across developmental subgroups.	The distal humerus is exposed to less bending but more compression compared to midshaft. Brachiation should place variable strain along the humerus compared to other locomotor patterns, reinforcing the section in multiple planes[1].	Yes	The distal humerus was circular with no significant differences identified among the developmental subgroups. Adults distributed more bone in the ML compared to juveniles but not infants.
	Midshaft	Circularity will increase incrementally or remain circular across developmental subgroups.	The humeral midshaft experiences peak bending loads[2]. Infant gibbons and siamangs exhibit circular humeral midshafts which should maintain their shape to mitigate bending in multiple planes during brachiation and suspensory locomotion[9].	Yes	The midshaft section was circular in each group across development. Adult midshafts were significantly more circular than infants but not juveniles.
	Proximal	Shape will remain relatively circular across development groups.	The proximal humerus is exposed to less bending compared to midshaft allowing for a more static shape regardless of bending regime[1]. Proximity to the glenohumeral joint grants more rotational mobility than the elbow, yielding a circular shape[3].	Yes	The proximal humerus was circular across all developmental subgroups. Tissue distribution in the anatomical planes did not differ between subgroups either.
Ulna	Distal	Shape will remain relatively circular between developmental groups.	Proximity to the radioulnar articulation grants the wrist multi-directional rotation[4], and thus, equal bone distribution to accommodate bending loads, irrespective of locomotor profile or developmental stage.	Yes	The midshaft section was circular in each subgroup across development. Juveniles and adults reinforced the AP and ML planes more evenly than infants.
	Midshaft	Incrementally more circular bone distribution across developmental subgroups.	The hylobatid ulna should not experience the same bending loads as other taxa during brachiation[9]. Shape change should not be as exaggerated compared to the humerus[5].	Yes	The ulnar midshaft was elliptical (AP), not circular, among each developmental subgroup.
	Proximal	Shape will remain elliptical (AP) across development.	Proximity to the elbow joint inhibits bending loads compared to the midshaft[2]. Further, the elbow is a hinge joint, limiting variable bending loads[1].	Yes	The section was elliptical (AP) in each developmental subgroup.
Femur	Distal	Shape will remain elliptical, with distribution in the ML plane across development	The distal femur experiences less bending and greater compression during locomotion[1]. Thus, it should scale with general isometry to accommodate an individual's size rather than conform its shape to bending loads.	No	The section was elliptical (ML) in each developmental subgroup but was more circular among adults compared to infants and juveniles.

Femur	Midshaft	Circularity will increase incrementally or remain circular across development.	The femoral midshaft experiences peak bending during locomotion[2]. Further, multidirectional bending loads during suspensory locomotion should distribute bone relatively evenly at the midshaft[9].	Yes	Each developmental subgroup revealed a circular shape at midshaft.
	Proximal	Elliptical shape with distribution in the ML plane across development.	The proximal femur should be more mobile than the distal section due to its proximity to the hip, especially under multidirectional suspensory loading[7,9]. It should also experience less bending compared to the midshaft.	No	Shape was more elliptical (ML) among adults compared to infants and juveniles.
Tibia	Distal	Elliptical shape, with distribution in the ML plane across development.	Bending loads are not as great at the distal tibia compared to midshaft[1]. Further, distal tibial structure is constrained by tissue economy and safety factors near the ankle[8].	Somewhat	The distal tibia was relatively circular in infants and juveniles while adults exhibited significantly more elliptical (between AP and ML) sections.
	Midshaft	More elliptical distribution in the AP over the course of development.	Because the knee-joint acts as a hinge, bending at the midshaft should be uniform in the AP plane[10]. Long-distance leaping and arboreal bipedal behaviour should influence midshaft shape.	Yes	Shape was significantly more elliptical (AP) in juveniles and adults compared to the relatively circular infants.
	Proximal	Elliptical shape, with distribution in the AP plane across development.	Proximal tibial bending should be constrained by its proximity to the adjacent knee joint[1]. As a hinge joint, mobility is limited to uniform loading in the AP. Thus, shape should be relatively static through development[10].	Yes	Shape was incrementally more elliptical (AP) among each developmental subgroup, with infants exhibiting the most circular sections and adults, most elliptical.

[1] Ruff and Runestad, 1992; Currey, 1984, 2002.
[2] Biewener and Taylor, 1986.
[3] Larson, 2015.
[4] Sarmineto, 1988.
[5] Lieberman et al., 2003.
[6] Rose, 1988.
[7] San Millán et al., 2015.
[8] Currey and Alexander, 1985; Skedros et al., 2003; Nadell and Shaw, 2016.
[9] Swartz et al., 1989; Patel et al., 2013.
[10] Demes et al., 2001.

TABLE 3.9e. Predictions for *Macaca* developmental shape variation by long bone element and cross-section site

Element	Section	Predicted shape change	Rationale	Prediction met?	Observation
Humerus	Distal	Shape will remain elliptical, with distribution in the ML across development.	The distal humerus is exposed to less bending but more compression compared to midshaft[1]. Thus, it should scale with general isometry to accommodate increased size rather than conform its shape to bending loads.	Yes	The distal humerus was elliptical (ML) in each developmental subgroup.
	Midshaft	More elliptical distribution in the ML plane across development.	The humeral midshaft experiences peak bending loads during locomotion[2]. Macaques achieve locomotor independence rapidly[11]. As they place greater strain on the midshaft from quadrupedal loading, shape should conform from circular to elliptical.	Yes	Midshaft shape was relatively circular among infants and juveniles and significantly elliptical (ML) among adult males and females.
	Proximal	Shape will remain relatively elliptical (ML) across development subgroups.	The proximal humerus is exposed to less bending compared to midshaft[1]. Unlike hominoids, shoulder mobility is relatively limited among catarrhines, yielding a less circular proximal shape[3]. However, macaques possess a proximal retroflexion which may obscure any adaptive signals.	Somewhat	Proximal humeral shape was elliptical (between AP and ML) among all developmental subgroups. However, it is difficult to determine whether this is more an adaptive effect or obstruction of the proximal humeral retroflexion.
Ulna	Distal	Shape will remain relatively circular between developmental groups.	Proximity to the radioulnar articulation grants the wrist multi-directional rotation[4], and thus, equal bone distribution to accommodate bending loads, irrespective of locomotor profile.	Yes	The section was relatively circular in each subgroup, no significant differences were identified at any stage of development.
	Midshaft	More elliptical distribution in the AP plane across development.	While it should be more constrained than the humerus[5], the ulnar midshaft should experience peak bending along the diaphysis and conform to the relatively uniform quadrupedal bending loads placed on it[2].	No	The section was elliptical (AP) in each subgroup, though no significant differences were identified between any stage of development.
	Proximal	Shape will remain elliptical (AP) across development.	Proximity to the elbow joint inhibits bending loads compared to midshaft combined with relatively uniform quadrupedal loading[1,2]. Further, the elbow is a hinge joint, limiting multi-directional loading patterns.	Yes	The section was elliptical (AP) across development.
Femur	Distal	Elliptical shape, with distribution in the ML plane across development.	The distal femur experiences less bending and greater compression during locomotion[1]. Thus, it should scale with general isometry to accommodate an individual's size rather than conform its shape to bending loads.	Yes	The distal femur was elliptical (ML) in each group. No significant differences were identified at any stage of development.

Femur	Midshaft	More elliptical distribution in the ML plane between infant and adult groups.	The femoral midshaft experiences peak bending during locomotion[2]. As body size increases and greater locomotor strain is applied to the midshaft from variable locomotor patterns and positions, its shape should conform[2,11].	No	The only change at femoral midshaft was identified between infants and adult males, where the adults exhibited significantly more circular midshafts.
	Proximal	Elliptical shape with distribution in the ML plane across development.	The proximal femur should grant greater mobility than the distal section due to its proximity to the hip[7]. It should also experience less bending compared to the midshaft[1,2].	Somewhat	Shape was circular across development apart from adult males, which exhibited relatively elliptical sections. However, no significant differences were identified.
Tibia	Distal	Elliptical shape, with distribution in the ML plane across development.	Distal tibial shape is constrained by safety factors and its proximity to the ankle[6]. Further, bending loads are not as great distally compared to midshaft[1].	No	The distal tibia was circular in each subgroup; no significant differences were identified at any stage of development. Adult males and females distributed bone more evenly about the anatomical axes.
	Midshaft	More elliptical distribution in the AP plane across development.	Uniform quadrupedal locomotion should influence shape at midshaft, particularly in the plane of bending (AP)[10]. Further, the midshaft experiences peak bending loads along the diaphysis[2].	Yes	Shape was significantly more elliptical (AP) among the relatively circular infants and juveniles compared to the adult males and females.
	Proximal	Elliptical shape, with distribution in the AP plane across development.	Proximal tibial bending should be constrained by its proximity to the adjacent knee joint, especially when placed under relatively uniform bending (AP)[10]. Thus, shape should be relatively static through development.	Somewhat	Shape was significantly more elliptical (AP) among juveniles and adults (pooled) compared to infants. Infants also displayed relatively elliptical proximal tibiae though.

[1] Ruff and Runestad, 1992; Currey, 1984, 2002.
[2] Biewener and Taylor, 1986.
[3] Hunt, 2016.
[4] Sarmineto, 1988.
[5] Lieberman et al., 2003.
[6] Rose, 1988.
[7] San Millán et al., 2015.
[8] Currey and Alexander, 1985; Skedros et al., 2003; Nadell and Shaw, 2016.
[9] Swartz et al., 1989; Patel et al., 2013.
[10] Demes et al., 2001.
[11] Wells and Turnquist, 2001.

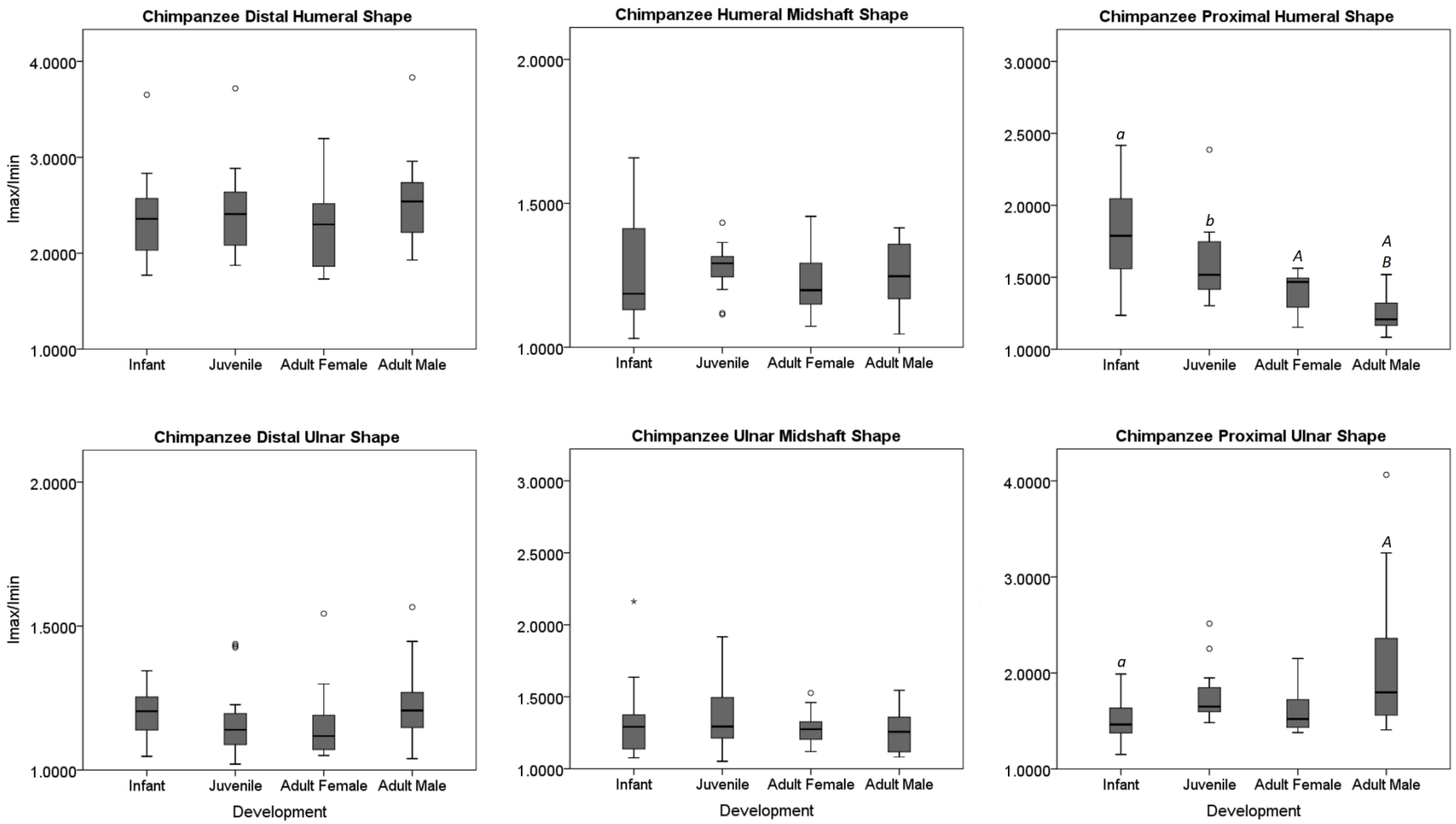

Fig. 3.2a. Box-and-whisker plot of chimpanzee forelimb circularity (I_{max}/I_{min}) variation over development. Rows depict limb elements (top, humerus; bottom, ulna) and columns depict scan section (left, distal; centre, midshaft; right, proximal). A ratio of 1.0 represents true circularity. Boxes represent 25th – 75th percentile range of a given developmental subgroup. Horizontal darkened lines indicate the median while whiskers extend to the maximum and minimum values within 1.5 box lengths. Outliers are denoted by an 'o' and extreme values, a star. Statistically significant between-group relationships are labelled with corresponding lower case and capital letters above their respective whisker bars.

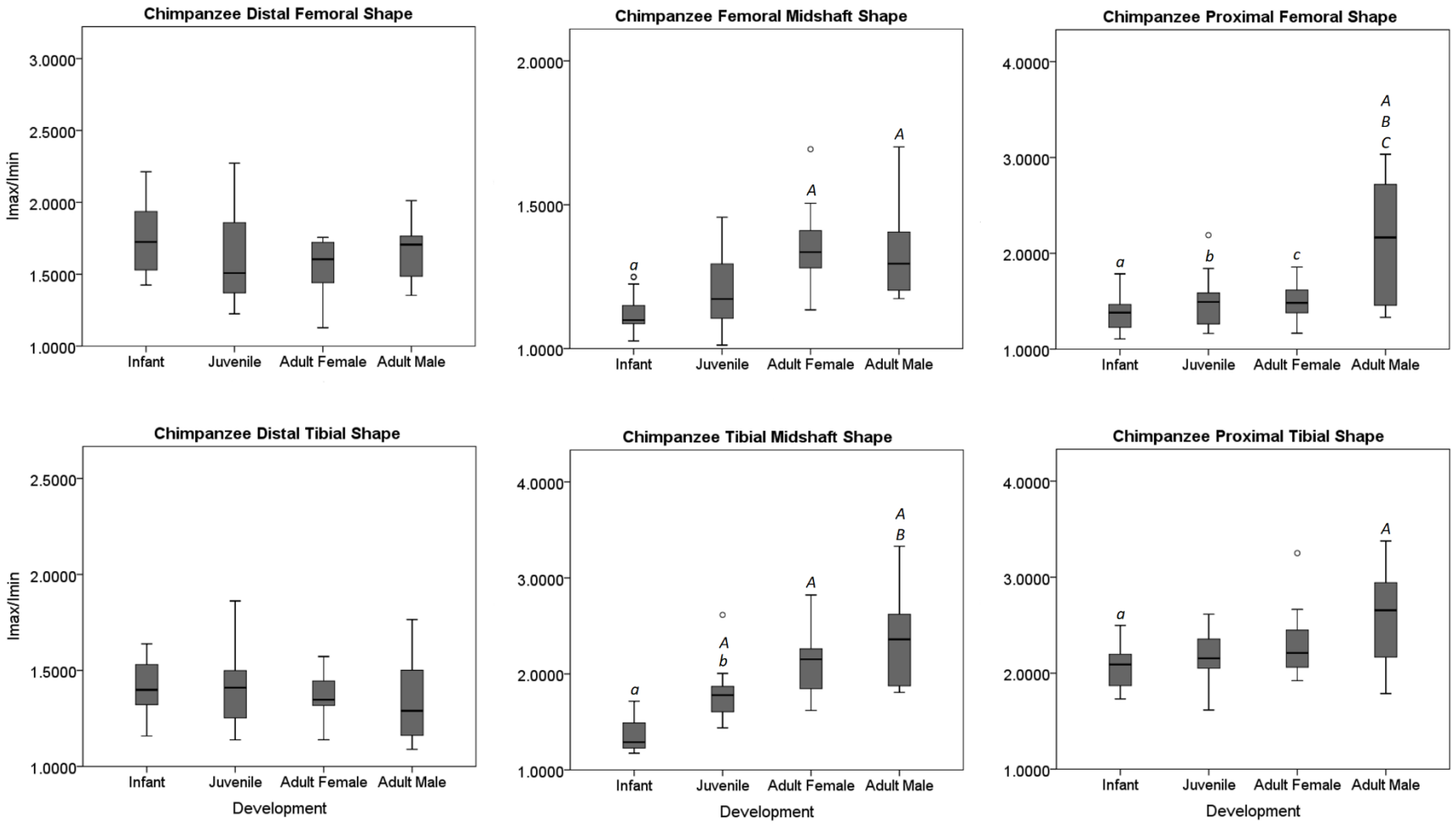

Fig. 3.2b. Box-and-whisker plot of chimpanzee hindlimb shape (I_{max}/I_{min}) variation over the course of development. Rows depict limb elements (top, femur; bottom, tibia) and columns depict scan section (left, distal; centre, midshaft; right, proximal). A ratio of 1.0 represents true circularity. Boxes represent 25th – 75th percentile range of developmental subgroups. Horizontal darkened lines indicate the median while whiskers extend to the maximum and minimum values within 1.5 box lengths. Outliers are denoted by an 'o' and extreme values, a star. Statistically significant between-group relationships are labelled with corresponding lower case and capital letters above their respective whisker bars.

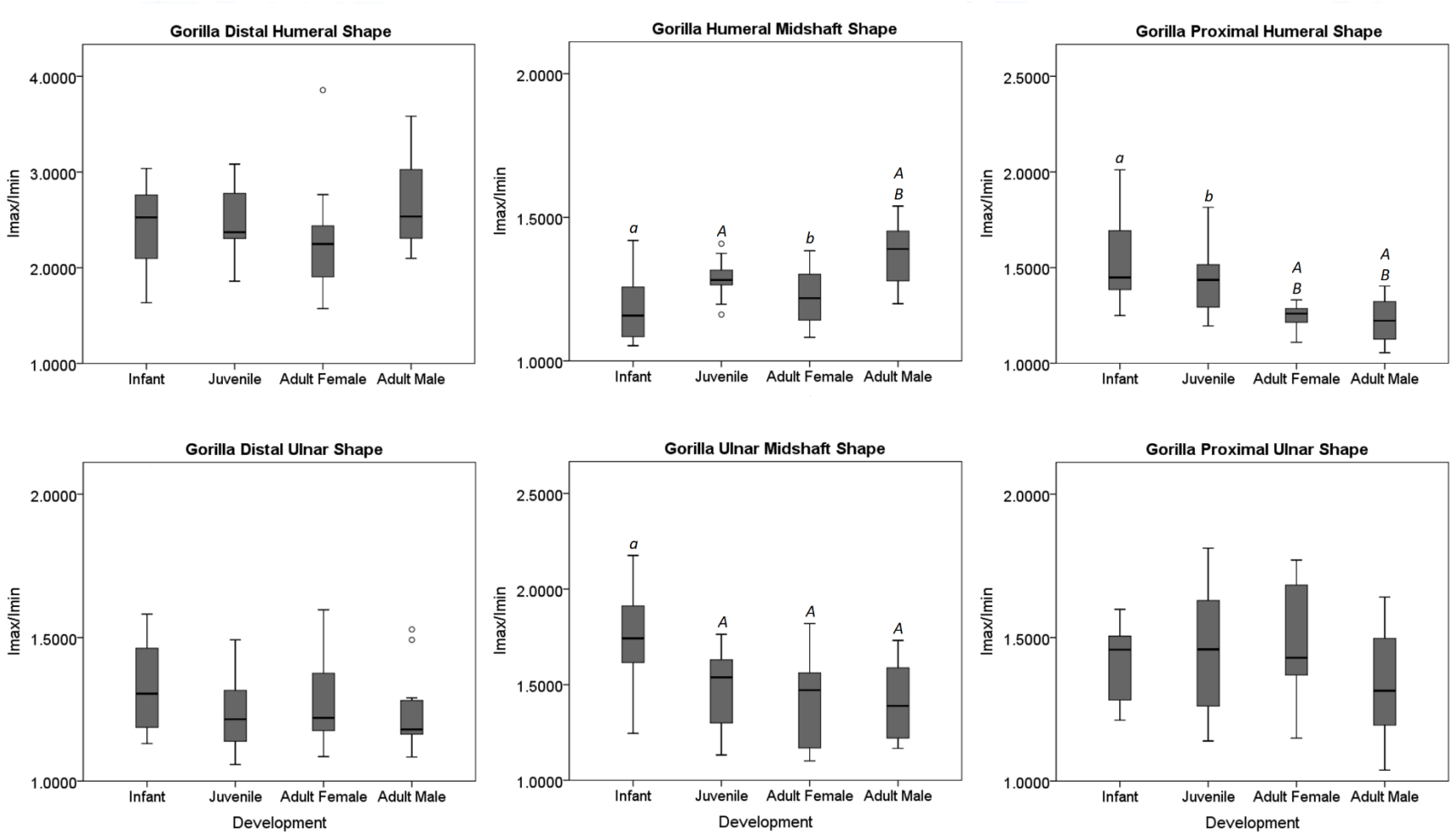

Fig. 3.2c. Box-and-whisker plot of gorilla forelimb shape (I_{max}/I_{min}) variation over the course of development. Rows depict limb elements (top, humerus; bottom, ulna) and columns depict scan section (left, distal; centre, midshaft; right, proximal). A ratio of 1.0 represents true circularity. Boxes represent 25th – 75th percentile range of a given developmental subgroup. Horizontal darkened lines indicate the median while whiskers extend to the maximum and minimum values within 1.5 box lengths. Outliers are denoted by an 'o' and extreme values, a star. Statistically significant between-group relationships are labelled with corresponding lower case and capital letters above their respective whisker bars.

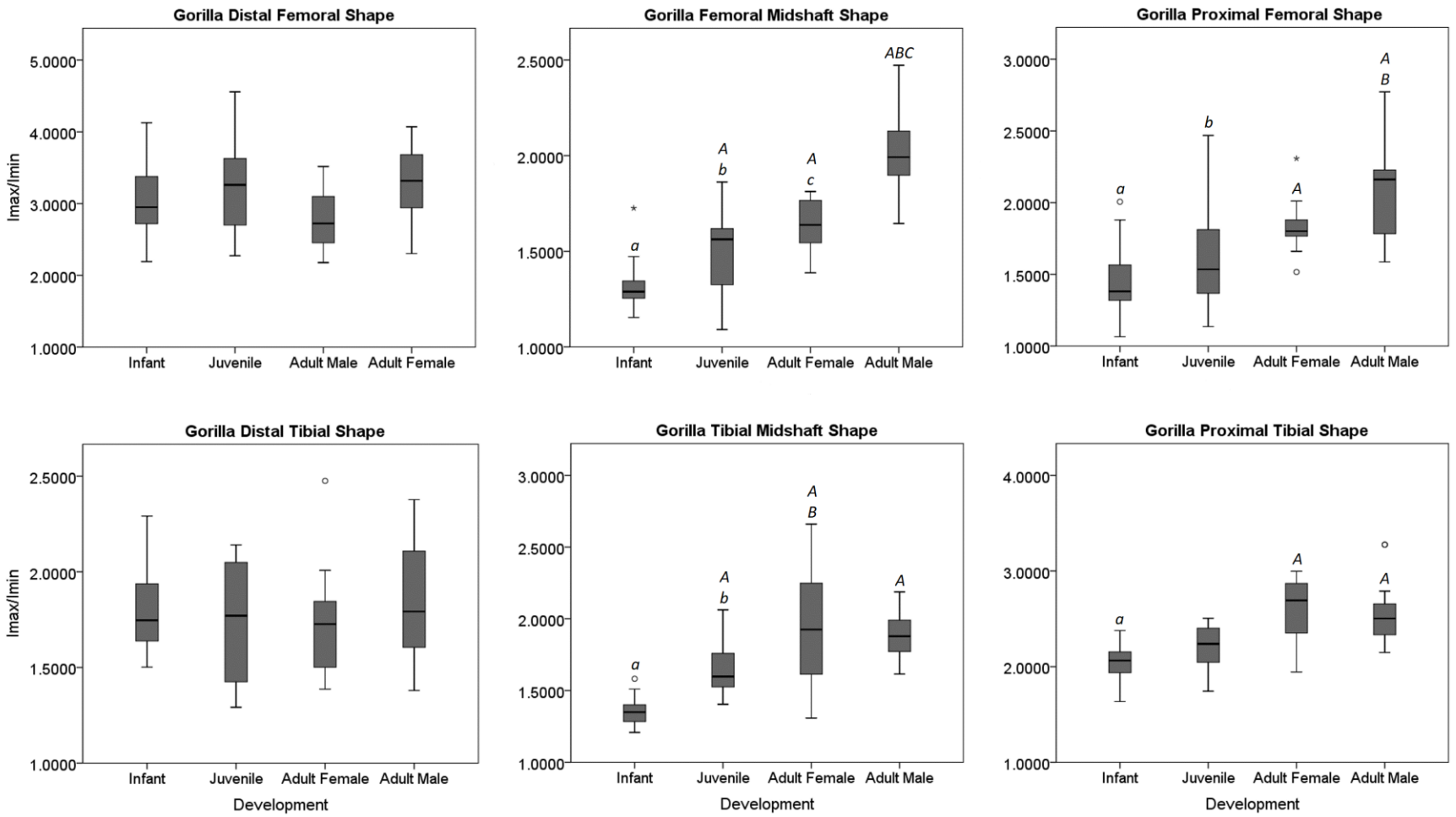

Fig. 3.2d. Box-and-whisker plot of gorilla hindlimb shape (I_{max}/I_{min}) variation over the course of development. A ratio of 1.0 represents true circularity. Rows depict limb elements (top, femur; bottom, tibia) and columns depict scan section (left, distal; centre, midshaft; right, proximal). Boxes represent 25th – 75th percentile range of developmental subgroups. Horizontal darkened lines indicate the median while whiskers extend to the maximum and minimum values within 1.5 box lengths. Outliers are denoted by an 'o' and extreme values, a star. Statistically significant between-group relationships are labelled with corresponding lower case and capital letters above their respective whisker bars.

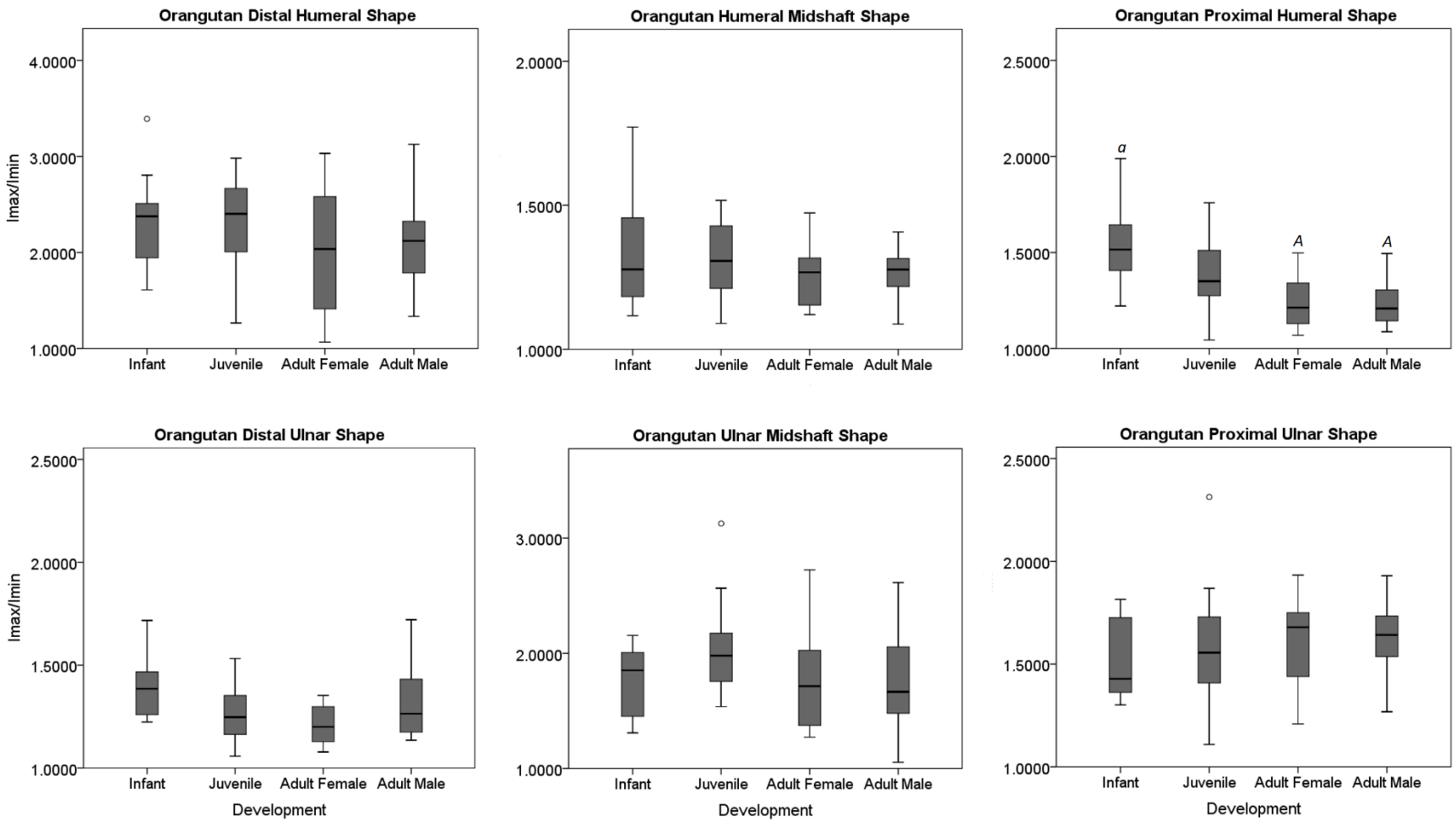

Fig. 3.2e. Box-and-whisker plot of orangutan forelimb shape (I_{max}/I_{min}) variation over the course of development. A ratio of 1.0 represents true circularity. Rows depict limb elements (top, humerus; bottom, ulna) and columns depict scan section (left, distal; centre, midshaft; right, proximal). Boxes represent 25th – 75th percentile range of a given developmental subgroup. Horizontal darkened lines indicate the median while whiskers extend to the maximum and minimum values within 1.5 box lengths. Outliers are denoted by an 'o' and extreme values, a star. Statistically significant between-group relationships are labelled with corresponding lower case and capital letters above their respective whisker bars.

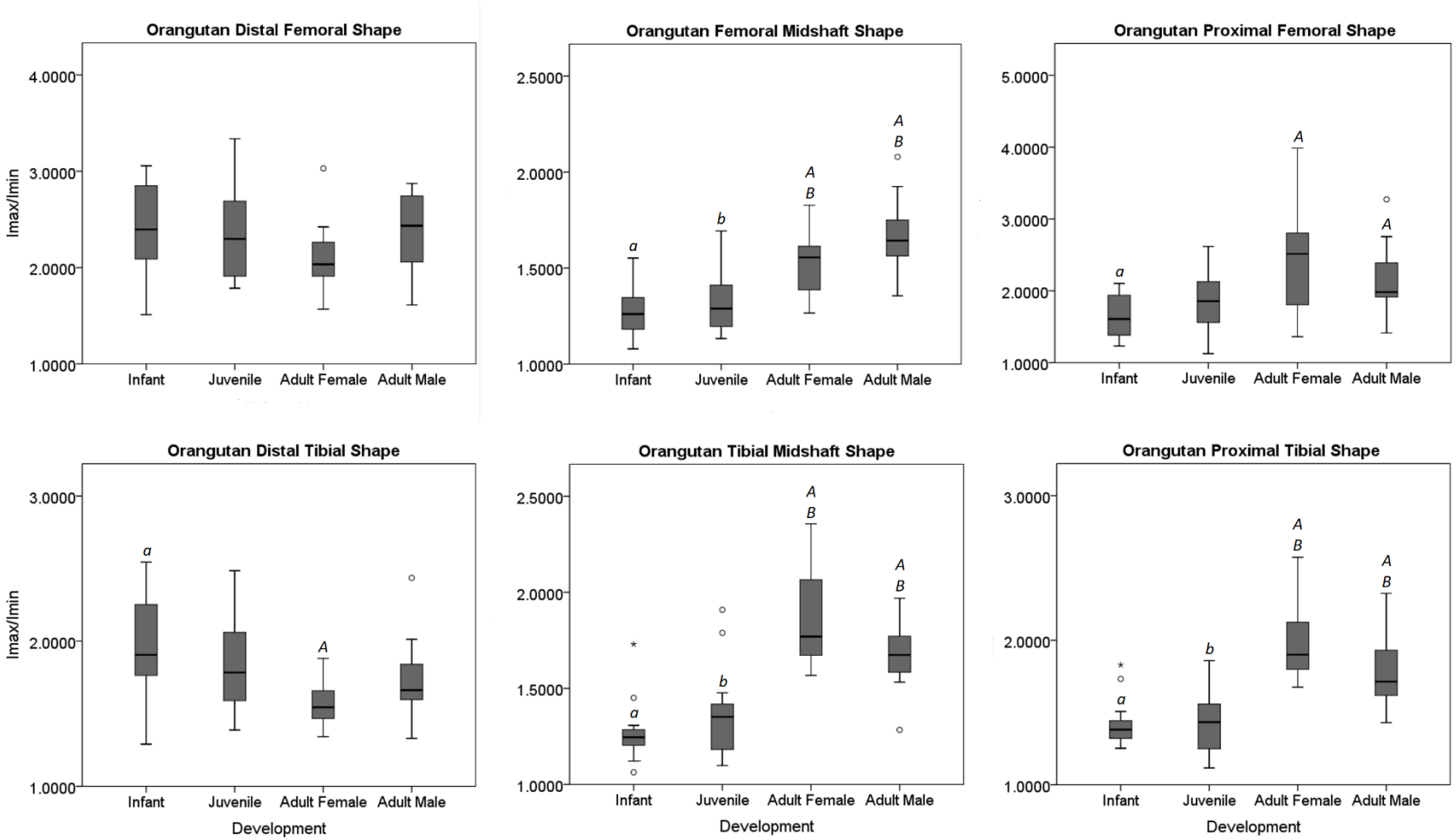

Fig. 3.2f. Box-and-whisker plot of orangutan hindlimb shape (I_{max}/I_{min}) variation over the course of development. A ratio of 1.0 represents true circularity. Rows depict limb elements (top, femur; bottom, tibia) and columns depict scan section (left, distal; centre, midshaft; right, proximal). Boxes represent 25th – 75th percentile range of developmental subgroups. Horizontal darkened lines indicate the median while whiskers extend to the maximum and minimum values within 1.5 box lengths. Outliers are denoted by an 'o' and extreme values, a star. Statistically significant between-group relationships are labelled with corresponding lower case and capital letters above their respective whisker bars.

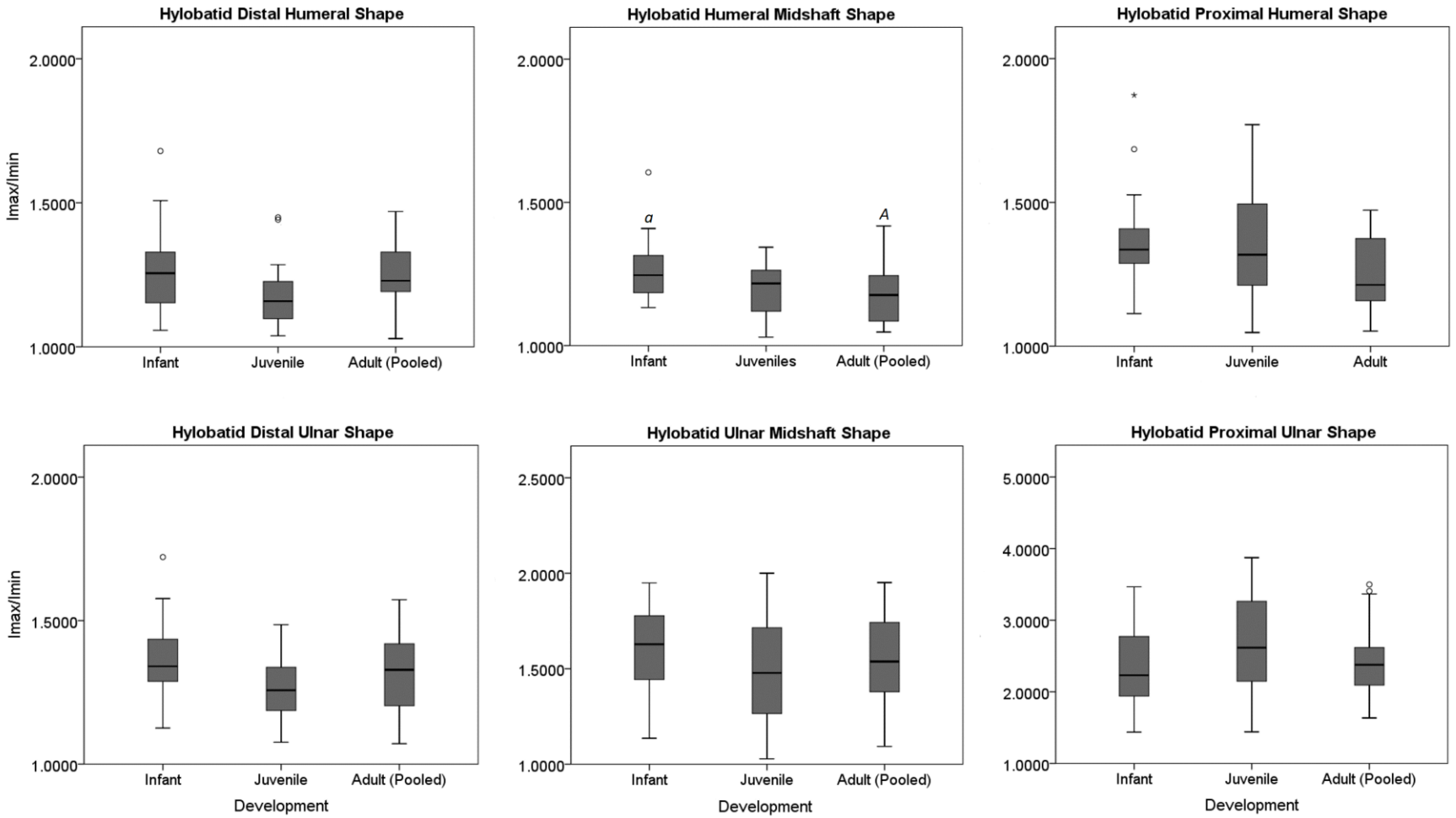

Fig. 3.2g. Box-and-whisker plot of hylobatid forelimb shape (I_{max}/I_{min}) variation over the course of development. A ratio of 1.0 represents true circularity. Rows depict limb elements (top, humerus; bottom, ulna) and columns depict scan section (left, distal; centre, midshaft; right, proximal). Boxes represent 25th – 75th percentile range of a given developmental subgroup. Horizontal darkened lines indicate the median while whiskers extend to the maximum and minimum values within 1.5 box lengths. Outliers are denoted by an 'o' and extreme values, a star. Statistically significant between-group relationships are labelled with corresponding lower case and capital letters above their respective whisker bars.

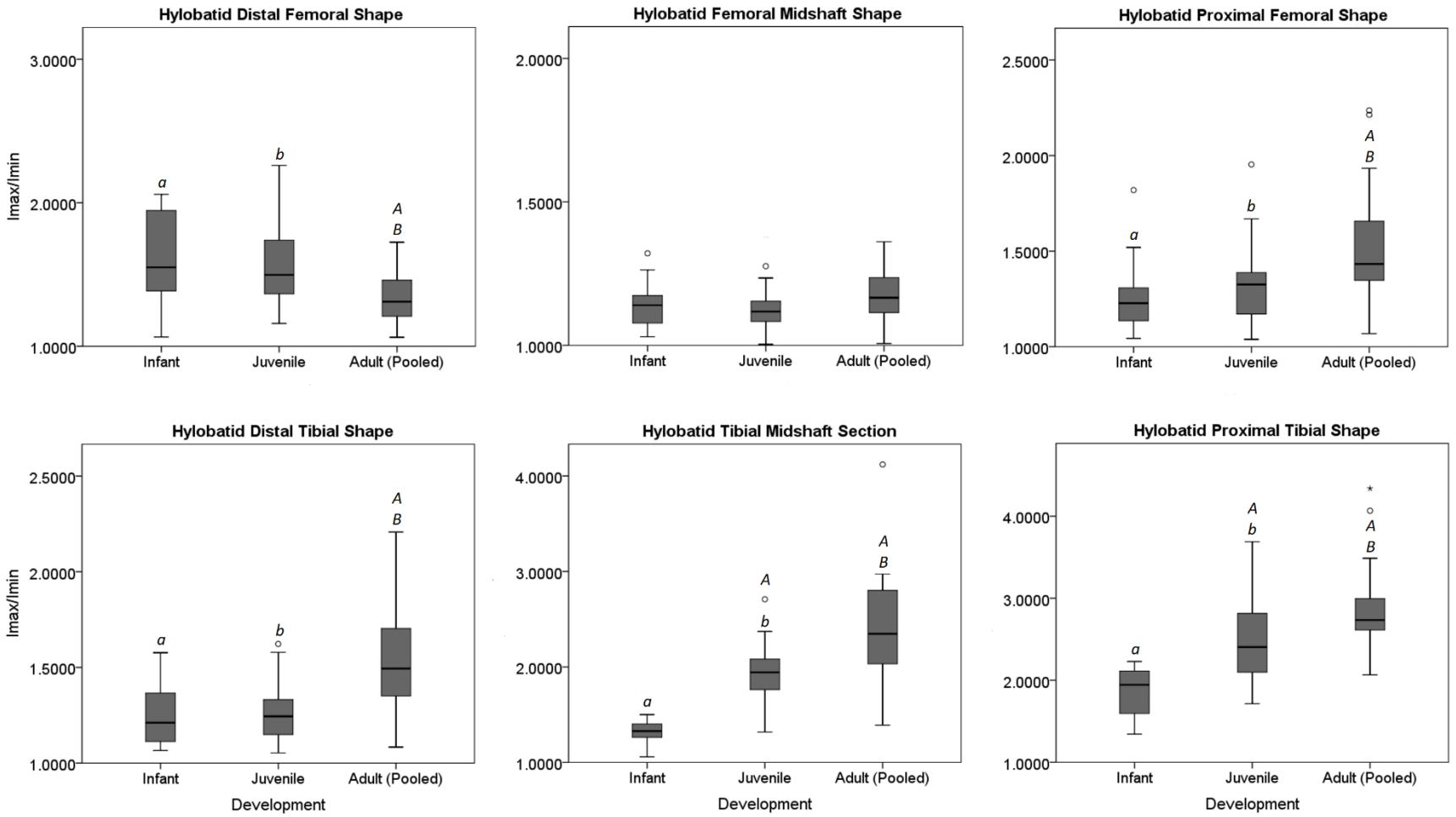

Fig. 3.2h. Box-and-whisker plot of hylobatid hindlimb shape (I_{max}/I_{min}) variation over the course of development. A ratio of 1.0 represents true circularity. Rows depict limb elements (top, femur; bottom, tibia) and columns depict scan section (left, distal; centre, midshaft; right, proximal). Boxes represent 25th – 75th percentile range of developmental subgroups. Horizontal darkened lines indicate the median while whiskers extend to the maximum and minimum values within 1.5 box lengths. Outliers are denoted by an 'o' and extreme values, a star. Statistically significant between-group relationships are labelled with corresponding lower case and capital letters above their respective whisker bars.

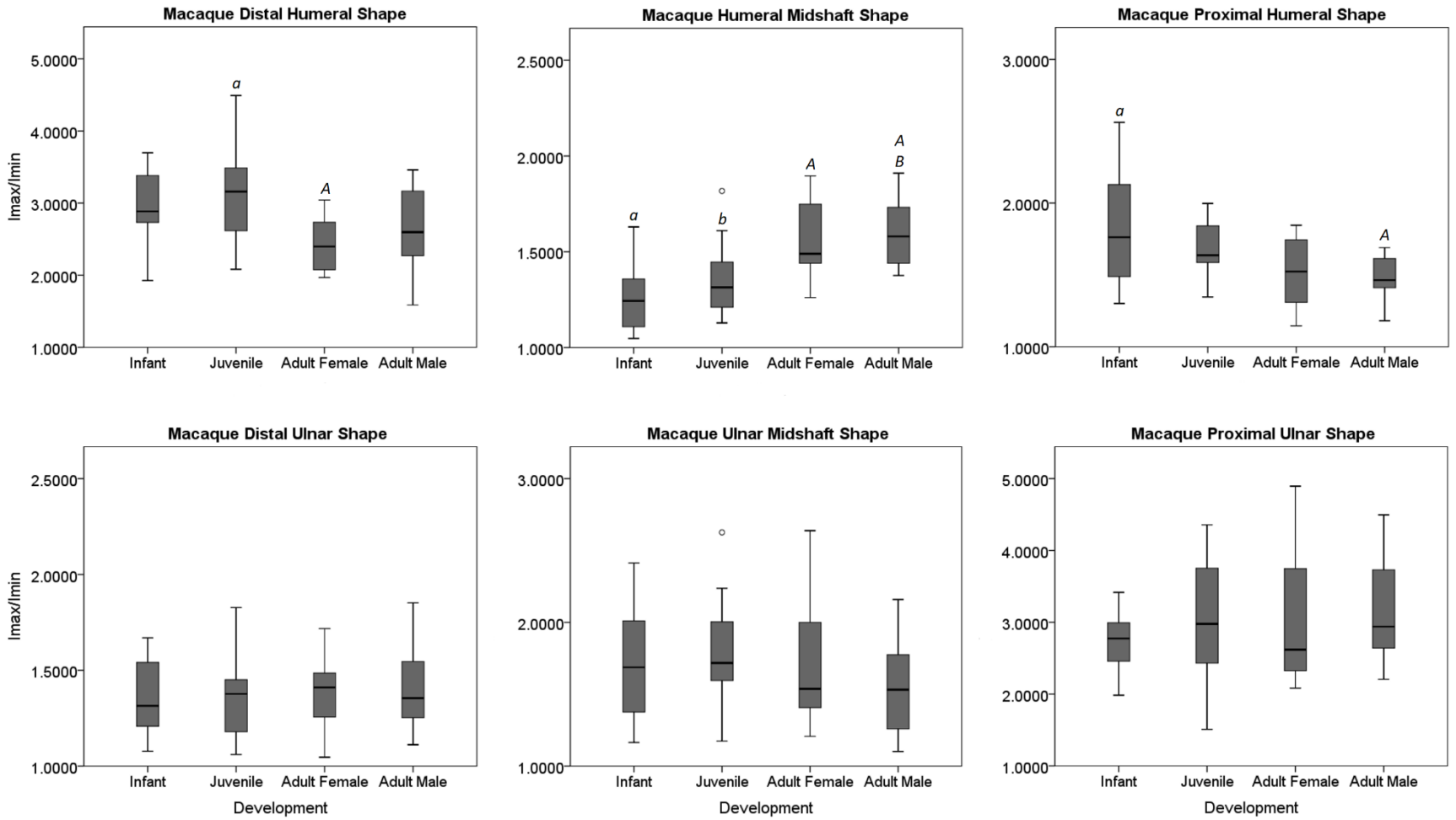

Fig. 3.2i. Box-and-whisker plot of macaque forelimb shape (I_{max}/I_{min}) variation over development. A ratio of 1.0 represents true circularity. Rows depict limb elements (top, humerus; bottom, ulna) and columns depict scan section (left, distal; centre, midshaft; right, proximal). Boxes represent 25th – 75th percentile range of a given developmental subgroup. Horizontal darkened lines indicate the median while whiskers extend to the maximum and minimum values within 1.5 box lengths. Outliers are denoted by an 'o' and extreme values, a star. Statistically significant between-group relationships are labelled with corresponding lower case and capital letters above their respective whisker bars.

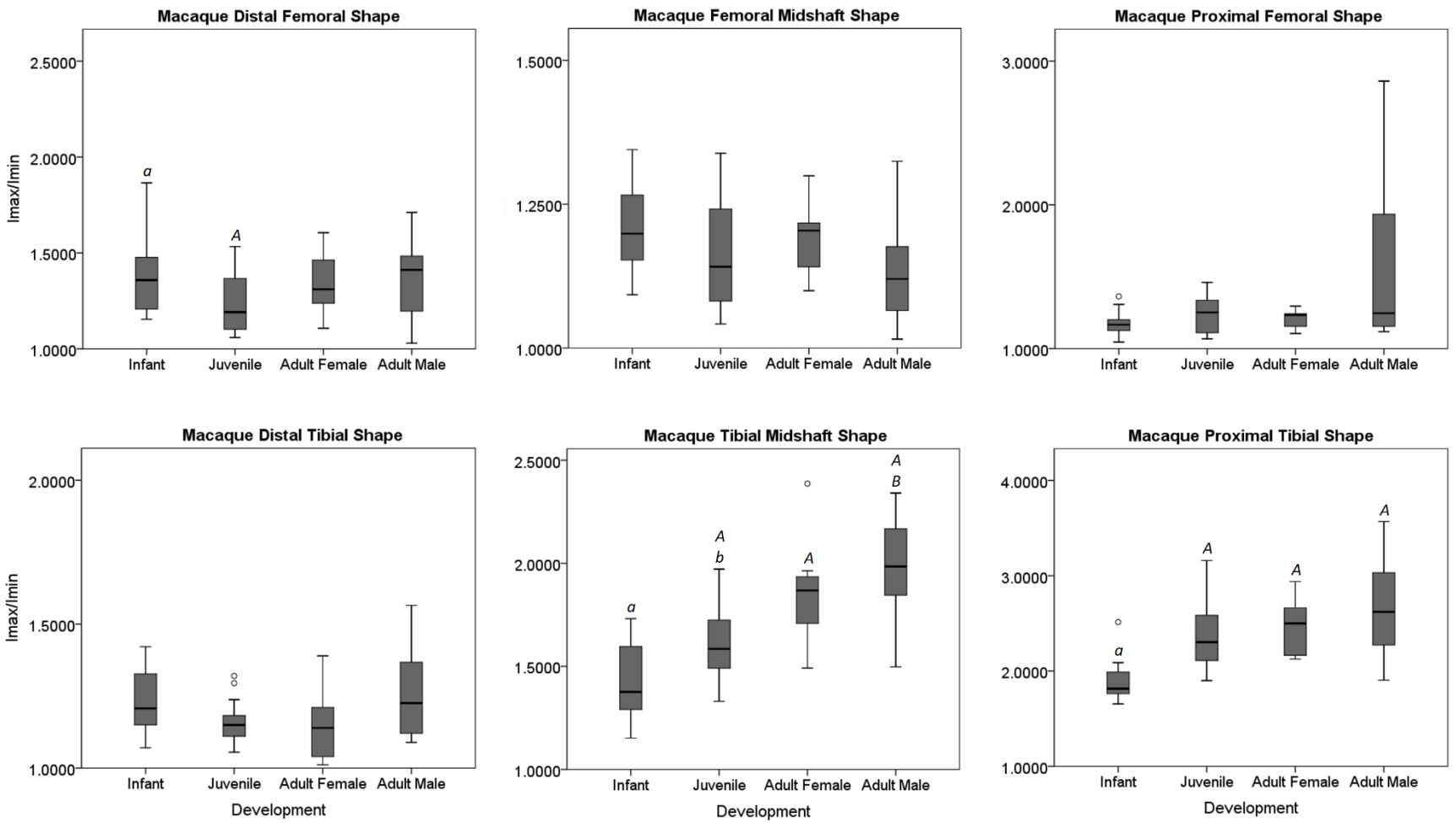

Fig. 3.2j. Box-and-whisker plot of macaque hindlimb shape (I_{max}/I_{min}) variation over the course of development. A ratio of 1.0 represents true circularity. Rows depict limb elements (top, femur; bottom, tibia) and columns depict scan section (left, distal; centre, midshaft; right, proximal). Boxes represent 25th – 75th percentile range of developmental subgroups. Horizontal darkened lines indicate the median while whiskers extend to the maximum and minimum values within 1.5 box lengths. Outliers are denoted by an 'o' and extreme values, a star. Statistically significant between-group relationships are labelled with corresponding lower case and capital letters above their respective whisker bars.

3.5 Discussion

The primary aim of this chapter was to evaluate how long bone diaphyseal shape varies at different stages of primate development. Specifically, two research objectives were addressed: first, to understand how cross-sectional shape varies between taxonomic groups with distinctly different ecologies and phylogenetic relationships to one another. Second, to determine whether cross-sectional shape changes across a given taxon's development. In addition to investigating these two broader topics, the preceding analysis considered shape variation at three discrete sites along each limb element. The results illustrate that shape variation along the limbs is site specific, where particular segments are more prone to shape change while others maintain their form over development. Limb shape appears to closely correspond to each taxon's locomotor profile at different stages of their development, and may be further influenced by factors including the substrates they negotiate, the gaits they employ and body sizes they possess as they mature. Further, it is apparent that specific aspects of limb elements, like midshafts typically experience more pronounced changes in shape, while distal sections tend to remain static throughout development.

3.5.1 Circularity along the forelimb

Analysis of forelimb circularity revealed that specific sections along the arm are more prone to change, while others largely maintain their shape over development. Because bone is highly responsive to mechanical loading during development, it was expected that variation along the forelimb would parallel the changing locomotor demands placed on each taxon as they matured. Indeed, it is evident that shape change at the humeral midshaft reflects the locomotor transitions undertaken during development. Of the five sampled genera, *Gorilla* engage in terrestrial positional behaviours most frequently (Tutin and Fernandez, 1985; Remis, 1994; Doran and McNeilage, 1998; Larson, 1998), particularly after infancy, when knuckle-walking accounts for up to 86% of all locomotor behaviour (Doran, 1997). This postural transition may account for the significantly more elliptical humeri exhibited among the juveniles compared to infants in the sample, especially in relation to the uniform loading pattern associated with terrestrial knuckle-walking (i.e., repetitive, unidirectional) (Schaffler et al., 1985). Further, the sexually dimorphic

shape variation found at the adult mid-humerus can be accounted for by male-female locomotor differences. Adult female mountain, and especially, western lowland gorillas, spend more time in an arboreal context compared to adult males (Kuroda, 1992; Remis, 1995, 1999); the variable loading regime of which likely fortifies their humeri in multiple planes compared to the concentrated ML reinforcement observed in male midshafts. Dynamic loading is capable of influencing cortical structure, even under loading regimes of short or infrequent duration (Rubin and Lanyon, 1984; Umemura et al., 1997; Judex et al., 2007), so long as strain magnitude exceeds that of typical loads (Frost, 1997). Thus, a semi-arboreal loading regime appears sufficient in distributing bone relatively evenly about the midshaft, even when terrestrial knuckle-walking occupies a majority of overall locomotor behaviour. The circular midshaft can subsequently support a female gorilla during unidirectional loading patterns like knuckle-walking, while also strengthening the planes of bending brought on by multi-directional suspensory loads. The same principle appears to govern mid-humeral shape in chimpanzees, who, like gorillas, transition from a forelimb- to hindlimb-dominant locomotor profile between infancy and adulthood (Doran, 1992a; Sarringhaus et al., 2014). One major difference between the African apes was that both male and female chimpanzees maintained their circular mid-humeri from infancy into adulthood. The most likely reason being that both sexes exhibit more frequent humeral abduction during suspension (i.e., arm-hanging, vertical climbing) compared to gorillas, throughout their lives (Tuttle and Watts, 1985; Hunt, 1991). These suspensory behaviours, combined with terrestrial knuckle-walking, require the humeral midshaft to remain rigid in multiple planes, similar to that observed among female gorillas. As such, humeral midshaft shape appears closely related to locomotor behaviour in the African apes, insofar that terrestrial and arboreal loading signals are capable of transcending sexual, and even generic differences, in driving humeral midshaft shape.

The application of second moment of area ratios (I_x/I_y) as a complement to principal moment of area ratios (I_{max}/I_{min}), granted further insight into the humeral midshaft's functionality. In agreement with Patel et al. (2013), examination of orangutan and gorilla mid-humeral I_{max}/I_{min} values determined that by adulthood, there was a general overlap in shape between the two genera, despite their considerably different locomotor profiles. Upon inspection of I_x/I_y ratios, however, it became apparent that orangutans distribute significantly more bone in the AP axis compared to gorillas, which distribute more bone along the ML, effectively discriminating the two ape genera by their mid-humeral shape. This finding demonstrates how cross-sectional shape can, in fact,

serve as a strong indicator of behaviour when paired with information on section distribution in the sagittal and coronal planes. It has been suggested that I_x/I_y ratios correlate to body mass while I_{max}/I_{min} ratios more readily predict locomotor behaviour (Carlson, 2005). However, the macaque sample – the lightest and smallest-bodied genus in this study – was the only taxon to distribute more bone along the ML axis than gorillas – the heaviest and largest taxon – at the humeral midshaft. Rather than a function of body mass, the greater elliptical ML distribution observed at the midshaft appears to be an equal determinant of locomotor behaviour as I_{max}/I_{min} ratios, especially in relation to quadrupedal loading patterns. Habitually quadrupedal primates apply vertical (braking and propulsive) and ML (side-to-side) forces to the ground each time the forelimb comes into contact with it (Biewener, 1989, 1990; Schmitt, 2003). As a result, the limb experiences an equal and opposite substrate reaction force, which acts on the bone in the form of a bending moment (Schmitt, 1999). Accordingly, repetitive ML bending via a quadrupedal gait should yield an elliptical ML section, like that observed in the gorilla and macaque midshafts in this study. Still, an intraspecific study of three macaque species determined that the mid-humerus revealed less morphological variation than the femur (Burr et al., 1989), which might be expected of a hindlimb-dominant primate (Wells and Turnquist, 2001). Thus, the findings discussed here may effectively differentiate between broad locomotor profiles, but caution should be taken when attempting to distinguish locomotor variation on a finer taxonomic level.

Like the primarily quadrupedal gorilla and macaque samples, the AP reinforced mid-humerus of the orangutans and chimpanzees is more likely an adaptation to above-branch suspensory behaviours rather than a function of body mass. Both *Pongo* and *Pan* allocate 16% of their total body mass to their forelimbs (Zihlman, 1992), underscoring the importance of their arm musculature and skeletal mass for suspensory behaviours like vertical climbing and arm-hanging (Thorpe et al., 1999). To place this in perspective, modern *Homo* and *Macaca* forelimb mass accounts for 9% and 13% of total body mass respectively, while the forelimb-dominant *Hylobates* dedicates more of its mass to the forelimb (20%) (Zihlman, 1992). Unlike the highly circular hylobatid midshafts adapted to brachiation and arm-swinging (Cannon and Leighton 1994; Fleagle, 2013), the AP distribution in the larger-bodied orangutans and chimpanzees may reflect the bending loads endured during arm-hanging feeding (Goodall, 1963; Sabater, 1979; Cant, 1987; Hunt, 2016). It is also possible that localised muscle-bone interactions could play a more dominant

role in driving humeral midshaft shape than sagittal bending, though orangutan and chimpanzee forelimb musculature vary decisively (Thorpe et al., 1999; Oishi et al., 2008, 2009).

Just as mid-humeral shape corresponded to locomotor behaviour, proximal and distal sections may adhere to broader evolutionary relationships. For instance, locomotor behaviour was not as easily discernible at the proximal humerus, where all five taxa exhibited a significant increase in circularity between infancy and adulthood, despite their markedly different ecologies. A similar phenomenon was observed at the distal humerus, which did not change shape between developmental stage among the entire sample. For one, proximal and distal sections should experience reduced bending moments compared to midshafts (Biewener and Taylor, 1986). Rather than adapting their shape to an ever-changing loading environment then, the primary function of proximal and distal sections should be to support the adjacent synovial joint (Currey, 1984). The type of neighbouring joint (i.e., socket, pivot, hinge), however, does appear to influence section shape as primates mature. Because primates (and particularly hominoids) are often defined by a high degree of shoulder mobility (Ashton and Oxnard, 1964; Schmidt et al., 2002; Chan, 2007, 2008; Larson, 2013), it is reasonable to expect that diaphyseal sections proximate to the glenohumeral joint would be circular in shape, in order to facilitate arm circumduction in multiple planes. Moreover, as individuals mature and locomotor competence improves, a rounded proximal humerus may aid in the support of more massive upper arm and rotator cuff musculature (Diogo and Wood, 2011; Diogo, 2015). Though proximal humeral shape becomes more circular over development in all five taxonomic groups, it is not to say that interspecific variation cannot also be distinguished between them. Compared to the high mobility of the hominoid glenohumeral joint and pectoral girdle, the cercopithecine shoulder region is specially adapted to forelimb movement in the parasagittal plane (Rose, 1983). Thus, the proximal humeral shape discrimination of *Macaca* from the four hominoid taxa may be more emblematic of primitive cercopithecine forelimb characters (Young et al., 2006; Schmidt and Krause, 2011) compared to the more derived hominoid upper arm and shoulder complex (Berger, 1994; Young et al., 2015). Similar to the proximal humerus, distal humeral structure should primarily serve to support the adjoining elbow (Currey, 1984; Ruff and Runestad, 1992). The fact that the elbow joint is limited in its mobility compared to the circumduction permitted by the shoulder, may influence its static shape throughout development. Prior studies on primate elbow structure have found derived characters adapted for specialised locomotor behaviours (Szalay and Dagosto, 1980; Jungers et al., 2002) while also

identifying similarities thought to aid in general mobility and stability across numerous forms of locomotion (Jenkins, 1973; Fleagle and Lieberman, 2015). Accordingly, the complete lack of developmental shape variation observed within each taxonomic group demonstrates that hinge joints and their congruent sections may not need to adapt their shape to the same capacity as sections near more mobile socket joints, let alone diaphyseal midshafts. Interspecific behavioural signals, on the other hand, are distinguishable by shape at the distal humerus. Such signals appear to be more discernible among taxa that possess highly specialised musculo-skeletal morphology, like that of the hylobatids (Andrews and Groves, 1975; Hallgrimsson and Swartz, 1995; Michilsens et al., 2009; Diogo et al., 2015), who support more than half of their body mass when the elbow is fully extended during brachiation (Hunt et al., 1996).

In direct contrast to the humerus, developmental shape variation along the ulnar diaphysis was minimal at each site and within each taxonomic group, demonstrating how variably arm segments develop in spite of their proximity to one another. Following limb optimality models (Currey and Alexander, 1985; Alexander, 1998; Raichlen, 2006), distal segments like the ulna must sustain proportionally greater loads than their proximal counterparts, all the while being slender and light enough to conserve energy during locomotion (Drapeau and Street, 2006). The lack of developmental variation in all taxa at the ulnar midshaft, despite the mechanical loads it endures, illustrates this fine trade-off between form and function in the forearm. Excessive structural variation during growth could risk mechanical failure in more gracile bones, in turn, constraining the midshaft's shape as an individual matures. The only taxon to exhibit any shape variation along the ulna over its development was *Gorilla*, where infant midshafts were significantly more circular than juveniles, adult females and adult males. Gorillas are not the only sampled taxon to undertake a major locomotor transition between infancy and adulthood, but they are the most massive (Smith and Jungers, 1999) and rapidly increase their mass up to ten years of age (Leigh and Shea, 1996). To put their size in perspective, the mean body mass of a four-year-old gorilla is roughly 30.5kg while an adult female chimpanzee is about 33kg (Doran, 1997). Thus, coupled with a transition to a more terrestrial posture shortly after infancy, an increase in body mass may be an adequate stimulus to evoke an adaptive response to midshaft bending loads. Another factor as to why so little developmental variation was observed at the ulnar midshaft in general, may be the mitigative role the radius plays in sustaining forearm bending loads (Birkbeck et al., 1997). Even among forelimb-driven specialists like gibbons (*H. lar*), which place

considerable strain on their forearms during brachiation (Swartz et al., 1989), have been shown to possess cross-sectionally stronger radii compared to ulnae (Ruff, 2002). Despite a lack of developmental variation within each taxon, the ulnar midshaft was effective at discriminating between taxa. For instance, both adult chimpanzee and gorilla circularity and axis distribution were significantly different compared to orangutans, hylobatids and macaques, but the African apes did not differ from one another in adulthood. While it is possible that the ulnar midshaft may be more adaptively responsive to terrestrial knuckle-walking behaviours than the humerus, given its proximity to ground impact (Skedros et al., 2003), both gorillas and chimpanzees may execute biomechanically different forms of knuckle-walking, facilitated by their hand, wrist and forearm morphology and orientation (Kivell and Schmitt, 2009). It is also possible that a locomotor-diverse taxon like *Pan* might benefit from an adaptively mosaic forelimb (i.e., a more suspensory-adapted humerus and a more terrestrially-adapted ulna), though it is more likely that the entire chimpanzee forelimb is suited to suspensory postures (Larson and Stern, 1987). Thus, the cross-sectional similarities between the African ape ulnae is likely more of a canalised effect than an adaptive response, especially if more gracile distal elements like the ulna are more adaptively constrained by tissue economy compared to the robust humerus (Plochocki et al., 2008).

While the distal ulna did not reveal any shape variation within each taxon, it is interesting that the section did not exhibit any interspecific variation either. In fact, the distal ulna was the only section across the entire adult fore- and hindlimb that was incapable of discriminating any taxon by means of principal area ratios (I_{max}/I_{min}). Though some taxonomic groups were distinguishable by second moment of area ratios (I_x/I_y) (e.g., adult macaques and orangutans), the shape overlap between taxa was most similar at the distal ulna than other sections of the diaphysis. A broad morphological pattern across the sample may be a solution to the dependence that all non-human primates place on wrist manoeuverability during locomotion. While studies have demonstrated how morphological diversity across primate wrists corresponds to their locomotor function (Kivell et al., 2013; Fleagle and Lieberman, 2015 and sources therein; Hunt, 2016), it is also apparent that broad locomotor profiles including suspension and quadrupedalism may not always leave a clear functional signal in their trabecular networks (Schilling et al., 2014). The highly circular distal ulnar section's proximity to the radio-ulnar joint may be a basal character among catarrhines, adjoining an equally primitive wrist (Kivell, 2016b), used to support forearm pronation and supination in a wide range of locomotor contexts. Shape homologies at the distal

ulna should not be over-interpreted, however, as significant differences in shape were identified between infant and juvenile taxonomic subgroups; the opposite pattern of what might be expected, as closely-related taxa tend to bear greater resemblance prior to maturity (de Beer, 1958; Lande, 2013). A closer investigation of the distal ulnar diaphysis that accounts for cortical, medullary and trabecular area and density, may help clarify whether the region is highly canalised among a more inclusive sample of primates and other arboreal mammals.

3.5.2 Circularity along the hindlimb

Like the forelimb, hindlimb midshafts were most similar between taxonomic groups during infancy, diverging into juvenility, and finally, displaying the greatest interspecific shape variation by adulthood. Similar research on the femoral and tibial morphology of two modern human populations (Frelat and Mittereocker, 2011) demonstrated that before adolescence, hindlimb form was largely similar between populations and similarly, went on to diverge with maturity. It is thus likely that environmental factors coupled with genetics each contribute to the adult condition in human and non-human primate limbs alike (Bogin and Rios, 2003; Tilkens et al., 2007; Gunz et al., 2010).

Comparisons along the hindlimb help demonstrate how shape corresponds to behaviour in some regions, while others resemble broader systematic relationships. Just as chimpanzee and gorilla humeral and femoral midshafts transition to a more ML oriented ellipse as they develop, mid-femoral shape is also capable of discriminating the two adult subgroups. For instance, chimpanzees exhibited a relatively circular midshaft compared to the highly elliptical condition seen in gorillas. Because terrestrial knuckle-walking has been demonstrated to place higher peak vertical forces on the hindlimb than the forelimb (Demes et al., 1994), it seems logical that hindlimb-driven primates like adult African apes would adapt their femora to mitigate substrate reaction forces produced during terrestrial locomotion. However, it is apparent that habitual quadrupeds like macaques, which are also hindlimb-dominant locomotors (Kimura, 1992), distribute bone virtually evenly between the ML and AP axes revealing a circular midshaft by adulthood. Thus, ML hindlimb distribution may not be a broad adaptive solution to quadrupedal loading forces, as it appeared to in the humerus. To determine whether a similar suspensory signal existed in the femur as it did in the humerus, the adult *Pan* sample was compared alongside *Pongo*.

Unlike the similar pattern found at the mid-humerus, mid-femoral shape differed significantly between the two ape genera. Furthermore, macaque and hylobatid shape did not vary between one another at any stage of their development in spite of the markedly different locomotor strategies they have evolved (Fleagle, 1976; Cant, 1988). It is therefore apparent that femoral midshaft shape is capable of distinguishing between the three sampled great ape taxa, though these differences do not appear to be explicitly correlated with locomotor behaviour. Femoral midshaft shape may instead be a better indicator of intraspecific locomotor patterns in primates, as has been demonstrated between human populations following femoral cross-sectional analyses (Larsen, 2002; Stock and Pfeiffer, 2001, 2004) and primate subspecies (Carlson, 2002, 2005; Ruff et al., 2013).

Rather than distinguishing between broad or specific locomotor signals, femoral cross-sectional shape may correspond more closely to overall body size. The weight-bearing aspects of the distal femur, including cross-sectional geometry and articular breadths and surface dimensions have made it an ideal candidate for body mass estimation techniques in modern and extinct *Homo* (Feldesman and Fountain, 1996; Auerbach and Ruff, 2004; Kurki et al., 2010; Grabowski et al., 2015; Will and Stock, 2015) as well as extant and extinct non-human primate skeletal specimens (Rafferty et al., 1995; Delson et al., 2000; Ruff, 2002, 2003b). Distal femoral principal and second moment ratios both closely correlated with the mean body size of the sampled taxa, where the smaller-bodied hylobatids and macaques overlapped in their relatively circular shape, followed by chimpanzees, orangutans and gorillas, each of which exhibited incrementally greater elliptical ML orientation in adulthood. While prior research has examined the relationship between I_{max}/I_{min} and I_x/I_y ratios and body size in human populations (Ruff, 1995, 2006; Pearson et al., 2014), those analyses were conducted solely at midshaft and failed to find a strong correlation between the two. To my knowledge, Old World primate size and its relationship with cross-sectional circularity at the distal femoral diaphysis has not been analysed before this study (see Chapter 6 for a preliminary analysis). While these initial results are hopeful, incorporating a more diverse taxonomic sample will help determine how closely body mass and shape relate and whether shape can accurately predict body mass across taxonomic groups.

One aspect of the femur shared with the sampled forelimb elements is the developmental constraint observed at their distal sections. In fact, only hylobatids and macaques exhibited any

I_{max}/I_{min} variation across developmental stages. One explanation as to why distal shape remains static during development is the proximity of the section to the knee joint. As discussed in the previous subsection, regions near hinge joints are not exposed to the same bending loads as midshafts and thus, are not required to adapt their external morphology to resist the variable or greater loads that midshafts endure when posture or profile change (Currey, 1984; Ruff, 1988). Instead, these sections do not adapt their shape dramatically as they grow. Maintaining shape over development allows the section to serve its primary function of supporting the joint as well as transferring mechanical loads between adjoining elements (Ruff and Runestad, 1992) without undergoing unnecessary structural changes that sections prone to bending otherwise might. Furthermore, because hinge joints like the knee operate in the same manner over development (i.e., permit or limit motion in a relatively confined sagittal plane), it appears more critical to change their size rather than shape, as observed across the sample. The exception of the hylobatids, whose distal femora became incrementally more elliptical between infancy, juvenility and adulthood, may be better explained by their specialised hindlimb musculature (Vereecke et al., 2006a,b). While all of the taxa in the sample undergo some form of locomotor transition as they mature, gibbons (*Hylobates lar* and *H. moloch*) and siamangs (*S. syndactylus*) have been shown to possess a voluminous rectus femoris and gastrocnemius; both of which act on their respective distal joints (the knee and ankle) during instances of leaping and climbing to a greater extent than other apes (Channon et al., 2010a). The musculature of the hylobatid hip and thigh may also help to explain their significantly more elliptical proximal femora, as gibbon and siamang gluteals feature relatively small moment arms and short fascicles (but see Payne at el. 2006b analysis of *Pan paniscus*) combined with a large physiological cross-sectional area (Channon et al., 2009). The advantage of this configuration is thought to reduce muscle mass at the thigh while increasing angular velocity and excursion near the hip (Crompton et al., 1996, Scholz et al., 2006); an effective locomotor strategy for a taxon that relies on lower limb propulsion to leap upwards of 15 metres (Fleagle, 1974).

Similar to the proximal humerus, significant developmental variation at the proximal femur was identified in all taxonomic groups apart from *Macaca*; the reason for which may be related to the limited range of motion at the acetabulofemoral joint in monkeys compared to hominoids. By studying the articular surface dimensions of the great apes with short-tailed macaques, Ruff (1988) found that the macaques had relatively small hindlimb articulations for their size, while orangutans

and modern humans possessed the largest articular surfaces and femoral heads, despite all three genera loading their limbs in markedly different ways. The smaller articulations found in the macaque sample may therefore be a factor of limited joint excursion, as joint mobility is understood to be greater among hominoids, irrespective of their locomotor repertoire (Ruff, 1988; Godfrey et al., 1991). In other words, limited joint movement at the macaque proximal femur may make it unnecessary to modify its shape and structure to the same capacity as their hominoid cousins.

Just as the proximal segments of each limb varied in their shape and development, analysis of the tibia demonstrated that the fore- and hindlimb are not serially homologous (Diogo and Molnar, 2014), but vary considerably in their shape development. Significant developmental variation was identified among each taxon at the proximal and mid-tibia in stark contrast to the developmental constraint observed along the ulnar diaphysis across the entire sample. There are several factors that may help explain why ulnar shape appears more constrained than tibial shape among taxa, despite their distal positions on their respective limbs. For one, the tibia is more robust than the ulna, which serves to support more body weight among hindlimb-dominant primates, including four of the five taxa sampled in this study (hylobatids being the forelimb-dominant exception) (Kimura et al., 1979; Schaffler et al., 1985; Demes et al., 1994). Further, it follows that a more robust element – given their similar material properties (Schmidt-Nielsen, 1992) – should more effectively resist deformation brought on by bending moments than a more gracile one. Coupled with experimental evidence demonstrating that the tibia experiences higher strains while supporting more body mass than the ulna during quadrupedal locomotion (Demes et al., 2001), it is plausible that tibial midshaft bone distribution primarily serves to counter the propulsive forces generated by the hindlimb during locomotion. From an adaptationist perspective, the fact that each taxonomic group develops a more AP oriented elliptical mid-tibia (irrespective of posture) suggests that the bending strains they endure move roughly anterior to posterior through the section. Even so, it is apparent that the degree by which AP distribution deviates from circularity may correspond to a taxon's locomotor behaviour. The orangutans serve as a particularly good example, as adults distributed bone more evenly at their mid-tibiae than any other adult taxon; significantly more so than chimpanzees, gorillas and hylobatids (Tables 3.7c and 3.8). Orangutan locomotor behaviour varies based on forest structure and support availability but locomotor manoeuver and substrate preferences are similar across species and populations in arboreal

contexts (Cant, 1987; Manduell et al., 2012; see Thorpe and Crompton, 2006 for terrestrial locomotor differences). Employing torso-orthograde and pronograde forms of suspensory locomotion to traverse branches and lianas of variable size and shape (Manduell et al., 2012) requires a great deal of locomotor dexterity, and in turn, likely influences bending strain and directionality about the section; especially compared to more uniform loading patterns (Carlson, 2002, 2005; Carlson and Judex, 2007). Of the diverse locomotor modes that orangutans assume in the wild and captivity (including pronograde quadrupedalism, orthograde climbing, and brachiation) (Cant, 1987; Gebo, 1996; Hebert and Bard, 2000), the bending loads endured via clambering and bipedalism may be the primary drivers of their tibial morphology. Though the frequencies and even definitions by which both behaviours have been reported varies (Cant, 1987; Hunt et al., 1996; Thorpe and Crompton, 2006), it is evident that hand-assisted bipedalism occupies approximately half of all orangutan locomotor postures. All great apes display heel-strike during quadrupedalism (Schmitt and Larson, 1995) but unlike their African relatives, orangutans have also been found to walk with an inverted foot, placing the entire lateral side on the ground during step-phase (Gebo, 1993; Schmitt and Larson, 1995). While postural and locomotor frequencies are relatively similar between orangutans and the African apes (aside from pronograde suspension behaviours) (Thorpe and Crompton, 2006), it is possible that the distinct footfall that orangutans employ could help with balance during variable loading on multiple supports like branches (Thorpe et al., 2007). Orangutan positional behaviour has also been described as broadly similar between development and sex (Thorpe and Crompton, 2006), despite the relatively circular pattern revealed by the pooled infant and juvenile subsamples. This observation may relate to the long period of maternal dependence that orangutans feature compared to other primate taxa (van Noordwijk and van Schaik, 2005), as maternal clinging is observed up to the age of six among sub-adults (van Adrichem et al. 2006).

The two sampled macaque species (*Macaca mulatta* and *M. fascicularis*) occupy a range of terrestrial and arboreal environments, both assuming habitual quadrupedal locomotor profiles (Nozawa et al., 1977; Cant, 1988; Huang et al., 2015). Analysis of their tibiae determined that like orangutans, the adult macaques reinforce their midshafts in the AP plane, but not to the extent that hylobatids and chimpanzees do. While arboreal species like *M. fascicularis* spend upwards of 70% of quadrupedal and climbing locomotion on continuous substrates, these behaviours are supplemented by more variable loading behaviours like pronograde and vertical clambering (14-

25%) (Cant, 1988). Furthermore, macaques support themselves on small branches oriented away from their bodies while traversing between substrates (Cant, 1988), as opposed to moving in a more predictable pattern like that of terrestrial knuckle-walking. The footfall pattern between arboreal and terrestrial primates may be driven by the variable substrates they negotiate as well, where arboreal primates tend to exhibit mid-foot/heel plantigrady compared to the heel-strike plantigrady found in the great apes (including humans) during terrestrial quadrupedalism (Rose, 1973a,b; Gebo, 1992; Schmitt and Larson, 1995). In line with this evidence, it is apparent that loading the hindlimb in multiple planes, coupled with placing a majority of strain approximately along the AP axis (Demes et al., 2001), is affiliated with a relatively even distribution of bone about the tibial midshaft to accommodate variable bending loads. By comparison, both African ape taxa exhibited more AP oriented midshafts which could be linked to the uniform loading pattern that terrestrial knuckle-walking incurs. The greater vertical forces experienced in the hind- compared to the forelimb may help explain the disparity of shape constraint and change between the ulna and tibia, respectively. Substantially higher vertical forces have also been reported to act on the chimpanzee hindlimb compared to forelimb (Li et al., 1996), as the small ground contact area (intermediate phalanges during knuckle walking) is arguably not as well adapted to apply propulsive or directional forces (Thorpe et al., 1999). Ultimately, the multi-directional loading patterns exhibited by orangutans and macaques appear to play an important role in more even distribution of bone about the tibial midshaft, while locomotor behaviours like knuckle-walking load the tibia in a more uniform parasagittal plane, necessitating greater bending rigidity along the AP axis (Figure 3.3). It is interesting to compare these patterns to those found in modern athletic studies, as mid-tibial shape in field hockey players also appears to be more evenly distributed about a section than distance runners, who load their tibiae more uniformly along the AP axis (Shaw and Stock, 2009b).

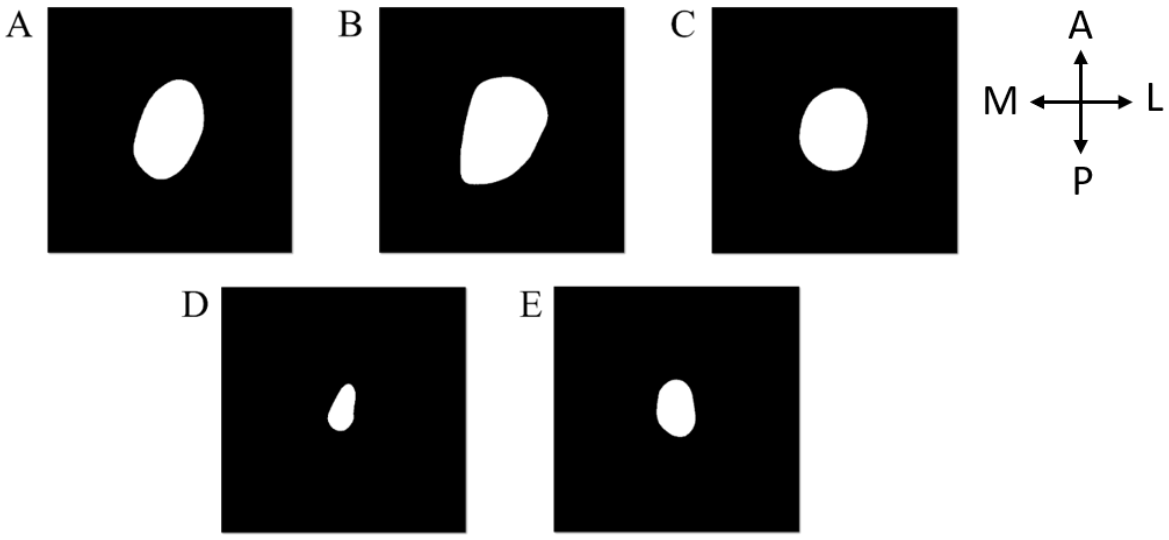

Fig. 3.3. Example of mid-tibial cross-sections from adult male individuals of each taxon: **A**. *Pan troglodytes troglodytes* **B.** *Gorilla gorilla gorilla* **C.** *Pongo pygmaeus* **D.** *Nomascus concolor* **E.** *Macaca mulatta.* Cross-sections oriented along the anatomical axes. Images not scaled.

To reduce mid-tibial shape to a mere product of arboreal or terrestrial locomotor directionality is insufficient, however. The hylobatid sample serves as a testament to this, in that their tibial midshafts are unequivocally more reinforced along the AP axis than any of the other sampled taxa in spite of their forelimb dominant, arboreal ecology (Sati and Alfred, 2002). While the hylobatids are often associated with forelimb-driven locomotor modes like brachiation, quadrumanous climbing, and scrambling (Carpenter, 1964; Tuttle, 1972; Fleagle, 1974, 1977; Cannon and Leighton, 1994; Usherwood and Bertram, 2003; Fan et al., 2013), the role of the hindlimb in leaping and hand-assisted/unassisted bipedal walking and running (Tuttle, 1986; Rafferty and Ruff, 1994; Hunt, 2004; Vereecke et al., 2006a) could grant insight into their tibial morphology. Though the hindlimb may not generate a great deal of thrust during leaping in *S. syndactylus*, the feet are the last part of the body to leave the branch, propelling them forward with momentum acquired by "pumping in place" (Fleagle, 1976). Further, hylobatids are capable arboreal and terrestrial bipedal locomotors, and employ low stride frequencies with high stride lengths (Demes et al., 1990) to achieve walking speeds that most humans would be required to run at to parallel (Vereecke et al., 2006a). Insights into hylobatid tibial morphology may be ascertained by their specialised musculature, as discussed earlier in this section. Their highly-developed

Achilles tendon compared with other hominoids, for instance, has been posited to more effectively store elastic energy for leaping or jumping behaviours (Vereecke et al., 2006b; Channon et al., 2010b). Equally, their hindlimb musculature may be an adaptation to brachiation, as lengthening tendons along the tibia is one strategy for decreasing distal mass (Payne et al., 2006a). Based on the close relationship between muscle and bone dimensions (Burr, 1997), it follows that the tibia too would reduce its mass by resorbing bone in planes that are not loaded as frequently or with the same intensity. Thus, the disproportionate AP distribution exhibited by adult hylobatids may be as much a function of stress mitigation from parasagittal leaping and bipedal loads as it is a mechanism for reducing the mass of a limb less integral to brachiation in contrast to the forelimb. Developmental change does not appear static along the entire tibial diaphysis, however, as no shape variation was reported among either the African apes or macaques at the distal section. Prior studies on distal tibial and ankle plasticity have presented conflicting results, where some research has found this region to be physiologically constrained (Venkataraman et al., 2013; Nadell and Shaw, 2016), while others have found the region to be more phenotypically plastic (DeSilva, 2009; Morimoto et al., 2011; Tsegai et al., 2017), in response to mechanical loading. Whether the comparatively uniform shape of the distal tibia is more a plastic phenomenon – as all apes and cercopithecoids exhibit a range of ankle dorsiflexion during locomotion (DeSilva, 2008, 2009) – or is better explained by intrinsic factors that appear to constrain the distal ulna in a similar way, is difficult to validate with circularity data alone. Though the correlation between circularity and size is not as strong at the distal tibia compared to the distal femur, future work should investigate how other cross-sectional properties like cortical area correspond to size and behaviour.

3.6 Chapter summary

The principal and second moment of area ratios reviewed here help contextualise several relationships between diaphyseal morphology and its association to the locomotor profiles and body sizes of the sampled taxa. For one, it is apparent that limb development is not only highly variable between the limb elements of primate taxa, but at specific sections along their diaphyses. Overall, distal sections appeared to be the most constrained regions in both the fore- and hindlimb, as their shape remained relatively static between developmental subgroups. The circular distal ulna in particular revealed no variation between developmental stages but also presented interspecific

circularity overlap between the adult subgroups of all five genera. This observation suggests that distal ulnar shape may be highly canalised among catarrhines, and potentially, primates in general. One reason a circular distal ulna would be selected is its function in wrist manipulation and manoeuverability; a primitive character important to all primates irrespective of posture. By comparison, diaphyseal sections predisposed to shape change over development often reflect behavioural transitions undertaken by a given taxon. For instance, the fore- to hindlimb locomotor transitions exhibited by the African apes between infancy and juvenility were echoed in the cross-sectional shape of their humeral midshafts, where I_{max}/I_{min} ratios reflected the loading patterns that each taxon assumed. These same comparisons showed that locomotor signals could also be differentiated at the sexual and generic levels, particularly when I_x/I_y ratios complement I_{max}/I_{min} ratios. Using both shape ratios together can help avoid observation errors by exposing differences in bone distribution rather than relying on one of them as a general index of circularity. The best example of which demonstrated that while ecologically different taxa like orangutans and gorillas both possess elliptical mid-humeral sections, they reinforce opposing planes within them to facilitate their distinct locomotor profiles. While I_{max}/I_{min} ratios continue to serve as stronger indicators of broad locomotor signals, incorporating I_x/I_y into cross-sectional shape analyses is strongly recommended. Fore- and hindlimb elements develop in different ways across taxa but some also reflect locomotor adaptations more readily than others. While arboreal locomotor behaviours often require dexterous use of both the fore- and hindlimb, for instance, mid-humeral shape appeared to be a stronger indicator of suspensory locomotion in chimpanzees compared to any other section along their fore- or hindlimb. In fact, chimpanzee and orangutan section shape closely overlapped at the humeral midshaft. By comparison, the chimpanzee tibial midshaft may reflect terrestrial knuckle-walking behaviours driven by the hindlimb, closely overlapping with gorilla mid-tibial shape. Sections like the distal femur, on the other hand, did not appear to correspond to behaviour very closely at all, but were correlated with body mass in all five taxa. These observations support other evidence that similar forces acting on separate limb elements (e.g., parasagittal strain on the femur and tibia) does not imply that they will alter their shape in the same way (Pearson et al., 2014).

Chapter Four:
The Ontogeny of Limb Strength

4.1 Introduction

Ontogenetic processes are the primary mechanisms responsible for biological character variation. Accordingly, the skeletal dimensions of primate limb bones are valuable to researchers interested in their form and function as they grow and adapt over an individual's life (Lumer, 1939; Cheverud, 1982; Shea, 1986; Jungers and Hartmann, 1988; Taylor 1995; Ruff et al., 2013). Along with intrinsic genetic factors that dictate bone growth, the biomechanical component of skeletal adaptation (i.e., interaction between bone and its loading environment, and its plastic response) is a key determinant of a limb's form (van der Meulen et al., 1993; Pearson and Lieberman, 2004). By studying growth trajectories between long bone diaphyses, it is possible to identify physical signals linked to behaviour, especially when said behaviours fluctuate over development (e.g., locomotor and postural transitions). However, research attempting to decipher these signals are often limited to observations of single developmental stages (Shaw and Ryan, 2012), focus exclusively on a single genus (Ruff et al., 2013), or consider only one aspect of the limb (e.g., proximal limb segments) (Sarringhaus et al., 2016). Incorporating an inclusive ontogenetic series of several distinct taxa allows for a side-by-side comparison of primate limb growth, granting an opportunity to study morphological adaptation through a behavioural and developmental lens.

The close correspondence between skeletal dimension and locomotor behaviour (Alexander, 1977; Currey and Alexander, 1985; Cowgill et al., 2010) means that discrete sections along a diaphysis must withstand the unique forces they are subject to (Schaffler et al. 1985). Thus, a cross-section's overall strength is a useful property for interpreting bone structure not only between elements, but along them as well. The two most common forces that act upon limb bone diaphyses during locomotion are bending, which strains opposing sides of a given section in compression and tension (Rubin and Lanyon, 1982); and torsion, placing shearing stress through a section when a bone is twisted along its long axis (Ruff, 2008). In this chapter, the polar section modulus (Z_p) – a geometric property proportional to a section's torsional strength as well as twice its average bending strength – is used to measure how bone structure varies regionally along the

limbs. Traditionally, Z_p is derived by dividing the polar second moment of area (J) by the distance of the section centroid to its outermost fiber. In the absence of cortical and medullary breadth data however, Z_p can be accurately estimated by raising J to 0.73 (Ruff, 1995). Using $J^{0.73}$ as a proxy for Z_p has been shown to estimate section strength in human and non-human primate long bones with precision (Ruff, 1995, 2002; Trinkaus and Ruff, 1999; Marchi, 2007; Young et al., 2010a).

While an elliptical section can theoretically withstand greater bending forces in its maximum compared to minimum plane (e.g., tibial strength along the AP is greater relative to its ML axis), the dynamic loads placed on the limbs in vivo are not always predictable and vary across taxa and locomotor types (Demes et al., 1998; Ruff, 2002; Lieberman et al. 2004). Therefore, Z_p is used to study each cross-section's average bending strength, effectively controlling for any variation in maximum or minimum strength between limb regions. When cross-sections depart from circularity (see Chapter 3 for a review of principal axis ratios), both J and Z_p become increasingly poorer indicators of a section's torsional rigidity and strength, respectively (Piziali et al., 1976; Daegling, 2002). That said, Daegling (2002) found that small departures from circularity result in negligible errors in predicting a bone's ability to resist torsion (errors < 5% were reported on departures from circularity as great as 50%; i.e., $I_{max}/I_{min} < 1.5$). Though J and Z_p are useful estimators of a section's ability to resist torsion and bending, the primary difference between the two properties lies in their proportionality to rigidity and strength. Regardless of the type of load, a given cross-section's ability to resist deformation before mechanical failure (fracture) is defined as rigidity, and a section's ability to resist fracturing itself denotes its strength (Ruff, 2008). More simply, a section's rigidity describes its ability to elastically return to its normal state after it is unloaded, while its strength is a measure of the stress it can resist before yielding to permanent deformation, or in a material like bone, breaking. Examples of variable strength and rigidity can be taken from ordinary objects. For instance, a piece of rubber tubing can only deflect a relatively small bending load before yielding its shape under it, yet it is strong enough to resist breaking under relatively greater force. A glass tube, on the other hand, must be comparatively rigid under a bending load in order to maintain its shape, but its strength may not be great enough to resist shattering as tension increases.

Caution should be taken when directly comparing individual element sections, however. Ontogenetic comparisons can clarify relationships between a species' morphology and ecology

but differences in bone microstructure play an important functional role in their ability to resist mechanical loads, as well (White et al., 2012). The material properties and growth processes of immature bone are demonstrably different than their mature counterparts (Enlow, 1963; Bass et al., 2002; Mcfarlin et al., 2008), where a greater composition of cartilage and trabeculae in cancellous tissue make young bones pliant compared to the thick and rigid cortices of adult bones (Burdi, 1969; Burdi et al., 1969; White et al., 2012). Moreover, bone microstructure varies along the diaphysis, where midshafts exhibit a thick cortex enveloping a large medullary cavity. Epiphyses, on the other hand, possess a comparatively thin cortical envelope surrounding a dense trabecular network (Currey, 2002; Chirchir et al., 2015). While this study compares distal diaphyses – which are more like midshafts in their endosteal morphology – rather than epiphyses, material differences cannot be controlled by comparing the relative dimensions of two discrete sections of the same diaphysis. Bearing that in mind, analysis of dimensional change between bone sections can still serve as an effective tool in understanding a primate's ecology, by considering how a section is reinforced and the forces it experiences during habitual loading episodes.

4.2 Research context and objectives

4.2.1 *Strength allometry along the diaphyses*

As an organism's size increases with growth, its shape typically changes as well (Huxley, 1932; Gould, 1966). The covariation between size and shape (form) in metric traits is central to the field of allometry, providing information on growth trajectory, ecology and phylogenetic relationships across the animal kingdom (Huxley and Teissier, 1936; Cock, 1966; Gould, 1975, 1989; Klingenberg and Spence, 1993; Klingenberg and Marugán-Lobón, 2013). The observations of Schultz (1924), that infant apes share greater morphological similarity than adults helped develop an early evolutionary framework for studying primate growth. Primate allometric research has since progressed from the scaling of soft tissue characters (Clutton-Brock and Harvey, 1980; Rilling, 2006, 2014; Taylor et al., 2015) to the correspondence between metabolism and behaviour (Hayssen and Lacy, 1985; Nunn and Barton, 2000; Simmen et al., 2015) and to bone structural adaptations (Boyer et al., 2015; Lewton, 2015; Arlegi et al., 2017).

Two primary research methods are employed in the study of primate allometry: the ecological approach and the engineering approach (Fleagle, 2013). The ecological approach seeks to answer questions on the matter of body size as it relates to behaviour. For example, research centred on the influence of a primate's caloric (energy) intake, and subsequently, the relationship between dietary adaptation and overall body mass – as per Kay's Threshold (Kay, 1975) – serves as an example of an ecological approach to allometry. The engineering approach seeks to answer which changes in body shape are necessary for two given animals of variable size to accomplish similar fundamental tasks, independent of inherent behavioural differences (i.e., how the metric dimensions of trait 'x' vary in conjunction between a larger and smaller primate). Take, for instance, a chimpanzee and a macaque. Both primates are equipped with distinctly different body dimensions and sizes and yet, must perform the same basic functions in order to survive. Even if their respective limb bones were adjusted for size, the robusticity of the chimpanzee's long bones would be greater than the macaque's, to preserve functional equivalence (McMahon, 1975) (Figure 4.1.); the reason being that bone cross-sectional areas in larger animals are disproportionately scaled to their linear dimensions to support their greater mass (Schmidt-Nielsen, 1992). The ecological and engineering approaches to allometry complement each other, as both perspectives are ultimately concerned with the same objective: the role of functional equivalence in relation to body size variation (McMahon, 1975).

Primate locomotor function can also be studied through the scaling of long bone cross-sectional geometry. Comparing section properties can identify locomotor patterns in a taxon and even inform about an element's adaptive response to mechanical loading, as strength ratios have been used to distinguish between fore- and hindlimb locomotor-dominant primates (Ruff, 2002; Shaw and Ryan, 2012). For instance, skeletally mature orangutans exhibit more rigid humeri, reinforced with greater cortical thickness compared to their femora, demonstrative of their suspensory lifestyle (Ruff, 2002; Shaw and Ryan, 2012). While several methods have been developed to estimate body mass in adult primates using cranial and postcranial skeletal dimensions (Aiello, 1981; Dagosto and Terranova, 1992; Delson et al., 2000; Ruff, 2002, 2003a,b), there is presently no way of estimating body mass in subadult specimens with the same accuracy.

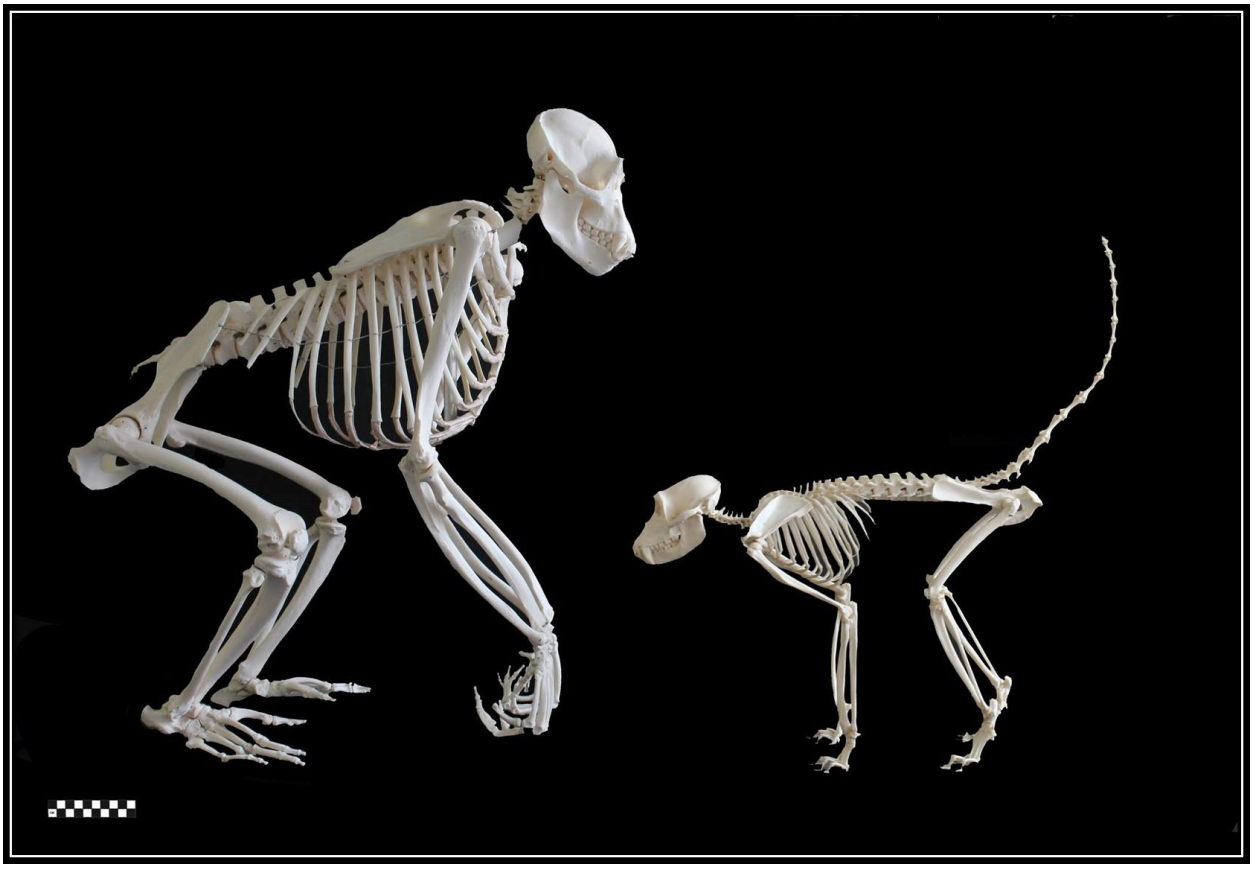

Fig. 4.1. Photograph of chimpanzee (*P. troglodytes* spp.) and macaque (*Macaca* sp.) skeletons side-by-side for visual comparison. Even when the limb elements of both individuals are size-scaled, variation in their cross-sectional geometry can provide information about their respective ecologies. Access to skeletons courtesy of the Bilsborough Laboratory, Durham University.

Using ratios to evaluate strength resolves this problem by allowing for the direct comparison of individuals at different stages of skeletal maturity. For example, Ruff and colleagues (2013) studied gorillas in an ontogenetic series to better understand limb growth trajectories between infancy and adulthood. By comparing Z_p proportions in mountain (*Gorilla beringei*) and western lowland (*Gorilla gorilla*) individuals, it was determined that inter-limb strength proportions closely correlate with transitions in locomotor behaviour exhibited between developmental stages, rather than scaling isometrically (Ruff et al., 2013). Their findings suggest that increases in strength relative to length dimensions are not merely products of continuous growth, but an adaptive response to shifts in locomotor behaviour. A similar study on limb strength ratios found

that chimpanzee femora became relatively stronger than humeri between infancy and adulthood (Sarringhaus et al., 2016). The findings of their research matched the locomotor transition chimpanzees experience shortly following infancy, when forelimb-driven arboreal locomotion is supplemented with hindlimb-driven knuckle-walking behaviour (Sarringhaus et al., 2014). While these two African ape studies help illuminate the morphological changes they experience as they mature, a lack of published research on other non-human primates makes it difficult to decipher whether proportional changes in limb strength are a function of similar locomotor behaviours or are more simply an inherent primate trait. Like inter-limb comparisons, prior studies have compared cross-sectional ratios within limb segments (e.g., radius/ulna; tibia/fibula), to understand the load-bearing capacities of adjacent bones (Marchi, 2007; Ruff et al., 2013). Though comparisons between and within limbs can be an effective method in evaluating their mechanical function, there is limited research comparing strength proportions along individual long bones themselves. Because midshafts are more disposed to bending moments compared to epiphyses or metaphyses (Currey, 1984), investigating how site-specific bone sections develop relative to each other can inform how entire diaphyses grow and adapt to their loading environments. Therefore, comparing strength changes between limbs, as well as along individual elements therein, can prove a useful method for studying limb functional ontogeny. While strength and rigidity ratios can be generated between any two locations along a diaphysis, comparisons of plastically adaptive cross-sections like the midshaft, with those understood to be more adaptively constrained, like distal sections (see results of Chapter 3), have the capacity to inform how diaphyses adapt different aspects of their structure. Even when elliptical sections exceed departures of circularity exceeding 50% (as several tibial distal sections did), they may not give an accurate interpretation of section structure but can be used as shape-constraint markers for which to compare shape-variable sections like their respective midshafts.

4.2.2 Research questions

The primary objective of this chapter is to investigate how cross-sectional strength changes along the limb bones of chimpanzees, gorillas, orangutans, hylobatids and macaques over their development. In doing so, I aim to determine whether adaptive signals exist within and between the limbs, with the potential to discriminate groups on the taxonomic, ontogenetic and locomotor

levels. To address this goal, polar section moduli ratios between the limbs and along individual elements are used to interpret limb and bone strength. Interspecific comparisons between infancy, juvenility and adulthood are explored to determine whether broad (i.e., quadrupedalism, suspension) and specific (i.e., terrestrial knuckle-walking, orthograde arm-hanging) locomotor behaviours emit physical signals along the upper and lower limbs. Two primary mechanisms responsible for dictating bone structure – plastic adaptation and genetic canalisation – are considered in relation to development-specific locomotor behaviours in each taxon. Femoral-to-humeral midshaft ratios are used to identify any disparity between fore- and hindlimb strength among the five taxonomic groups. Because both the humeral and femoral midshafts of the five taxa are relatively circular, Z_p ratios between the two elements provide an accurate depiction of their maximum bending and torsional strength. If a taxon assumes a developmental locomotor transition between the fore- or hindlimb, the shift should be reflected by a change in strength from the former to newly dominant limb (Kimura et al., 1979; Kimura, 1992; Demes et al., 1994). Specifically, it is expected that the African apes and macaques will exhibit stronger humeri early in life, transitioning to relatively stronger femora by the time adulthood is achieved, based on the arboreal- to terrestrial-dominant postures they come to assume by adulthood (Doran, 1997; Wells and Turnquist, 2001), and findings from previous studies (Ruff et al., 2013; Sarringhaus et al., 2016). The Asian apes, by comparison, are expected to display stronger or equally strong humeri relative to femora across all three stages of development, given the propulsive role of the forelimb in suspensory locomotion and their relatively fixed locomotor profiles beginning in infancy and carrying on through to adulthood (van Adrichem et al., 2006; Chappell et al., 2015). In Chapter 3, I demonstrated that the distal ulna and tibia remained relatively static in shape compared to their respective midshaft sections over the course of development. Therefore, strength between the ulnar midshaft and distal ulna is compared in the forearm while mid- to distal tibial ratios will be used to measure strength differences in the lower leg. Unlike inter-limb comparisons, strength ratios between two sections of the same diaphysis can place structural variation into a finer context. Accordingly, intra-limb comparisons will help quantify any distinct strength changes between proximate bone sections exposed to similar forces, rather than between dissociated limbs. Because midshafts must resist greater bending and torsional forces compared to sections neighbouring synovial joints (Ruff and Runestad, 1992), it is expected that all five taxa will display an incremental increase in midshaft strength between developmental stages. However, if locomotor

patterns place variable strain along the diaphyses, these differences should still be distinguishable between taxonomic and developmental groups.

4.3 Methods

The following section details the protocol used to calculate and compare strength ratios along the limbs. The respective developmental subgroups (infants, juveniles and adults) of the five anthropoid taxa (*Pan, Gorilla*, *Pongo*, Hylobatidae and *Macaca*) were incorporated in the following analyses. Midshaft and distal cross-sections along the four sampled long bones (humerus, ulna, femur and tibia) were also assessed among each taxonomic and developmental subgroup. For a review of the primate skeletal sample and the laser scanning method used to obtain the cross-sectional data discussed ahead, please see Chapter 2.

Polar section moduli (Z_p) were used to evaluate bending and torsional strength at discrete sections along the fore- and hindlimb across the sample. Each section's Z_p was estimated by raising the polar second moment of area to 0.73 ($J^{0.73}$) (Ruff, 2002). To control for the effects of body size variation within and between developmental groups, discrete sections along the limbs were compared within each individual using ratios. Rather than making direct comparisons of Z_p between limbs, the use of ratios made it possible to interpret strength changes while neutralising the effects of individual body mass. In doing so, direct comparisons between developmental stages and taxonomic groups could be made.

Three separate Z_p ratios were generated to compare variation in inter- and intra-element strength. To normalise each data set, all ratios were transformed by their natural logarithm (Ln), so that the data could be expressed linearly. These log-log linear regressions first assessed the structure of the femoral and humeral midshafts against each other (50% of total element length) (F/H), in order to measure fore- and hindlimb strength proportions in the proximal segments. The second and third Z_p ratios were designated between the mid- (50%) and distal (20%) ulna (U50/U20), to identify structural changes within the forearm, as well as the mid- (50%) and distal (20%) tibia (T50/T20), to examine changes in the lower leg. Bivariate plots were used to illustrate how the log-transformed Z_p values influenced each inter- and intralimb ratio. The slope of each plot represents the allometric coefficient, where a value above 1.0 represents a positive allometric

relationship and a number below 1.0 signifies negative allometry (Figure 4.2). Bivariate scatters across taxonomic and locomotor variable groups are expected to adhere to a typically isometric pattern (Ruff, 2002), making even subtle allometric differences informative. The coefficient of determination (R^2) was included in each plot to show the fit of the data to the regression line.

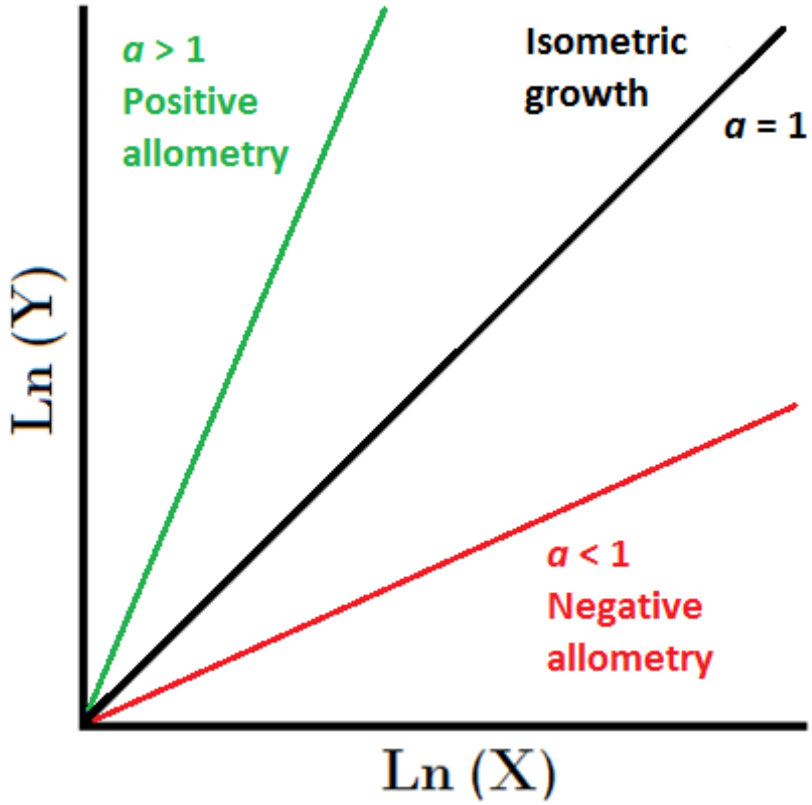

Fig. 4.2. Generalised bivariate plot of the allometric equation describing a positive correlation between two morphological characters, 'x' and 'y', as they increase in size. By log-transforming a property of interest like Z_p, data points of the two characters change from a curved to linear relationship, allowing for comparisons between size-variable groups. Image adapted from Carr, 2005.

After log-transforming the F/H, U50/U20 and T50/T20 values, general linear models of each ratio were used to investigate effect size of taxonomic and sex differences among the developmental groups. Because distal sections acted as points of comparison for the intra-ulnar and intra-tibial ratios, the effects of distal shape (I_{max}/I_{min}) were accounted for as covariates in each

model (ANCOVA). To improve statistical power for testing main effects, Type II sums of squares (SS) was considered when the interaction between taxa and sex was insignificant, while Type III SS was referred to for any significant interactions between taxonomic and sex differences (Langsrud, 2003). Most interspecific comparisons were deemed significant using one of two *post hoc* correction methods. When assumptions of homogeneity were met, Scheffé's method was consulted. When homogeneity of variance was violated, the Games-Howell test was used to interpret the results. Brown-Forsythe and Welch tests were both consulted to determine whether developmental and taxonomic subgroups were normally distributed in each comparison. In instances when they were not, a Kruskal-Wallis H test was used to control for variance in each subgroup and to test for significant interactions (Sokal and Rohlf, 1995). Significance was recognised at $P < 0.05$ in all comparisons.

4.4 Results

4.4.1 Femoral-to-humeral strength proportions

Descriptive statistics for F/H strength are given for all taxa across infancy, juvenility and adulthood in Table 4.1. Compared to juvenile and adult taxa, sexual differences did not account for any variance in the infant F/H model. Instead, taxonomic differences accounted for approximately 61% of infant variance (Table 4.2a). Following infancy, sex accounted for 1.9% and 2.9% of variance in juveniles and adults, respectively, though these differences did not account for any significant variation in their respective models (Table 4.2a – 4.2c). By comparison, taxonomic differences accounted for the largest effect size.

TABLE 4.1. Mean and standard deviation for mid- femoral and humeral strength ratios (raw Z_p)

Development Stage/Sex	*Pan*	*Gorilla*	*Pongo*	Hylobatidae	*Macaca*
Infant	0.9 ± 0.09	1.09 ± 0.21	0.77 ± 0.05	0.87 ± 0.24	1.39 ± 0.18
Juvenile	1.11 ± 0.12	1.33 ± 0.32	0.73 ± 0.11	1.05 ± 0.16	1.65 ± 0.23
Adult Female	1.21 ± 0.16	1.27 ± 0.12	0.84 ± 0.1	1.01 ± 0.1	1.38 ± 0.25
Adult Male	1.21 ± 0.12	1.06 ± 0.36	0.77 ± 0.1	1.01 ± 0.11	1.31 ± 0.18

Polar section modulus mean and standard deviation for each taxonomic group by developmental stage.

TABLE 4.2a. Between-subject effects for strength ($\mathrm{Ln}Z_p$) of the infant mid- femur and humerus

Source	SS (II)[1]	df[2]	Mean Square	*F*	*P*[3]	Variance[4]
Corrected Model	3.53	12	0.26	8.01	**0.0001**	0.628
Intercept	74.4	1	0.002	0.06	0.801	0.001
Taxa	3.45	4	0.72	21.9	**0.0001**	0.606
Sex	0.001	2	0.002	0.06	0.939	0.002
Taxa*Sex	0.017	6	0.011	0.32	0.921	0.033

[1] Type II sum of squares.
[2] Degrees of freedom.
[3] Significance accepted at $P < 0.05$ and listed in bold font.
[4] Model variance expressed as partial eta squared (η_p^2).

TABLE 4.2b. Between-subject effects for strength (LnZ_p) of the juvenile mid- femur and humerus

Source	SS (II)[1]	df[2]	Mean Square	*F*	*P*[3]	Variance[4]
Corrected Model	6.81	9	0.76	28.9	**0.0001**	0.758
Intercept	0.642	1	0.64	24.5	**0.0001**	0.228
Taxa	6.68	4	1.67	63.7	**0.0001**	0.755
Sex	0.042	1	0.04	1.59	0.210	0.019
Taxa*Sex	0.131	4	0.03	1.24	0.297	0.057

[1] Type II sum of squares.
[2] Degrees of freedom.
[3] Significance accepted at $P < 0.05$ and listed in bold font.
[4] Model variance expressed as partial eta squared (η_p^2).

TABLE 4.2c. Between-subject effects for strength (LnZ_p) of the adult mid- femur and humerus

Source	SS (II)[1]	df[2]	Mean Square	*F*	*P*[3]	Variance[4]
Corrected Model	4.05	9	0.451	6.01	**0.0001**	0.356
Intercept	0.3	1	0.3	4	**0.048**	0.039
Taxa	3.6	4	0.9	12	**0.0001**	0.328
Sex	0.22	1	0.22	2.9	0.093	0.029
Taxa*Sex	0.37	4	0.09	1.2	0.297	0.048

[1] Type II sum of squares.
[2] Degrees of freedom.
[3] Significance accepted at $P < 0.05$ and listed in bold font.
[4] Model variance expressed as partial eta squared (η_p^2).

Chimpanzee and gorilla F/H proportions did not differ from one another at any stage of development. The two African ape taxa exhibited a modest positive allometric F/H relationship, where a relatively strong humerus in infancy was followed by an increase in femoral strength by adulthood (Table 4.3a – 4.3c).

Growth trajectory plots for F/H for each of the five taxa are given in Figures 4.3a – 4.3e. Infant chimpanzees in particular displayed significantly smaller F/H values compared to juvenile and adult male and female chimpanzees (Figure 4.4). Infant gorillas, by comparison, did not exhibit any significant developmental differences despite their similar positive allometric trajectory with chimpanzees. Like the African apes, infant orangutan and hylobatid F/H strength did not differ from each other. Overall, orangutans exhibited the strongest humeri compared to femora across development among the entire sample, while hylobatids transitioned from significantly stronger humeri to femora following infancy. Orangutan F/H strength proportions were largely consistent over development, by comparison (Figure 4.4.). Infant and juvenile macaque F/H values were significantly greater compared to all other infant taxonomic subgroups, effectively discriminating all apes from macaques by limb strength proportions early in development. By adulthood though, macaques, chimpanzees and gorillas did not display any significant differences in F/H strength from one another.

TABLE 4.3a. Mid- femoral and humeral strength ($\mathrm{Ln}Z_p$) ratio *post hoc* tests for pooled infants

	Pan	*Gorilla*	*Pongo*	Hylobatidae	*Macaca*
Pan	-	n.s	n.s	n.s	0.0001
Gorilla	n.s	-	0.001	0.035	0.008
Pongo	n.s	0.001	-	n.s	0.0001
Hylobatidae	n.s	0.035	n.s	-	0.0001
Macaca	0.0001	0.008	0.0001	0.0001	-

Significant values accepted at $P < 0.05$ and given in the table, non-significant values denoted by n.s.

TABLE 4.3b. Mid- femoral and humeral strength (LnZ_p) ratio *post hoc* tests for pooled juveniles

	Pan	*Gorilla*	*Pongo*	Hylobatidae	*Macaca*
Pan	-	n.s	0.0001	n.s	0.0001
Gorilla	n.s	-	0.0001	0.039	0.028
Pongo	0.0001	0.0001	-	0.0001	0.0001
Hylobatidae	n.s	0.039	0.0001	-	0.0001
Macaca	0.0001	0.028	0.0001	0.0001	-

Significant values accepted at $P < 0.05$ and given in the table, non-significant values denoted by n.s.

TABLE 4.3c. Mid- femoral and humeral strength (LnZ_p) ratio *post hoc* tests for pooled adults

	Pan	*Gorilla*	*Pongo*	Hylobatidae	*Macaca*
Pan	-	n.s	0.0001	n.s	n.s
Gorilla	n.s	-	0.0001	n.s	n.s
Pongo	0.0001	0.026	-	0.02	0.0001
Hylobatidae	n.s	n.s	0.02	-	0.025
Macaca	n.s	n.s	0.0001	0.025	-

Significant values accepted at $P < 0.05$ and given in the table, non-significant values denoted by n.s.

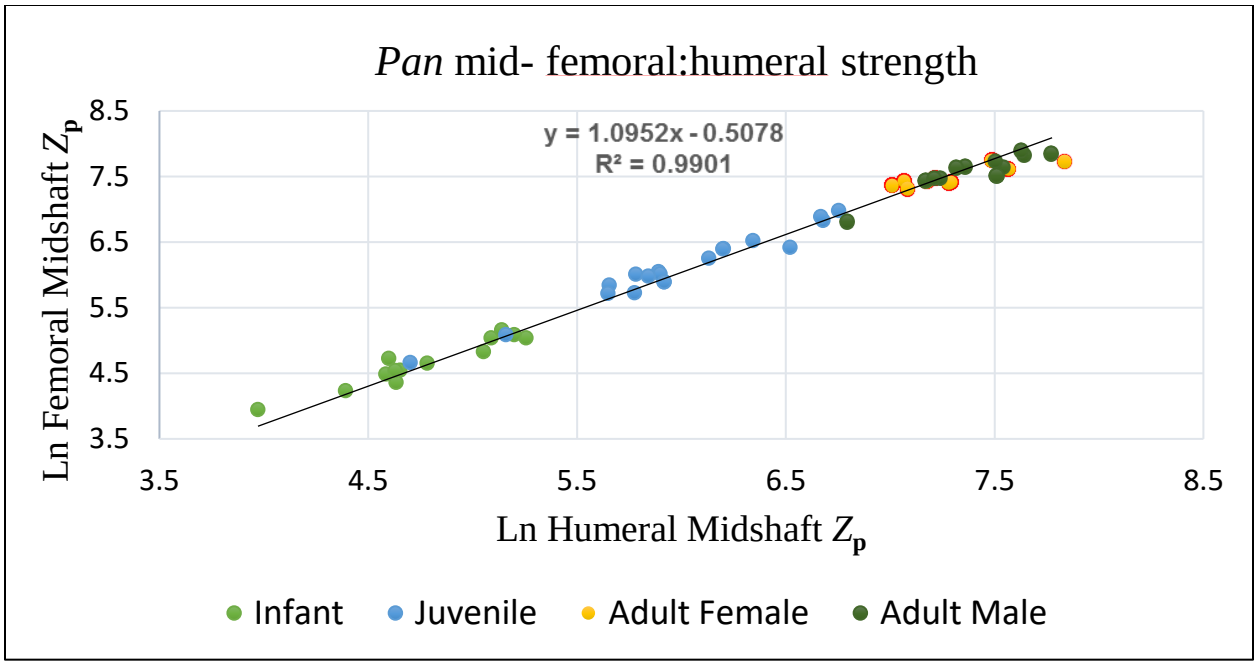

Fig. 4.3a. Log-log bivariate plot comparing *Pan* F/H over development. The allometric coefficient (slope) reveals a positive allometric relationship, where the femur increases in strength relative to the humerus between infancy and adulthood.

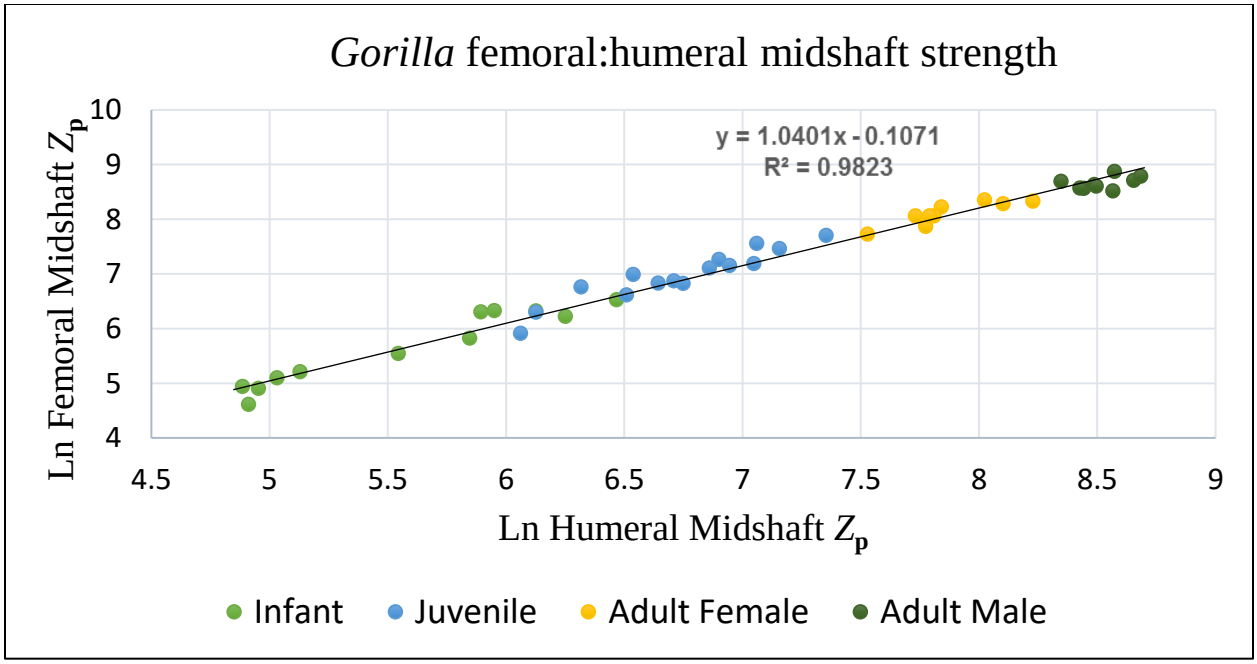

Fig. 4.3b. Log-log bivariate plot comparing *Gorilla* F/H over development. The allometric coefficient (slope) reveals a slightly positively allometric relationship, where the femur increases in strength relative to the humerus between infancy and adulthood.

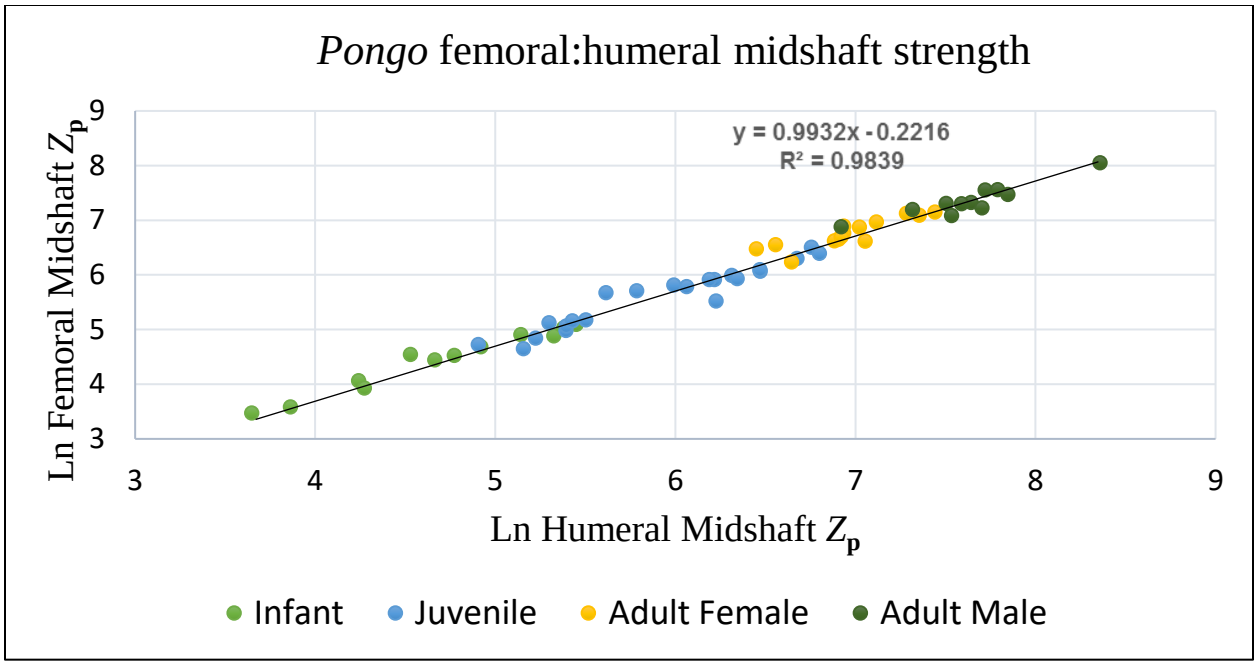

Fig. 4.3c. Log-log bivariate plot comparing *Pongo* F/H over development. The allometric coefficient (slope) reveals a virtually isometric relationship, where the humerus remained slightly stronger than the femur across all three stages of development.

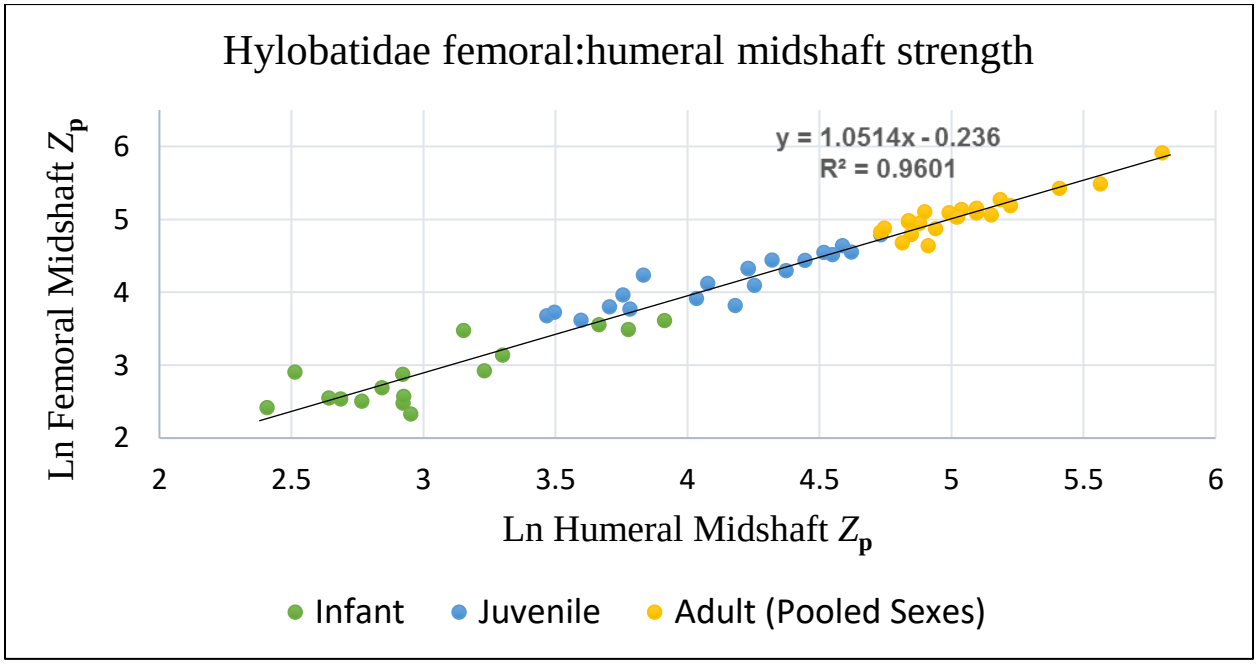

Fig. 4.3d. Log-log bivariate plot comparing Hylobatidae F/H over development. The allometric coefficient (slope) reveals a slightly positively allometric relationship, where the femur increases in strength relative to the humerus between infancy and juvenility.

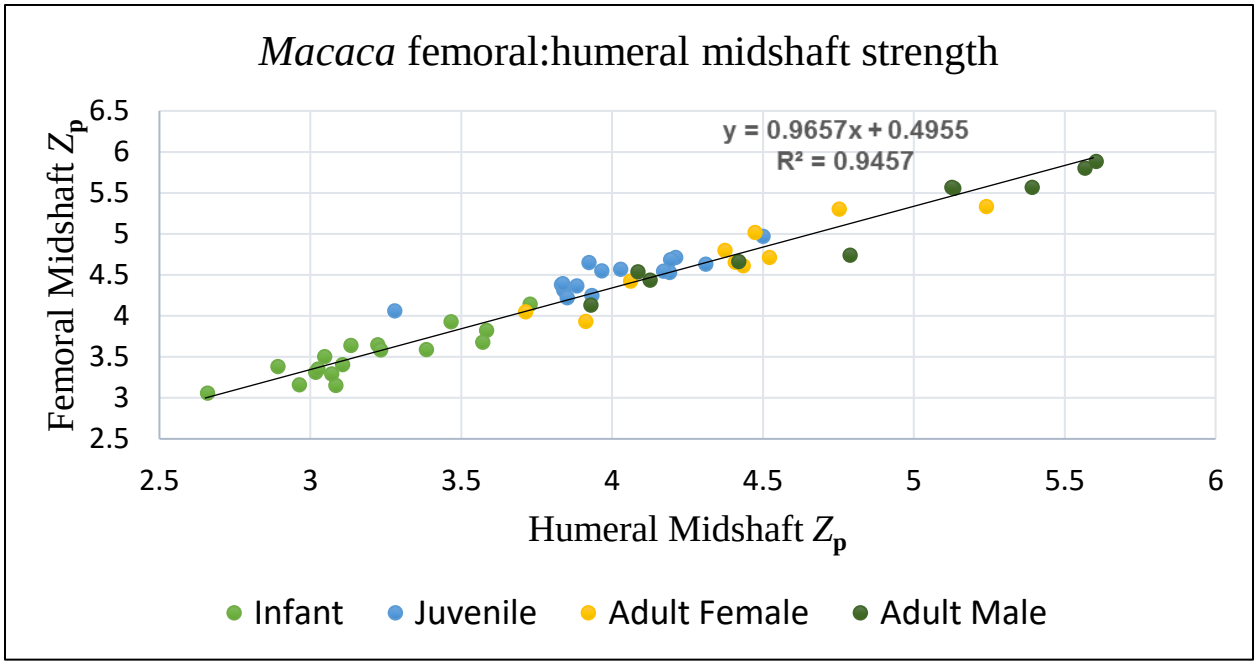

Fig. 4.3e. Log-log bivariate plot comparing *Macaca* F/H over development. The allometric coefficient (slope) reveals a slightly negative allometric relationship, where the femur initially increases in strength between infancy and juvenility but then equalises with the humerus by adulthood.

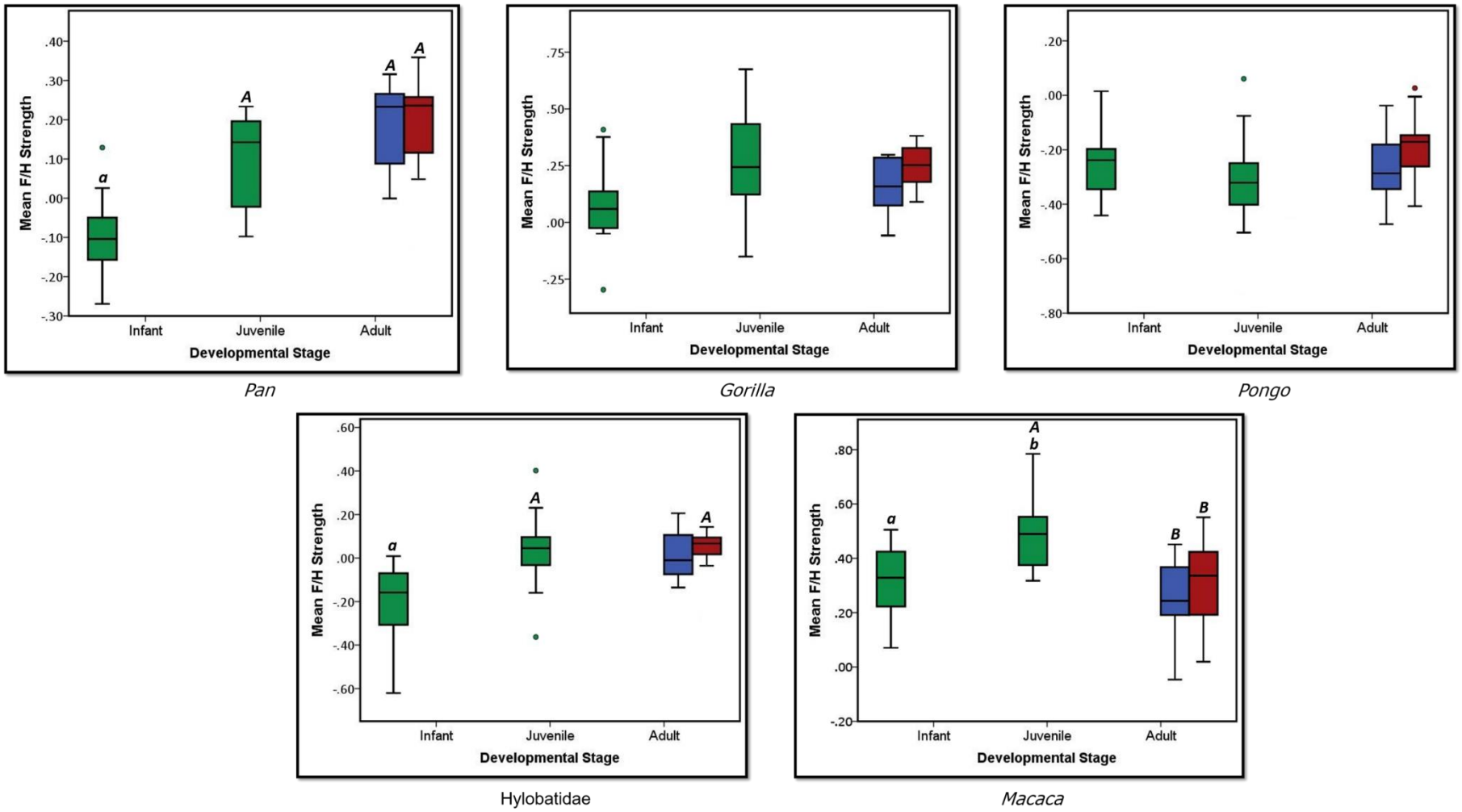

Fig 4.4. Box-and-whisker plot depicting femoral-to-humeral strength variation across development among the five sampled taxa. Male (blue) and female (red) adult sub-groups are discriminated while the immature sub-groups are shown in green. Boxes represent 25th – 75th percentile range of a given developmental subgroup. Horizontal darkened lines indicate the median while whiskers extend to the maximum and minimum values within 1.5 box lengths. Outliers are denoted by an 'o'. Statistically significant between-group relationships are labelled with corresponding lower case and capital letters above their respective whisker bars.

4.4.2 Mid-distal ulnar strength proportions

Descriptive statistics for ulnar strength are given in Table 4.4. Taxonomy was the only main effect to account for significant variance in both the infant (29.4%) and juvenile (22.9%) models (Tables 4.5a and 4.5b). By adulthood though, fixed factors including taxonomy, sex and their interaction effect, taxonomy*sex, each covaried significantly with ulnar strength (Table 4.5c). Taxonomic and sexual differences were not as pronounced along the ulna as they were between the femur and the humerus however, resulting in a relatively small effect size in each developmental model.

TABLE 4.4. Mean and standard deviation for mid- distal ulnar strength ratios (raw Z_p)

Development Stage/Sex	*Pan*	*Gorilla*	*Pongo*	Hylobatidae	*Macaca*
Infant	1.24 ± 0.33	1.62 ± 0.19	1.12 ± 0.3	1.4 ± 0.17	1.49 ± 0.33
Juvenile	1.41 ± 0.21	1.68 ± 0.22	1.52 ± 0.33	1.69 ± 0.25	1.89 ± 0.3
Adult Female	1.77 ± 0.16	2.32 ± 0.26	2.28 ± 0.3	2 ± 0.24	2.54 ± 0.42
Adult Male	1.75 ± 0.16	2.23 ± 0.2	1.96 ± 0.23	1.82 ± 0.23	1.8 ± 0.32

Polar section modulus mean and standard deviation for each taxonomic group by developmental stage.

TABLE 4.5a. Between-subject effects for strength (LnZ_p) of the infant mid- and distal ulna

Source	SS (II)[2]	df[3]	Mean Square	*F*	*P*[4]	Variance[5]
Corrected Model	1.74	10	0.17	3.4	**0.001**	0.358
Intercept	0.09	1	0.09	1713.2	0.185	0.029
Taxa	1.3	4	0.33	6.58	**0.0001**	0.294
Sex	0.001	1	0.001	.008	0.905	0.0001
Taxa*Sex	0.38	4	0.1	1.68	0.13	0.109
Ulnar 20% I_{max}/I_{min}[1]	9.25^{-005}	1	9.25^{-005}	.002	0.966	0.0001

[1] Distal ulnar circularity (I_{max}/I_{min}) was included as a covariate in the model to measure the effect size of section shape.
[2] Type II sum of squares.
[3] Degrees of freedom.
[4] Significance accepted at $P < 0.05$ and listed in bold font.
[5] Model variance expressed as partial eta squared (η_p^2).

TABLE 4.5b. Between-subject effects for strength (LnZ_p) of the juvenile mid- and distal ulna

Source	SS (II)[2]	df[3]	Mean Square	*F*	*P*[4]	Variance[5]
Corrected Model	1.09	10	0.1	3.07	**0.002**	0.286
Intercept	0.16	1	0.16	4.71	**0.033**	0.058
Taxa	0.8	4	0.2	5.71	**0.0001**	0.229
Sex	0.02	1	0.02	0.63	0.429	0.008
Taxa*Sex	0.12	4	0.03	0.87	0.486	0.043
Ulnar 20% I_{max}/I_{min}[1]	0.002	1	0.002	0.059	0.809	0.001

[1] Distal ulnar circularity (I_{max}/I_{min}) was included as a covariate in the model to measure the effect size of section shape.
[2] Type II sum of squares.
[3] Degrees of freedom.
[4] Significance accepted at $P < 0.05$ and listed in bold font.
[5] Model variance expressed as partial eta squared (η_p^2).

TABLE 4.5c. Between-subject effects for strength (LnZ_p) of the adult mid- and distal ulna

Source	SS (III)[2]	df[3]	Mean Square	*F*	*P*[4]	Variance[5]
Corrected Model	1.15	10	1.15	9.2	**0.0001**	0.508
Intercept	1.21	1	1.21	75.3	**0.0001**	0.458
Taxa	0.76	4	0.19	11.8	**0.0001**	0.346
Sex	0.43	1	0.43	26.9	**0.0001**	0.232
Taxa*Sex	0.31	4	0.08	4.8	**0.001**	0.179
Ulnar 20% I_{max}/I_{min}[1]	0.004	1	0.004	0.231	0.632	0.003

[1] Distal ulnar circularity (I_{max}/I_{min}) was included as a covariate in the model to measure the effect size of section shape.
[2] Type II sum of squares.
[3] Degrees of freedom.
[4] Significance accepted at $P < 0.05$ and listed in bold font.
[5] Model variance expressed as partial eta squared (η_p^2).

Among the hominoids, strength proportions varied across development, in that U50/U20 variation was most pronounced in infancy and adulthood, but was virtually indistinguishable between the juvenile taxonomic subgroups (Tables 4.6a – 4.6c). An inverse pattern was found between the hominoids and macaques, where no significant differences were identified among their respective infant or adult subgroups. Of the infant sample, gorillas exhibited stronger midshafts compared to the other taxa, though this difference was not significant when compared to macaques (Table 4.6a). By juvenility, gorilla midshaft dimensions remained static from infancy, while the other ape taxa displayed an increase in midshaft strength, revealing relatively equal U50/U20 values among the four hominoid groups (Figures 4.5a – 4.5e). The relatively low allometric coefficient exhibited by the macaques, despite a marked increase in their mid-ulnar strength by adulthood, may be an artefact of the sample's taxonomic and ecological diversity. Figures 4.6a and 4.6b help to illustrate the interspecific and sexual variation as both macaque species mature. The marked increase in gorilla mid-ulnar strength in adulthood distinguished them

from the chimpanzee and hylobatid subgroups, who distributed bone more proportionally between the distal and mid-ulna.

Intraspecifically, ulnar midshaft strength among all five taxonomic groups increased relative to the distal section either between infancy and juvenility, between juvenility and adulthood, or across all three stages. Adult male and female chimpanzees and gorillas displayed stronger midshafts than both their respective infant and juvenile counterparts. However, no difference in strength proportion was found between infancy and juvenility in either African ape taxon, unlike those observed between the humeral and femoral midshafts. Moreover, no difference in ulnar strength was found between male and female adult chimpanzees or gorillas either (Figure 4.7). The orangutan, hylobatid and macaque groups each exhibited significant increases in U50/U20 values over development but unlike the African apes, these taxa revealed an increase in ulnar midshaft strength between infancy and juvenility, as well as between juvenility and adulthood.

TABLE 4.6a. Mid- and distal ulnar strength (LnZ_p) ratio *post hoc* tests for pooled infants

	Pan	*Gorilla*	*Pongo*	Hylobatidae	*Macaca*
Pan	-	0.016	n.s	n.s	n.s
Gorilla	0.027	-	0.010	0.031	n.s
Pongo	n.s	0.010	-	n.s	n.s
Hylobatidae	n.s	0.031	n.s	-	n.s
Macaca	n.s	n.s	n.s	n.s	-

Significant values accepted at $P < 0.05$ and given in the table, non-significant values denoted by n.s.

TABLE 4.6b. Mid- and distal ulnar strength ($\ln Z_p$) ratio *post hoc* tests for pooled juveniles

	Pan	*Gorilla*	*Pongo*	Hylobatidae	*Macaca*
Pan	-	n.s	n.s	n.s	0.001
Gorilla	n.s	-	n.s	n.s	n.s
Pongo	n.s	n.s	-	n.s	0.004
Hylobatidae	n.s	n.s	n.s	-	n.s
Macaca	0.001	n.s	0.004	n.s	-

Significant values accepted at $P < 0.05$ and given in the table, non-significant values denoted by n.s.

TABLE 4.6c. Mid- and distal ulnar strength ($\ln Z_p$) ratio *post hoc* tests for pooled adults

	Pan	*Gorilla*	*Pongo*	Hylobatidae	*Macaca*
Pan	-	0.0001	0.0001	n.s	n.s
Gorilla	0.0001	-	n.s	0.001	n.s
Pongo	0.0001	n.s	-	n.s	n.s
Hylobatidae	n.s	0.001	n.s	-	n.s
Macaca	n.s	n.s	n.s	n.s	-

Significant values accepted at $P < 0.05$ and given in the table, non-significant values denoted by n.s.

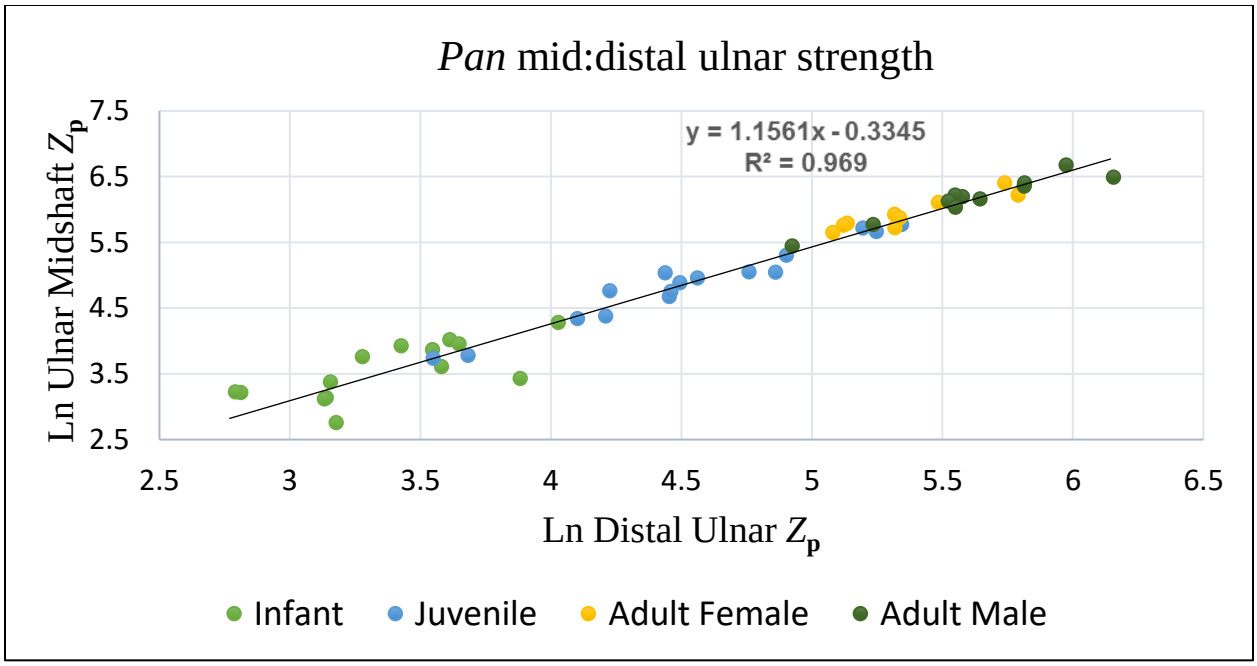

Fig. 4.5a. Log-log bivariate plot comparing chimpanzee U50/U20 over development. The allometric coefficient (slope) reveals a positive allometric relationship, where the midshaft increases in strength relative to the distal diaphysis between infancy and adulthood.

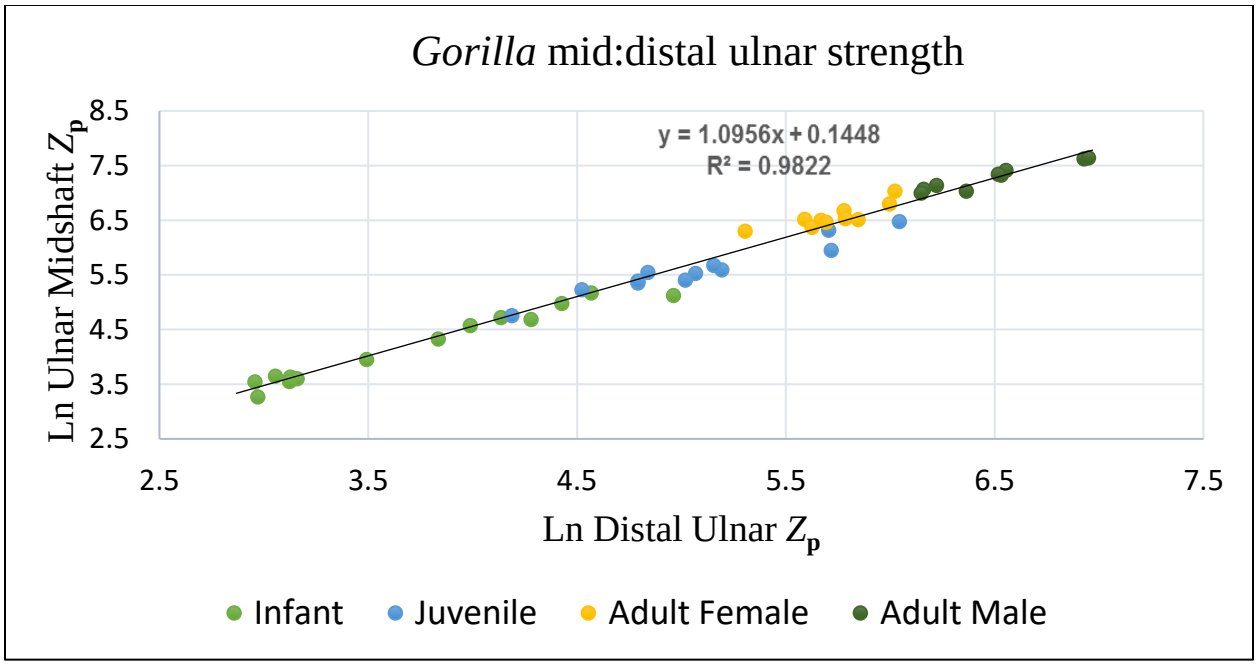

Fig. 4.5b. Log-log bivariate plot comparing gorilla U50/U20 over development. The allometric coefficient (slope) reveals a positive allometric relationship, where the midshaft increases in strength relative to the distal diaphysis between infancy and adulthood.

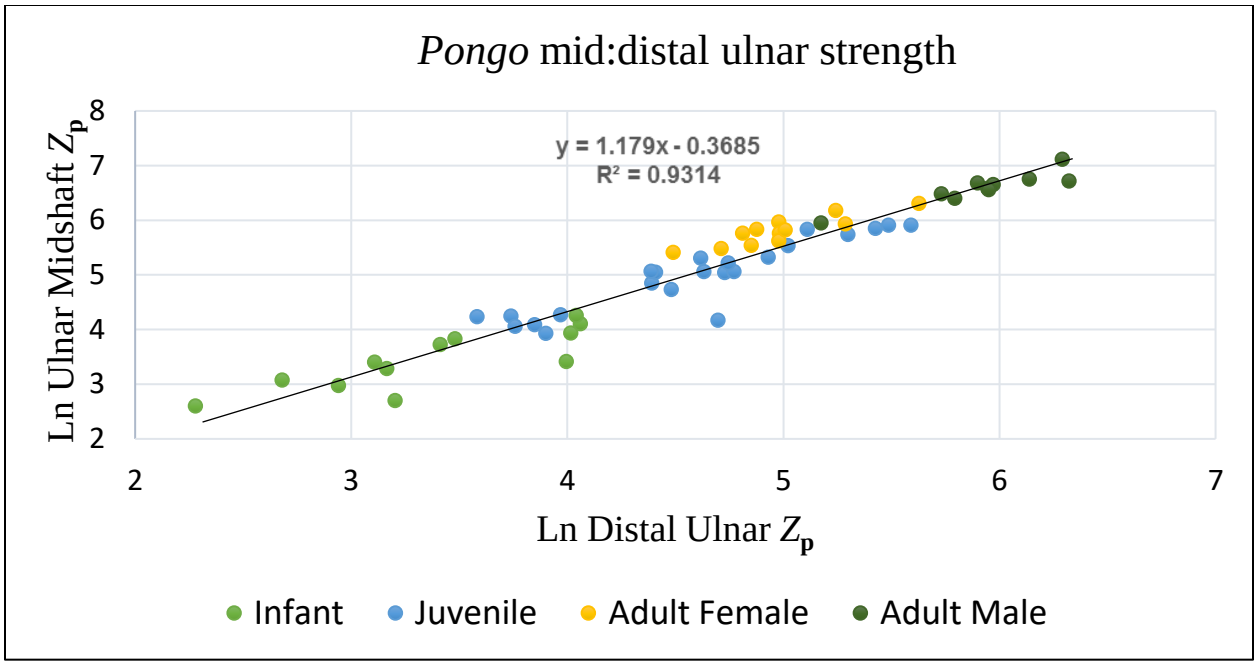

Fig. 4.5c. Log-log bivariate plot comparing orangutan U50/U20 over development. The allometric coefficient (slope) reveals a positive allometric relationship, where the midshaft increases in strength relative to the distal section between infancy and adulthood.

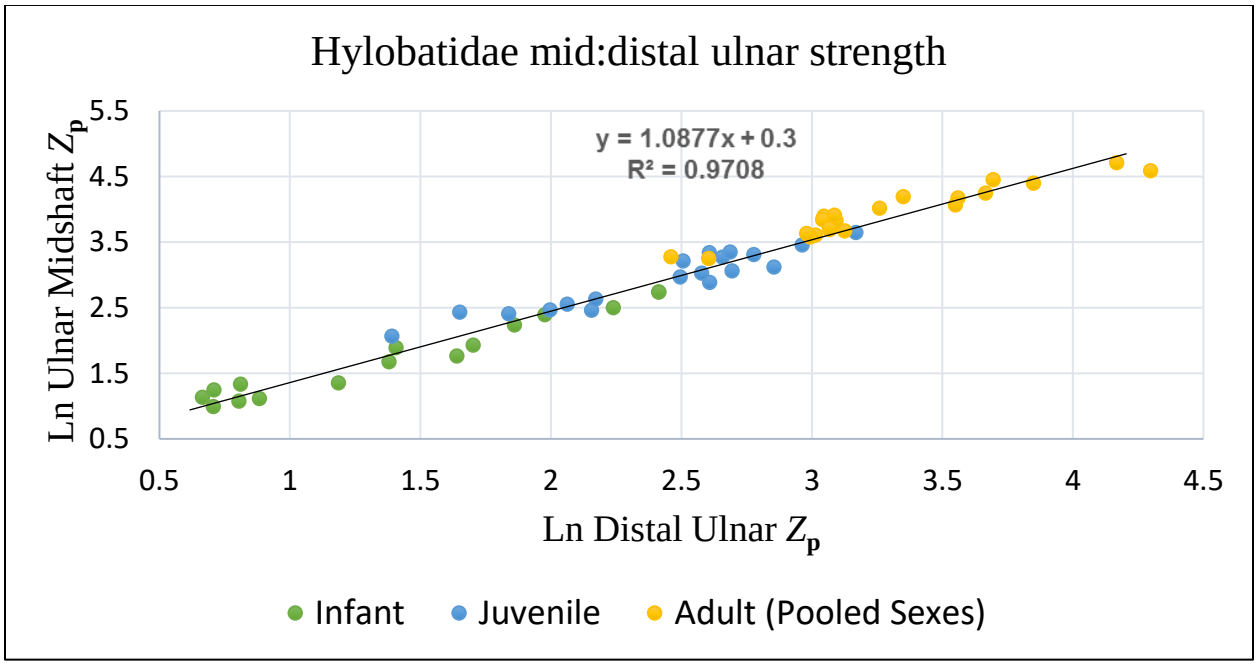

Fig. 4.5d. Log-log bivariate plot comparing hylobatid U50/U20 over development. The allometric coefficient (slope) reveals a positive allometric relationship, where the midshaft increases in strength relative to the distal diaphysis between infancy and adulthood.

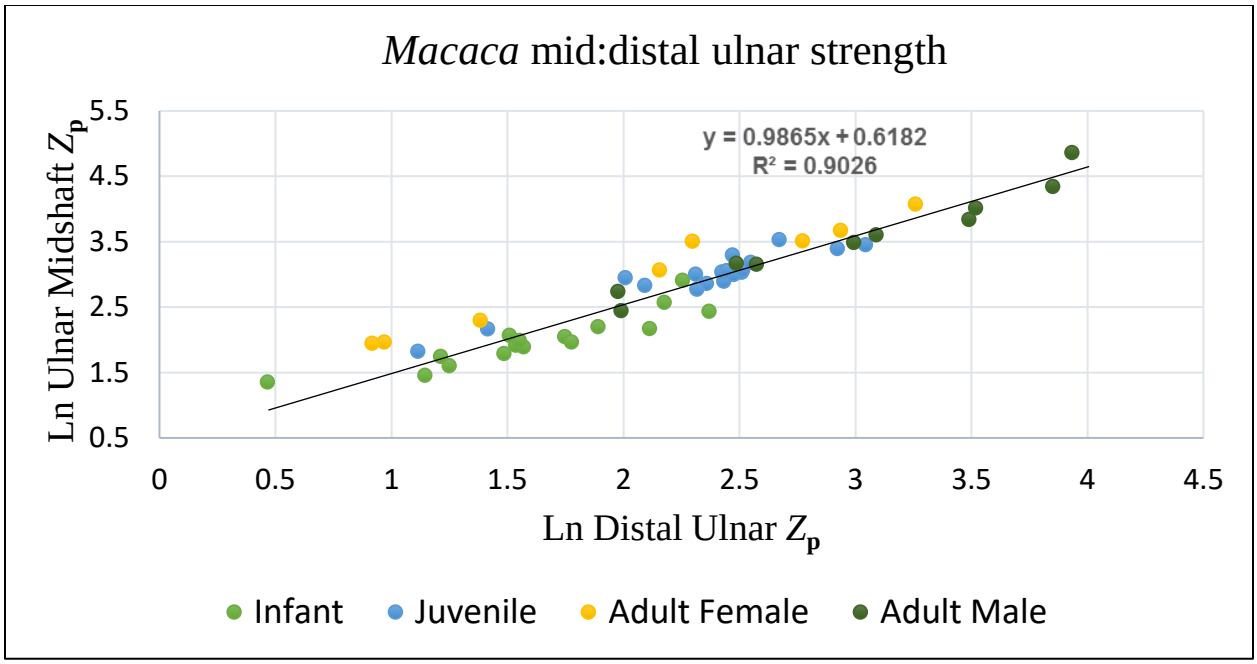

Fig. 4.5e. Log-log bivariate plot comparing macaque U50/U20 over development. The allometric coefficient (slope) reveals a virtually isometric relationship, where the midshaft increases in strength in juvenility and remains stronger relative to the distal diaphysis between through to adulthood.

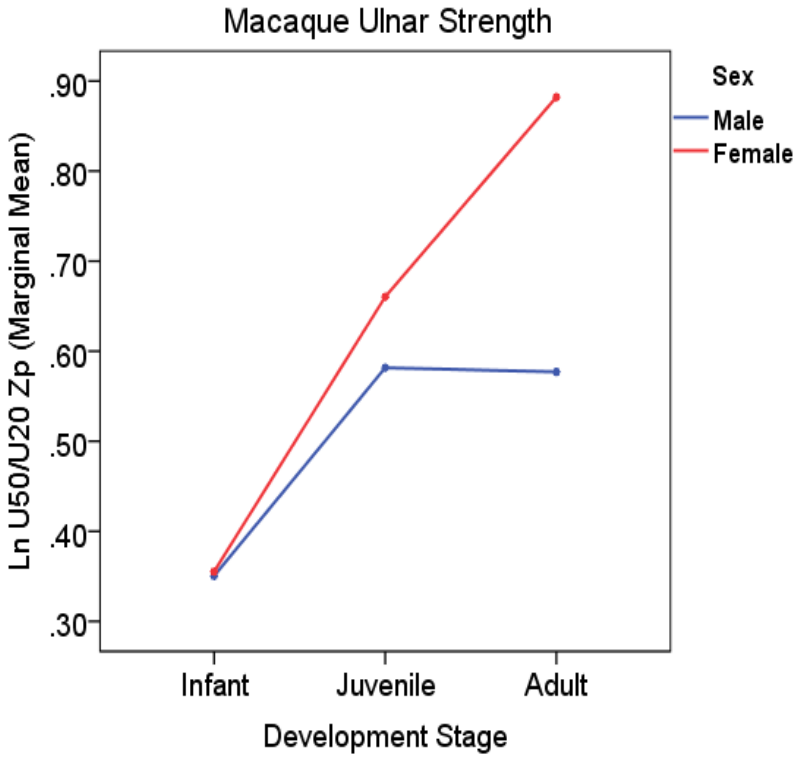

Fig. 4.6a Linear plot describing the significant variation between adult male and female macaque ulnar proportions. *M. mulatta* and *M. fascicularis* are combined. Distal ulnar shape (I_{max}/I_{min}) was accounted for as a covariate in the model (U = 1.39).

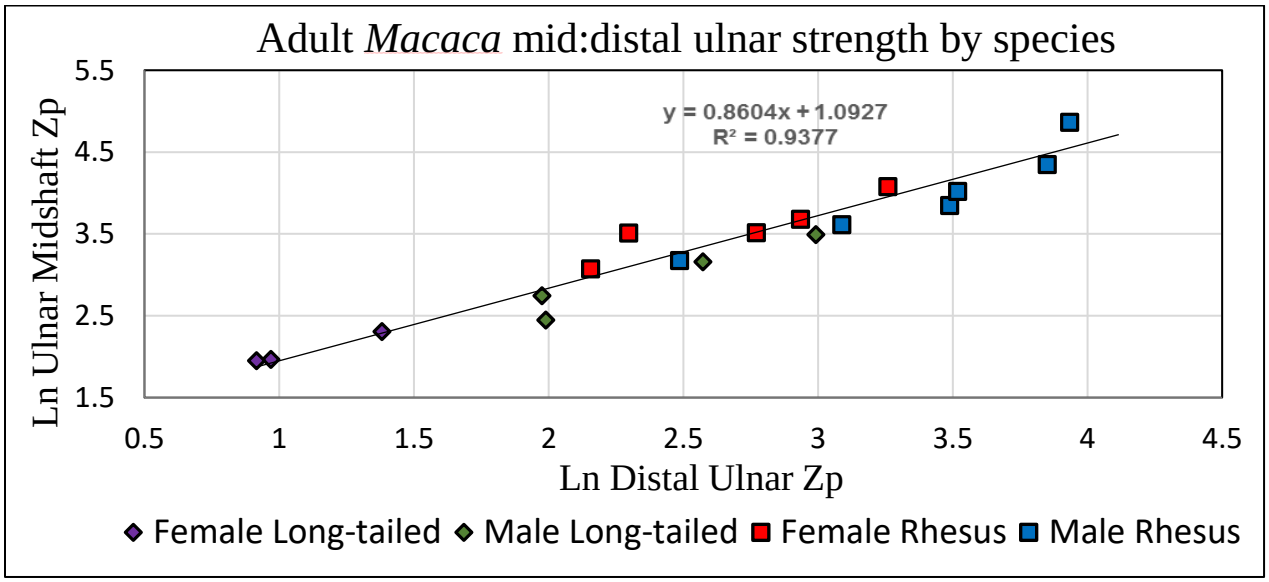

Fig. 4.6b. Log-log bivariate plot comparing ulnar proportions (U50/U20) in adult rhesus and long-tailed macaque species.

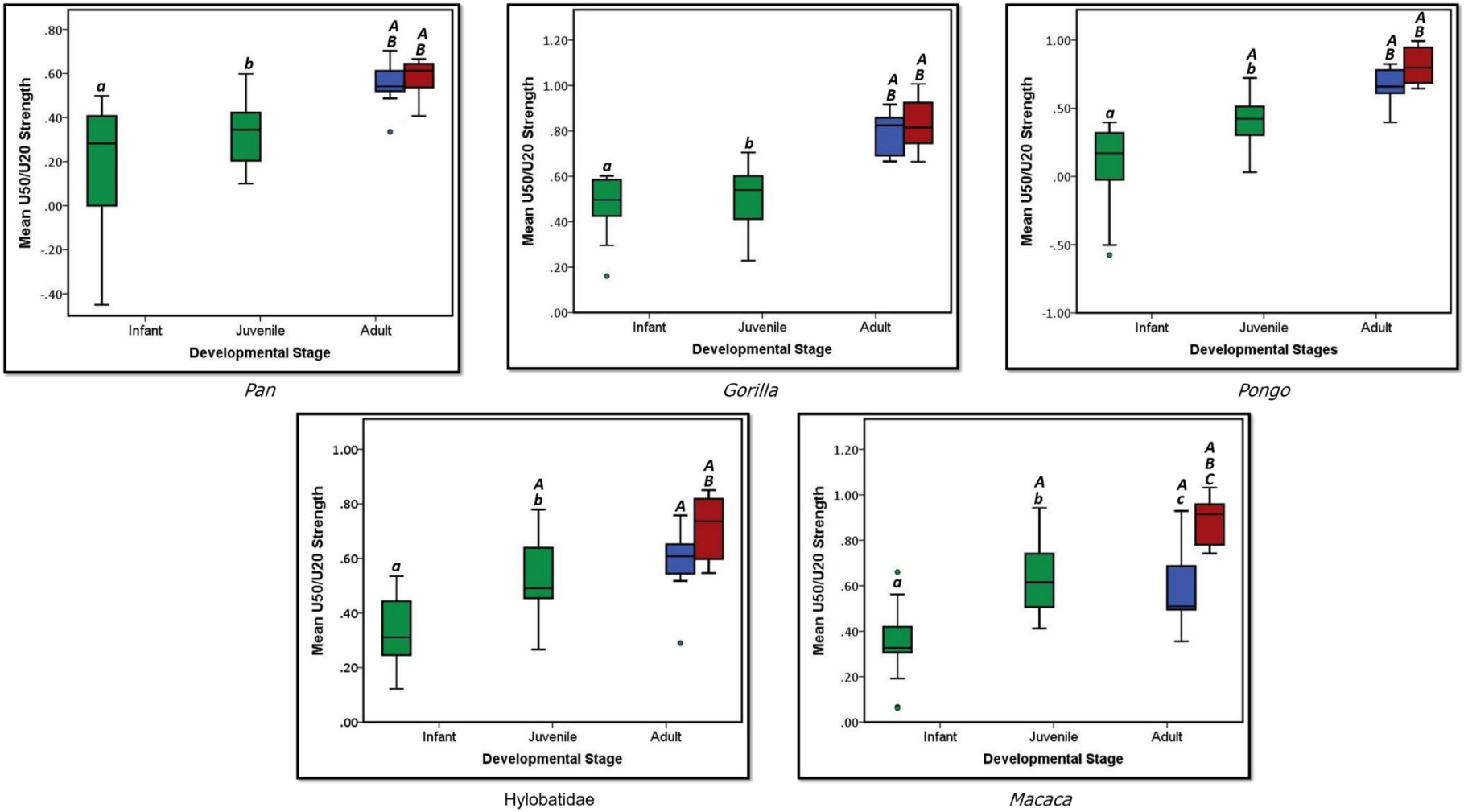

Fig 4.7. Box-and-whisker plot depicting mid-to-distal ulnar strength variation across development among the five sampled taxa. Male (blue) and female (red) adult sub-groups are discriminated while the immature sub-groups are shown in green. Boxes represent 25th – 75th percentile range of a given developmental subgroup. Horizontal darkened lines indicate the median while whiskers extend to the maximum and minimum values within 1.5 box lengths. Outliers are denoted by an 'o'. Statistically significant between-group relationships are labelled with corresponding lower case and capital letters above their respective whisker bars.

4.4.3 Mid- distal tibial strength proportions

Descriptive statistics for intra-element T50/T20 strength ratios are given in Table 4.7. Unlike the U50/U20 between-subject effects, T50/T20 sexual differences did not account for significant variation in any of the three developmental models. That said, taxonomic differences accounted for a greater effect size at each stage of development between infancy (8.7%) and adulthood (67.2%) (Tables 4.8a – 4.8c). The interaction between taxa and sex was deemed non-significant in each of the developmental models.

TABLE 4.7. Mean and standard deviation for mid- distal tibial strength ratios (raw Z_p)

Development Stage/Sex	*Pan*	*Gorilla*	*Pongo*	Hylobatidae	*Macaca*
Infant	0.78 ± 0.21	0.69 ± 0.06	0.69 ± 0.12	0.86 ± 0.22	0.93 ± 0.11
Juvenile	0.82 ± 0.11	0.75 ± 0.1	0.8 ± 0.14	1.16 ± 0.18	1.06 ± 0.09
Adult Female	0.95 ± 0.12	0.81 ± 0.12	1.01 ± 0.09	1.44 ± 0.23	1.26 ± 0.15
Adult Male	0.92 ± 0.15	0.76 ± 0.07	1.01 ± 0.15	1.39 ± 0.24	1.28 ± 0.14

Polar section modulus mean and standard deviation for each taxonomic group by developmental stage.

TABLE 4.8a. Between-subject effects for strength (LnZ_p) of the infant mid- and distal tibia

Source	SS (II)[2]	df[3]	Mean Square	*F*	*P*[4]	Variance[5]
Corrected Model	1.81	10	0.118	2.49	**0.014**	0.297
Intercept	0.13	1	0.129	2.71	0.104	0.044
Taxa	0.27	4	0.066	1.4	0.244	0.087
Sex	0.002	1	0.002	0.04	0.85	0.001
Taxa*Sex	0.2	4	0.051	1.08	0.376	0.068
Tibial 20% I_{max}/I_{min}[1]	0.04	1	0.39	0.83	0.366	0.014

[1] Distal tibial circularity (I_{max}/I_{min}) was included as a covariate in the model to measure the effect size of section shape.
[2] Type II sum of squares.
[3] Degrees of freedom.
[4] Significance accepted at $P < 0.05$ and listed in bold font.
[5] Model variance expressed as partial eta squared (η_p^2).

TABLE 4.8b. Between-subject effects for strength (LnZ_p) of the juvenile mid- and distal tibia

Source	SS (II)[2]	df[3]	Mean Square	*F*	*P*[4]	Variance[5]
Corrected Model	2.8	10	0.28	12.6	**0.0001**	0.616
Intercept	1	1	1	45.7	**0.0001**	0.367
Taxa	1.14	4	0.28	12.9	**0.0001**	0.395
Sex	0.01	1	0.01	0.25	0.622	0.003
Taxa*Sex	0.11	4	0.03	1.23	0.306	0.059
Tibial 20% I_{max}/I_{min}[1]	0.08	1	0.08	3.8	0.056	0.046

[1] Distal tibial circularity (I_{max}/I_{min}) was included as a covariate in the model to measure the effect size of section shape.
[2] Type II sum of squares.
[3] Degrees of freedom.
[4] Significance accepted at $P < 0.05$ and listed in bold font.
[5] Model variance expressed as partial eta squared (η_p^2).

TABLE 4.8c. Between-subject effects for strength (Z_p) of the adult mid- and distal tibia

Source	SS (II)[2]	df[3]	Mean Square	*F*	*P*[4]	Variance[5]
Corrected Model	4.67	10	0.47	22.5	**0.0001**	0.704
Intercept	0.74	1	0.74	35.9	**0.0001**	0.274
Taxa	4.03	4	1.01	48.7	**0.0001**	0.672
Sex	0.02	1	0.02	0.8	0.385	0.008
Taxa*Sex	0.02	4	0.01	0.23	0.919	0.01
Tibial 20% I_{max}/I_{min}[1]	0.02	1	0.001	0.05	0.828	0.0001

[1] Distal tibial circularity (I_{max}/I_{min}) was included as a covariate in the model to measure the effect size of section shape.
[2] Type II sum of squares.
[3] Degrees of freedom.
[4] Significance accepted at $P < 0.05$ and listed in bold font.
[5] Model variance expressed as partial eta squared (η_p^2).

Strength proportions along the tibial diaphysis were more variable between the primate groups compared to the mid-ulnar strength increase found among all five taxa. However, these differences were not discernible in infancy. For instance, the T50/T20 ratios of the five infant subgroups were all below 1.0, indicative of stronger distal sections relative to the tibial midshaft across taxa (Table 4.7 and 4.9a). By juvenility though, the same pattern was not recognisable, as hylobatids and macaques each displayed a significant increase in strength at the mid-tibia, while chimpanzees and gorillas did not reveal any change in strength proportions following infancy (Tables 4.9a – 4.9c). Growth trajectories along the tibia complement these findings by illustrating the degree of proportional strength change as each taxon matures (Figures 4.8a – 4.8e). Adult hylobatids and macaques possessed significantly greater T50/T20 values compared to the great apes, who did not reinforce their mid-tibiae to the same degree. Tibial strength ratios did not vary between the three great ape taxa among infant and juvenile groups at all (Tables 4.9a and 4.9b). It was only among adults that strength proportions were distinguishable among the hominids, where gorillas exhibited significantly stronger distal, relative to mid-tibiae, compared to chimpanzees

and orangutans (Figure 4.8). Orangutans, by comparison, displayed the greatest T50/T20 values of the great apes, with both males and females reinforcing their midshafts to a greater degree in adulthood compared to infancy.

TABLE 4.9a. Mid- and distal tibial strength (LnZ_p) ratio *post hoc* tests for pooled infants

	Pan	*Gorilla*	*Pongo*	Hylobatidae	*Macaca*
Pan	-	n.s	n.s	n.s	n.s
Gorilla	n.s	-	n.s	n.s	0.0001
Pongo	n.s	n.s	-	n.s	0.002
Hylobatidae	n.s	n.s	n.s	-	n.s
Macaca	n.s	0.0001	0.002	n.s	-

Significant values accepted at $P < 0.05$ and given in the table, non-significant values denoted by n.s.

TABLE 4.9b. Mid- and distal tibial strength (LnZ_p) ratio *post hoc* tests for pooled juveniles[1]

	Pan	*Gorilla*	*Pongo*	Hylobatidae	*Macaca*
Pan	-	n.s	n.s	0.0001	0.0001
Gorilla	n.s	-	n.s	0.0001	0.0001
Pongo	n.s	n.s	-	0.0001	0.0001
Hylobatidae	0.0001	0.0001	0.0001	-	n.s
Macaca	0.0001	0.0001	0.0001	n.s	-

Significant values accepted at $P < 0.05$ and given in the table, non-significant values denoted by n.s.

TABLE 4.9c. Mid- and distal tibial strength (LnZ_p) ratio *post hoc* tests for pooled adults

	Pan	*Gorilla*	*Pongo*	Hylobatidae	*Macaca*
Pan	-	0.007	n.s	0.0001	0.0001
Gorilla	0.007	-	0.0001	0.0001	0.0001
Pongo	n.s	0.0001	-	0.0001	0.0001
Hylobatidae	0.0001	0.0001	0.0001	-	n.s
Macaca	0.0001	0.0001	0.0001	n.s	-

Significant values accepted at $P < 0.05$ and given in the table, non-significant values denoted by n.s.

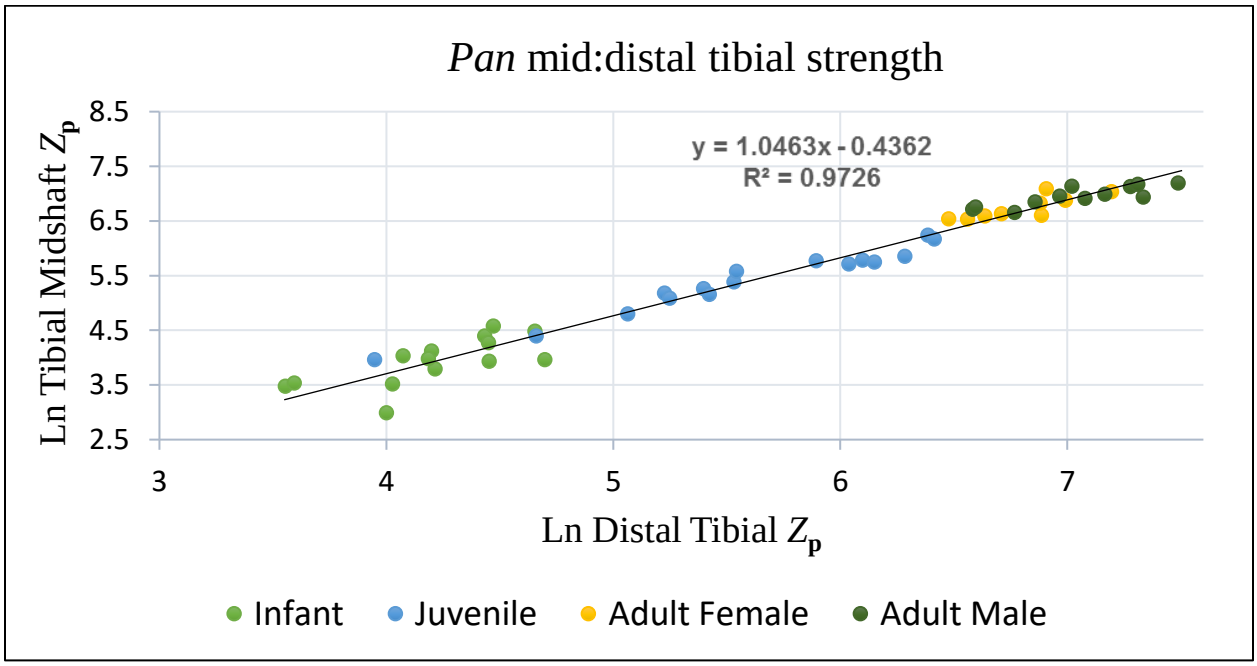

Fig. 4.8a. Log-log bivariate plot comparing *Pan* mid- and distal tibial strength (T50/T20) over development. The allometric coefficient (slope) reveals a slightly positively allometric relationship, where the midshaft increases in strength relative to the distal diaphysis between infancy and adulthood.

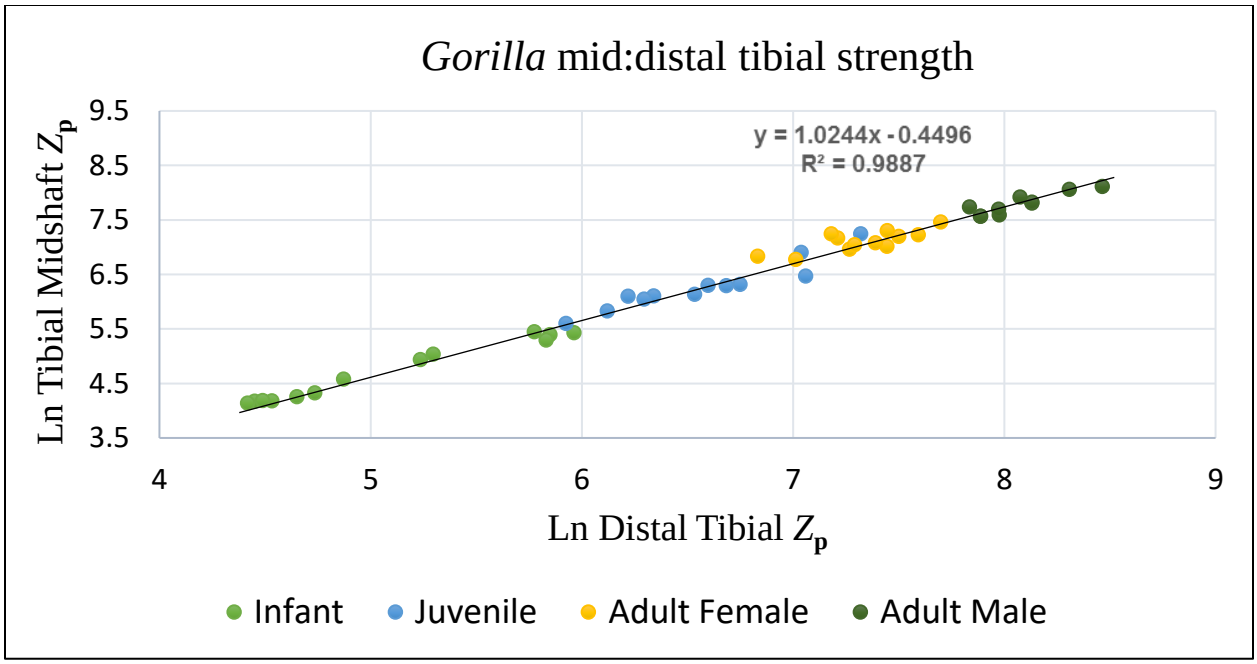

Fig. 4.8b. Log-log bivariate plot comparing *Gorilla* mid- and distal tibial strength (T50/T20) over development. The allometric coefficient (slope) reveals a virtually isometric relationship, where midshaft and distal strength remain roughly static between infancy and adulthood.

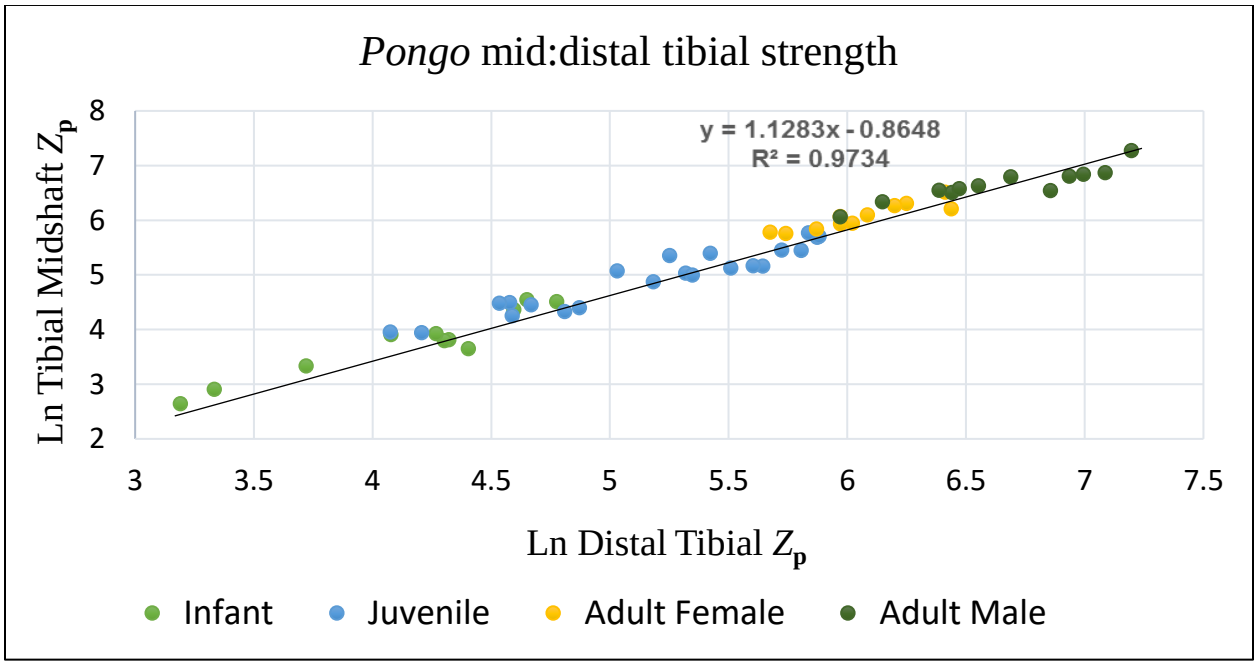

Fig. 4.8c. Log-log bivariate plot comparing *Pongo* mid- and distal tibial strength (T50/T20) over development. The allometric coefficient (slope) reveals a positive allometric relationship, where the midshaft increases in strength relative to the distal diaphysis between infancy and adulthood.

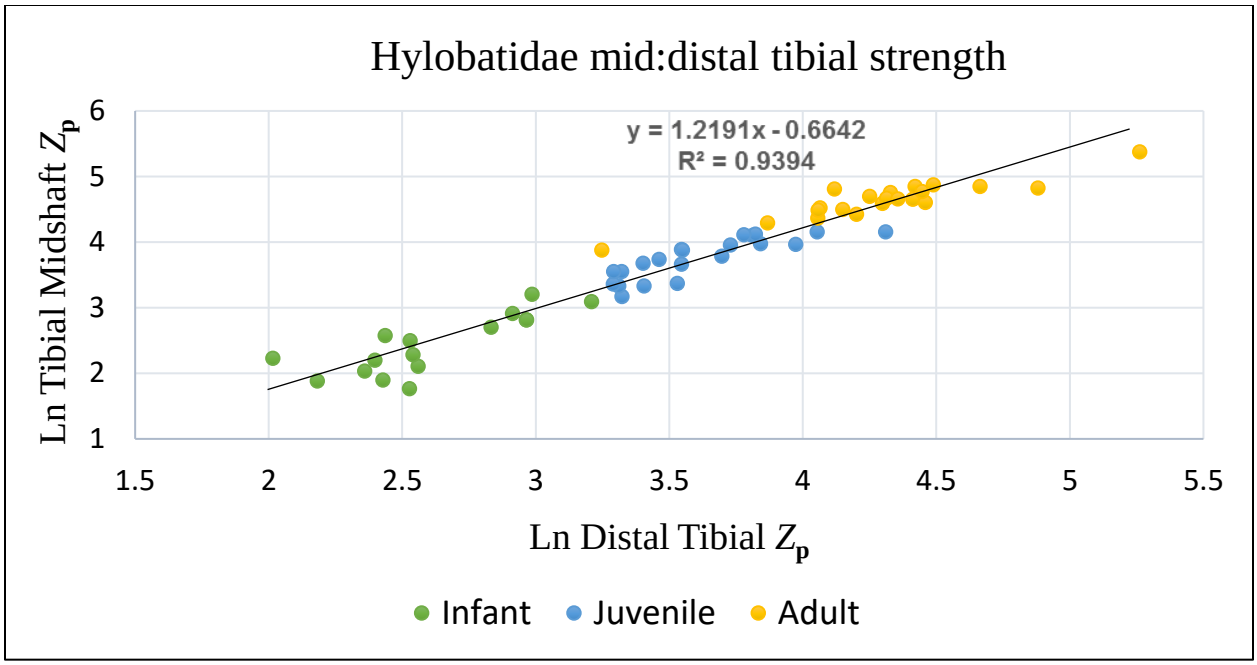

Fig. 4.8d. Log-log bivariate plot comparing Hylobatidae mid- and distal tibial strength (T50/T20) over development. The allometric coefficient (slope) reveals a positive allometric relationship, where the midshaft increases in strength relative to the distal diaphysis between infancy and adulthood.

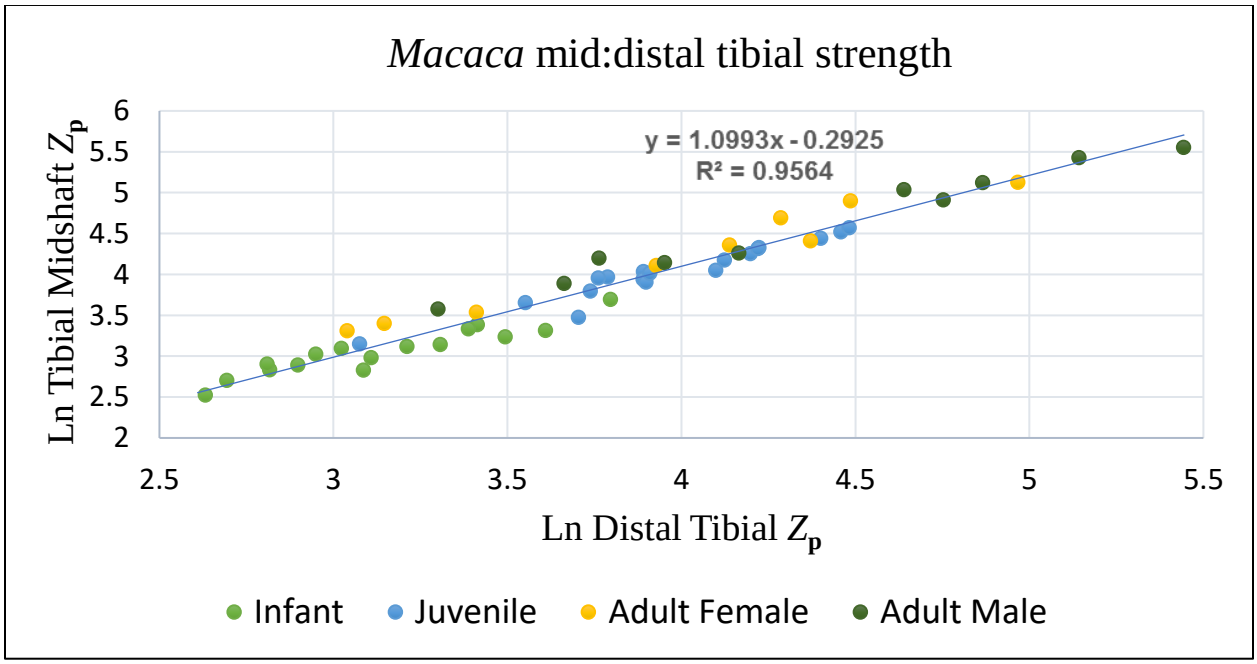

Fig. 4.8e. Log-log bivariate plot comparing *Macaca* mid- and distal tibial strength (T50/T20) over development. The allometric coefficient (slope) reveals a positive allometric relationship, where the midshaft increases in strength relative to the distal diaphysis between infancy and adulthood.

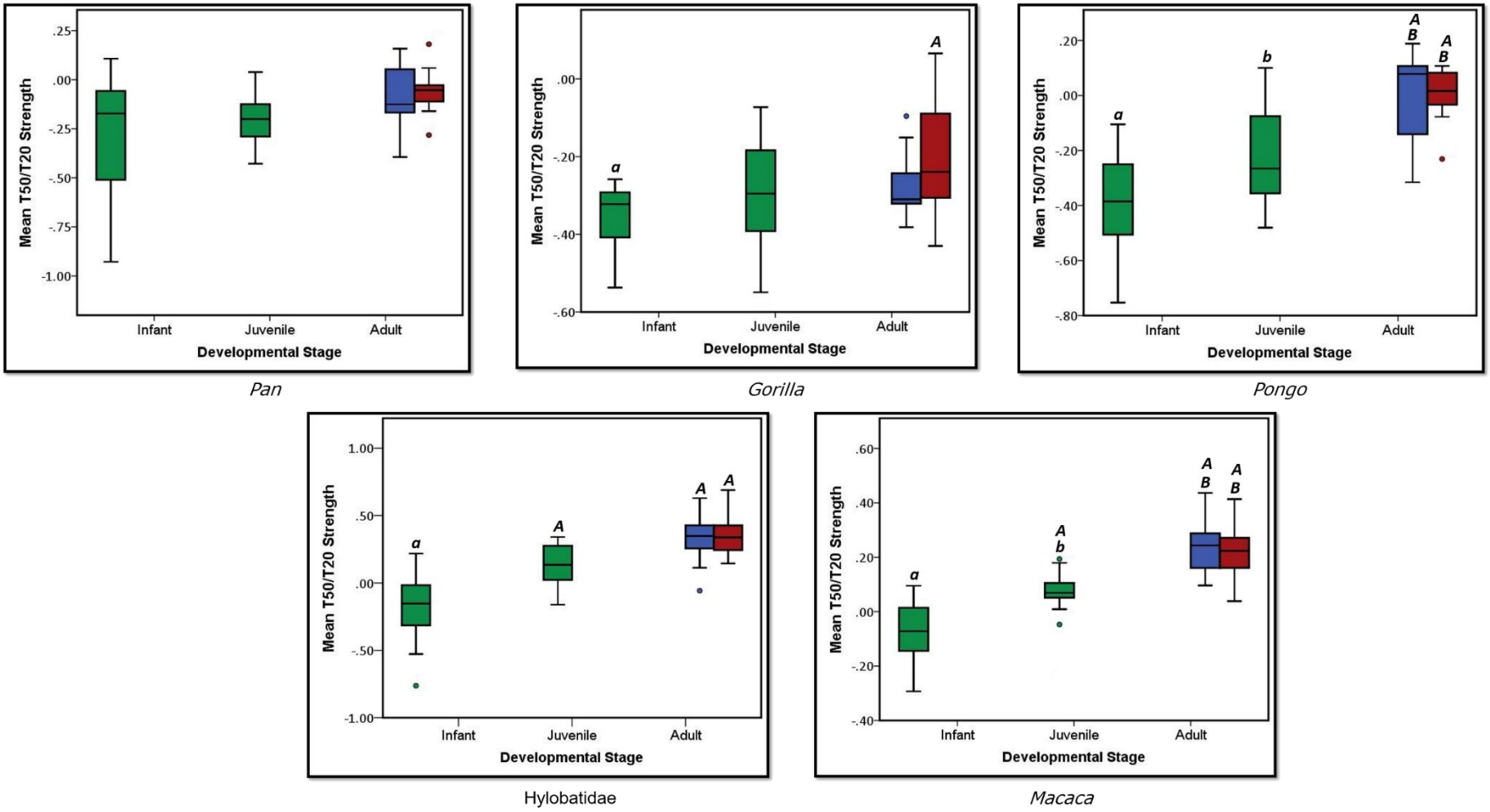

Fig 4.9. Box-and-whisker plot depicting mid-to-distal tibial strength variation across development among the five sampled taxa. Male (blue) and female (red) adult sub-groups are discriminated while the immature sub-groups are shown in green. Boxes represent 25th – 75th percentile range of a given developmental subgroup. Horizontal darkened lines indicate the median while whiskers extend to the maximum and minimum values within 1.5 box lengths. Outliers are denoted by an 'o'. Statistically significant relationships between-groups are labelled with corresponding lower case and capital letters above their respective whisker bars.

4.5 Discussion

In this chapter, limb strength proportions were compared among five primate ontogenetic series to measure how long bone cross-sectional strength changes over development. Cross-sectional ratios derived from the polar section modulus (Z_p) were generated between and within the elements of the fore- and hindlimb. To measure broader developmental strength changes between the limbs, femoral-to-humeral midshaft ratios were calculated. To measure changes along individual elements more precisely, Z_p ratios between the midshafts and more structurally constrained distal sections of the ulna and tibia were generated, respectively. Both the inter- and intra-limb comparisons helped illustrate the correspondence between locomotor behaviours and limb morphology in two different ways: comparisons of F/H underscored ontogenetic locomotor transitions particularly well. Ulnar comparisons highlighted morphological changes that may reflect adaptive responses to habitual loading as well but the sample-wide increase in strength proportions, combined with the load-sharing role of the radius makes the interpretation of the ulnar results more complex. Tibial strength comparisons also appear to elicit behavioural signals along the diaphysis but may serve as a better index for body mass across the sample.

4.5.1 Strength ontogeny between the limbs

Femoral-to-humeral ratios closely correlate with ontogenetic locomotor transitions, where increases in strength are identified in limbs primarily responsible for propulsion. The relatively strong femora exhibited by macaques, for instance, differentiated them from all four hominoid taxa among the infant and juvenile subgroups. By adulthood though, F/H values between the macaques and both African ape genera were comparable, which may be explained by the quadrupedal postures exhibited by the three taxa in adulthood. The locomotor ontogeny of rhesus macaques fluctuates considerably after infants achieve locomotor independence. Juvenile conspecifics in particular, exhibit more frequent arboreal quadrupedal behaviours compared to any other developmental stage, steadily transitioning into more terrestrial behaviours in adulthood (Rawlins, 1976). Fore- and hindlimb strength proportions in the macaque sample reflected these transitions, where F/H values were greater among juveniles than both infants and adults (male and

female). Just as juveniles spend a majority of their activity time exploring and playing in an arboreal context while navigating variable support surfaces, locomotor behaviour among infants and adults is comparatively terrestrial (Wells and Turnquist, 2001). Infants tend to approach new supports cautiously, staying close to their mothers on the ground, while both adult males and females adopt a more sedentary terrestrial lifestyle following juvenility (Wells and Turnquist, 2001). Macaque limb development is also reflective of the forelimb-to-hindlimb-dominant transition shared with other primate hindlimb locomotors (Kimura et al., 1979; Reynolds, 1985a; Demes et al., 1994; Schmitt, 1994). For instance, rhesus macaque body segment lengths and weights change rapidly during infancy, orienting their centre of mass from the head and torso more caudally and inferiorly on the body (Turnquist and Wells, 1994). The similar fore- to hindlimb locomotor transition assumed by chimpanzees and gorillas (Doran, 1992a,b; 1996, 1997; Doran and Hunt, 1994; Remis, 1999; Masi, 2004; Sarringhaus et al., 2014) may help explain the F/H dimensions they share with macaques by the time all three taxa reach skeletal maturity, despite their disparate orthograde and pronograde postures. While adult chimpanzees, gorillas and macaques each exhibit distinctly different forms of quadrupedal locomotion (Schmitt and Larson, 1995; Hunt et al., 1996; Kivell and Schmitt, 2009), the fundamental mechanics behind their gaits are analogous, where the hindlimb propels the body forward and is both directed and checked by the forelimb (Kimura, 1992). Ultimately, the differences between macaque palmigrady and the two distinct forms of knuckle-walking exhibited by African apes appear negligible in relation to the fore- and hindlimb strength proportions they develop in adulthood, as a strong femur relative to humerus may be a general pattern associated with a quadrupedally-driven gait. As such, quadrupedal primates may differ from one another in their long bone cross-sectional shape, but may share a broader fore- to hindlimb strength configuration by the time their bones are fully developed, irrespective of phylogenetic affinity. If F/H values are similar across other quadrupedal primates as they mature, it would help clarify whether a stronger femur relative to humerus is a mechanical adaptation for a propulsive hindlimb. This signal may further supersede sub- and superstrate types, as the macaque footfall pattern and locomotor behaviour in general are similar between large-diameter branches and the ground (Dunbar, 1989). The fact that a stronger femur is not necessarily as pronounced before adulthood should be considered when interpreting posture among immature fossil individuals as well.

Though chimpanzee and gorilla limb strength proportions are similar, the developmental strategies they employ to achieve their stronger hindlimb-to-forelimb skeletal configuration is seemingly different. For instance, a relatively late transition in locomotor posture in chimpanzees, but not gorillas (despite both taxa exhibiting more quadrupedal and less suspensory behaviours with increasing size and age) (Doran, 1997) can help explain how both African apes grow. In particular, the significant increase in femoral strength exhibited by chimpanzees between infancy and adulthood mirrored the transition between climbing and suspensory-dominant, to terrestrial quadrupedal-dominant locomotor behaviours (Sarringhaus et al., 2014). Gorilla F/H values remained consistent between infancy and adulthood, despite undergoing a similar change in locomotor behaviour following their second year of life. The relative timing of these transitions is key in explaining the significant limb strength changes present in *Pan*, but absent in *Gorilla* (Figure 4.10). Though both African apes dedicate most of their locomotor time to climbing and suspensory behaviour in their first five months, infant chimpanzees and gorillas differ significantly in their frequency and use of substrates (Doran, 1997). Moreover, chimpanzees do not adapt their locomotor pattern substantially until they reach the age of two, while gorillas adopt a quadrupedal-dominant locomotor profile before two, due to their comparatively greater body mass (Doran, 1997). The static F/H values observed across gorilla development may therefore act to serve the mechanical demands placed on the hindlimb early in infancy, when regular terrestrial quadrupedal locomotion begins. Chimpanzee femoral strength first exceeds that of the humerus by juvenility (2-5 years); around the same time the transition to a quadrupedal, hindlimb-dominant gait is adopted (Doran, 1997). Modern humans undergo a similar postural change, where femoral and humeral strength are virtually equal until the adoption of bipedality, when femoral strength exceeds the humerus and grows at a more rapid rate (Ruff, 2003a). Similar research has demonstrated that bone strengths and lengths do not develop linearly, suggesting that plastically adaptive and genetic mechanisms dictate long bone form discretely (Ruff et al., 2013; Sarringhaus et al., 2016). Humans, chimpanzees and gorillas share especially close ancestry among anthropoids, which is reflected in their morphological similarities (Schultz, 1924; Mann and Weiss, 1996; Young, 2003). Though it is possible that specific limb growth trajectories are an ontogenetic artefact of Homininae, the close correspondence between strength proportions and locomotor ontogeny support an adaptationist perspective to limb morphology: where bone strength

actively conforms to the unique mechanical demands placed on it at specific stages of development.

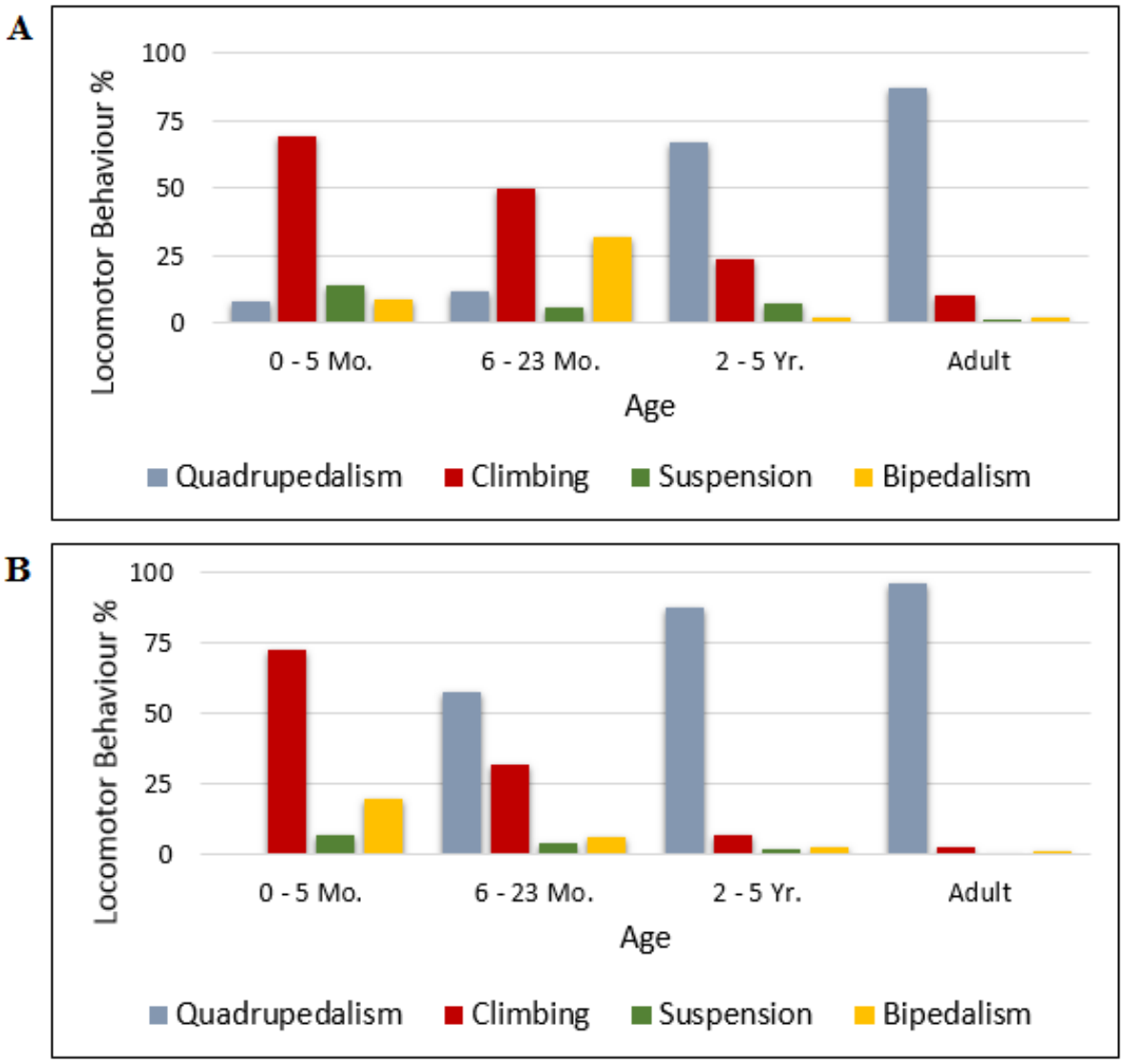

Fig. 4.10. Comparison of chimpanzee (**A**) and gorilla (**B**) locomotor behaviour frequency with age classification. Observational data was collected from the same general populations. Figure and data adapted from Doran (1997).

Further evidence for a mechanical interpretation of limb development was found in the F/H comparisons of the Asian apes. Orangutans and hylobatids have evolved markedly different locomotor strategies to negotiate generally similar environments (Gebo, 1996), as a solution to their distinct body sizes (Napier and Walker, 1967; Cartmill, 1985). While both apes rely on a relatively strong forelimb during suspension, the unique movements they use to navigate the canopy can inform about their growth trajectories. In infancy, the orangutan and hylobatid subgroups each exhibited stronger humeri compared to femora, consistent with an arboreal locomotor profile. Both taxa also have long immature periods and are highly dependent on parental care in infancy (van Adrichem et al., 2006; Lappan, 2008; Reichard et al., 2012), though the exceptionally slow life history of orangutans distinguishes them from the other apes (Charnov, 1993; Stearns, 2000; Wich et al., 2004; Leighton et al., 2014, but see van Noordwijk and van Schaik, 2005). Research on orangutan locomotor ontogeny has shown that while subadults transition between postures as they mature (van Adrichem et al., 2006) even infants can execute the complex substrate-crossing manoeuvres employed by adults (Chappell et al., 2015). Regardless of age or size, gap crossing is initiated by pulling branches or lianas from the destination tree (Chappell et al., 2015), granting an advantage to elongated (Schmitt and Larson, 1995), and as observed in this study, strong forelimbs. By executing similar locomotor behaviours across development, it is reasonable to assume that limb morphology would not vary dramatically with maturity in order to preserve their habitual locomotor patterns. Indeed, the strong forelimb configuration was found to persist in orangutans through to adulthood, in agreement with Shaw and Ryan's (2012) findings in adults, where individuals exhibited significantly greater humeral-to-femoral strength than the other sampled taxa.

Unlike the static F/H strength signal seen in orangutans, hylobatid limb trajectory changes significantly following infancy. For one, it was evident that a considerable increase in femoral strength occurred by juvenility, but not between juvenility and adulthood. Unfortunately, a lack of research on hylobatid locomotor ontogeny makes it difficult to make direct comparisons between behavioural transitions and limb morphology. Even so, extrapolating from known behaviours and life history events can place the observed limb proportional changes into context. Weaning in the lar (*Hylobates lar*) and hoolock gibbons (*Hoolock hoolock*), as well as siamangs (*S. syndactylus*), occurs at approximately two years of age (Harvey and Clutton-Brock, 1985; Pereira and Altman,

1985; but see Morino and Borries, 2016, for a discussion on extended dependence in siamangs), combined with parental carrying. These adult-infant interactions signify some degree of parental dependence among infants, and in accordance with the locomotor changes that follow weaning in *Pan* (Horvat and Kraemer, 1982; Doran, 1992a), *Gorilla* (Nowell and Fletcher, 2007), and *Pongo* (van Noordwijk and van Schaik, 2005), it is likely that hylobatids do not achieve complete locomotor independence during infancy. The significant increase in mid-femoral strength among the juvenile subgroup may therefore mark a behavioural change between infancy and juvenility where a transition to locomotor independence would be expected. The greater femoral-to-humeral strength configuration is then preserved through to adulthood. Specifically, spring-mass bipedalism and leaping behaviours occupy 4 – 12% and 6 – 15% of adult locomotor time in gibbons and siamangs (Carpenter, 1964; Whitmoor, 1975; Crompton et al., 2008). The comparatively similar humeral and femoral strength observed in juveniles and adults may therefore be a locomotor adaptation if bipedalism and leaping are, in fact, used with less frequency among infants. Further focal studies on hylobatid behavioural ontogeny are crucial to answering these questions. If leaping behaviours do increase among hylobatids following infancy, F/H ratios could serve as an accurate method in deciphering primate locomotor behaviour among specific taxa and at discrete developmental stages. Nevertheless, a high F/H value among a unique forelimb dominant locomotor repertoire like the brachiating hylobatids shows that the relationship between interlimb strength is not always straightforward.

4.5.2 Strength ontogeny along the elements: the ulna

Comparing dimensions along individual long bone elements granted a unique perspective into their growth. Like the F/H comparisons, ulnar ratios appear sensitive to ontogenetic locomotor behaviours and transitions, but also help illuminate how the structure of more adaptively constrained sections, like the distal diaphysis, covary with sections more disposed to bending deformation, like the midshaft.

The taxa-wide increase in mid- ulnar strength over development may be a highly canalised trait shared among primates. When bending forces act on a long bone, the midshaft mitigates peak strains to offset the risk of fracture (Biewener and Taylor, 1986; Currey, 2002). By contrast,

sections closer to articular surfaces transfer loads between elements, and thus, do not require the reinforcement of a thick cortex (Ruff and Runestad, 1992; McFarlin et al., 2008). Regardless of posture, it is apparent that a disproportionately stronger ulnar midshaft relative to distal diaphysis is a valuable adaptation following infancy in both hominoids and macaques. Aside from the general benefit of improved bending strength and rigidity at midshaft, explanation of the strong distal infant pattern is probably more complex. The interosseous membrane adjoining the ulna and radius stabilises the forearm during loading (Hotchkiss et al., 1989) and is also responsible for transferring loads proximally to the elbow (Rabinowitz et al., 1994). Though experimental research is lacking in extant primates, insight on forearm loading can be attained from human subjects. A study on force transfer along the forearm determined that during supination, the distal ulna supports approximately 32% of a given load compared to 68% in the distal radius (Birkbeck et al., 1997). The proximal sections of each bone, on the other hand, assume roughly equal capacity of the load as it is transferred proximally along the forearm (51% in the radius, 49% in the ulna) (Birkbeck et al., 1997). Because periosteal bone deposition serves to structurally reinforce vulnerable diaphyseal regions (Lieberman et al., 2003), the relatively light loads the distal ulna must support may explain why each taxon experiences a net increase in mid-ulnar strength relative to the distal section. This concept is further supported by the lack of ontogenetic and taxonomic shape variation found at the distal ulna, discussed in Chapter 3. Ultimately, a relative increase in ulnar midshaft strength appears advantageous across catarrhines and could serve as an example of an ancestral primate character if a similar configuration could be substantiated or falsified among developing platyrrhine and strepsirrhine taxa.

Despite the ontogenetic increase in U50/U20 values across the sample, interspecific variation was still discernible between taxa, but did not display as clear a pattern to that found in the inter-limb F/H comparisons. During infancy, gorillas exhibited significantly stronger midshafts relative to distal ulnar sections than any other infant hominoid subgroup. By juvenility though, the strength disparity between taxonomic groups disappears, largely due to a lack of dimensional change in the gorillas following infancy. Similar to the findings between their femora and humeri, maintaining strength dimensions in the ulna is likely a product of a conserved locomotor pattern in young gorillas. While forelimb-driven arboreal behaviours are more prominent among infant gorillas than at any other stage of their development, a majority of locomotor behaviour in the first

two years is dedicated to quadrupedalism (Doran, 1997). A more robust mid-ulna may therefore be necessary in aiding the hindlimb to support their mass during locomotion from around six months of age.

Infant macaques exhibited the most similar ulnar proportions to gorillas; the two most quadrupedal taxa in the sample (Grand, 1983; Wells and Tunrquist, 2001; Huang et al., 2015). The frequency of quadrupedal behaviours they share in conjunction with their vastly different body sizes implies a more mechanical than allometric effect may be responsible for the observed change in ulnar proportions in both taxa. The morphological changes that enable early locomotor independence in macaques develop within the first six months of birth, achieving adult body dimensions (but not size) by 18 months (Turnquist and Wells, 1994). Though linear skeletal dimensions appear to stabilise early in life, the comparisons made here suggest that macaque limb structure continues to change between infancy, juvenility and adulthood. The sexual variation between adult macaque ulnar proportions was statistically significant; a pattern not found in any other adult taxon (Figure 4.6a and 4.6b). For one, the higher U50/U20 values of adult females compared to males cannot be easily corroborated from a sexual dimorphic behavioural standpoint, as both sexes of *M. mulatta* and *M. fascicularis* share similar locomotor profiles, respective to species (Burr et al., 1989; Wells and Turnquist, 2001; Huang et al., 2015). The allometric effect of body size could be a factor contributing to sexual variation – as adult males of both species are considerably larger than females (*M. mulatta* female: 7.45kg, male: 10.95kg; *M. fascicularis* female: 4.85, male: 7.08kg) (Napier and Napier, 1967; Leigh, 1992; species mean mass calculated from Hamada et al., 2016) – though there is a lack of significant sexual variation between the other sampled sexually dimorphic taxa along the ulna. Rates of growth cessation and bimaturism between the two macaque species may also contribute in part to the observed variation but once again, compared to similar patterns in size found among the other taxa (Leigh, 1992), it is unlikely the primary cause. Instead, the variation is likely at least partially driven by interspecific noise within the macaque sample. Among the adult macaque subgroups, the highest U50/U20 values were identified among long-tailed macaques, while the lowest ratios were associated with rhesus macaques. Considering the close ancestry of the two species (Tosi, et al., 2002; Osada et al., 2008; Hamada et al., 2016), along with the overlap of ulnar dimensions in the subadult specimens, the morphological divergence found in adulthood may be related to the unique postures and loading

patterns exhibited by each species. In particular, the smaller long-tailed macaque spends less than 2% of its total time on the ground (Rodman, 1979), compared to rhesus macaques, who engage in terrestrial and arboreal locomotion more evenly (Rodman, 1979; Rodman and McHenry, 1980). Prior research on the two species also found that differences in their cross-sectional long bone dimensions corresponded to their respective arboreal and terrestrial behaviours in adulthood (Burr et al., 1989). Macaques are not the only genus to display interspecific locomotor differences among the sample, however. For instance, western lowland and mountain gorillas exhibit tangible locomotor differences, where the former species is relatively more arboreal than the latter, even in adulthood (Remis, 1999; Masi, 2004; Doran-Sheehy, 2009; but see Neufuss et al., 2017). Compared to the hominoids though, the markedly different sizes, ecologies and loading environments associated with rhesus and long-tailed macaques appears sufficient in influencing their ulnar dimensions in different ways. Due to the small sample size of each species and their respective sexes, a more comprehensive analysis on a larger macaque sample is necessary to determine the impact that behaviour places on their tibial and ulnar intra-limb proportions, though these initial results are encouraging that such a behavioural signal is capable of distinguishing differences between species in comparisons along single elements.

4.5.3 Strength ontogeny along the elements: the tibia

Interspecific comparisons along the tibia reflected a similar pattern of mid-ulnar strength increase exhibited by all five taxa. Despite this general developmental pattern however, taxa like the African apes maintained stronger distal sections from infancy into adulthood (Table 4.7). Moreover, tibial dimensions did not reveal a strong behavioural or phylogenetic signal across the infant subgroups, but went on to reflect moderate locomotor differences in juvenility, followed by the most discernible locomotor differences by adulthood. First, the lack of variation between the infant hominoids suggests that tibial proportions are generally similar early in life, irrespective of loading pattern. Second, the low T50/T20 ratios (below 1.0) among all five infant subgroups, suggests that distal dimensions must be relatively stronger than midshafts early in life. A generalised primate configuration along the tibia could afford several locomotor benefits to infants. One potential advantage is the ability to acclimate immature limbs to a new loading environment.

Young individuals can afford soft and cartilaginous elements because their function of body mass support is not imperative in infancy; instead, rapid growth is prioritised (White et al., 2012). It is not until juvenility that mechanical loading elicits a strong anabolic response for bone formation, followed by ossification and a rapid increase in linear growth (Bertram and Swartz, 1991; Robling et al., 2006). It follows that a generalised primate tibia in infancy can permit adequate mobility in a variety of locomotor contexts before the skeleton plastically conforms, and eventually, specialises its morphology in response to the loads it experiences (Haapasalo et al., 1996; Bass et al., 2002). Another reason a generalised tibial configuration may be beneficial to infants is the advantage of increased safety factors before ecological independence is achieved. A study on capuchin (*Cebus albifrons*: *C. apella*) limb bones found that size and Z_p values scale with negative allometry, so that cross-sectional strength peaks at birth (Young et al., 2010a), when arboreal species are more prone to falling injuries (van Lawick-Goodall, 1967; Morland, 1990; Dunbar and Badam, 1998). As locomotor competence improves with maturity, bone lengths are prioritised over robusticity (Main and Biewener, 2004, 2007; Young et al., 2010a); a trade-off which may subsequently improve agility and energy expenditure in more mature, locomotor proficient individuals. Indeed, declines in strength among comparatively terrestrial primates, which are less prone to falling injuries like baboons (*Papio cynocephalus*) (Ruff, 2003a) and gorillas (*G. beringei*; *G. gorilla*) (Ruff et al., 2013), are not as exaggerated as they are in arboreal capuchin monkeys (Young et al., 2010a). While all five infant subgroups exhibited low T50/T20 values, the relatively high ratio observed among the macaque sample could be attributed to the rapid onset of locomotor independence they undergo in the first 12-18 months of life (Cheverud, 1981; DeRousseau et al., 1983) compared to the extended infancy period characteristic to the hominoids.

Following infancy, a structural change was identified among the juvenile hylobatid and macaque subgroups. While both taxa are morphologically and behaviourally dissimilar, each exhibited a marked increase in midshaft strength relative to their distal tibiae by juvenility which may be explained by an overlap in foraging behaviours in a similar loading environment. Siamangs, gibbons and long-tailed macaques share a dietary overlap of about 35%, with a focus on many of the same fruits, which comprise the majority of the gibbon and macaque, and nearly half of the siamang diet (44%) (MacKinnon and MacKinnon, 1978). To rapidly move through the canopy and exploit these nutritional resources, hylobatids and macaques developed a proficiency

in arboreal leaping (Fleagle, 1976; Gittins, 1983; Cant, 1988; Wells and Turnquist, 2001). The biomechanics that govern leaping behaviour vary widely across primates dependent on body size variation and support type and availability (Demes and Gunther, 1989; Aerts, 1998; Preuschoft et al., 1998; Crompton and Sellers, 2007; Crompton et al., 2010; Gebo, 2011; Granatosky et al., 2016). Compared to research conducted on vertical-clinging-and-leaping (VCL) specialists like Indriidae, Galagidae, and Tarsiiformes (Anemone, 1990; Demes et al., 1991; Anemone and Nachman, 2003; Gebo et al., 2012), relatively few biomechanical studies have focused specifically on leaping behaviour in hylobatids and macaques. Due to the disjointed and variable structure of the forest canopy, leaping can be an energy efficient method of movement compared to climbing up or down to cross a gap terrestrially or via bridging (Sellers, 1992; Thorpe et al., 2007) and is an important part of the hylobatid and macaque locomotor repertoire in spite of its relatively infrequent use (Whitmoor, 1975; Cant, 1988). Lar gibbons in particular execute four distinct types of leaping influenced by their environment in the wild and captivity, each of which is derived from a proximo-distal extension of the hindlimb (i.e., hip extension, followed by the knee, and finally ankle) (Channon et al., 2010b). During even modest leaps of one metre, their voluminous hip and knee extensor muscles generate forces of 1.5-3 times their body mass, and are likely to increase with gap distance (Channon et al., 2010a). Compared to gibbons (*H. agilis*), macaques (*M. fascicularis*) traverse smaller gaps via leaping but are still capable of crossing distances up to 6 metres in a single bound (Cannon and Leighton, 1994). Similar mechanical forces pass through the macaque hindlimb during pronograde forward leaps in adults, and VCL episodes in older infant and juvenile macaques (*M. mulatta*) (Dunbar, 1994). It is likely that the orthograde and squatting leaps used by gibbons (Channon et al., 2010b) apply similar forces to the tibia, as well. Thus, the leaping strategies of these two sympatric genera may vary in their execution, but the forces which are generated by the proximal leg and pass through lower leg (i.e. bending, torsion, shearing) are likely similar (Calow and Alexander, 1973; Alexander, 1974; Dunbar, 1994) and accordingly, may reflect morphological adaptations to high-intensity leaping behaviours over their development. Incorporating other leaping primates with variable ecologies, sizes and masses (i.e., *Lemuridae, Tarsiidae, Galagidae, Cebus*), would make for an interesting comparative study and could help determine whether tibial proportions closely correlate with mechanical loading elicited through leaping behaviours.

Among juvenile great apes, tibial morphology does not exhibit the sharp increase in midshaft-to-distal strength found in the hylobatids and macaques. Diaphyseal dimensions remain relatively similar after infancy despite the ecological and locomotor differences exhibited by chimpanzees, gorillas and orangutans. If tibial strength proportions are canalised among the great apes, then it should be related to a synapomorphic trait they share. While all hominoids share an orthograde posture in common (Ward, 2007), the large-bodied hominids evolved unique locomotor and life history adaptations to facilitate their relatively large sizes. Body mass is one of the most important aspects of a taxon's biology and ecology, with direct implications to their life history, energy metabolism, social and mating systems, and locomotor behaviour (Clutton-Brock et al., 1977,1980; Western, 1979; Jungers, 1985; Cant, 1992; Knott, 2005; Speakman, 2005; Rayadin and Spehar, 2015). Moreover, body mass closely correlates with hindlimb cross-sectional geometric properties or midshaft diameters (van der Meulen et al., 1996), and thus, correlations between the two are often cited as an effective tool for estimating mass in extinct and extant human and non-human primate taxa (Delson et al., 2000; Ruff, 2003b; Grabowski et al., 2015). Even when mass is disproportionately distributed across the limbs during locomotion, hindlimb cross-sectional properties and articular surfaces accurately reflect habitual locomotor patterns in both bipeds and quadrupeds (Ruff, 1990). The two African ape genera employ a hindlimb-dominant locomotor gait following infancy (Kimura et al., 1979; Carrier and Leon, 1990; Sarringhaus et al. 2014). Orangutans rely on the fore- and hindlimb in different capacities during suspensory locomotion (Cant, 1987; Thorpe and Crompton, 2006; Chappell et al., 2015) as discussed above, but still bear more weight on the hindlimb than the forelimb (Reynolds, 1981, 1985a,b; Larson et al., 1991; Schmitt, 1994). Furthermore, kinematic research on primate locomotor gaits determined that vertical forces are significantly higher on orangutan hindlimbs than forelimbs, even compared to habitual quadrupedal taxa like vervet monkeys (*Chlorocebus pygerythrus*) (Demes et al., 1994). As such, the weight-bearing function of the hindlimb may supersede any behavioural signals in the tibiae of the three apes. Further evidence that tibial strength proportions reflect body mass more accurately than behaviour in interspecific comparisons is found among the adult great ape subgroups in this study. By adulthood, gorilla T50/T20 values were significantly smaller compared to both adult chimpanzees and orangutans, while the latter exhibited no significant structural variation from their African counterparts. Indeed, adult gorilla mean body mass exceeds that of

chimpanzees and orangutans considerably (Smith and Jungers, 1997). For instance, female gorilla body mass is 98.2% greater than female chimpanzees and 124% greater than that of female orangutans, while male gorilla body mass exceeds that of male chimpanzees by 241.7% and male orangutans by 116.6% (based on species means calculated from Smith and Jungers, 1997). Moreover, both chimpanzee and gorilla tibial midshaft shape is significantly more elliptical than orangutans (see Chapters 3 and 5), suggesting that strength proportions may be better indicators of overall body mass while bone shape and distribution may be more indicative of behaviour. It is also possible that the interspecific differences between the five taxa are the result of genetic canalisation rather than products of body mass. Prior morphometric research on primate trunk and forearm elements have shown that great ape postcranial characters exhibit significant overlap, while hylobatid morphology bears more similarity to the brachiating atelids (Young, 2003). A more refined sample (i.e., on the species level) may also prove more effective at differentiating loading patterns as demonstrated among human populations that load their tibiae in distinctly different ways (Macdonald et al., 2009; Shaw and Stock, 2009b). However, the significant strength proportional difference between gorillas with that of chimpanzees and orangutans, as well as the similar tibial strength-mass configuration of the hylobatids and macaques, lends further support to a body mass-driven interpretation.

Like the radius and ulna in the forearm, tibial locomotor loads are mitigated by the fibula along the leg, though the extent of which varies based on factors including the orientation and articulation of both bones with the talocrural joint (Stern and Susman, 1983; Latimer et al., 1987). Though the cross-sectional geometry of the fibula can grant insight into the broad locomotor behaviours of human and non-human primates (Marchi, 2007; DeSilva, 2009; Marchi and Shaw, 2011; Marchi, 2015a,b), it is not as responsive to load-driven adaptation compared to the tibia (Ireland et al., 2016). Moreover, its role in body mass support does not appear to obscure locomotor or body size signals derived from cross-sectional properties (Trinkaus et al., 1999; Trinkaus and Ruff, 2012).

4.6 Chapter Summary

Both inter- and intra-limb strength comparisons have their respective benefits for investigating growth and adaptation in the catarrhine skeleton. Overall, F/H comparisons prove to be an effective tool for distinguishing taxa by locomotor behaviour not only in adulthood, but in infancy and juvenility. The great apes in particular serve as prime examples, as humeral and femoral strength proportions corresponded to chronological locomotor transitions across chimpanzee and gorilla development (and a lack thereof in orangutans). Given that both African ape taxa adopt a hind-limb driven quadrupedal posture by adulthood, identifying bone dimensional changes at discrete points of development can effectively inform about a taxon's locomotor behaviour over ontogeny. This study affirms prior research on intraspecific locomotor ontogeny in chimpanzees (Sarringhaus et al., 2016) and gorillas (Ruff et al., 2013) but also builds upon it through interspecific comparative analyses between the taxa. Further support for a mechanical interpretation for F/H values is substantiated in the sampled orangutans, which are the only taxon to exhibit stronger humeri relative to femora across all three stages of their development. In demonstrating that orangutans do not only exhibit greater humeral strength in adulthood but during infancy and juvenility, it is evident that the roughly isometric scaling of F/H strength may be associated with the generally static locomotor repertoire adopted by orangutans from infancy.

Along the ulna, a net increase in U50/U20 values across the total sample helped establish how increased strength across behaviourally and taxonomically diverse species is an important mechanical adaptation, and possibly, an ancestral primate character. Even with the taxa-wide U50/U20 increase, significant variation between taxa and developmental stage were distinguishable down to the species level, though consideration should be given to the load-mitigative function of the radius as well. Ulnar comparisons further revealed a potential sensitivity to intraspecific noise within the macaque sample, which comprises pooled rhesus and long-tailed species, each of which inhabit distinctly different ecologies and locomotor environments. If intra-ulnar strength comparisons can discriminate between macaques or other primate species, subspecies and populations with a range of ecological and behavioural diversity (e.g., *Lemuridae*), it could prove an effective method for making more precise comparative analyses when interlimb comparisons like F/H are ambiguous or unavailable. Tibial strength proportions may be a strong indicator of dynamic, high-intensity locomotor behaviours like leaping, even when executed

infrequently and in different ways (i.e., VCL, pronograde forward leaping, orthograde one-footed or two-footed leaps) or by different taxa. Moreover, tibial strength proportions do not necessarily correlate with section circularity, as demonstrated in Chapter 3. Similarities among the great apes lent support to the correspondence between T50/T20 proportions and body mass. While the sampled hominids allied themselves across infancy and juvenility, tibial strength proportions were distinguishable between gorillas compared to chimpanzees and orangutans by adulthood, when mass is at its peak and locomotor profile is fixed. Indeed, the virtually identical body masses of the hylobatids and macaques help validate this observation, given their drastically different ecologies and behaviours but similar sizes. Ultimately, intralimb ratios can prove highly effective in teasing apart behavioural and phylogenetic signals, though each method has its respective strengths and weaknesses. Further exploration of ulnar and tibial strength comparisons can verify their accuracy across a wider sample of more diverse primate taxa. If effective, their ability to elucidate behaviour and mass in skeletal remains could be beneficial, particularly when only fragmented or single skeletal elements are available for analysis. Additionally, structural comparisons between the matched sections of proximate elements, like the radius and ulna (Ruff et al., 2013) or the tibia and fibula (Marchi, 2015a) may aid in interpreting changes along individual elements and should be investigated in future studies.

Though intra- ulnar and tibial comparisons appeared to correspond to locomotor transitions throughout the sample, there are some matters to consider. For one, ratios between the midshafts of two separate elements (e.g., F/H) effectively compare morphologically-like bone sections. Intra-element ratios do not account for the microstructural differences in bone material properties between each section which may obscure interpretation. Fully mature long bone midshafts, for instance, are defined by their relatively thick cortices and medullary cavities, while epiphyseal and metaphyseal section morphology comprise a thin cortex enveloping a dense trabecular network (Robling et al., 2006). Because the distal sections evaluated in this study were taken from the diaphysis, microstructural differences from midshaft sections would not be as exaggerated as an epiphyseal section, though caution is still warranted when interpreting results.

Chapter Five:

Size or Shape? Biological Pathways of Limb Development

5.1 Introduction

Research on biological form (size and shape) experienced a renaissance in the 1980s and early 1990s, largely driven by technical advances in the field of geometric morphometrics (GM) (Bookstein, 1989, 1991; Rohlf and Slice, 1990; Rohlf and Marcus, 1993). While classic morphometrics approaches the analysis of form through linear or volumetric measurements, GM defines a given object's dimensions using landmark coordinates (Zelditch et al., 2012). Doing so not only introduces the potential for greater statistical power and analytical opportunity but helps visualise an object's form in ways that traditional measurements cannot. By applying new analytical techniques to classical biological concepts, GM methods have served as a cornerstone for research based on morphological and allometric variation for the past two decades (Strand Vidarsdóttir et al., 2002; Cardini and Elton, 2007, 2008a,b, 2009; Klingenberg, 2009; Tallman, 2012; O'Higgins and Nicholas, 2013; Arias-Martorell et al., 2015). Nevertheless, traditional beam modelling methods, including ratios along principal and anatomical axes, have remained standard practice for interpreting cross-sectional shape in extant and fossil primate limb elements (Burgess et al., 2016; Miller et al., 2017; Weatherholt and Warden, 2017). The aim of this chapter is to quantify limb cross-sectional form along the periosteal contour using a GM approach, rather than through the cross-section as with traditional geometric measures. Doing so will introduce a novel and potentially more comprehensive way of comparing taxonomic and developmental form variation in catarrhine long bone geometry.

One distinct advantage that GM provides over conventional ratio analyses is the detail that can be captured about the periosteal contour (Wilson and Humphrey, 2015). Because principal and anatomical area ratios inform about two discrete aspects of a cross-section, both are limited in their ability to describe shape beyond their respective axes. With a morphometric approach, control over how much or little detail is considered for analysis is established through the manual placement of Cartesian landmarks (Bookstein, 1991), granting a more complete view of a cross-section's entire curve. A second advantage of GM is its ability to directly account for size differences between

specimens. While cross-section ratios act as natural size controls along specific axes, morphometric analyses scale all dimensions of an object by a central point (centroid), so that all aspects of its shape can be considered together. Just as removing the size component of a cross-section is necessary before any meaningful biomechanical comparisons can be made, the inclusion of size can be useful for studying allometric variation, especially in an ontogenetic context (Monteiro, 1999). In instances when the scale of a group of objects is preserved, comparisons of form can be made (Dryden and Mardia, 1998; Klingenberg, 2016). Regressions of an organism's shape by its size, for instance, have been used to inform about the morphological changes they experience as they mature (Ponssa and Candioti, 2012; Turley and Frost, 2014; Murta-Fonseca and Fernandes, 2016), as well as identify the relative timing of these changes (heterochrony) (Klingenberg and Spencer, 1993; Mitteroecker et al., 2004). Area ratios situated along defined axes can also be used to visualise how form varies across development (Ruff et al., 2013), but again, are restricted to the predesignated planes of a given section. By incorporating multiple shape variables along a section's curve using GM, even subtle allometric effects, which might otherwise be overlooked using shape ratios alone, can be interpreted.

5.2 Research context and objectives

5.2.1 Geometric morphometrics and primate allometry

Primate skeletal variation has been of interest to researchers studying ontogeny (Schultz, 1924, 1926; Jungers, 1984; Leigh, 1992; Leigh et al., 2005; Raichlen, 2005a,b; Young et al., 2010a,b) and phylogeny (Schultz, 1937; Gingerich and Schoeninger, 1977; Young, 2006; Diogo and Wood, 2011; Fleagle and Lieberman, 2015) for the better part of the past century. Among extant primates, the implementation of GM has illuminated relationships between skeletal characters and their behavioural ecology, including the great apes (Lockwood et al., 2002; Smith et al., 2015), macaques (Ito et al., 2014) and guenons (Cardini and Elton, 2008a,b). Geometric morphometrics have also been used to describe cranial and postcranial variation within populations and species (Baab, 2008; Baab and McNulty, 2009; Lordkipanidze et al., 2013) as well as between species (Tallman, 2012; Almécija et al., 2013; Lordkipanidze et al., 2013; Tallman et al., 2013; Püschel and Sellers, 2016).

Primate form, and the ontogenetic trajectories that achieve that form, are subject to selection pressures (Gould, 1966; Janson and van Schaik, 1993). To discern how adult morphological patterns arise from infant phenotypes, Mitteroecker and colleagues (2004) compared the ontogenetic craniofacial trajectories of an extant hominid sample. By regressing 3D cranial shape variables with size, they identified how, and at which stages of their development, each taxonomic group overlapped and diverged in craniofacial form (Mitteroecker et al., 2004). Another study conducted on hominin ontogenetic facial trajectories demonstrated that taxonomic shape differences are largely established postnatally (Cobb and O'Higgins, 2004). Subsequent studies have taken similar approaches to investigate the effects of ape sexual dimorphism over ontogeny, by comparing the angles formed between shape variable vectors (Strand Vidarsdottir et al., 2002; Cobb and O'Higgins, 2004, 2007; Schaefer et al., 2004; Klingenberg and Marugán-Lobón, 2013). These angles describe developmental changes between two or more taxa by connecting a vector between the mean shape values of immature and mature specimens. The size of the angle formed between the vectors of two taxa can be used as a proxy for how little or great their ontogenetic trajectories diverge. The greater representation of cranial over postcranial material in ontogenetic studies of GM may be due to the stronger phylogenetic compared to functional signal the skull emits (Lieberman, 1996). While crania do elicit an anabolic response for bone formation when mechanically loaded, a higher strain threshold must be passed to stimulate the same osteoblastic activity as found in limb bones (Rawlinson et al., 1995; Terhune et al., 2014). That said, studying growth trajectories through an adaptive lens could be an insightful way of studying long bone shape variation, especially when infant taxa appear to exhibit greater similarity to one another than their adult counterparts do. Therefore, studying midshaft ontogenetic trajectories may not only inform how different species mature but grant insight into the environmental forces that influence their adult form.

To date, the only study to apply any form of GM (morphometric mapping), to non-human primate long bone growth trajectories specifically, was conducted along the cross-sections of the chimpanzee femur (Morimoto et al., 2011). In that study, Morimoto and colleagues (2011) compared shape and structure along the femoral diaphyses of wild and captive chimpanzees over development. Their method broke ground by demonstrating the accuracy and effectiveness of a morphometric approach to cross-sectional geometry. Wilson and Humphrey (2015) applied a GM

approach to cross-sectional geometry more recently, where humeral bilateral asymmetry was compared among a population of indigenous Andaman Islanders. They also found that GM methods yield more accurate shape information than second moment of area ratios and conclude that their method should be equally capable of distinguishing between ontogenetic groups or those that exhibit different locomotor patterns (Wilson and Humphrey, 2015).

In this chapter, three types of allometry are considered, including: static allometry, ontogenetic allometry, and evolutionary allometry (Gould, 1975). 1) Static allometry refers to any intraspecific size and trait variation identified among individuals belonging to the same age and taxonomic group (Klingenberg, 1996). To take an example from the present postcranial dataset, a comparison between the shape and size of an ulnar cross-section among a sample of infant chimpanzees would serve as a study of static allometry. 2) Ontogenetic allometry, or growth allometry, focuses on the emergence of variation over the course of either an individual or group's development. An example of an ontogenetic allometric study might evaluate the size and shape variation of ulnar cross-sections sampled from a group of infant and adult chimpanzees together, for instance. 3) Evolutionary allometry is concerned with the covariation of character traits over the course of evolutionary history, with a particular focus on related members of a phylogenetic group (Klingenberg and Marugán-Lobón, 2013). Unlike intraspecific scaling employed in static intragroup analyses, evolutionary allometry aims to scale traits on the species level. Studying the covariation of ulnar cross-sectional size and shape between adult chimpanzee and gorilla ulnae would serve as an example of studying African ape evolutionary allometry.

5.2.2 Research questions

To understand how long bone cross-sectional form varies across primate taxa over development, I will address two primary research objectives. The first is whether form variation within and between taxonomic groups can be measured with accuracy using a GM approach, and if so, whether the observed variation appears to correspond to biological or behavioural adaptations. In Chapters 3 and 4, cross-sectional circularity (defined by second moment of area ratios within each cross-section) and strength (derived from log-linear polar section moduli ratios

between and within limb segments) were found to correlate with broad locomotor behaviours, but were also sensitive to intrinsic factors like body size. If a GM approach can discriminate between taxonomic and developmental groups, it should also be possible to infer whether these differences are related to locomotor behaviour, body size or some combination of the two. In the forelimb, stronger locomotor signals should be found at the humeral midshaft compared to the ulnar midshaft, while a weaker body mass signal is expected to be found in both forelimb elements compared to the hindlimb. These predictions stem from mammalian optimality models of limb form suggesting that more robust proximal limb segments are less constrained by tissue economy (Alexander, 1981, 1998; Lieberman et al., 2003), as well as findings from the two prior research chapters. This should be reflected by greater structural adaptation in response to loading (Skedros et al., 2003). Moreover, forearm loads are distributed between the ulna and the radius (Rabinowitz et al., 1994), meaning that any adaptive ulnar signals may be more difficult to discern without the context of radial shape – though GM may be capable of highlighting patterns previously indistinguishable by circularity ratios alone. Among the femur and tibia, the effects of both behaviour and size should be discernible within and between taxa due to their propensity to adapt to habitual loading patterns (Shaw et al., 2014), as well as their role in supporting an individual's mass in terrestrial and arboreal contexts. Therefore, a stronger allometric signal should be detectable in the hindlimb, as both elements adapt their shape to accommodate increases in body mass.

The second objective addresses whether cross-sectional shape vectors can discriminate taxa between infancy and adulthood. Studying cross-sectional form rather than shape alone can inform about both the static and ontogenetic allometry of the limb. Because most other GM studies on hominid growth have focused exclusively on cranial form variation (Mitteroecker et al., 2004; Schaefer et al., 2004; Cobb and O'Higgins, 2007), the current dataset will determine whether cross-sections can distinguish between the variable ontogenetic trajectories of the fore- and hindlimb. While plastic adaptation of the midshaft adds an element of noise to the analysis (as individual loading histories are unknown in the majority of museum specimens), broad taxonomic comparisons should be more easily distinguishable than between populations or individuals. Furthermore, regressions of Procrustes distance and the natural logarithm of centroid size (log CS) will accurately define how much shape variation can be attributed to increases in size within each

taxon. Following the geometric analyses in Chapters 3 and 4, it is expected that taxa that exhibit fewer locomotor transitions over their lives (i.e., *Gorilla*, *Pongo*) will exhibit greater increases in size, but fewer dramatic changes in shape to accommodate the locomotor loads they experience as they grow. By comparison, taxa that undertake more dramatic postural, substrate or locomotor changes as they develop (i.e., *Pan*, *Macaca* and potentially Hylobatidae) should not only exhibit larger overall cross-sections as they grow, but more variable section shapes as an adaptive mechanism.

5.3 Methods

The following section details the geometric morphometric approach used to compare cross-sectional shape of the humerus, ulna, femur and tibia of the sampled taxa. Analysis was conducted exclusively at the midshaft location (50% of total length) of each bone due to its high adaptive sensitivity to biomechanical stress (Biewener and Taylor, 1986). All three developmental subgroups (infants, juveniles and adults) of the five primate taxa (*Pan*, *Gorilla*, *Pongo*, Hylobatidae and *Macaca*) were incorporated in the following analyses. For an inclusive review of the primate skeletal sample and the laser scanning method used to obtain the cross-sections discussed ahead, please revisit Chapter 2.

5.3.1 Semilandmarking and Procrustes superimposition

A total of 21 semilandmarks were manually placed approximately equidistantly and at corresponding locations of each 2D cross-section, beginning at the anterior and working clockwise along the periosteal contour (Figure 5.1). All semilandmarks were placed using tpsDig of the TPS software series (Rohlf, 2015). To preserve lateral symmetry across the sample, images of all left elements were mirrored to reflect the right side before landmarking. Unlike a traditional photograph where a size marker (i.e., a ruler or measuring tape) can be positioned to give a sense of scale, cross-sectional images generated by AsciiSection do not include a marker. To set a consistent reference length for each cross-section, 1,000 pixels (the total length of an AsciiSection image file) were measured manually so size could be integrated or omitted during statistical

analysis. The semilandmarks were slid along the digitised curve of each cross-section using tpsUtil (Rohlf, 2015) to minimise spacing and shape differences (Gunz and Mitteroecker, 2013). After all semilandmarks were placed, the coordinate data were divided into developmental groups and taxonomic subgroups therein (e.g., infant gorilla, juvenile gorilla, adult gorilla). The TPS .txt files were then imported to MorphoJ: an integrated software package for geometric morphometric analysis (Klingenberg, 2011). All groups and subgroups were checked for outliers by comparing the theoretical and observed distribution of landmarks using comparisons of squared Mahalanobis distance: a measure indicative of dissimilarity between individuals relative to the rest of the group (Klingenberg and Monteiro, 2005). This allowed for the identification of any displaced or swapped semilandmarks so that their position could be manually adjusted prior to analysis.

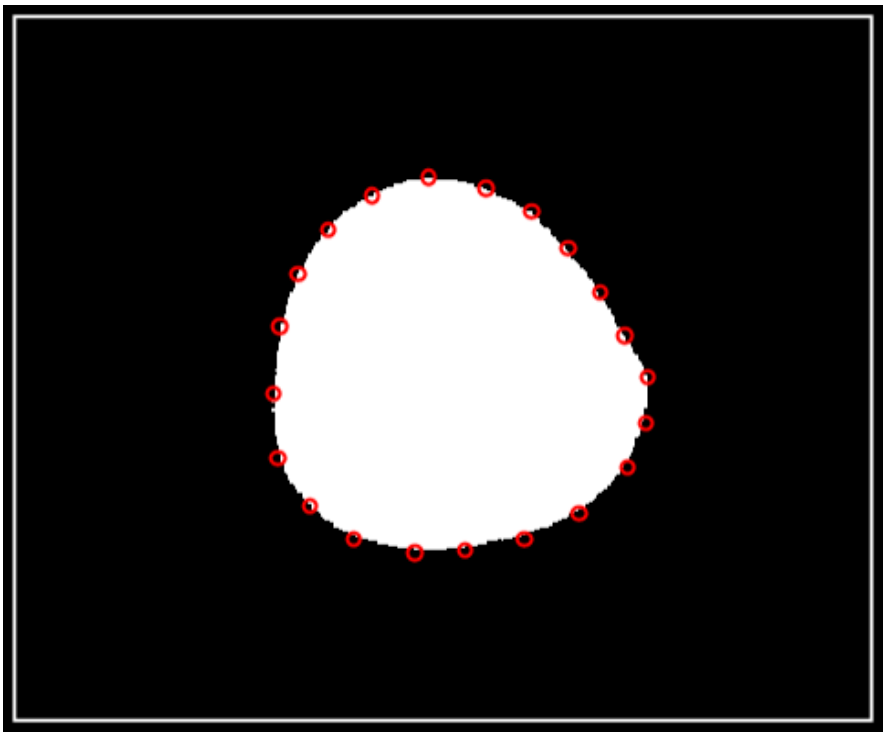

Fig. 5.1. Cross-section of an adult male chimpanzee's right ulnar midshaft (not to scale) after placement of 21 semilandmarks. Note that these landmarks have not yet been slid or superimposed along the curve.

Uniformly scaling a group of objects by their size is the first of three steps of a shape analysis technique called Generalised Procrustes Analysis (GPA), a statistical method used to optimally superimpose two or more objects upon each other so their shapes may be directly compared (Gower, 1975; Rohlf, 2015). By proportionately increasing or decreasing an object's dimensions relative to its centroid, size can be controlled while preserving shape (Figure 5.2). An object's centroid size is defined as the square root of the summed squared distance from its landmarks to its centroid (Zelditch et al., 2012).

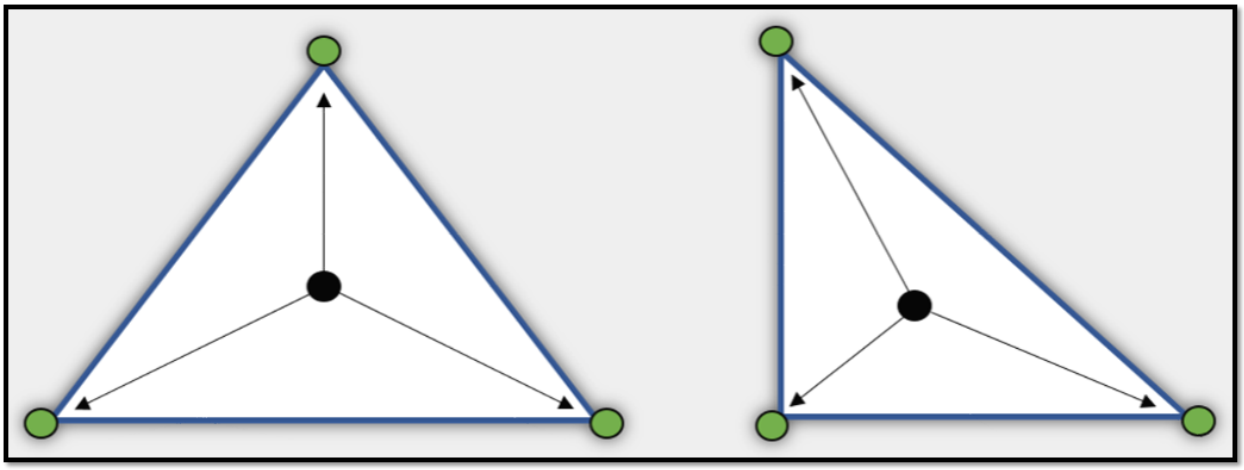

Fig. 5.2. Illustration of two geometric objects scaled by their respective centroids (black circles), relative to three landmarks (green circles). By proportionately adjusting the dimensions of each triangle, both shapes can be compared independent of their original sizes.

In the translation step of GPA, each object is moved to the same point in space so that their centroids are aligned at a common origin. Finally, the cross-sectional figures are rotated in space relative to the origin, minimising the sum of the squared distances between their corresponding points (Rohlf and Slice, 1990). When aspects of scale (size-variation), translation (positional differences in space) and rotation (orientation about the centroid) are removed from the Cartesian coordinate data, the remaining component is the object's shape, which is expressed using Procrustes shape coordinates (Figure 5.3) (Bookstein, 1997; Mitteroecker and Gunz, 2009).

Variation between the data can then be quantified by comparing the sum of squared distances between the Procrustes coordinates between an object and the superimposed group mean (Procrustes distance) (Slice, 2005; Zelditch et al., 2012). In essence, two objects are considered the same shape when their Procrustes distances do not vary after size, position, and orientation are removed from the comparison (Mitteroecker et al., 2013). Zelditch et al. (2012) provide an in-depth summary of Procrustes superimposition including differences between the full and partial fitting techniques.

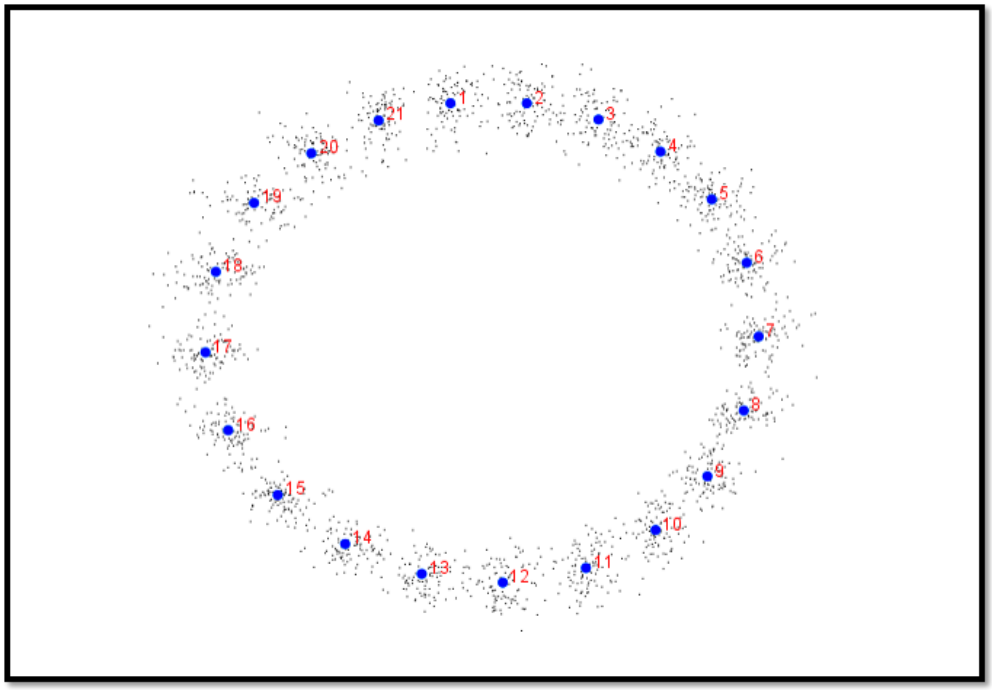

Fig. 5.3. The 21 semilandmarks of the adult (aggregate) mid-femur following Procrustes superimposition and sliding. The large blue dots and their corresponding red numbers depict the semilandmarks of the cumulative reference configuration, the small grey dots surrounding them depict the semilandmark positions of each individual adult specimen.

5.3.2 Statistical analyses

Covariance matrices of the 21 Procrustes aligned coordinates (42X42 matrix), were generated for each taxonomic and developmental subgroup and served as the basis of all analyses described ahead (Jolicoeur, 1963; Klingenberg and Spencer, 1993). A dimensionality of 38 (4 degrees of freedom were deducted from the 42-column matrix during translation, scaling and rotation) was applied to all calculations of shape variance (Klingenberg, 2011). Principal component analysis (PCA) – a multivariate method used to analyse shape variability on Procrustes coordinate data (Gibson et al., 1978; Baab & McNulty, 2009; Faccia et al., 2014) – was carried out for each taxon and element to compare midshaft shape variation between developmental stages, as well as between the sexes among adult specimens. Principal component analysis describes shape variation using a series of orthogonal vectors called principal components (PCs). Each PC acts as a linear and independent combination of an object's original shape variables making it easier to compare the primary differences between objects without having to investigate their every detail. Moreover, the first several PCs of a PCA typically describe the majority of total variance (Jackson, 1993), eliminating the need to investigate minor, inconsequential differences between objects. Eigenvalues were < 1.0 in each PCA, so Cattell's scree test advised which PCs were most meaningful in identifying shape variation (Jackson, 1993). However, bivariate scatter plots of only the first and second PCs were compared in this study, granting a broad view of developmental shape change across the sample.

After measuring midshaft shape change between infants, juveniles and adult taxonomic groups, the next step was to compare their ontogenetic trajectories. The first PC typically acts as the allometric shape component in single-species ontogenetic samples (Cobb and O'Higgins, 2004; Mitteroecker et al., 2004). Therefore, interspecific comparisons of PC1 vectors were evaluated for a more comprehensive view of developmental change than can be found comparing discrete developmental stages alone. Vector angles between 0° and 90° were compared in a pairwise fashion between taxa, where smaller angles corresponded to a similar ontogenetic trajectory and larger angles corresponded to greater ontogenetic divergence between taxa. Because cross-section size was dissociated from shape during the scaling phase of GPA, it was possible to test whether size and shape were statistically correlated. Multivariate regressions of size and shape have previously been used to investigate the effects of allometry over development (Monteiro,

1999; Klingenberg, 2009) and so were extended to the ontogenetic series here. Specifically, Procrustes coordinate distances of each cross-section were regressed by log CS, for each taxonomic group. The allometric effect was expressed as a percentage of the predicted sum of squares from the total sum of squares in each regression (Klingenberg, 2016). To test whether the effects of allometry were statistically significant, permutation tests of 10,000 iterations reassigned size and shape values to specimens at random (Klingenberg, 2009; Good, 2013; Martín-Serra et al., 2014). Following resampling, the null hypothesis of size and shape independence was rejected if $P < 0.05$.

In addition to intraspecific developmental comparisons of bone shape, interspecific tests were conducted at each of the three developmental stages. Canonical variate analyses (CVA) were carried out to compare midshaft shape between taxa. Similar to PCA, CVA extracts linear combinations of an object's original shape variables and constructs a new orthogonal coordinate system with them (CVs) (Zelditch et al., 2012). The fundamental difference between the two analyses is that PCA describes differences among individuals while CVA describes differences among groups (chosen *a priori*), essentially acting as a PCA for group means. Unlike PCA, the axes of a CVA are scaled relative to patterns of intragroup variation (in units of Mahalanobis distance), and so should not be interpreted as a simple rotation of the original shape variables (Tallman et al., 2013). As such, distances between groups along the first CV are not always correlated (Zelditch et al., 2012). Permutation tests of 10,000 iterations were again used to test for significant differences of Mahalanobis and Procrustes distance between taxonomic groups. Because separate analyses were conducted on each developmental group, the canonical axes of each scatter plot may describe different shape configurations. For example, high values on the CV1 axis of an infant scatter plot and a juvenile scatter plot do not necessarily correspond to the same shape, and therefore, each plot should be interpreted separately. Because differences in Procrustes distance were always more conservative than Mahalanobis distance (every instance of significant variation in Procrustes distance was also identified in permutation tests of Mahalanobis distance), variation in Procrustes distance was the primary comparative focus of the chapter.

5.4 Results

5.4.1 Intraspecific shape variation at the humeral midshaft

Humeral midshaft PCAs and size-shape regressions of the five taxa are given in Tables 5.1a – e. The scree plots of each PCA and scatter plots of the allometric regressions (size against shape) are given in the Appendix (Figures A5.1 – A5.8) for the mid-humerus and all subsequent elements. Over 75% of cumulative shape variance was explained within the first four PCs across the total sample. Multivariate regressions of allometry determined that size accounted for a significant portion of humeral shape variation in each taxon, though gorillas and orangutans exhibited a slightly weaker allometric relationship than the other taxa (Tables 5.1b and c). Scatter plots of PC1 and PC2 illustrate mid-humeral shape variation across development in each taxon (Figures 5.4a – e), and are complemented by wireframe graphs depicting the direction of shape change along both axes. The orangutan PCA scatter plot showed the greatest overlap between developmental stages, where the infant, juvenile and adult scatters were distributed relatively evenly across PCs 1 and 2, exhibiting a circular midshaft configuration (Figure 5.4c). By comparison, chimpanzee infants aligned themselves more closely along the lower end of PC1, where midshaft shape was distinguishably more circular than the elliptical pattern evident among juveniles and adults (Figure 5.4a). PC2 effectively discriminated both adult chimpanzees and gorillas by sex, where males were largely situated at the higher end of the factor, exhibiting a more mediolateral-elliptical shape compared to the more circular female mid-humerus. Gorilla infants were also defined by a more circular midshaft on the lower end of PC2 (Figure 5.4b). Unlike the great apes, infant hylobatids and macaques each aligned themselves on the higher end of PC1, exhibiting more elliptical midshafts than their juvenile and adult counterparts. Adult hylobatids exhibited a relatively circular midshaft (Figure 5.4d) while adult macaques revealed a more mediolateral elliptical shape (Figure 5.4e). Adult shape was not distinguishable between sexes in either taxon. While developmental subgroups displayed variable overlap in the other taxa, the infant macaque scatter was discriminated from adults along PC1.

TABLE 5.1a. Ontogenetic shape variation at the chimpanzee humeral midshaft

PC	Eigenvalues	% Variance	% Cumulative	Allometry	
1	0.00204839	40.313	40.313	Size variance	12.8%
2	0.00086843	17.091	57.404	*P*	0.0001
3	0.00067813	13.346	70.750	Total SS	0.254
4	0.00044935	8.843	79.593	Predicted SS	0.0324
5	0.00025622	5.042	84.636	Residual SS	0.2215
6	0.00020182	3.972	88.608		

PCA results including eigenvalues and shape variance are given on the left side of the table, results of the multivariate regression of shape and size are given on the right.

TABLE 5.1b. Ontogenetic shape variation at the gorilla humeral midshaft

PC	Eigenvalues	% Variance	% Cumulative	Allometry	
1	0.00156276	35.350	35.350	Size variance	8.1%
2	0.00081919	18.530	53.881	*P*	0.0019
3	0.00061536	13.920	67.800	Total SS	0.2166
4	0.00043561	9.854	77.654	Predicted SS	0.0174
5	0.00022199	5.022	82.676	Residual SS	0.1991
6	0.00016493	3.731	86.406		

PCA results including eigenvalues and shape variance are given on the left side of the table, results of the multivariate regression of shape and size are given on the right.

TABLE 5.1c. Ontogenetic shape variation at the orangutan humeral midshaft

PC	Eigenvalues	% Variance	% Cumulative	Allometry	
1	0.00159994	35.488	35.488	Size variance	6.7%
2	0.00089721	19.901	55.389	*P*	0.0019
3	0.00059792	13.263	68.652	Total SS	0.2614
4	0.00045322	10.053	78.705	Predicted SS	0.0174
5	0.00021678	4.808	83.513	Residual SS	0.244
6	0.00017913	3.973	87.487		

PCA results including eigenvalues and shape variance are given on the left side of the table, results of the multivariate regression of shape and size are given on the right.

TABLE 5.1d. Ontogenetic shape variation at the hylobatid humeral midshaft

PC	Eigenvalues	% Variance	% Cumulative	Allometry	
1	0.00118023	32.828	32.828	Size variance	13.1%
2	0.00069604	19.360	52.188	*P*	0.0001
3	0.00050765	14.120	66.308	Total SS	0.2121
4	0.00045663	12.701	79.009	Predicted SS	0.0277
5	0.00018372	5.110	84.120	Residual SS	0.1843
6	0.00015517	4.316	88.436		

PCA results including eigenvalues and shape variance are given on the left side of the table, results of the multivariate regression of shape and size are given on the right.

TABLE 5.1e. Ontogenetic shape variation at the macaque humeral midshaft

PC	Eigenvalues	% Variance	% Cumulative	Allometry	
1	0.00144662	35.171	35.171	Size variance	12.4%
2	0.00099793	24.263	59.434	*P*	0.0001
3	0.00055443	13.480	72.914	Total SS	0.2015
4	0.00039154	9.519	82.433	Predicted SS	0.0249
5	0.00014823	3.604	86.037	Residual SS	0.1765
6	0.00012110	2.944	88.981		

PCA results including eigenvalues and shape variance are given on the left side of the table, results of the multivariate regression of shape and size are given on the right.

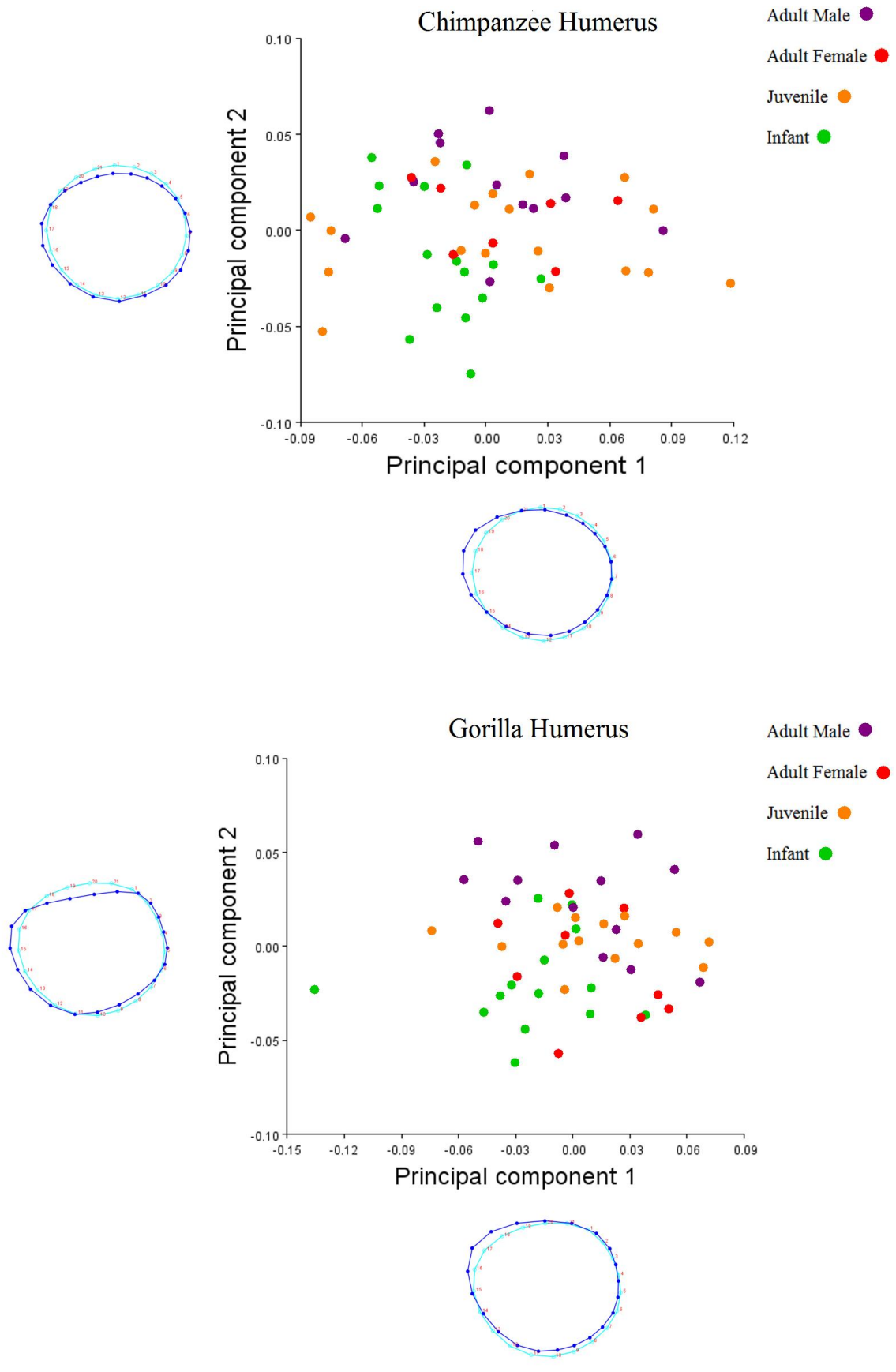

Fig. 5.4a and b. Scatter plot of humeral midshaft developmental variation projected onto PC1 and PC2 in shape space. Wireframes along the axes represent shape variation; the light blue outlines depict shape at the low ends of their respective axes and the dark blue outlines depict the high ends.

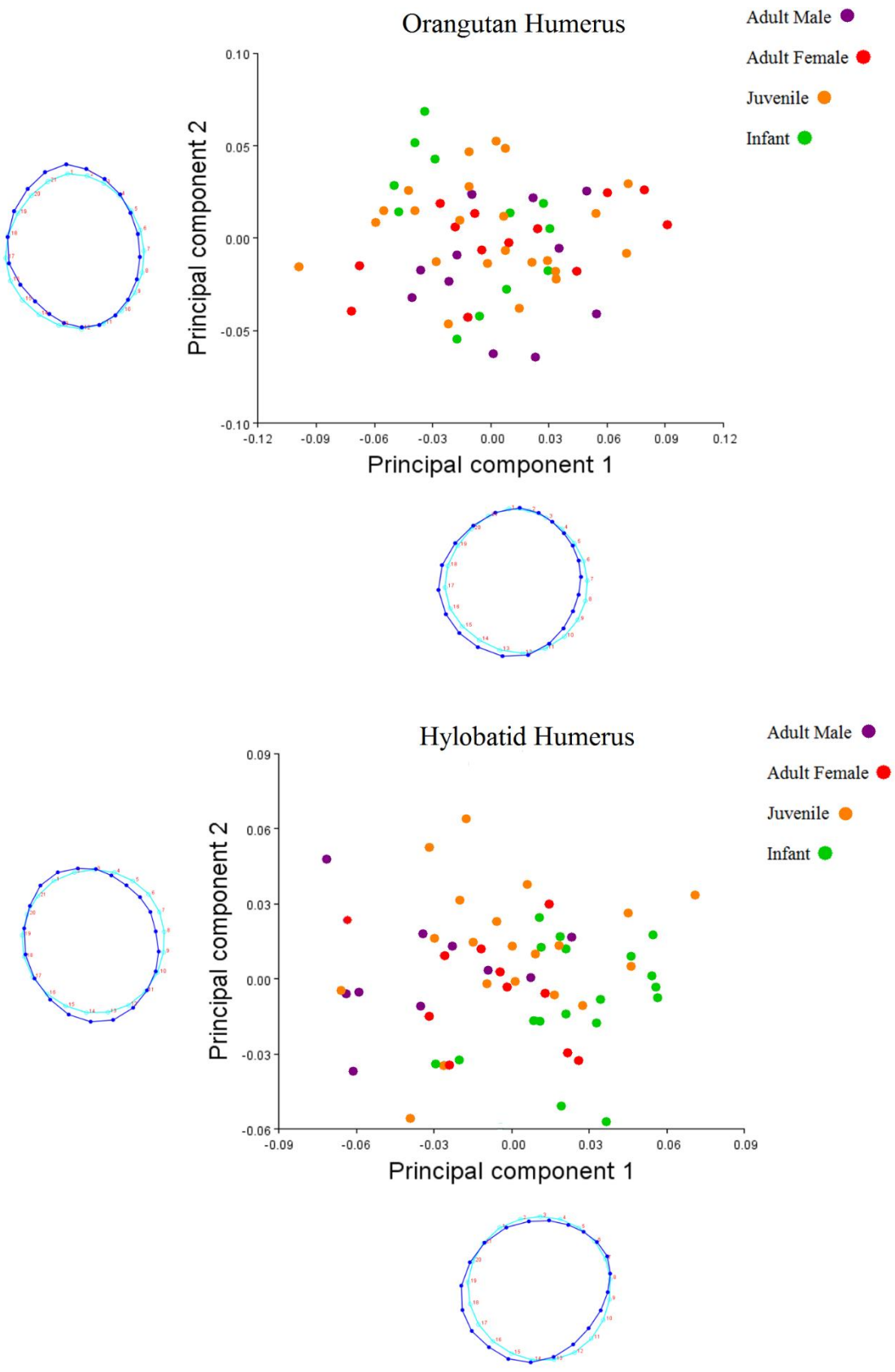

Fig. 5.4c and d. Scatter plot of humeral midshaft developmental variation projected onto PC1 and PC2 in shape space. Wireframes along the axes represent shape variation; the light blue outlines depict shape at the low ends of their respective axes and the dark blue outlines depict the high ends.

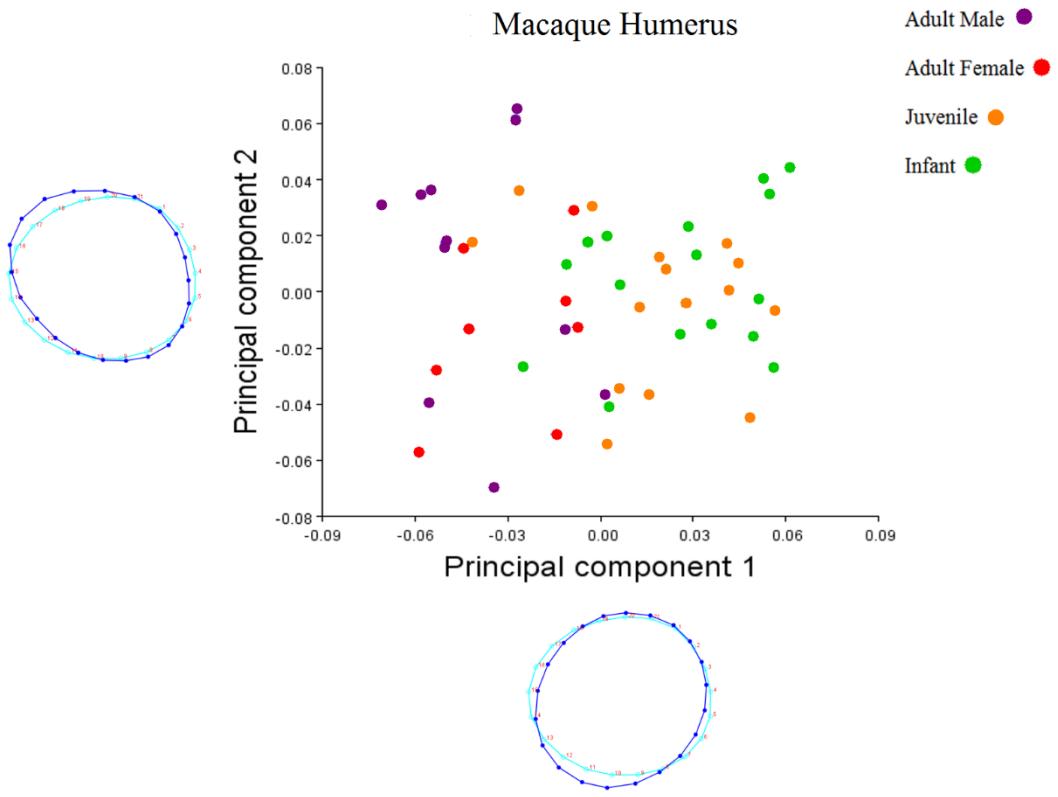

Fig. 5.4e. Scatter plot of humeral midshaft developmental variation projected onto PC1 and PC2 in shape space. Wireframes along the axes represent shape variation; the light blue outlines depict shape at the low ends of their respective axes and the dark blue outlines depict the high ends.

5.4.2 Interspecific shape variation at the humeral midshaft

Angles formed between humeral midshaft PC1 vectors are given in Table 5.2. The range of angle sizes suggests that mid-humeral shape change is highly variable across primate development. Of the entire sample, the smallest vector angle was identified between the chimpanzees and orangutans, and the largest between the hylobatids and macaques. Shape trajectories between the great apes were intermediate, ranging between 20.8° and 50.6°, though the chimpanzee and gorilla samples exhibited greater shape divergence between each other than they each did with orangutans. The macaque humeral vector formed a significantly small angle with gorillas but approached perpendicularity with the other taxa, including an 89.1° angle with the similar-sized hylobatids.

TABLE 5.2. Vector angle comparisons between PC1s of mid-humeral ontogenetic series

	Macaca	*Pan*	*Gorilla*	*Pongo*
Pan	85.6° (< 0.645)			
Gorilla	38.6° (< 0.001)	50.6° (< 0.001)		
Pongo	81.1° (< 0.346)	20.8° (< 0.001)	44.5° (< 0.001)	
Hylobatidae	89.1° (< 0.923)	38.3° (< 0.001)	62.1° (< 0.003)	45.4° (< 0.001)

P-values given in parentheses beside the vector angles.

CVA and permutation tests of group means were used to compare and test humeral shape differences between taxa at each stage of their development. All pairwise comparisons of Mahalanobis distance were significantly different across infant, juvenile and adult subgroups (Appendix; Figure A5.9). Results of the infant mid-humeral CVA, including *P*-values of Procrustes distance are given in Table 5.3a – c. Among the infant subgroups, chimpanzee, orangutan and hylobatid midshaft shape did not differ from one another but were each significantly different from gorillas and macaques. Moreover, gorilla and macaque mid-humeral shape did not differ from each other at infancy. Juvenile subgroups exhibited greater variation, making the taxa more easily distinguishable compared to their infant counterparts (Table 5.3b). For instance, hylobatids were discriminated from all other taxonomic groups by juvenility. However, several juvenile taxa exhibited shape overlap like that found among the infants, such as the chimpanzee and orangutan subgroups. Similarly, the juvenile macaques and gorillas exhibited no significant shape differences with one another but were each discriminated from the other taxa, as in infancy. Humeral midshaft shape variation was greatest among the adult subgroups, where each taxon differed significantly from the others to the exception of chimpanzees and orangutans, which overlapped at each stage of their development (Table 5.9).

TABLE 5.3a. Procrustes distance group mean comparisons of infant mid-humeral shape

	Pan	*Gorilla*	*Pongo*	Hylobatidae	*Macaca*
Pan	**x**	0.0001	n.s	n.s	0.0001
Gorilla	0.062	**x**	0.0001	0.0001	n.s
Pongo	0.023	0.08	**x**	n.s	0.0001
Hylobatidae	0.021	0.051	0.03	**x**	0.0001
Macaca	0.06	0.02	0.072	0.052	**x**

The diagonal-left side of the table denotes Procrustes distances among groups. *P*-values derived from 10,000 permutation rounds are given on the right side of the table, non-significant relationships denoted by 'n.s'.

TABLE 5.3b. Procrustes distance group mean comparisons of juvenile mid-humeral shape

	Pan	*Gorilla*	*Pongo*	Hylobatidae	*Macaca*
Pan	**x**	0.0001	n.s	0.0473	0.0007
Gorilla	0.073	**x**	0.0001	0.0001	n.s
Pongo	0.024	0.09	**x**	0.0001	0.0001
Hylobatidae	0.032	0.05	0.044	**x**	0.0067
Macaca	0.052	0.03	0.07	0.035	**x**

The diagonal-left side of the table denotes Procrustes distances among groups. *P*-values derived from 10,000 permutation rounds are given on the right side of the table, non-significant relationships denoted by 'n.s'.

TABLE 5.3c. Procrustes distance group mean comparisons of adult mid-humeral shape

	Pan	*Gorilla*	*Pongo*	Hylobatidae	*Macaca*
Pan	**x**	0.0001	n.s	0.0001	0.0001
Gorilla	0.082	**x**	0.0001	0.0001	0.0074
Pongo	0.031	0.084	**x**	0.0023	0.0001
Hylobatidae	0.052	0.07	0.037	**x**	0.0001
Macaca	0.064	0.037	0.08	0.078	**x**

The diagonal-left side of the table denotes Procrustes distances among groups. *P*-values derived from 10,000 permutation rounds are given on the right side of the table, non-significant relationships denoted by 'n.s'.

5.4.3 Intraspecific shape variation at the ulnar midshaft

Tables 5.4a – e give the PCA and size-shape regression results for each taxon over development. The majority of cumulative variance was explained by PC2 and over 75% of variance was accounted for by PC3 among all taxa apart from chimpanzees. In fact, chimpanzees exhibited the least shape variance across PC1 and PC2 of the whole sample (Table 5.4a). Accordingly, shape variation along the first two chimpanzee PCs was not closely associated with any particular developmental stage. Regressions of Procrustes distance on log CS revealed that size covaried significantly with shape among gorillas, orangutans and hylobatids. Unlike the humerus, there was a weak allometric effect at the chimpanzee and macaque mid-ulna, where size and shape change were not significantly correlated (Figure 5.4a and 5.4e).

Bivariate scatter plots describing shape change along the first two PCs are given with their corresponding wireframe graphs in Figures 5.5a – e. Gorillas exhibited a different developmental dispersion pattern, where infant shape (distributed along the lower end of PC1) was more ML oriented than the more circular pattern assumed by juveniles and adults (Figures 5.5b). Orangutans exhibited a similar pattern but departed from circularity following infancy and adopted a distinctly different shape configuration by adulthood, exhibiting a more AP elliptical midshaft (Figure 5.5c). The only two taxa to emit a discernible sexually dimorphic signal among the adult subgroups were chimpanzees and gorillas, where females of both taxa exhibited more circular ulnar midshafts than their male counterparts. That said, overlap between the scatters of both sexes was more pronounced at the ulna than at the humerus. Hylobatid infants were also distinguishable from their juvenile and adult counterparts, particularly along PC2, where midshaft shape assumed more of an AP elliptical shape over development (Figure 5.5d). Similar to the chimpanzee sample, the four macaque subgroups each exhibited a wide distribution pattern across PC 1 and 2, making it difficult to assign a clear ulnar shape profile with any particular stage of development.

TABLE 5.4a. Ontogenetic shape variation at the chimpanzee ulnar midshaft

PC	Eigenvalues	% Variance	% Cumulative	Allometry	
1	0.00189655	32.904	32.904	Size variance	2.1%
2	0.00127212	22.071	54.975	*P*	0.3635
3	0.00079589	13.808	68.783	Total SS	0.2939
4	0.00053061	9.206	77.989	Predicted SS	0.0061
5	0.00037732	6.546	84.536	Residual SS	0.2878
6	0.00031142	5.403	89.939		

PCA results including eigenvalues and shape variance are given on the left side of the table, results of the multivariate regression of shape and size are given on the right.

TABLE 5.4b. Ontogenetic shape variation at the gorilla ulnar midshaft

PC	Eigenvalues	% Variance	% Cumulative	Allometry	
1	0.00339790	44.455	44.455	Size variance	11.6%
2	0.00179658	23.505	67.960	*P*	0.0004
3	0.00076884	10.059	78.019	Total SS	0.3592
4	0.00050704	6.634	84.653	Predicted SS	0.0417
5	0.00035245	4.611	89.264	Residual SS	0.3174
6	0.00021647	2.832	92.096		

PCA results including eigenvalues and shape variance are given on the left side of the table, results of the multivariate regression of shape and size are given on the right.

TABLE 5.4c. Ontogenetic shape variation at the orangutan ulnar midshaft

PC	Eigenvalues	% Variance	% Cumulative	Allometry	
1	0.00516569	47.650	47.650	Size variance	12.9%
2	0.00175824	16.219	63.869	*P*	0.0001
3	0.00156153	14.404	78.273	Total SS	0.6287
4	0.00070682	6.520	84.793	Predicted SS	0.0814
5	0.00047700	4.400	89.194	Residual SS	0.5472
6	0.00032491	2.997	92.191		

PCA results including eigenvalues and shape variance are given on the left side of the table, results of the multivariate regression of shape and size are given on the right.

TABLE 5.4d. Ontogenetic shape variation at the hylobatid ulnar midshaft

PC	Eigenvalues	% Variance	% Cumulative	Allometry	
1	0.00283091	36.880	36.880	Size variance	11.5%
2	0.00186567	24.305	61.185	*P*	0.0001
3	0.00108709	14.162	75.347	Total SS	0.4375
4	0.00074054	9.647	84.995	Predicted SS	0.0504
5	0.00034571	4.504	89.498	Residual SS	0.387
6	0.00024847	3.237	92.735		

PCA results including eigenvalues and shape variance are given on the left side of the table, results of the multivariate regression of shape and size are given on the right.

TABLE 5.4e. Ontogenetic shape variation at the macaque ulnar midshaft

PC	Eigenvalues	% Variance	% Cumulative	Allometry	
1	0.00242149	36.086	36.086	Size variance	2.2%
2	0.00195651	29.157	65.243	*P*	0.3297
3	0.00071981	10.727	75.970	Total SS	0.3355
4	0.00047518	7.081	83.052	Predicted SS	0.0074
5	0.00032145	4.790	87.842	Residual SS	0.328
6	0.00022929	3.417	91.259		

PCA results including eigenvalues and shape variance are given on the left side of the table, results of the multivariate regression of shape and size are given on the right.

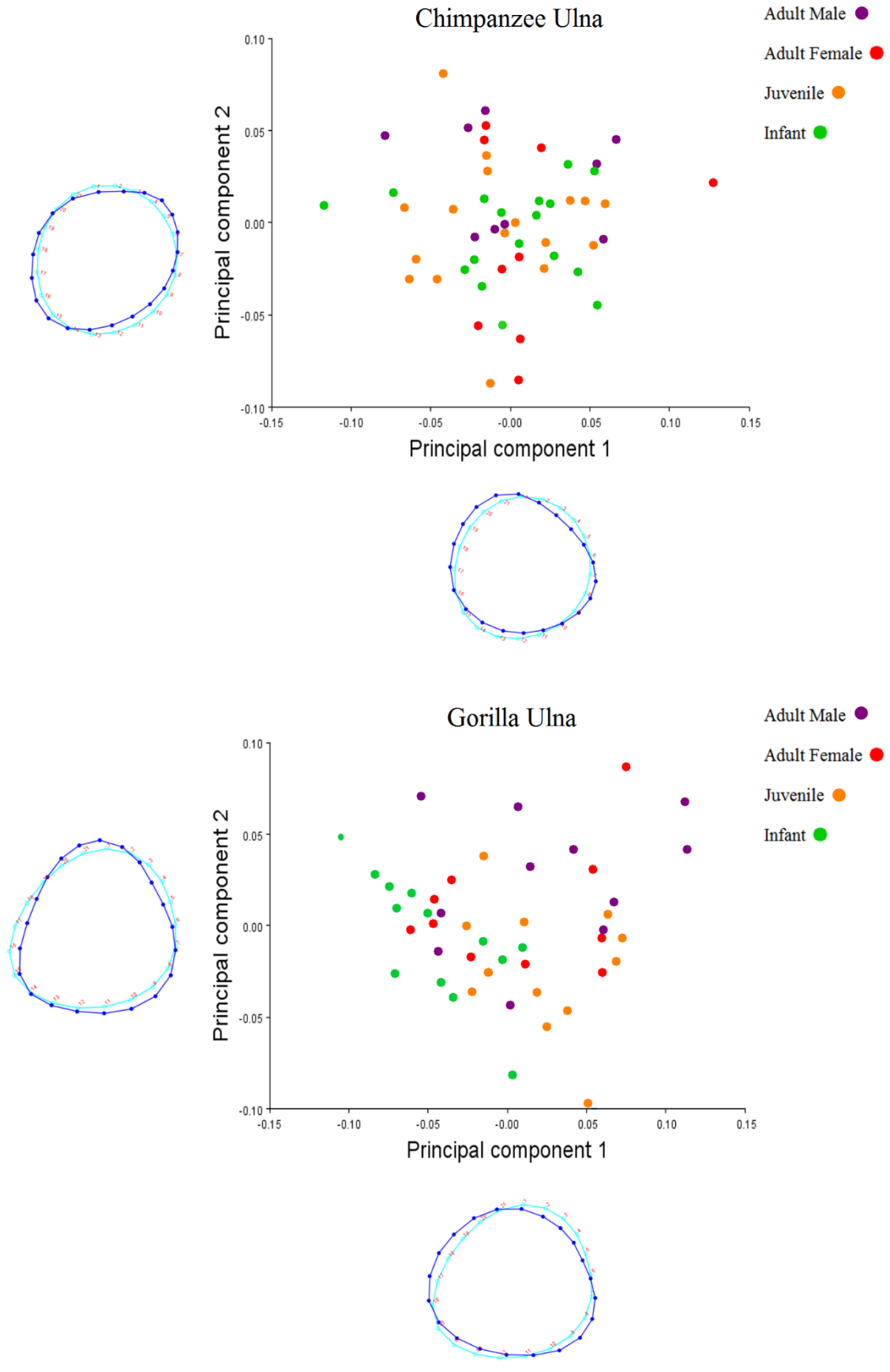

Fig. 5.5a and b. Scatter plot of ulnar midshaft developmental variation projected onto PC1 and PC2 in shape space. Wireframes along the axes represent shape variation; the light blue outlines depict shape at the low ends of their respective axes and the dark blue outlines depict the high ends.

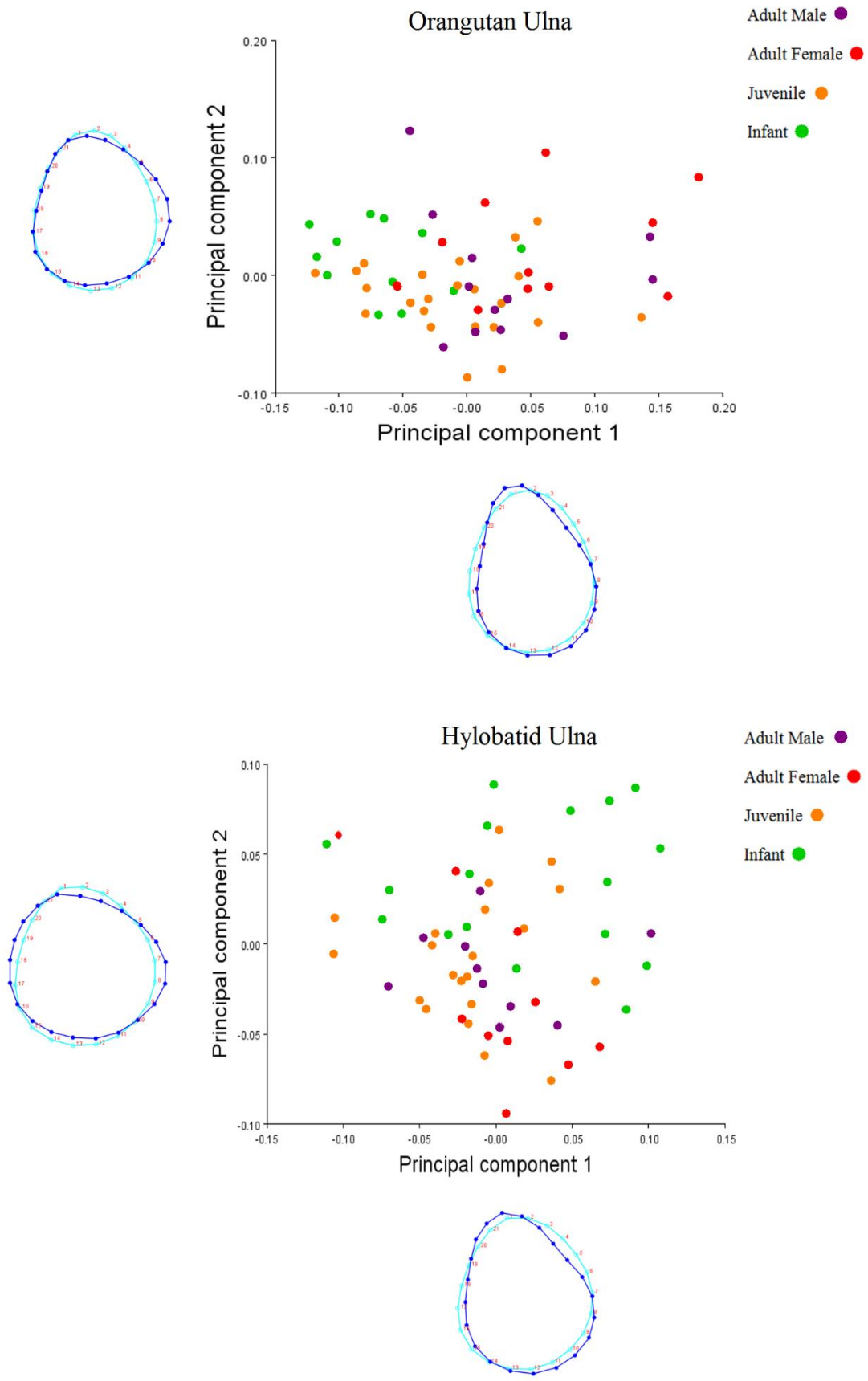

Fig. 5.5c and d. Scatter plot of ulnar midshaft developmental variation projected onto PC1 and PC2 in shape space. Wireframes along the axes represent shape variation; the light blue outlines depict shape at the low ends of their respective axes and the dark blue outlines depict the high ends.

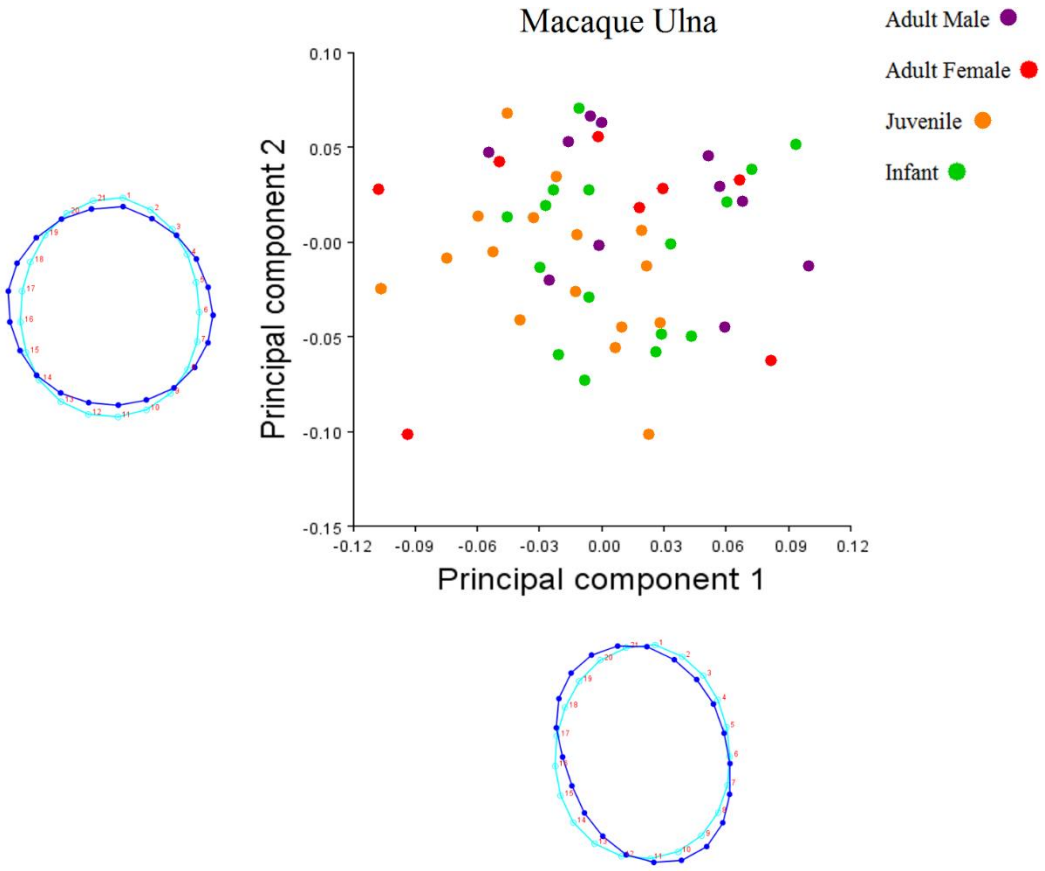

Fig. 5.5e. Scatter plot of ulnar midshaft developmental variation projected onto PC1 and PC2 in shape space. Wireframes along the axes represent shape variation; the light blue outlines depict shape at the low ends of their respective axes and the dark blue outlines depict the high ends.

5.4.4 Interspecific shape variation at the ulnar midshaft

PC1 vectors at the mid-ulna ranged from 30.4° between orangutans and hylobatids, to 83.3° between chimpanzees and hylobatids (Table 5.5). Similar to the humerus, the relatively large angles at the mid-ulna highlighted the wide diversity of ontogenetic shape variation in the forelimb, even among genetically and behaviourally similar genera. Unlike the humerus, hominid shape trajectories were widely variable. For instance, the angle formed between chimpanzees and orangutans was relatively large compared to that formed in the humerus. However, the angles formed between orangutans and hylobatids, as well as between gorillas and macaques were

smaller. The hylobatid and macaque angle was considerably smaller in the ulna compared to the humerus.

TABLE 5.5. Vector angle comparisons between PC1s of mid-ulnar ontogenetic series

	Macaca	*Pan*	*Gorilla*	*Pongo*
Pan	77.5° (< 0.186)			
Gorilla	31.3° (< 0.001)	74.6° (< 0.102)		
Pongo	52° (< 0.001)	73.2° (< 0.074)	56° (< 0.001)	
Hylobatidae	33.5° (< 0.001)	83.3° (< 0.479)	36.2° (< 0.001)	30.4° (< 0.001)

P-values given in parentheses beside the vector angles.

Through CVA, permutation tests of group means of mid-ulnar Mahalanobis and Procrustes distance were compared to determine how interspecific shape varied across development. Mahalanobis distance was significantly different among all taxa at each developmental stage (Appendix; Figure A5.10). Comparisons of Procrustes distance were more conservative (Tables 5.6a – 5.6c) but also discriminated each taxon by mid-ulnar shape more successfully than the principal and second moment of area ratios reviewed in Chapter 3. The only two subgroups that could not be discriminated by Procrustes distance were the infant gorillas and orangutans, suggesting that shape variation is greater at the mid-ulna than the mid-humerus across development (Table 5.6a).

TABLE 5.6a. Procrustes distance group mean comparisons of infant mid-ulnar shape

	Pan	*Gorilla*	*Pongo*	Hylobatidae	*Macaca*
Pan	**x**	0.0007	0.0001	0.0100	0.0001
Gorilla	0.068	**x**	n.s	0.0001	0.0100
Pongo	0.073	0.043	**x**	0.0100	0.0001
Hylobatidae	0.055	0.1	0.105	**x**	0.0113
Macaca	0.1	0.144	0.14	0.058	**x**

The diagonal-left side of the table denotes Procrustes distances among groups. *P*-values derived from 10,000 permutation rounds are given on the diagonal-right, non-significant relationships denoted by 'n.s'.

TABLE 5.6b. Procrustes distance group mean comparisons of juvenile mid-ulnar shape

	Pan	*Gorilla*	*Pongo*	Hylobatidae	*Macaca*
Pan	**x**	0.0041	0.0001	0.0081	0.0024
Gorilla	0.053	**x**	0.0001	0.0007	0.0001
Pongo	0.096	0.133	**x**	0.0001	0.0001
Hylobatidae	0.044	0.056	0.08	**x**	0.0001
Macaca	0.054	0.1	0.075	0.072	**x**

The diagonal-left side of the table denotes Procrustes distances among groups. *P*-values derived from 10,000 permutation rounds are given on the diagonal-right, non-significant relationships denoted by 'n.s'.

TABLE 5.6c. Procrustes distance group mean comparisons of adult mid-ulnar shape

	Pan	*Gorilla*	*Pongo*	Hylobatidae	*Macaca*
Pan	**x**	0.0025	0.0001	0.0001	0.0001
Gorilla	0.053	**x**	0.0001	0.0001	0.0001
Pongo	0.124	0.129	**x**	0.0006	0.0001
Hylobatidae	0.077	0.073	0.066	**x**	0.0001
Macaca	0.085	0.115	0.098	0.087	**x**

The diagonal-left side of the table denotes Procrustes distances among groups. *P*-values derived from 10,000 permutation rounds are given on the diagonal-right, non-significant relationships denoted by 'n.s'.

5.4.5 Intraspecific shape variation at the femoral midshaft

Eigenvalues, shape variance and size effects of the mid-femur are given in Tables 5.7a – 5.7e. Cumulative shape variance among the great apes ranged between 59.1% (chimpanzees) and 66.1% (gorillas) by PC2. Multivariate regressions of femoral size and shape highlighted a strong allometric effect among the great ape taxa, where size accounted for a considerable portion of midshaft shape variation (Tables 5.7a – 5.7c) compared to either upper limb element. Size had a smaller influence on shape in both the hylobatids and macaques, though allometry was still a significant factor in both taxa (Tables 5.7d and 5.7e).

Figure 5.6a – 5.6e describes the mid-femoral shape change over each taxon's development as well as between adult males and females. All three great ape taxa transitioned from a relatively circular to ML elliptical shape configuration between infancy and adulthood. Gorillas and orangutans exhibited a pronounced sexually dimorphic signal among adults, where females of both genera possessed more circular midshafts than their male counterparts (Figures 5.6b and 5.6c). By comparison, chimpanzees exhibited more of an overlap between adult male and female scatters (Figure 5.6a). In addition to the chimpanzee sample, the hylobatids, and especially macaques, exhibited considerable sexual and developmental shape overlap (Figures 5.6d and 5.6e). Moreover, neither of the two smaller-bodied taxa displayed the same ML elliptical configuration found among the great apes. Instead, adult hylobatids possessed highly circular midshaft sections with greater bone distributed in the posterior plane compared to infants. The extensive overlap across the macaque subgroups made it difficult to discern and assign a shape pattern to any one developmental group. However, this did not appear to be an effect of interspecific variation, as *M. mulatta* and *M. fascicularis* adult scatters overlapped across PC1 and PC2 (Figure 5.7).

TABLE 5.7a. Ontogenetic shape variation at the chimpanzee femoral midshaft

PC	Eigenvalues	% Variance	% Cumulative	Allometry	
1	0.00228188	40.342	40.342	Size variance	21.7%
2	0.00105856	18.715	59.057	*P*	0.0001
3	0.00091590	16.193	75.249	Total SS	0.2884
4	0.00044954	7.948	83.197	Predicted SS	0.0625
5	0.00018437	3.260	86.456	Residual SS	0.2259
6	0.00017194	3.040	89.496		

PCA results including eigenvalues and shape variance are given on the left side of the table, results of the multivariate regression of shape and size are given on the right.

TABLE 5.7b. Ontogenetic shape variation at the gorilla femoral midshaft

PC	Eigenvalues	% Variance	% Cumulative	Allometry	
1	0.00311793	35.814	35.814	Size variance	17.2%
2	0.00263341	30.248	66.062	*P*	0.0001
3	0.00101743	11.687	77.749	Total SS	0.4091
4	0.00059586	6.844	84.593	Predicted SS	0.0705
5	0.00032921	3.781	88.375	Residual SS	0.3386
6	0.00022231	2.554	90.928		

PCA results including eigenvalues and shape variance are given on the left side of the table, results of the multivariate regression of shape and size are given on the right.

TABLE 5.7c. Ontogenetic shape variation at the orangutan femoral midshaft

PC	Eigenvalues	% Shape Variance	% Cumulative	Allometry	
1	0.00219781	34.350	34.350	Size variance	19.4%
2	0.00169227	26.449	60.798	*P*	0.0001
3	0.00096211	15.037	75.835	Total SS	0.3519
4	0.00047235	7.382	83.218	Predicted SS	0.0684
5	0.00023533	3.678	86.896	Residual SS	02835
6	0.00019167	2.996	89.891		

PCA results including eigenvalues and shape variance are given on the left side of the table, results of the multivariate regression of shape and size are given on the right.

TABLE 5.7d. Ontogenetic shape variation at the hylobatid femoral midshaft

PC	Eigenvalues	% Variance	% Cumulative	Allometry	
1	0.00134360	31.783	31.783	Size variance	5%
2	0.00096163	22.748	54.531	*P*	0.009
3	0.00051416	12.163	66.693	Total SS	0.3519
4	0.00047037	11.127	77.820	Predicted SS	0.0684
5	0.00023043	5.451	83.271	Residual SS	02835
6	0.00016411	3.882	87.153		

PCA results including eigenvalues and shape variance are given on the left side of the table, results of the multivariate regression of shape and size are given on the right.

TABLE 5.7e. Ontogenetic shape variation at the macaque femoral midshaft

PC	Eigenvalues	% Variance	% Cumulative	Allometry	
1	0.00108993	29.312	29.312	Size variance	7%
2	0.00073641	19.804	49.116	*P*	0.0014
3	0.00055983	15.056	64.172	Total SS	0.2045
4	0.00038200	10.273	74.445	Predicted SS	0.0143
5	0.00024480	6.583	81.028	Residual SS	0.1901
6	0.00018498	4.975	86.003		

PCA results including eigenvalues and shape variance are given on the left side of the table, results of the multivariate regression of shape and size are given on the right.

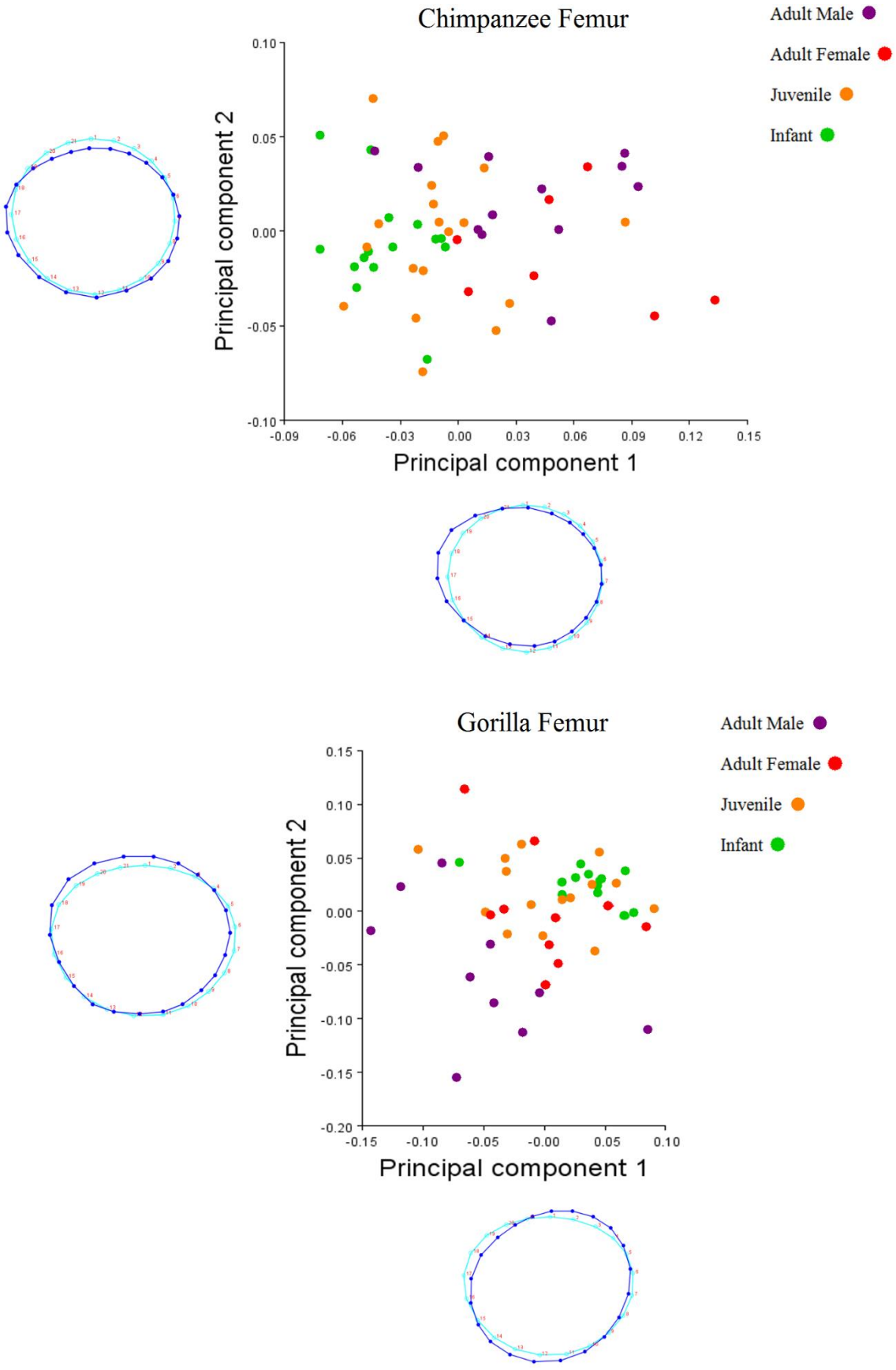

Fig. 5.6a and b. Scatter plot of femoral midshaft developmental variation projected onto PC1 and PC2 in shape space. Wireframes along the axes represent shape variation; the light blue outlines depict shape at the low ends of their respective axes and the dark blue outlines depict the high ends.

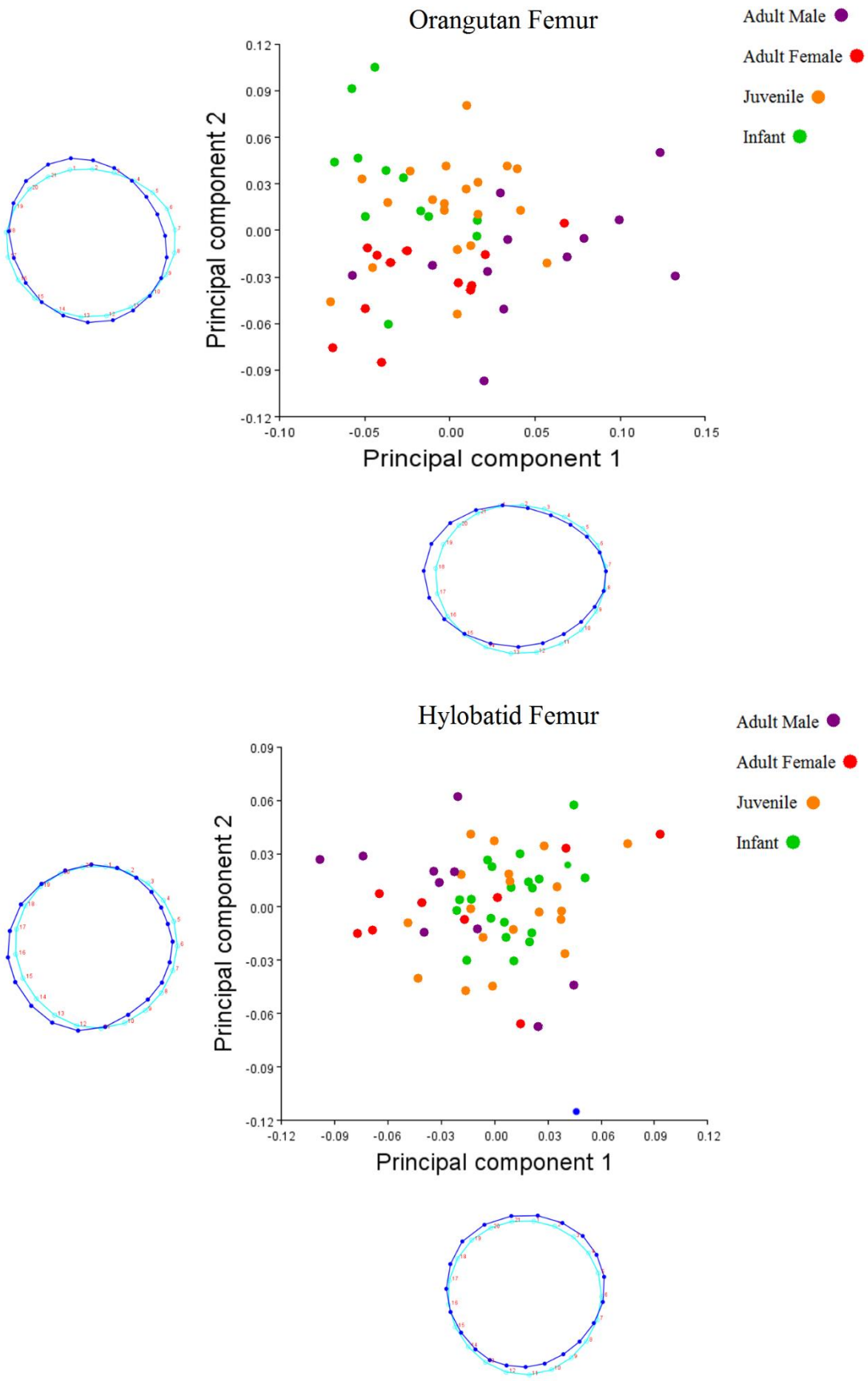

Fig. 5.6c and d. Scatter plot of femoral midshaft developmental variation projected onto PC1 and PC2 in shape space. Wireframes along the axes represent shape variation; the light blue outlines depict shape at the low ends of their respective axes and the dark blue outlines depict the high ends.

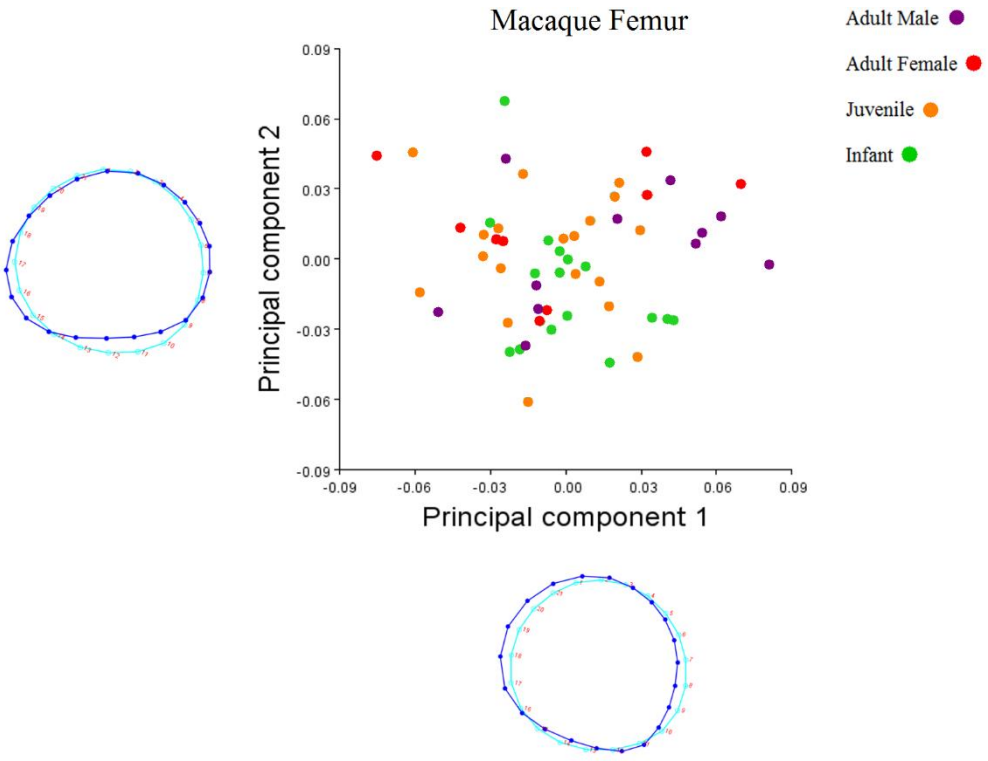

Fig. 5.6e. Scatter plot of femoral midshaft developmental variation projected onto PC1 and PC2 in shape space. Wireframes along the axes represent shape variation; the light blue outlines depict shape at the low ends of their respective axes and the dark blue outlines depict the high ends.

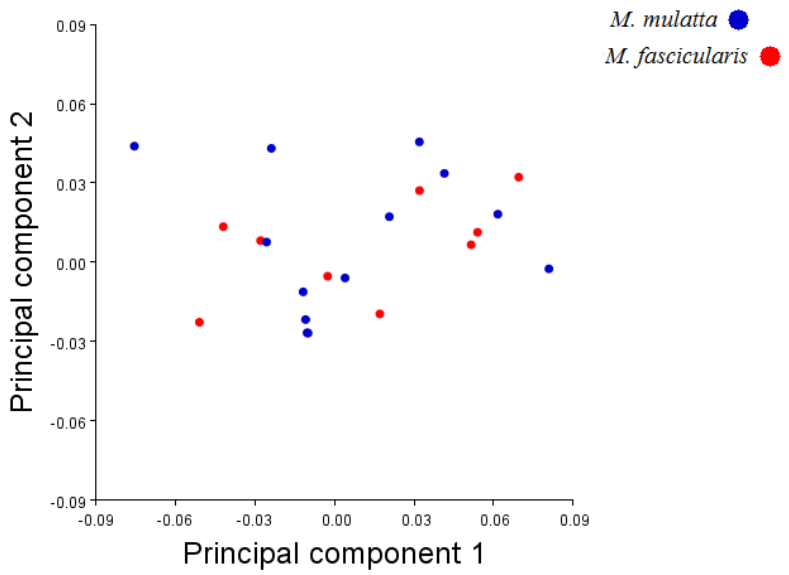

Fig. 5.7. PCA scatter plot describing mid-femoral shape dispersion between the adult rhesus and long-tailed macaque subgroups. See wireframes from Figure 5.6e.

5.4.6 Interspecific shape variation at the femoral midshaft

Mid-femoral PC1 vector angles ranged between 23.2° and 57.4°. Femoral vectors did not appear to reflect the angles formed in the upper limb elements and for the most part, were generally smaller in size and range. The vectors formed particularly small angles between the great ape taxa. The chimpanzee-gorilla vector angle was the smallest in the analysis in contrast to the relatively large angles formed between the two African apes in the upper limb elements. Both the hylobatids and macaques generated smaller angles with the Asian apes compared to the African apes. Permutation tests comparing interspecific Mahalanobis distances were significant between the means of all taxonomic groups at each developmental stage (Appendix; Figure A5.11). Comparisons of Procrustes distance also identified significant femoral shape variation across development, though these differences were more conservative between taxa (Tables 5.9a – 5.9c). For instance, mid-femoral shape did not differ between infant chimpanzees or orangutans (Table 6.10a), but did among juveniles and adults. Chimpanzee and macaque mid- femoral shape exhibited some overlap among the juvenile subgroups, though shape was ultimately found to be significantly different between the two taxonomic subgroups (Table 5.9b).

TABLE 5.8. Vector angle comparisons between PC1s of mid-femoral ontogenetic series

	Macaca	*Pan*	*Gorilla*	*Pongo*
Pan	41.3° (< 0.001)			
Gorilla	46.3° (< 0.001)	23.2° (< 0.001)		
Pongo	27.3° (< 0.001)	28.1° (< 0.001)	26° (< 0.001)	
Hylobatidae	37° (< 0.001)	55.8° (< 0.001)	57.4° (< 0.001)	39.2° (< 0.001)

P-values given in parentheses beside the vector angles.

TABLE 5.9a Procrustes distance group mean comparisons of infant mid-femoral shape

	Pan	*Gorilla*	*Pongo*	Hylobatidae	*Macaca*
Pan	**x**	0.0001	n.s	0.0015	0.0001
Gorilla	0.063	**x**	0.0008	0.0001	0.0001
Pongo	0.026	0.053	**x**	0.0004	0.0137
Hylobatidae	0.032	0.062	0.044	**x**	0.0001
Macaca	0.046	0.071	0.039	0.04	**x**

The diagonal-left side of the table denotes Procrustes distances among groups. *P*-values derived from 10,000 permutation rounds are given on the diagonal-right side of the table, non-significant relationships denoted by 'n.s'.

TABLE 5.9b Procrustes distance group mean comparisons of juvenile mid-femoral shape[1]

	Pan	*Gorilla*	*Pongo*	Hylobatidae	*Macaca*
Pan	**x**	0.0001	0.0105	0.0245	0.0481
Gorilla	0.063	**x**	0.0001	0.0001	0.0001
Pongo	0.037	0.055	**x**	0.0013	0.0001
Hylobatidae	0.031	0.08	0.055	**x**	0.0076
Macaca	0.03	0.077	0.047	0.03	**x**

The diagonal-left side of the table denotes Procrustes distances among groups. *P*-values derived from 10,000 permutation rounds are given on the diagonal-right side of the table, non-significant relationships denoted by 'n.s'.

TABLE 5.9c Procrustes distance group mean comparisons of adult mid-femoral shape

	Pan	*Gorilla*	*Pongo*	Hylobatidae	*Macaca*
Pan	**x**	0.0001	0.0047	0.0001	0.0002
Gorilla	0.084	**x**	0.0003	0.0001	0.0001
Pongo	0.052	0.071	**x**	0.0001	0.0001
Hylobatidae	0.088	0.133	0.095	**x**	0.0393
Macaca	0.062	0.117	0.079	0.037	**x**

The diagonal-left side of the table denotes Procrustes distances among groups. *P*-values derived from 10,000 permutation rounds are given on the diagonal-right side of the table, non-significant relationships denoted by 'n.s'.

5.4.7 Intraspecific shape variation at the tibial midshaft

Tables 5.10a – 5.10e give the PCA and regression results of the five taxa over development. The first two tibial PCs explained more shape variance than the other three elements, ranging from 63.8% among the macaque sample to 76.5% among the hylobatids. Size accounted for greater variation at the mid-tibia than any other element, as well. The effects of size were most evident in the hylobatid sample, though size had a significant influence on shape in the four other taxa as well (Table 5.10d).

Overall, intraspecific developmental stages were more easily distinguished by mid-tibial shape than any other element. Moreover, the tibia was the only element where all five taxa followed the same general shape-change pattern over development, characterised by a relatively circular configuration in infancy and an AP elliptical configuration by adulthood (Figures 5.8a – 5.8e). Sexual dimorphism was not as pronounced in the tibia as it was in the femur, though four adult female orangutans aligned themselves away from the adult cloud, on the low end of PC2 (Figure 5.8c). Adult macaques exhibited some sexual variation as well, where male midshafts were, in all instances but one, more AP elliptical than their female counterparts (Figure 5.8e).

TABLE 5.10a. Ontogenetic shape variation at the chimpanzee tibial midshaft

PC	Eigenvalues	% Variance	% Cumulative	Allometry	
1	0.00323891	45.345	45.345	Size variance	32.7%
2	0.00195881	27.423	72.768	*P*	0.0001
3	0.00084146	11.780	84.548	Total SS	0.3571
4	0.00030606	4.285	88.833	Predicted SS	0.1168
5	0.00021361	2.991	91.824	Residual SS	0.2403
6	0.00018022	2.523	94.347		32.7%

PCA results including eigenvalues and shape variance are given on the left side of the table, results of the multivariate regression of shape and size are given on the right.

TABLE 5.10b. Ontogenetic shape variation at the gorilla tibial midshaft

PC	Eigenvalues	% Variance	% Cumulative	Allometry	
1	0.00284770	42.583	42.583	Size variance	23.5%
2	0.00176212	26.350	68.933	*P*	0.0001
3	0.00072409	10.828	79.761	Total SS	0.3209
4	0.00040196	6.011	85.772	Predicted SS	0.0754
5	0.00026681	3.990	89.762	Residual SS	0.2455
6	0.00015163	2.267	92.029		

PCA results including eigenvalues and shape variance are given on the left side of the table, results of the multivariate regression of shape and size are given on the right.

TABLE 5.10c. Ontogenetic shape variation at the orangutan tibial midshaft

PC	Eigenvalues	% Variance	% Cumulative	Allometry	
1	0.00285142	49.232	49.232	Size variance	29.5%
2	0.00137497	23.740	72.973	*P*	0.0001
3	0.00052788	9.114	82.087	Total SS	0.3243
4	0.00027063	4.673	86.760	Predicted SS	0.0956
5	0.00023244	4.013	90.773	Residual SS	0.2286
6	0.00017015	2.938	93.711		

PCA results including eigenvalues and shape variance are given on the left side of the table, results of the multivariate regression of shape and size are given on the right.

TABLE 5.10d. Ontogenetic shape variation at the hylobatid tibial midshaft

PC	Eigenvalues	% Variance	% Cumulative	Allometry	
1	0.00437495	64.762	64.762	% Size variance	43.9%
2	0.00079423	11.757	76.519	*P*	0.0001
3	0.00041926	6.206	82.725	Total SS	0.3783
4	0.00033460	4.953	87.678	Predicted SS	0.166
5	0.00023507	3.480	91.158	Residual SS	0.2122
6	0.00015787	2.337	93.495		

PCA results including eigenvalues and shape variance are given on the left side of the table, results of the multivariate regression of shape and size are given on the right.

TABLE 5.10e. Ontogenetic shape variation at the macaque tibial midshaft

PC	Eigenvalues	% Variance	% Cumulative	Allometry	
1	0.00155843	39.863	39.863	% Size variance	22.5%
2	0.00093743	23.979	63.842	*P*	0.0001
3	0.00050414	12.896	76.738	Total SS	0.2032
4	0.00036062	9.224	85.962	Predicted SS	0.0457
5	0.00015968	4.085	90.047	Residual SS	0.1575
6	0.00008129	2.079	92.126		

PCA results including eigenvalues and shape variance are given on the left side of the table, results of the multivariate regression of shape and size are given on the right.

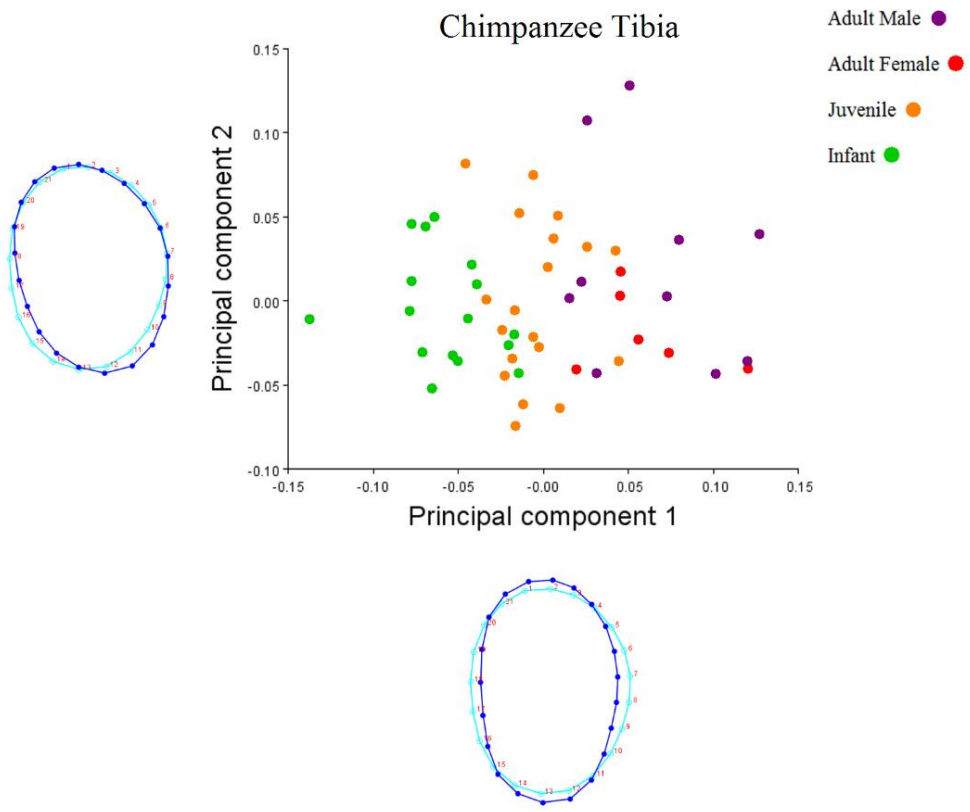

Fig. 5.8a. Scatter plot of tibial midshaft developmental variation projected onto PC1 and PC2 in shape space. Wireframes along the axes represent shape variation; the light blue outlines depict shape at the low ends of their respective axes and the dark blue outlines depict the high ends.

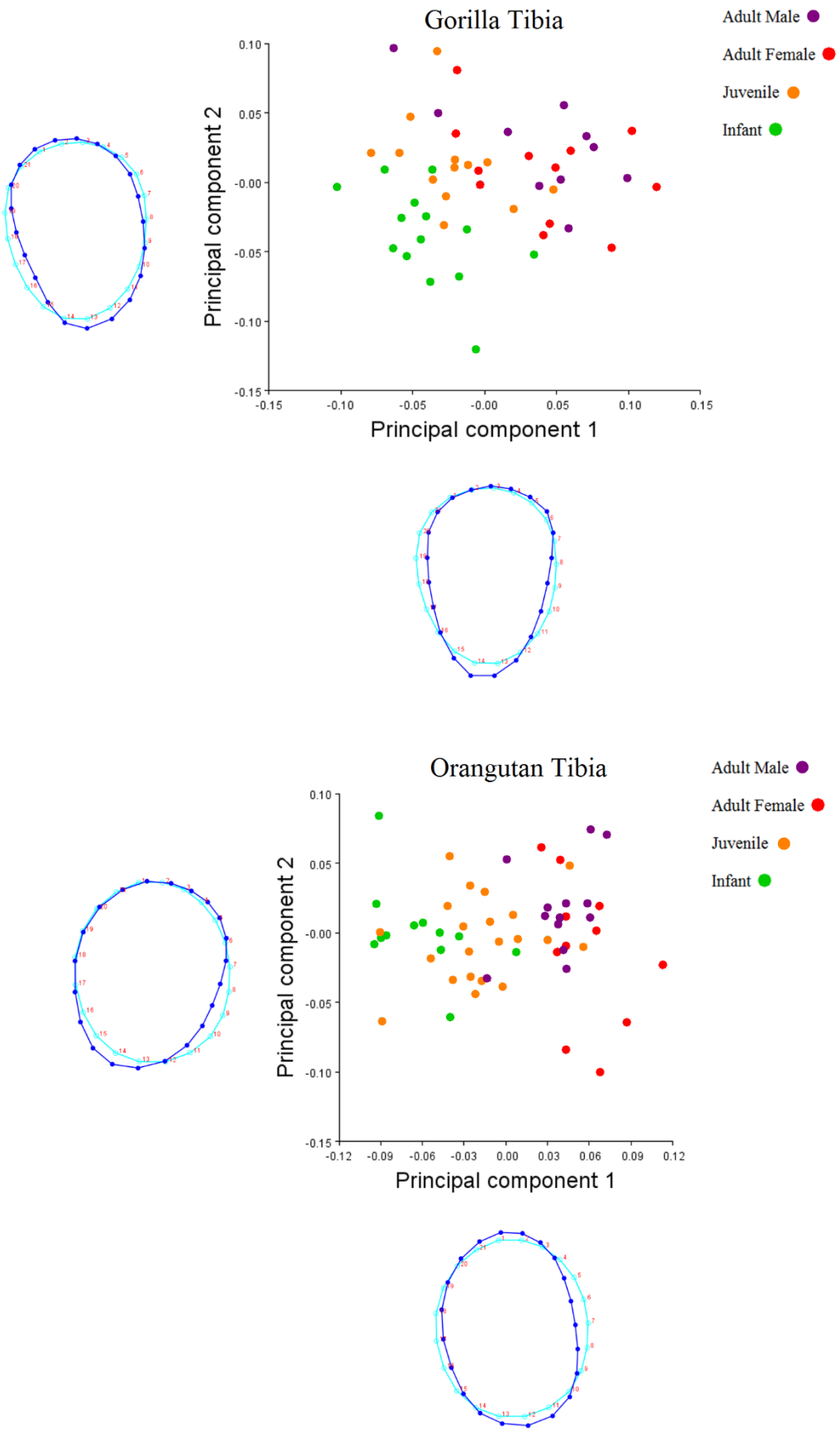

Fig. 5.8b and c. Scatter plot of tibial midshaft developmental variation projected onto PC1 and PC2 in shape space. Wireframes along the axes represent shape variation; the light blue outlines depict shape at the low ends of their respective axes and the dark blue outlines depict the high ends.

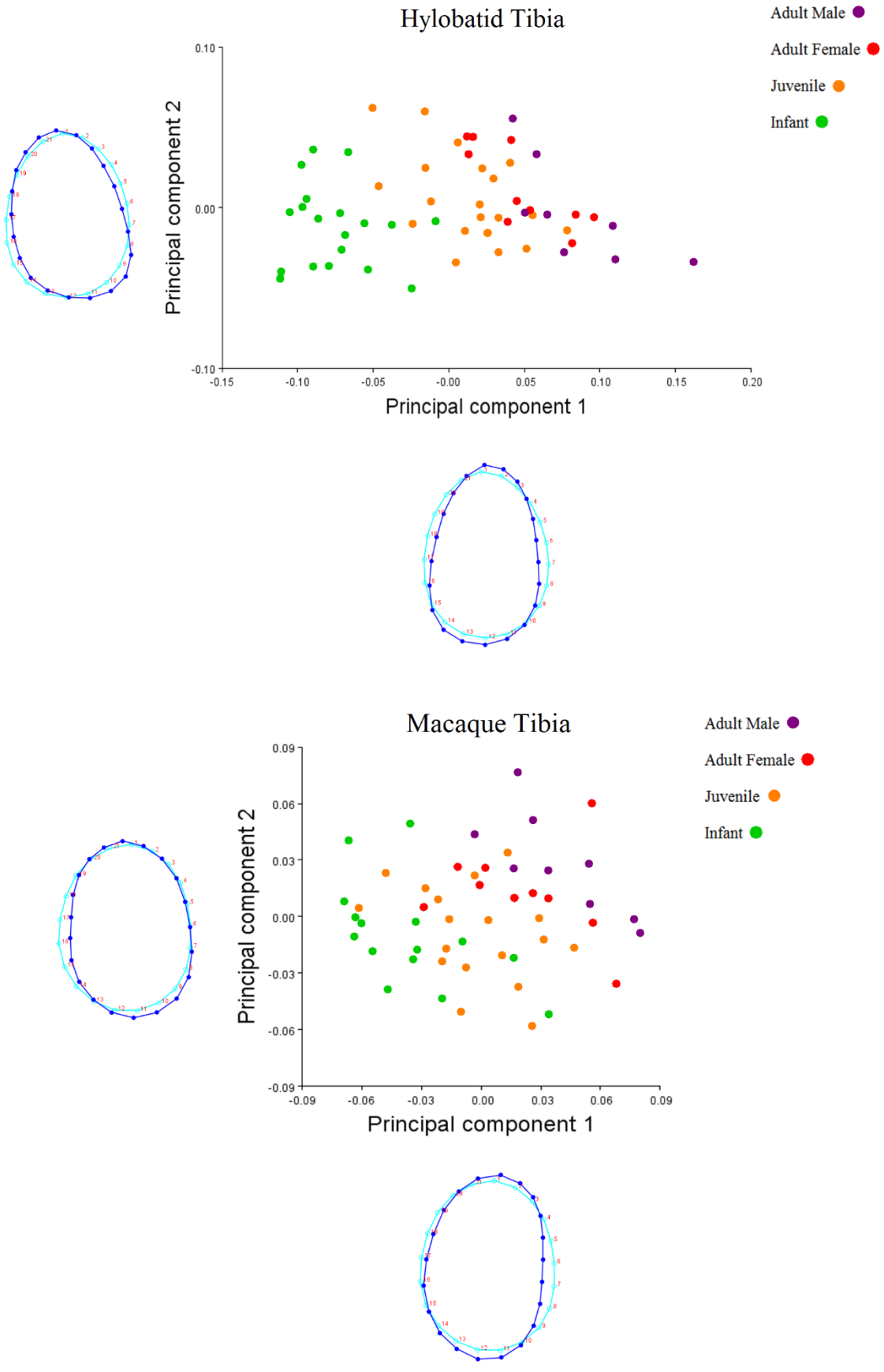

Fig. 5.8d and e. Scatter plot of tibial midshaft developmental variation projected onto PC1 and PC2 in shape space. Wireframes along the axes represent shape variation; the light blue outlines depict shape at the low ends of their respective axes and the dark blue outlines depict the high ends.

5.4.8 Interspecific shape variation at the tibial midshaft

Similar to the femur, interspecific vector angles along tibial-PC1 were overall smaller than either the mid-humerus or ulna (Table 5.11). The smallest angle formed between tibial vectors was identified between chimpanzee and orangutan ontogenetic series, and was also the smallest angle formed among all four long bone midshafts. The angle formed between hylobatids and macaques was also relatively small, suggesting that not only shape, but growth trajectory, are similar between the tibiae of the two taxa. Hominid comparisons yielded smaller angles than those found between hylobatids and macaques, but each great ape taxon formed a larger angle with the hylobatid series than they did with each other. Gorillas and hylobatids formed the largest tibial vector angle, for instance, which may be a product of the distinct ways both apes deposit bone at the midshaft as they mature.

TABLE 5.11. Vector angle comparisons between PC1s of mid-tibial ontogenetic series

	Macaca	*Pan*	*Gorilla*	*Pongo*
Pan	47.6° (< 0.001)			
Gorilla	64.5° (< 0.006)	24.8° (< 0.001)		
Pongo	49.9° (< 0.001)	15.8° (< 0.001)	28° (< 0.001)	
Hylobatidae	33.8° (< 0.001)	54.5° (< 0.001)	67.7° (< 0.017)	52.9° (< 0.001)

P-values given in parentheses beside the vector angles.

Group means comparisons of Mahalanobis distance found that all taxa exhibited significant variation from one another over their development (Appendix; Figure A5.12). Comparisons of Procrustes distance also discriminated all infant taxa, apart from orangutans and gorillas, as well as hylobatids and macaques (Table 5.12a). As with the other skeletal elements, greater interspecific shape variation was identified following infancy. For example, only the chimpanzee and hylobatid juvenile subgroups could not be discriminated from one another by mid-tibial shape (Table 5.12b).

By adulthood, all taxa could be discriminated by shape, despite their relatively similar bone distribution patterns in the AP plane (Table 5.12c).

TABLE 5.12a Procrustes distance group mean comparisons of infant mid-tibial shape

	Pan	*Gorilla*	*Pongo*	Hylobatidae	*Macaca*
Pan	**x**	0.0079	0.0103	0.0001	0.0001
Gorilla	0.044	**x**	n.s	0.0001	0.0001
Pongo	0.041	0.037	**x**	0.0001	0.0001
Hylobatidae	0.049	0.076	0.058	**x**	n.s
Macaca	0.062	0.094	0.074	0.023	**x**

The diagonal-left side of the table denotes Procrustes distances among groups. *P*-values derived from 10,000 permutation rounds are given on the diagonal-right side of the table, non-significant relationships denoted by 'n.s'.

TABLE 5.12b Procrustes distance group mean comparisons of juvenile mid-tibial shape

	Pan	*Gorilla*	*Pongo*	Hylobatidae	*Macaca*
Pan	**x**	0.0224	0.0006	n.s	0.0048
Gorilla	0.047	**x**	0.0038	0.0001	0.0004
Pongo	0.053	0.046	**x**	0.0001	0.0363
Hylobatidae	0.023	0.062	0.073	**x**	0.0001
Macaca	0.044	0.055	0.03	0.06	**x**

The diagonal-left side of the table denotes Procrustes distances among groups. *P*-values derived from 10,000 permutation rounds are given on the diagonal-right side of the table, non-significant relationships denoted by 'n.s'.

TABLE 5.12c Procrustes distance group mean comparisons of adult mid-tibial shape

	Pan	*Gorilla*	*Pongo*	Hylobatidae	*Macaca*
Pan	**x**	0.0001	0.0001	0.0001	0.0001
Gorilla	0.069	**x**	0.0001	0.0001	0.0001
Pongo	0.072	0.088	**x**	0.0001	0.0001
Hylobatidae	0.067	0.115	0.077	**x**	0.0001
Macaca	0.103	0.124	0.062	0.075	**x**

The diagonal-left side of the table denotes Procrustes distances among groups. *P*-values derived from 10,000 permutation rounds are given on the diagonal-right side of the table, non-significant relationships denoted by 'n.s'.

5.5 Discussion

The primary aim of Chapter 5 was to investigate the covariation of long bone cross-sectional size and shape over catarrhine development, using a geometric morphometric approach. Compared to the classic beam modelling methods employed in the two previous chapters, GM offered a more nuanced view of cross-sectional form by considering the dimensions of the entire contour, rather than relying solely on linear ratios within or between sections. Two primary research objectives were addressed in this chapter. The first sought to classify taxa by the interaction of their cross-sectional shape and size. To accomplish this, intraspecific PCAs were used to assign shape profiles to taxa at different stages of their development. Additionally, multivariate regressions of Procrustes distance and log CS evaluated the effects of allometry within each sample. The second objective attempted to classify taxa by their ontogenetic shape trajectories by analysing the angles formed by their respective shape vectors. To discriminate taxa at discrete stages of their development, groups means of Mahalanobis and Procrustes distance were compared using CVA. Vector angle size appeared contingent on the skeletal element in question more than any other factor, offering a new method for interpreting skeletal ontogeny between taxa. The results demonstrate that a geometric morphometric approach to cross-sectional shape analysis is as effective as using principal and area ratios, and depending on the research objectives, potentially a more powerful way of interpreting developmental and taxonomic variation within

and between limbs. Comparisons of form also offer an ontogenetic perspective that can further complement analyses of other geometric properties (i.e., measures of rigidity and strength).

5.5.1 Long bone growth trajectories

Vector angles paired with Procrustes group means comparisons provided a novel approach to studying primate limb development. While research on primate cranial ontogeny can inform about the genetic or systemic factors that govern skull form (Ponce de León and Zollikofer, 2001; Schaefer et al., 2004), the analysis of midshaft development introduce a third factor: adaptive plasticity. In agreement with comparisons of hominid skull form (Cobb and O'Higgins, 2004), none of the sampled primates share a common ontogeny, nor a common point of shape divergence for any one long bone, suggesting that most morphological variation is established pre- or neonatally, then further developed through genetic pathways and finally, plastically refined by the loading environment. Compared to shape-canalised postcranial elements linked to locomotion like the scapula though (Young, 2006), humeral midshafts do appear more generalised among young primates. The variation that is present during infancy also appears to bear more of a locomotor than a phylogenetic signal. For instance, infant humeral shape variation between phylogenetically disparate taxa like gorillas and macaques is negligible, while gorilla and chimpanzee shape is easily distinguishable in infancy. In fact, the vector angle formed between gorillas and macaques is smaller than those formed between gorillas and either of the other two great apes. Rather than genetic or size variation, the terrestrial quadrupedal locomotor behaviour employed by gorillas (Taylor, 1997; Remis, 1998) and macaques (Wells and Turnquist, 2001) during infancy is a more likely explanation for the humeral shape they share. As the two taxa grow and their postures change, humeral shape becomes distinctly discernible between them. The similar humeral shape of chimpanzees and orangutans over their development also favours an adaptationist perspective. From infancy, both chimpanzees and orangutans exhibit circular humeral midshafts which may facilitate their largely arboreal lifestyles. Compared to the other apes, chimpanzees are not fully adapted to either arboreal or terrestrial locomotion (Rose, 1991), though both are important components to their daily active periods (Hunt, 1991, 1992; Doran, 1992a,b); especially among infants (Doran, 1997). Even after their transition to a more terrestrial posture in juvenility (Doran,

1997), vertical climbing is up to ten times more energy efficient than terrestrial travel among chimpanzees (Pontzer and Wrangham, 2004) emphasising the importance of arboreality to their survival (Hunt, 2016). Thus, the dynamic loads brought on during suspension and climbing may govern the humeral shape of both chimpanzees and orangutans into adulthood. If humeral cross-sectional shape were more a product of phylogeny, gorillas would be expected to bear some resemblance to their hominid cousins, at least in infancy. Instead, infant hylobatids exhibit greater overlap with chimpanzees and orangutans, suggesting that some adaptation to suspensory locomotion early in life yields a relatively consistent pattern at the humeral midshaft, followed by further specialisation to whatever unique locomotor repertoire with maturity.

The discrimination of adult male and female chimpanzee humeral shape found using PCA was overlooked by circularity analyses used in Chapter 3, likely due to small dimensional differences beyond the detection of geometric ratios. While postcranial dimorphism in *Pan* is not as pronounced as in *Gorilla* or *Homo* (Reno et al., 2003), significant sexual variation in forearm length has been identified among adult *P. troglodytes*, and attributed to differences in somatic growth (Behringer et al., 2016). It is likely that the sexual cross-sectional differences found here are more closely related to body size than locomotor variation however, as there are few differences in positional and locomotor behaviour between male and female chimpanzees in both arboreal and terrestrial contexts (Doran, 1993), but moderate variation in mass and size (Shea, 1985; Smith and Jungers, 1997). While there is male-female overlap in adult humeral shape (Figure 6.4a), a more exaggerated ML configuration among males suggests that body mass signals may be detectable in intraspecific comparisons. Moreover, this observation has implications to Chapter 3's findings of significant shape variation between male and female gorillas, as well as prior research that has attributed cross-sectional geometric differences strictly to products of positional behaviour (Ruff et al., 2013).

The upper arm and forearm diaphyses do not follow parallel growth trajectories, however. Overall, the ulnar midshaft appears more canalised than the humerus for two reasons. First, the humeral shape overlap among posture-similar infant taxa was not mirrored in the ulna (i.e., significant differences in ulnar shape were established between chimpanzees and orangutans; gorillas and macaques). Instead, most ulnar shape variation is already established among infant catarrhines. Second, shape appears developmentally constrained compared to the humerus

following infancy. This is likely due to the ulna's gracility and load-sharing role with the radius (Birkbeck et al., 1997), which may confine tissue economy in the forearm to a greater extent than in more robust weight-bearing bones like the humerus. Optimality models of bone formation have indeed found that remodelling is dominant in distal limb segments, with frequency incrementally declining toward the axial skeleton in favour of new bone deposition (Lieberman, et al., 2003; Skedros et al., 2003). In other words, the mechanical strain placed on the humerus may be sufficient to adaptively model its structure to an individual's locomotor needs, while the more canalised ulna more readily repairs its predefined shape when microfractured. Ulnar vector analysis also lends some support to this view, particularly in the Asian apes. The angles formed between orangutans and hylobatids were considerably smaller in the ulna than they were in the humerus, which suggests that forearm development may be similar among the two taxa. Support for this premise is weakened by ulnar vector comparisons between hylobatids with gorillas and macaques, however, which form angles only a few degrees larger than those with orangutans. With no clear locomotor or size signal visible, mid-ulnar shape trajectories do not appear as reliable as humeral trajectories at classifying taxa on an ecological basis. The developmental and morphological differences between the humerus and ulna are a testament to how durable gracile bones must be to function effectively, while also remaining strong enough to withstand mechanical failure (Alexander, 1981, 1998). It follows that specialised element characters like those in the forearm must be more adaptively constrained, and therefore, may be better suited for distinguishing subtle mechanical differences between locomotor-diverse species or populations (as opposed to genera or families), as has been conducted with success among modern humans (Stock, 2006; Shaw and Stock, 2009a; Hagihara and Takashi, 2017). It is also possible that the mid-ulnar periosteal contour alone is inadequate at identifying developmental relationships but may be more informative when complemented with endosteal data. While one study successfully discriminated *G. beringei* from *G. g. gorilla* by their radial/ulnar cross-sectional strength (Ruff et al., 2013), there are a multitude of primate species, subspecies and populations that exhibit variable locomotor profiles as adaptations to their unique loading environments, across *Pan*, *Papio*, *Macaca*, and *Cercopithecus*, to name a few. Combining ontogenetic cranial data with limb cross-sectional data would give an impression of how locomotor adaptations factor into phylogenetic inertia, constraint and radiation across a given group, by measuring how adaptively constrained

facets of the skeleton covary with adaptively plastic facets. Additional comparisons including GM analysis of distal ulnar sections may be helpful in discerning signals between groups as well, especially given how little its shape changes across development in any given taxon (See results of Chapter 3).

Unlike the forelimb elements, the femur and tibia exhibited a common pattern of bone deposition across each taxon's development, generating relatively small vector angles in the hindlimb compared to the forelimb. Specifically, femora are typically circular in infancy, with shape becoming more ML elliptical by adulthood (to the exception of hylobatids, which exhibit little femoral shape change as they mature). Tibial midshafts also assume a relatively circular shape early in life before bone is deposited primarily along the AP plane. The most parsimonious explanation for a common hindlimb deposition pattern among apes and monkeys is the stereotypic, and generally parasagittal limb excursion permitted by the hip and knee, compared to the dynamic movements permitted by the shoulder and elbow (Jenkins, 1973; Rose, 1993). Even when the upper arm is loaded in a predominantly parasagittal fashion as in gorillas and macaques, the humeral midshaft adapts itself in a manner similar to the femur by depositing more bone along the ML axis in both taxa. Despite the interspecific similarities of hindlimb deposition, the detail captured using GM not only made it possible to discriminate taxa by shape, but to specifically identify which aspects of a section differentiate them. One of the strongest examples came from the gorilla and hylobatid tibia. In Chapter 3, area ratios demonstrated that while both apes deposit new bone in the AP plane as they mature, hylobatids displayed a higher ratio than gorillas, indicative of a more elliptical section. By studying aspects of section shape beyond the principal and anatomical axes, it became evident that only gorillas reinforce the antero-medial and lateral planes of their tibiae from infancy through to adulthood. As hylobatids mature, they deposit new bone anteriorly and posteriorly and possibly resorb bone from the medial and lateral sides relatively evenly (Figure 5.9). While ratios generated from conventional geometric axes are useful tools for inferring general locomotor patterns between taxa (Carlson, 2005; Patel et al., 2013; Burgess et al., 2016), quantifying shape change about the entire contour offers an opportunity to study intricate allometric differences that ratios simply cannot describe. The subtle variation in distribution may be valuable for inferring limb evolution and adaptation, especially considering

how precise the GM group means comparisons are at differentiating taxa compared to either of the linear ratio comparisons made in Chapter 3.

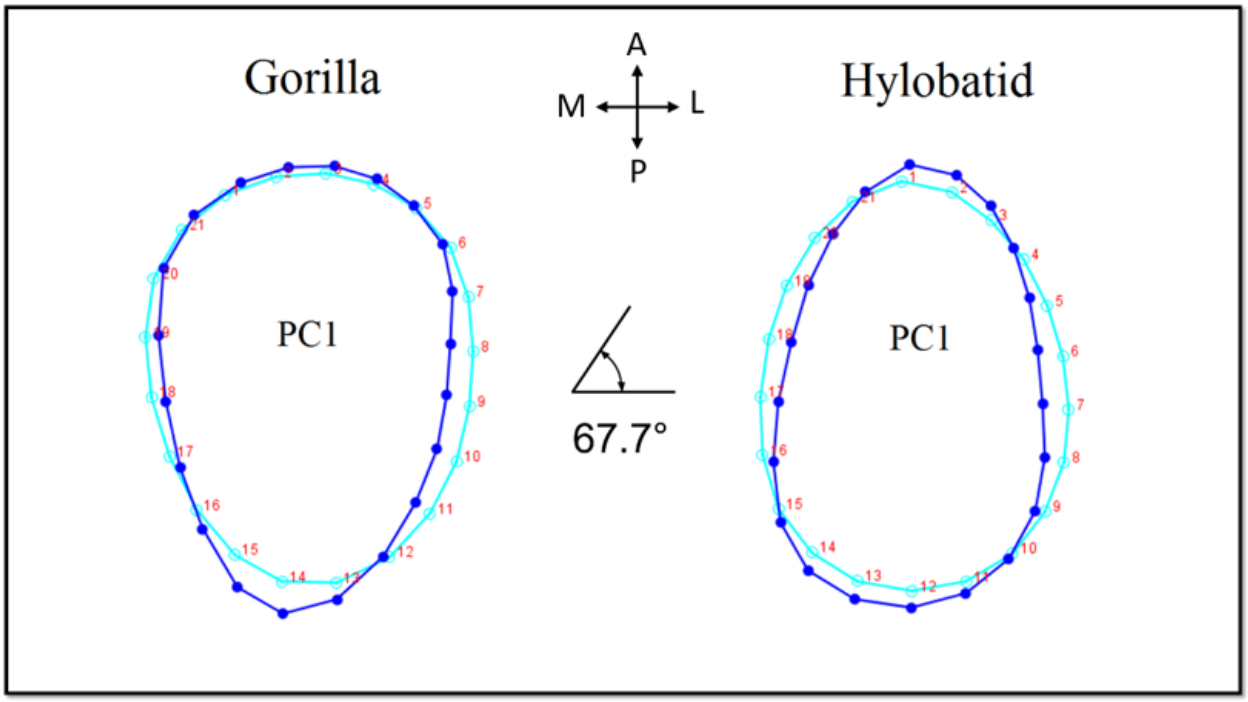

Fig. 5.9. Size-scaled wireframe comparison and PC1 vector angle of pooled gorilla and hylobatid mid-tibial development. The light blue outline illustrates the infant condition while the dark blue outline illustrates the adult condition. Though both taxa deposit bone along the AP axis as they mature, PCA defined potential planes of deposition and resorption with precision, revealing a distinctly different ontogenetic pattern between the two taxa. Cross-sections oriented along the anatomical axes.

The wide range of angles described how variable each element's development is, in that no two taxa of similar genetic, postural or size affiliation revealed any analogous growth pattern when considering the four skeletal elements together. From a developmental standpoint, primate skeletons are mosaics, with each limb element reflecting different adaptive signals at different stages of their development. For example, humeral, femoral and tibial form follow a relatively similar developmental trajectory among chimpanzees and orangutans (20.8°, 28.1° and 15.7°, respectively), whereas their ulnae follow a dramatically different path to growth cessation (73.1°). To place this disparity in perspective, the craniofacial ontogeny of *P. troglodytes* and *P. paniscus*

yield an angle of approximately 22° (Cobb and O'Higgins, 2004), suggesting that even highly canalised structures of like-species develop along unique trajectories. While linear ratio analyses have shown that adult chimpanzee and bonobo diaphyses do differ in their shape and structure (Carlson, 2005), others suggest the differences are inconsequential for distinguishing locomotor behaviour (Patel et al., 2013). An ontogenetic investigation like that presented here could reveal how variable long bone development is in the limbs of *Pan*, and may further elucidate whether adult variation is more a factor of genetic diversity (Won and Hey, 2005; Prado-Martinez et al., 2014) or the product of a more arboreal posture in bonobos compared to chimpanzees (Doran, 1993, 1996). Even when ontogenetic series are unavailable or limited like in the fragmented hominin fossil record, describing morphological characters in detail is critical if comparisons to modern humans or extant primates are to be made. The application of GM on cranial and postcranial fossil material has improved our understanding of extinct and extant primate ecology in ways that traditional analyses (e.g., linear metrics and angle-based methods) cannot (Baab, 2008; Tallman, 2012; Almécija et al., 2013; Green et al., 2015), while others have combined finite element analysis with GM to study the biomechanical implications of form-function relationships in anthropology (Panagiotopoulou, 2009; Smith et al., 2015). The next logical step is not to replace, but unite, traditional cross-sectional geometric techniques with GM, to provide a holistic approach to the study of biomechanics and limb adaptation.

5.5.2 Ontogenetic and evolutionary allometry of long bone midshafts

Allometry is a major component of primate limb form, but its effects are especially limb and element-dependent. Though associations between behaviour and body mass have been linked to cross-sectional structure of the forelimb relative to the hindlimb (Ruff, 1990, 2003), the GM approach used here described the timing of these changes in each limb separately. Broadly, humeral midshaft form correlates with locomotor transitions undertaken throughout development, while femoral midshaft form appears to correspond to major shifts in body mass. The strongest evidence for this observation came from the extant hominids, the variable sizes and growth trajectories of which act as a basis for comparing generally similar body proportions (Rose, 1983; Jungers and Susman, 1984; Leigh, 1993). Though allometry accounted for a statistically significant

proportion of humeral form among all three great apes, its effects were disproportionately greater in the femur, exhibiting between 8.9% to 12.7% more size variance than the humerus (6.7a – c). Whether the disparity between limb development is more a product of locomotor function or more an allometric effect of body mass can be considered in light of each taxon's ecology. Among the three great apes, chimpanzees revealed the most pronounced change in both mid- humeral and femoral form. They also undertake the most clearly defined locomotor transition, from an arboreal, forelimb-driven posture, to a semi-arboreal/terrestrial, hindlimb-driven posture, shortly after infancy (Sarringhaus et al., 2014). In the humerus, the infant condition exhibited some shape overlap, but was clearly distinguishable from the juvenile and adult configurations, implying a close correspondence between loading pattern and humeral form. If locomotor behaviour impacts the hindlimb to the same capacity, a similar adaptive change between infancy and juvenility should be observable in the femur, as well. Upon examination of chimpanzee femoral shape, however, it is evident that this is not the case. Instead, infant and juvenile shape overlapped extensively, this time to the exclusion of adults. Rather than reflecting a locomotor adaptation apparent in the humerus, the timing of mid-femoral shape change corresponds more closely to a pubertal body size increase exclusive to *P. troglodytes* (Leigh and Shea, 1996). Male and female chimpanzees follow a nearly identical growth trajectory until around eight years of age, when growth velocity peaks for females (approx. 4kg per year), and males experience a growth spurt (approx. 8kg per year) (Leigh and Shea, 1996). The adoption of a more ML oriented mid-femur late in juvenility may therefore provide an important means of body mass support to accommodate rapid growth, and further, suggests that femoral form may better reflect changes in chimpanzee mass rather than changes in their locomotor behaviour. Thus, future studies employing humeral-to-femoral strength ratios (Ruff et al., 2013; Sarringhaus et al., 2016), including those implemented in Chapter 4, should take caution when interpreting relative changes in fore-to-hindlimb bone dimensions as strict proxies for posture or limb locomotor dominance.

Compared to chimpanzees, gorillas and especially orangutans assume a relatively static locomotor repertoire over their lives, reflected by the least humeral size variance of all five sampled taxa (8.1% and 6.7%, respectively; Table 5.1b and c). Similar to chimpanzees though, gorillas and orangutans each exhibit a pronounced allometric effect at the mid-femur, in support of a body mass interpretation of femoral form. For one, both gorillas and orangutans experience

growth spurts at an earlier age than chimpanzees, and further, express stronger dimorphic variability in growth rate and duration compared to their cousins (Shea, 1983; Leigh, 1993; Leigh and Shea, 1995). While their interspecific growth rates differ from one another following cessation, gorilla and orangutan males both initiate their pubertal growth spurt at approximately five years of age, while females of both taxa initiate earlier (approx. 4.5 years in *Gorilla*; approx. 3.5 years in *Pongo*) (Leigh and Shea, 1995). Principal component analyses of the femur reflected these dimorphic differences well, where gorillas and orangutans both exhibited a clear sexual signal in the femur while chimpanzees did not. Moreover, the only major locomotor transition undertaken by gorillas happens early in infancy (Doran, 1997), whereas orangutans can execute the complex gap-crossing manoeuvers employed by adults even before weaning (Chappell et al., 2015), suggesting that femoral shape change after infancy is unlikely to be an adaptation to locomotor behaviour. The association of mid-femoral form and body mass can be expanded to the two smaller bodied taxa in the study, as well: the hylobatids and macaques, each of which exhibited the smallest allometric effect in analyses of femoral form (5% and 7%, respectively; Table 6.7d and e). This observation is unsurprising among the hylobatids, who employ forelimb-driven brachiation above any other form of locomotion (50% – 80% of total locomotor time) (Fleagle, 1974; Michilsens et al., 2009), and thus, rely on the hindlimb to support their full mass to a lesser extent than the hominids. Though the hylobatid locomotor ontogeny literature is limited, it is understood that infants do not achieve full locomotor independence until at least two years of age in both gibbons and siamangs (Harvey and Clutton-Brock, 1985; Lappan, 2009; Morino and Borries, 2016). While there is considerable humeral shape overlap across hylobatid developmental stages, differences are still discernible between infants and the other developmental subgroups, suggesting that the acquisition of new locomotor techniques, or their increased intensity and frequency, may be expressed as physical signals in the humerus following infancy. More experimental and wild focal studies could confirm whether the morphological relationships identified here are in fact products of a developmental locomotor shift.

At first glance, the small allometric effect in the macaque femur suggests that increases in body mass have little impact on the bone's shape, despite a large size and mass disparity between immature and adult individuals of *M. mulatta* (Turnquist and Wells, 1994). However, the ways in which cercopithecids support their body mass during locomotion may help explain the small

degree of femoral shape change among the macaque sample. The extant cercopithecids have maintained a number of pronograde locomotor adaptations since their divergence with the proto-apes some 23 million years ago (Raaum et al., 2005), including a relatively low intermembral index, small and restrictive humeral and femoral heads, proximally extended greater trochanters, short clavicles and narrow pelvises and scapulae (Hunt, 2016). While the functionality of some cercopithecid postcranial characters remain unclear (e.g., humeral diaphyseal retroflexion), most are adaptions that enable efficient, though predominantly parasagittal locomotor postures with limited joint excursion relative to apes. To execute arboreal and terrestrial walking, running and leaping effectively, monkeys orient their torsos horizontally along substrates, which should theoretically distribute their mass more evenly between the fore- and hindlimb compared to a torso-orthograde posture, which would place greater mass on the hindlimb. Experimental evidence suggests that while most primates are hindlimb-driven locomotors (Kimura et al., 1979; Kimura, 1992), markedly quadrupedal cercopithecids like vervet monkeys (*Chlorocebus pygerythrus*), tend to place peak forces on the fore- and hindlimb equally, while even suspensory species like orangutans apply greater force to the hindlimb (Demes et al., 1994). Even among macaques, infant and adult *M. fuscata* exhibit little variation in vertical force application between the fore- and hindlimb (Kimura, 2000). While the macaque hindlimb contributes to a greater percentage of overall body mass than the forelimb over development (Turnquist and Wells, 1994), an increase in cross-sectional size may simply be a means of supporting greater body mass. In other words, maintaining cross-sectional shape while increasing absolute size could serve as an effective alternative developmental pathway for offsetting locomotor demands as certain taxa grow.

Just as mid-humeral and ulnar growth trajectories do not emit a common signal (for behaviour, size or phylogeny), femoral and tibial form also develop independently to serve different purposes. Though both sampled hindlimb bones revealed a greater allometric effect than either forelimb bone, the femur and tibia exhibit a different allometric pattern. Among the hylobatids for instance, the smallest overall allometric effect in the femur (5%) was countered by the greatest effect in the tibia (43%). Though intrasectional and intralimb ratios helped illustrate the high degree of AP deposition and ML resorption the hylobatid tibia adopts with maturation, PCAs and size-shape regressions demonstrated that the change in form is more likely an effect of locomotor adaptation than body mass support. One contributing factor to the hylobatids'

exaggerated AP deposition could be bipedal locomotion, which is employed by the Asian apes more frequently than any other taxon in this study (Hunt, 2016). In fact, the adult hylobatid I_{max}/I_{min} values obtained in Chapter 3 overlap with those of modern humans (Shaw and Stock, 2009b). If bipedal behaviour alone could dictate mid-tibial shape though, a similar deposition and allometric pattern should be observable in the orangutan sample. Instead, the adult hylobatid condition is more likely an adaptation to facilitate muscle moment arms and bending loads related to leaping behaviour interspersed with brachiation (see the Discussion sections of Chapters 3 and 4 for a review). The first two tibial PCs explained more shape variance than the femur in each ontogenetic series; similar to the pattern observed between the humerus and ulna (to the exception of chimpanzees). Accounting for major shape differences in distal segments more readily than their proximal counterparts lends further support to an optimality model where zeugopodial elements are more genetically canalised and adaptively constrained compared to stylopodial elements, whose robusticity allows for greater plastic flexibility. Histological research, especially with a focus on cortical and trabecular structure, can help clarify how proximal limb elements respond to different forms of mechanical stimulation. Moreover, a similar method of semilandmarking to that used here could be introduced to such analyses, making it possible to incorporate a section's endosteal contour to explore cortical, trabecular or medullary geometry as well. The most practical step forward will be to apply these methods more narrowly to study variation at the population level, i.e., how groups of humans or non-human primates who load their bones specific to their ecology and environment differ.

5.6 Chapter Summary

Chapter 5 explored ontogenetic changes along the midshaft periosteal contours of the catarrhine sample, including the ways cross-sections change their shape independent of increases in size. The primary research objectives of the chapter were to determine whether limb form could be accurately discriminated between taxa as well as over the course of their development, by using GM rather than traditional beam modelling methods. One major advantage of taking a GM approach was the freedom to study shape and size without relying upon body mass or linear ratios as size controls. Studying shape variables directly along each section's contour not only helped

confirm the validity of GM on cross-sectional analysis in general, but placed several biomechanical and ecological inferences made in Chapters 3 and 4 into a clearer context.

In addition to the chapter's overarching objectives, several key findings should be considered in future studies interested in extant and extinct primate limb morphology. For one, shape variables like Procrustes coordinates offer a more comprehensive look at a section's contour than principal or anatomical ratios can, highlighting interspecific differences that were not previously discernable in the two previous chapters. Certain relationships established by linear ratios, like the humeral shape overlap between chimpanzees and orangutans were upheld using a GM approach, offering further evidence that the mid-humerus serves as a more effective proxy for posture and locomotion than size or taxonomic affinity. Patterns of long bone adaptation are not universal along the limbs as was found in the femur however, where a stronger signal for pubertal body mass spikes acted as a better explanatory factor for shape than locomotor transitions, especially among the hominids. The hindlimb elements generally deposit bone in the same planes over development (ML in the femur; AP in the tibia) though taxa can still be distinguished within these two broad patterns. For instance, the minimal influence of size on shape in the hylobatid femur is probably a product of the greater weight-bearing role of the forelimb during suspension and brachiation compared to the hindlimb (Fleagle and Lieberman, 2015). Similarly, the small allometric effect in the macaque femur could be a consequence of their mass distribution between the fore- and hindlimb during pronogrady compared to a torso-orthograde posture. Just as the humerus and femur emit different signals between taxa, the ulna and tibia are independent of their respective proximal limb segments. The more gracile ulnar diaphysis is likely too constrained by tissue economy to model itself in a manner identifiable across broad locomotor patterns like in the humerus. Instead, cross-sectional analyses of highly specialised elements like the ulna may be more useful for discriminating habitual loading patterns intraspecifically (Hagihara and Nara, 2017), or better still, among environmentally-dissimilar populations (e.g., Tai Forest populations compared to the Fongoli savanna-woodland populations of chimpanzees).

Vector analysis illustrated how primate diaphyseal form changes across development, rather than at discrete developmental stages as performed in the analyses of the prior research chapters. Comparisons of the angles formed between vectors helped contextualise how developmentally plastic or constrained each element is, while CVA determined how much

variation is established between taxa in infancy compared to adulthood. Combining these two techniques revealed precisely which aspects of a section are subject to bone deposition, resorption, or if they remain generally isometric as they grow. Accordingly, the high detail conveyed by GM can be especially useful when comparing contours that exhibit general deposition patterns across taxa, like the tibia. For instance, linear ratio comparisons between gorillas and hylobatid tibiae showed that both apes deposit bone along the AP axis, but a GM investigation of the contour revealed that gorillas deposited virtually the same proportion of bone anteriorly in infancy as they do in adulthood. Compared to their hylobatid cousins, gorillas place most new bone posteriorly, a pattern undetectable by linear ratios alone. Subtle differences in bone deposition like that found here can inform about an individual's ecology, and thus, may be helpful for interpreting locomotor or body size variation in the fossil record. Moreover, greater detail about the contour allows for the investigations of non-circular or asymmetrical cross-sections that are normally avoided in conventional beam modelling analysis (i.e., to avoid the deltoid tuberosity in the humerus) (Ruff, 2008) by scanning at locations proximal or distal to true midshaft.

Chapter Six:
Discussion

6.1 A review of key findings

To investigate the ways catarrhine limbs develop and adapt between infancy and adulthood, this thesis expanded upon two traditional beam modelling methods and helped establish a new approach for studying long bone cross-sectional form using geometric morphometrics (GM). Chapters 3, 4 and 5 used these three techniques to study variation in limb form among and between the sampled primate taxa (Figure 2.4). The specific research objectives addressed in this thesis are summarised in Table 1.2.

In Chapter 3, considering two cross-sectional area ratios together (I_{max}/I_{min} and I_x/I_y) clarified some ambiguous findings from previous studies attempting to interpret midshaft circularity and locomotor behaviour (Carlson, 2005; Patel et al., 2013). A clear example came from comparisons of the great ape ontogenetic series, where humeral shape overlap among the taxa in the principal plane was clarified by consulting shape variation along the anatomical axes. Applying both ratios together revealed that despite the similar maximum and minimum values shared by the apes, habitually quadrupedal taxa like gorillas deposit more bone along the humeral ML axis compared to relatively suspensory taxa like chimpanzees and orangutans, which reinforce the AP axis to a greater capacity. In other words, the similar shape proportions previously reported along the principal axis are achieved through distinctly different deposition patterns which appear closely related to posture. It is therefore recommended that researchers who rely on circularity ratios to report on broad shape differences between groups employ both principal and anatomical axes together rather than selecting one over the other. Distinct distribution patterns were also identifiable among infants, though immature diaphyses exhibited less interspecific variation overall, making shape more difficult to discern on the taxonomic level early in life. Just as generalised muscle groups enable a range of movements across locomotor environments (Rauwerdink, 1991), a similarly generalised skeleton in infancy appears to allow individuals to adapt their cross-sectional dimensions to the ecological pressures they encounter as they mature.

The results of Chapter 3 demonstrate how proximal and distal aspects of long bones are also effective at discriminating taxa by shape, despite the vastly different signals the sections emit during development. Specifically, the distal aspects of elements like the humerus, ulna and tibia appeared relatively static in shape between developmental stages, even when locomotor patterns changed. A clear signal of developmental constraint was identified at the distal ulna, which exhibited little or no significant variation in circularity over the course of both hominoid and macaque development. Further, relatively little interspecific variation was identified in the ulna compared to the other distal diaphyses, as well. It follows that a distal section adjoining the wrist must remain static in shape to facilitate pro- and supination (O'Connor and Rarey, 1979), irrespective of posture or body size. The mid- and proximal ulnar periosteum on the other hand, appears to adapt its shape more readily over development, which may be a function of its comparatively robust structure relative to a gracile distal section, as well as its role in mitigating and transferring greater mechanical loads between the radius and the humerus (Ruff and Runestad, 1992; Birkbeck et al., 1997). A lack of shape variation may also result from the different ways midshafts and distal sections model themselves, in that a more pronounced behavioural signal may be apparent in the distal endosteal rather than periosteal envelope (Bass et al., 2002). In the hindlimb, both mid- and especially distal femoral shape closely corresponded to size in all five taxonomic groups, where a greater I_{max}/I_{min} ratio was closely associated with average adult body mass (explored in further detail in section 6.2). In addition to the above findings, Chapter 3's results provided a foundation for the research methods used in Chapters 4 and 5. Specifically, the constrained distal sections of the ulna and tibia made it possible to investigate strength variation relative to their midshafts in Chapter 4, while ratio-generated shape indices at midshaft served as points of comparison for the GM method used in Chapter 5.

The objective of Chapter 4 was first to compare cross-sectional strength variation, expressed as the polar section modulus (Z_p), between the fore- and hindlimb; a method previously used to compare diaphyseal development within primate genera (Ruff et al., 2013; Sarringhaus et al., 2016) and interspecific comparisons of mature individuals between taxa (Shaw and Ryan, 2012). By incorporating ontogenetic samples from multiple taxa, this study demonstrated that interspecific strength variation typically reflects locomotor transitions during development, and further, that these locomotor signals appear to overshadow taxonomic relationships. For instance,

the similar femoral-to-humeral strength proportions between gorillas and macaques are more likely demonstrative of a habitual quadrupedal posture than a shared ancestral morphology, considering their distant divergence (Steiper and Young, 2006). This is further supported by the chimpanzee ontogenetic series: the femoral-to-humeral strength of which appears to reflect a stronger fore- to hindlimb configuration during infancy, when an arboreal posture is dominant (Doran, 1997). The hindlimb of gorillas, on the other hand, is a critical component of quadrupedal locomotion by six months of age (Doran, 1997) and before the first six months in rhesus macaques (Turnquist and Wells, 1994). The study also demonstrated that orangutans were the only taxon to exhibit a stronger humerus relative to femur from infancy through to adulthood, suggesting that strength proportions scale with general isometry when posture remains relatively static over development. Because orangutans acquire most of their locomotor repertoire by the time they turn one (though the frequency of manoeuvers is closely associated with age) (Chappell et al., 2015), it is reasonable that a strong humerus would be a defining characteristic of their morphology from an early age. A lack of published literature on hylobatid locomotor ontogeny made it more difficult to validate the relationship between locomotor behaviour and strength proportions, though wild focal studies lent some support. While femoral-to-humeral strength proportions are relatively similar across hylobatid development, a stronger femur relative to humerus emerged by juvenility, suggesting that the introduction of leaping and bipedal locomotion to their repertoire may underlie their unique limb configurations across ontogeny. Further support can be taken from observations that gibbons and siamangs do not achieve complete independence until at least two years of age (Morino and Borries, 2016). Thus, interspecific body size variation does not appear to be a strong contributing factor to whether locomotor transitions do or do not occur among taxa, and considering the similar locomotor environments of the Asian apes, broad postures like "suspension" may not either. Additional research on wild and captive hylobatids would confirm the relationship between limb strength and locomotor pattern, though these initial results indicate a strong correspondence between femoral and humeral form and function over the development of all five of the sampled taxa.

In addition to interlimb comparisons, Chapter 4 examined strength allometry along the ulna and tibia by comparing relatively plastic midshafts to their respective constrained distal sections. The intralimb results established that distal limb strength tends to develop uniformly in catarrhines,

where the midshaft becomes stronger than the distal diaphysis between infancy and adulthood, irrespective of posture. Accordingly, developing a stronger ulnar midshaft relative to the distal region is likely canalised among the sampled catarrhines but may be synapomorphic to the entire order Primates. While interspecific ulnar variation did not follow a strict locomotor or phylogenetic pattern, intraspecific comparisons of the rhesus and long-tailed macaques revealed that the more terrestrial rhesus monkeys may exhibit stronger midshaft sections by adulthood than their arboreal, long-tailed counterparts. Though larger sample sizes and a greater variety of taxa are necessary for verification, applying an intra-ulnar comparison may be an effective method for discriminating between species, subspecies and perhaps populations, dependent on their posture. Comparisons along the tibia demonstrated that distal limb segments also develop uniformly with increased AP deposition over time but unlike the ulna, tibial strength was approximately equal among all five infant subgroups, and even remained similar into adulthood between the African apes. Indeed, the African apes were the only two taxa to exhibit relatively proportionate strength along the diaphysis, while the other sampled taxa revealed considerably stronger midshafts among the adult subgroups. Overall, interspecific tibial dimensional variation was not as pronounced over development compared to the ulna, but the changes in strength that were observed may be linked to a combination of body mass and locomotor behaviour in each taxon.

Chapter 5 took a geometric morphometric approach to the analysis of cross-sectional shape, to determine whether semilandmarks could more accurately inform about section contours compared to conventional moment area ratios. By expressing midshaft dimensions as Procrustes coordinates, shape was quantified in each long bone and at each of the three developmental stages. The method proved especially effective in describing shape because it did not rely on ratios to control for individual size, but instead, scaled each cross-section by its centroid. Results revealed a close correspondence between ontogenetic shape and locomotor behaviour at the humeral midshaft across taxa, highlighting any postural transitions in taxa that exhibit them (e.g., *Pan* and *Macaca*) and a more isometric pattern in taxa that do not (*Pongo*). The comparatively gracile ulnar midshaft's shape changed over development as well, particularly in taxa that did not present any ostensible humeral shape variation over development, like gorillas and orangutans. The greater constraint placed on gracile elements like the ulna suggests that any developmental shape change is more likely a product of systemic factors than a local response to mechanical loading. While no

clear locomotor or size signal could be retrieved from the ulnar midshaft, it is not to say that such signals do not exist, but that they may simply be imperceivable across a highly diverse taxonomic sample. Instead, a species- or population-level study may better serve to identify locomotor differences that may otherwise be obscured across the sampled catarrhines. Just as the humerus reflected locomotor transitions in detail, shape and size variation in the femur appeared closely linked to genus-specific growth spurts, where changes in midshaft shape corresponded to increases in size. Nevertheless, the ability to accurately compare changes in form during development make the method valuable for studying ontogenetic series.

Another major advantage of a GM approach to an ontogenetic dataset was the use of vector analysis for comparisons of midshaft growth trajectories. Rather than a universal developmental pattern governing the skeleton, the fore- and hindlimbs appear to adapt their form in response to key life events; namely locomotor transitions in the forelimb and growth spurts in the hindlimb. For one, forelimb element vector angles formed along PC1 were relatively larger than those of the hindlimb. The comparatively small humeral angles formed between the suspensory apes (chimpanzees, orangutans and hylobatids) with respect to the habitual quadrupeds (gorillas and macaques) lent further support to a behavioural interpretation of humeral form that dominates phylogenetic or body size similarities. Unlike the humerus, ulnar shape trajectories did not appear to follow a clear postural, phylogenetic or body size signal, making ulnar midshaft shape vectors poor candidates for exploring interspecific ecological patterns as well. As discussed above, the ulna's gracile form likely limits its capacity for plastic adaptation compared to larger, more robust bones (at least periosteally), suggesting that any locomotor specialisation is more likely dictated by intrinsic than extrinsic factors. In addition to the femur and tibia exhibiting comparatively smaller vector angles than the forelimb elements, they also revealed a greater allometric effect of size over development, demonstrating that shape is more dependent on size in the hindlimb than it is in the forelimb. A GM approach to limb cross-sectional analysis also offered a more nuanced view of bone deposition patterns between developmental and taxonomic groups that were otherwise beyond the scope of shape ratios alone. When principal and anatomical ratios demonstrate that two different taxa distribute bone approximately in the same planes, for instance, wireframe graphs generated with Procrustes coordinate data could illustrate whether a distribution

pattern is homologous or if deposition varies subtly about the contour, offering an accurate depiction of each taxon's cross-sectional development (Figure 6.2).

6.2 Old dog, new tricks: future research applications

6.2.1 Applications of cross-sectional circularity

Bearing the above findings in mind, the following section considers several avenues for studying limb cross-sectional morphology in new ways that may identify ontogenetic and evolutionary patterns among extinct and extant primates. Though the objectives behind each study varied, their results introduced several findings that require further investigation. Of the four long bone elements and section locations analysed, the mid-humerus emitted the clearest locomotor signal across the sample, grouping taxa by their posture above other variables such as body size or phylogeny. Distal and proximal humeral shape was more constrained by comparison, demonstrating that like epiphyses, diaphyseal sections with increased distance from midshaft may be more genetically canalised. A study comparing tibial sections of varsity athletes and sedentary controls similarly found that the midshaft was most effective at discriminating athletic groups, followed by the 38% distal section, and finally, the 4% distal section, where virtually no differences could be identified between athletes or controls (Nadell and Shaw, 2016). Given their exposure to peak bending loads (Biewener and Taylor, 1986), an adaptive response for tissue deposition at midshaft compared to the metaphyses, which must remain rigid to support joint function (Ruff and Runestad, 1992), is a reasonable expectation. If the effects of plasticity and constraint are continuous along the diaphysis though, it will be helpful to study these elements with a finer lens, rather can broadly classifying the diaphysis, metaphysis and epiphysis as disconnected regions. In this sense, the mechanisms that drive long bone form may be better explained on a tissue-economy spectrum, where not only midshafts but proximate regions are most adaptively responsive to the loading environment, while regions with increasing distance from midshaft epiphyses are more closely governed by intrinsic factors (Figure 6.2).

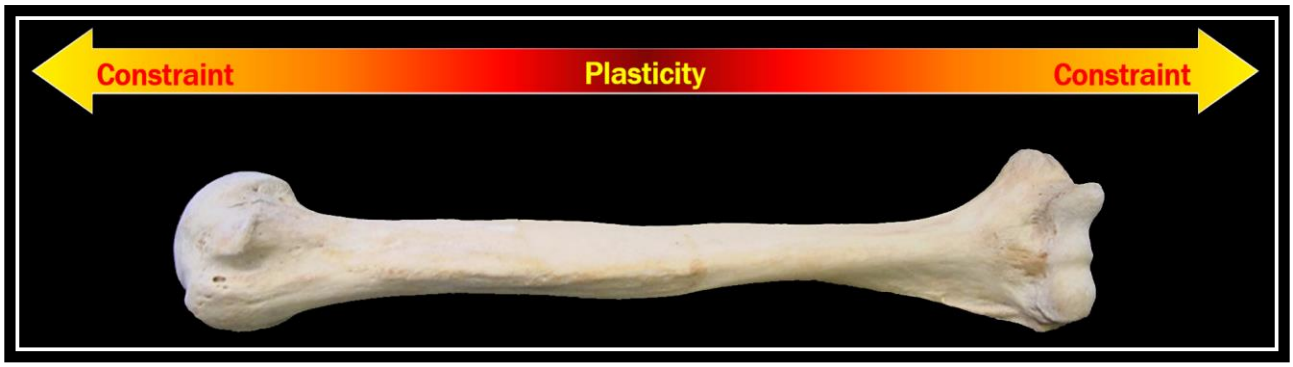

Fig. 6.2. A hypothetical spectrum of tissue-economy that may better explain the development of an element's form into adulthood. Rather than responses to adaptation acting at discrete regions along a bone's length (i.e., diaphysis, metaphysis, epiphysis), changes in form may be better described continuously in either direction from midshaft.

AsciiSection permits this type of analysis directly, where cross-sectional variation could hypothetically be evaluated at 1% increments of length, rather than the three discrete sections studied here. Of the results that arose from comparing contour circularity along the diaphysis in Chapter 3, this overarching concept of studying the limb as a sum of its parts (rather than disconnected components) was one of the most valuable aspects of the chapter's findings. Taking an example from the humerus, it is evident that all five taxa exhibit a relatively ML oriented distal section at each stage of their development (save for the hylobatids, which distribute bone more evenly until adopting a slight ML configuration in adulthood). Shifting focus from the distal section to midshaft, a different pattern begins to emerge, where distal ML flaring in the suspensory apes quickly gives way to greater bone distribution about the AP axis by the middiaphysis, or an almost perfectly circular configuration as seen in the hylobatids. By comparison, the habitual quadrupeds maintain a more ML oriented configuration from the 20% location. Of the five taxa, the habitual quadrupeds experience higher magnitude ML reaction forces during locomotion (Rose, 1988) which may explain why this exaggerated buttressing is not only vital for load mitigation distally in the humerus, but through to the midshaft and proximal aspects of the bone (Biewener, 1989, 1990; Schmitt, 2003). Moving proximally still to 80% of length, the surgical necks of chimpanzees and orangutans culminate into a more circular distribution pattern, gorillas and macaques maintain a similar ML shape (though the proximal humeral retroflexion of

macaques gives the impression of greater AP distribution) and hylobatids distribute more bone in the AP. In other words, direct shape comparisons at discrete sections can discriminate taxa, but studying how one section's shape transitions into another may offer substantially more information about a bone's function and the mechanical forces that influence its form. The distinct shape patterns identified among suspensory apes in particular, may serve as an effective tool for distinguishing potential forelimb suspensory locomotors in the fossil record (e.g., *Morotopithecus*) (Young and MacLatchy, 2004) from larger hindlimb-driven suspensory apes (e.g., *Dryopithecus*, *Oreopithecus*, *Sivapithecus*) (Larson, 1998; Begun, 2007). Identifying regions along the humerus where distinct shape transitions exist could potentially serve as an index for posture and should be applied to platyrrhines and strepsirrhines to determine its accuracy. Though no New World monkeys or lemurs were analysed here, a provisional comparison of their humeral form (i.e., highly circular diaphyses among the brachiating atelines; ML orientation among arboreal quadrupeds like the cebids and lemurids) suggests that common patterns of cross-sectional shape and structure may be identifiable across the order (Figure 6.3). While humeral shape presented the clearest signal for locomotor adaptation, the concept of interpreting cross-sectional geometry along the diaphyses in relation to each other can be applied to any limb element. In instances where shape serves as a poor index though, measures of strength and rigidity as dictated by cortical or trabecular volume and density may prove to be more effective alternatives.

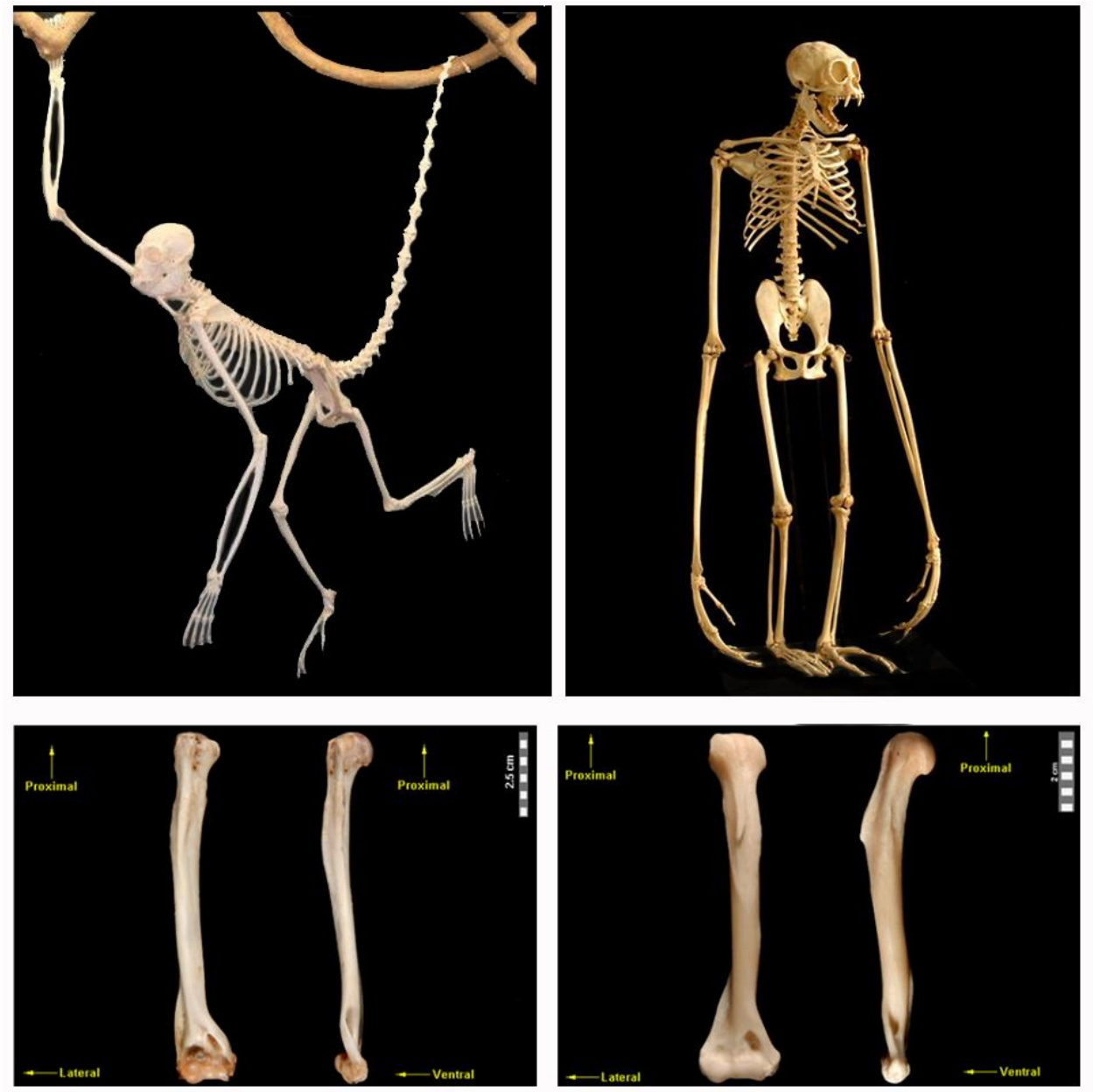

Fig. 6.3. Top: Spider monkey (*Ateles* sp.) (left) and gibbon (*Hylobates lar*) (right) skeletons. Despite variable intermembral index scores, atelids and hylobatids share long, gracile limb elements to facilitate brachiation and vertical climbing. Said similarities should be identifiable in cross-sectional shape analyses as well. **Bottom**: squirrel monkey (*Saimiri oerstedii*) (left) and ruffed lemur (*Varecia variegata*) (right) humeri. Though phylogenetically divergent, both taxa occupy above-branch arboreal quadrupedal postures which may be reflected by an ML distribution pattern at midshaft. Photos courtesy of the Museum of Osteology, Oklahoma City, Oklahoma and eSkeletons.org.

Complete long bone elements are rare in the primate fossil record, though a collection of well-preserved humeri spanning the African and Eurasian Miocene (Begun, 1992; Alba et al., 2011; Begun et al., 2012) could validate the methods used throughout the thesis. These include the distal and mid-distal diaphyseal fragment of a *Dryopithecus fontani* (IPS4334) from Castell de Barberà and a mid-diaphysis of the *D. fontani* type specimen (HGP 3) from Saint Gaudens; a shaft fragment (distal metaphysis and midshaft) from the Klein Hadersdorf *Griphopithecus darwini* specimen (1991/580); a partial humerus belonging to *Proconsul heseloni* (KNM-RU 2036 AH) from Rusinga; a *Sivapithecus indicus* specimen lacking the proximal epiphysis but with complete distal diaphysis and shaft (GSP 30730) from the Potwar Plateau, and a *S. parvada* partial distal and midshaft specimen (GSP 30734), also of the Potwar Plateau (Siwiliks locality Y311). While none of these specimens are complete, they each retain an intact distal diaphysis as defined by this study (20% total length), while most also feature a midshaft (or at least a mid-distal diaphysis) and proximal shaft, which would be valuable for intralimb cross-sectional comparisons. In addition to verifying the accuracy of the current methods, incorporating a fossil sample can further elucidate early hominid locomotor behaviour. Compared to the humerus, the ulna's gracility and restrictive tissue economy, as well as its load-bearing relationship with the radius are key to interpreting its morphology. The perceived canalisation of the ulna relative to the humerus makes for a great opportunity to compare locomotor variation on a smaller scale. Intraspecific differences between locomotor variable taxa should make strong candidates for comparison, as demonstrated by the preliminary look at strength proportions of the two macaque species (*Macaca fascicularis* and *M. mulatta*) studied here (Figure 4.6a and b). On the other hand, distal ulnar shape similarities established over development and even between the adult taxa would serve as a tool for describing broader taxonomic differences among primates and their ancestors, especially if a larger sample of taxa is found to share a familiar shape configuration.

Modelling the femur as a functional unit revealed a common pattern across the sample as well, but unlike the humerus, no clear association between shape and locomotor behaviour could be established. Instead, a strong correspondence between shape and body mass was found (Figure 6.4). Cross-sectional circularity became an incrementally poorer proxy for mass with increased distance from the 20% location, however. Whether the correlation between shape and mass

improves or degrades distal to the 20% location will require further investigation, but could prove to be a useful contribution to contemporary body mass estimation methods if effective.

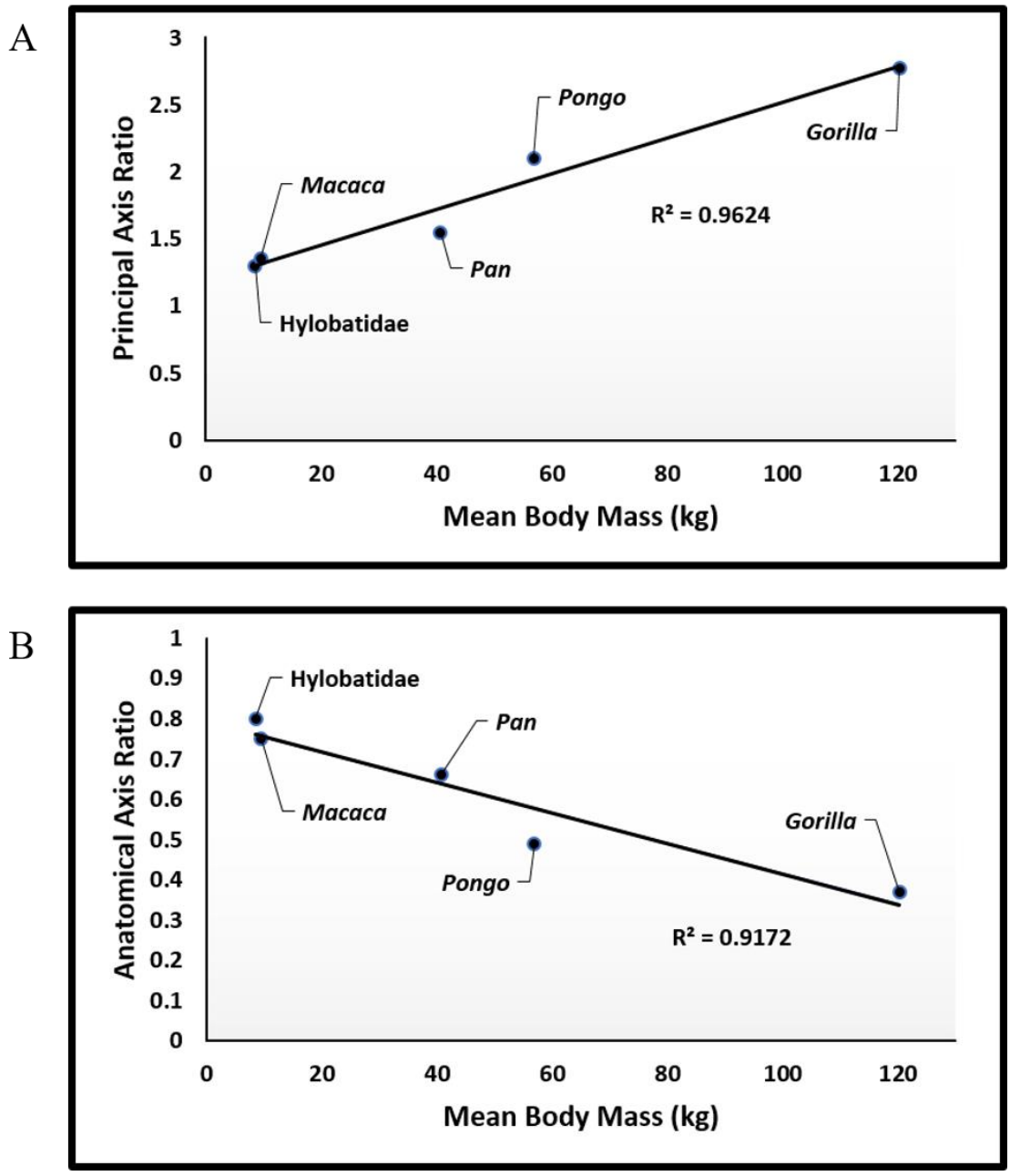

Fig. 6.4. Regressions illustrating the relationship between distal femoral shape (20% total length) and adult body mass (pooled sexes). Both **A.** principal moment of area ratios (I_{max}/I_{min}) and **B.** second moment of area ratios about the anatomical axes (I_x/I_y) reveal a closer correlation between shape and size than with locomotor behaviour or taxonomic affinity.

Accurately estimating size is especially important given that body mass is rarely recorded in museum skeletal collections, usually due to the period and means of their acquisition (Gordon et al., 2013). Body mass estimation equations have been developed to solve this problem using a number of cranial and postcranial measurements (Rafferty et al., 1995; Delson et al., 2000; Ruff, 2002, 2003b), and implementing circularity ratios at the distal femur as a predictive variable is a promising addition to the literature if accurate. Prior work on mass estimation derived from femoral articular breadths have yielded small error margins even in "locomotor blind" analyses (Ruff, 2002, 2003b), expanding their application across the primate order. If mass is previously established among individuals in a sample and distal femoral shape values are available for measure (e.g., I_{max}/I_{min}), the correlation between mass and shape in log-log space can be calculated to estimate mass in individuals where it is unknown, using the power-law model ($y = a^{*}b^{x}$) (Newman, 1993). Taking the principal axis as an example, the linear equation of Figure 6.4A. is $y = 0.013x + 1.186$. Implementing the slope and Y-intercept, the body mass prediction equation could be expressed as Ln Body Mass = $10^{1.186}$ (Ln I_{max}/I_{min})$^{0.013}$. After generating a value for log-mass in each individual, the inverse of the log can be derived, yielding an estimate for individual body mass rather than for group means as portrayed in Figure 6.4. If effective, the method can be applied to fossil specimens when distal femora are preserved. A preliminary test was conducted using the current sample and supplemented with known body mass data made available by Ruff (2003b), using tibial plateau medial condylar breadth in place of distal femoral circularity (Appendix; Table A6.1) with success. Other aspects of the femur (specifically locations distal of 20% length) as well as the tibia should be further tested to determine whether accuracy can be improved regionally along the diaphysis.

Femoral diaphyseal shape and structure play an important role in understanding temporal trends in human skeletal robusticity and mobility pattern (Trinkaus et al., 1994; Stock and Pfeiffer, 2001; Holt, 2003; Stock, 2006; Lieverse et al., 2011; Trinkaus and Ruff, 2012; Pearson et al., 2014; Macintosh et al., 2015; Stock and Macintosh, 2016). While geometric differences can reflect activity and mobility between populations, they appear to be obscured in interspecific comparisons like those made here. A lack of locomotor signal in femoral morphology may not be limited to the diaphyseal cortices, as the distribution and density of trabecular tissue in the femoral neck did not appear to correspond to posture among locomotor-diverse primate species either (Fajardo et al.,

2007). Comparisons of midshaft geometry and trabecular tissue also suggest that humeral midshaft cortical bone corresponds closely to trabecular strength in the humeral head, while the same relationship could not be established between the femoral diaphysis and neck (Ryan and Shaw, 2012). Though no obligate bipeds were considered in this thesis, it should be noted that ML bone distribution at the femoral condyle has been interpreted as a plastic response to habitual bipedality (resultant from medially concave bending moments acting on the diaphysis) (Preuschoft and Tardieu, 1996). As such, incorporating the distal femoral cross-sections of early hominins (e.g. *Orrorin tugenensis*, *Ardipithecus* sp.) and bipedal candidates of Hominidae (*Oreopithecus bambolii*) may reveal a postural signal that is lost among broader locomotor samples like those examined here.

6.2.2 Applications of diaphyseal strength proportions

A new approach to studying long bone form when diaphyses are largely intact is possible through geometric comparisons of two sections relative to each other. Generating ratios of shape or strength in this manner not only provides information about both sections discretely but any changes that occur between their locations, as well. The original circularity ratios applied along the elements informed the analyses of Chapter 3, making these comparisons possible. As might be expected of cross-sections closer to articular surfaces (Ruff and Runestad, 1992), distal aspects of the humerus, ulna and tibia each appeared more constrained in their shape and structure over development. Indeed, research on the distal fibula (20% of total length) also found that locomotor signals were more ambiguous compared to midshafts (Marchi, 2015a). Applying intra-element ratios to additional ontogenetic series can inform how bone structure changes with development and specifically, if the general patterns identified in the ulna and tibia (i.e., increased midshaft strength relative to distal strength with maturity, irrespective of locomotor mode) is common to primates. For example, if a similar developmental configuration can be established among platyrrhine and strepsirrhine taxa, it is parsimonious to expect a common growth pattern among fossil taxa. A study on lemur forearm morphology found that the ulna, and especially the radius, emitted strong locomotor signals between species that exploit robust supports compared to thin branch milieu (Fabre et al., 2017). The comparatively arboreal and terrestrial contexts of long-

tailed and rhesus macaques respectively, lend further support to their discrimination using ulnar strength proportions (Figure 5.15). Expanding upon the intra-ulnar results of Chapter 4 with a larger macaque sample and the inclusion of the radius would be useful in confirming the method's effectiveness among another Old World genus.

If geometric proportions are also comparable within fossil genera, comparisons of distal-to-midshaft sections can illuminate the locomotor behaviour of extinct primates. Two candidate taxa for investigation are *Proconsul* and *Dryopithecus* for their postcranial availability. Controlling for sex, age and intraspecific morphological variation in the fossil record can be difficult when limited specimens are available (Wood et al., 1991; O'Higgins, 2000), though further intraspecific analyses of extant primates can aid in discerning how much variation exists across individuals. For example, an investigation of limb strength proportions across *Pan paniscus, P. troglodytes troglodytes, P. t. verus* and *P. t. schweinfurthii* could incorporate matched *Dryopithecus* elements. Doing so would determine how geometric properties vary between the fossil and extant genera, including how said variation may relate to each species' ecology. Even in the absence of subadult fossil specimens, distal sections can serve as canalised markers and offer a glimpse of how the infant and juvenile condition may have appeared by studying ontogenetic patterns in extant taxa. Similar analyses could be conducted between the gorillines and *Dryopithecus* or *Gigantopithecus;* or the pongines with *Sivapithecus* and *Ramapithecus*. While combined samples of extant and fossil taxa morphology are not new, comparisons of linear surface dimensions (Berger, 1994; Lague and Jungers, 1996; Tallman, 2012; Almécija et al., 2013; Tallman et al., 2013) dominate the literature, though recent studies have helped draw attention to bone cross-sectional geometry and bone microstructure (Schilling et al., 2014; Marchi and Patel, 2015; Skinner et al., 2015; Wilson and Humphrey, 2015; Ruff et al., 2016; Stock and Macintosh, 2016; Tsegai et al., 2017). Additional cross-sectional analyses like those employed in this thesis can explore locomotor adaptations beyond limb surface features, opening new avenues of interpretation of hominid ecology. While hominins were not considered in this thesis, the strength ratio approach is also ideal for investigating the relationship between bipedal loading and bone structure in developing fossil taxonomic groups. Two candidates for study are the juvenile male *Homo ergaster*, KNM-WT 15000 (Turkana Boy), whose well preserved upper and lower limb would allow for intra- limb and element strength analyses, as well as the juvenile male *Australopithecus sediba*, MH1 (Karabo),

whose partial tibia could illuminate strength proportions between the midshaft and distal diaphysis. Comparing relative strength proportions in both specimens with a larger sample of juvenile and adult modern humans would highlight the functional differences associated with each species' locomotor behaviour and gait.

6.2.3 Applications of geometric morphometrics

Applying geometric morphometrics to midshaft section contours was successful at discriminating shape between developmental stages and taxa, offering greater detail than traditional methods could (i.e., $I_{max}/I_{min,}$ I_x/I_y). Because these traditional ratios act as indices of circularity strictly in the principal and anatomical planes, changes in shape along adjacent planes can go overlooked in comparison tests. By defining shape as a series of variables (i.e., Procrustes coordinates) around a section's perimeter, the dimensions of the entire contour can be studied, resolving this problem. A comparison of the GM permutation test results (Table 6.3a) with those of the I_x/I_y ANOVA (Table 4.4) at the mid-humerus, revealed the same statistically significant relationships between the infant taxonomic subgroups. In other instances, however, results of the GM and ratio analyses were inconsistent, like how the PCA of chimpanzee mid-humeral form exhibited notable developmental change (Figure 6.4a), while a lack of shape variation was reported along the principal plane (Figure 4.2). Because the GM and ratio methods each inform about different aspects of a cross-section though, one approach is not necessarily superior to the other, but instead, should be applied contingent on the research context and objectives. Taking this perspective, bone distribution about a section approximately reflects the direction along which it is primarily loaded (Carlson and Judex, 2007; Macdonald et al., 2009; Shaw and Stock, 2009b; but see the findings of Demes et al., 1998), suggesting that circularity ratios may better serve investigations of mechanically-driven plastic adaptation. Not surprisingly, these types of studies often favour principal ratios, as the primary plane of bending is more likely to reveal significant variation among locomotor-variable groups than the fixed anatomical plane (Carlson, 2005; Shaw and Stock, 2009a,b; Patel et al., 2013; Sarringhaus et al., 2016). The GM approach, on the other hand, is sensitive to variation about the entire contour, including aspects that may experience comparatively fewer bending moments relative to the principal plane. For instance, the

discrimination of adult male and female chimpanzee humeral shape found using PCA was overlooked by analyses used in Chapter 3, likely due to small dimensional differences beyond the detection of geometric ratios. Thus, the GM approach should not replace traditional beam modelling methods, but complement them, by considering total shape change relative to aspects that experience disproportionately greater bending moments.

Though vector angle sizes were element-dependent, the general pattern of high forelimb variation (larger angles) relative to hindlimb variation (smaller) was in agreement with the previous findings of the thesis: that forelimbs emit shape signals associated with locomotor behaviour while the hindlimb exhibits a balance between locomotor adaptation and body mass support. The moderate hindlimb variation – likely due to femoral and tibial bone deposition patterns (ML and AP, respectively) – is present across the sample apart from in the hylobatids, who do not rely primarily on the hindlimb for propulsion. The degree of variation between limb vector trajectories further illustrates the skeleton as a behavioural mosaic, where the cross-sectional properties of each element highlight unique adaptive signals. Without the context of the hindlimb for instance, the humeral and ulnar trajectories would group gorillas with macaques based on their cross-sectional shape before any of the other great apes. When the hindlimb is considered, gorilla and macaque trajectories bear little resemblance, and instead, both genera group with size-similar taxa; an important distinction to make, especially when evaluating behaviour in the fossil record using fragmented or individual elements. The vector method's dependence on ontogenetic data hinders its applicability, but it can be modified for smaller samples than the one used here. For instance, a sample of several modern human populations that exhibit markedly different mobility patterns would make for an interesting study of morphological variation between two ontogenetic groups, like pre-pubescent adolescents and skeletally mature adults. Such a study could compare the long bone cross-sectional properties of an adolescent group with those of several mobility-variable adult groups, effectively creating several vector angles from a single point. To control for variation unrelated to mechanical adaptation, a genetically homogenous population that exhibits diverse forms of mobility, such as professional athletes from a fixed geographic region, would make for an ideal sample. Alternatively, angles from locomotor-variable groups can be generated from separate immature and mature group means, following a method similar to Cobb and O'Higgins (2004). This approach would allow for greater geographic and

genetic control by sampling multiple adolescent groups as opposed to one, and so would be well suited for behaviourally and ecologically disparate populations (e.g., vector angle comparisons between the Khoisan of South Africa, Andaman Islanders of Southeast Asia, Yaghan of Tierra del Fuego, Inupiat of Alaska).

In addition to its application to modern humans and extant non-human primates, combining long bone cross-sectional GM with environmental (Bishop et al., 2011; Kovarovic et al., 2013), dietary (Sponheimer et al., 2013; Levin et al., 2015) and life history (Raichlen et al., 2015; Cameron et al., 2017) data can be a valuable asset to ongoing debates in the primate fossil record. The postcranial remains of *Oreopithecus bambolii* (IGF 11778) in particular, have continued to generate new discussions on hominid locomotor behaviour since they were first described by Hürzeler (1949). While there is general consensus that *O. bambolii* was primarily arboreal, some researchers have designated IGF 11778 a habitual biped (Straus, 1962; Köhler and Moyà-Solà, 1997; Rook et al., 1999, 2004) as well as a suspensory and climbing specialist (Schultz, 1960; Jungers, 1987; Begun, 2007; Russo and Shapiro, 2013; Billington, 2016). As new research clarifies the posture of the Upper Miocene ape, PCA and CVA of forelimb cross-sectional shape, like those performed in Chapter 5, could classify *O. bambolii*'s locomotor behaviour in relation to the extant apes, as well as bipedal taxa including extinct members of *Homo* and *Australopithecus*. Limb adaptations specific to the Miocene hominids' fore- (specialised elbow joints, elongated arm elements, pollical-assisted grip (Rose, 1988; Begun, 2007; Nakatsukasa et al., 2016) and hindlimb (reduced length, larger femoral head, derived lateral protrusion of the greater trochanter (Jungers, 1987; Almécija et al., 2013) would make shape comparisons of their diaphyses all the more interesting. Moreover, the ability to analyse the limb elements in relation to each other rather than focusing specifically on a single morphological character, can place IGF 11778's appendicular skeleton into a broader ecological context; especially considering its primitive-derived mosaic features (Köhler and Moyà-Solà, 1997). Other debates centred on early hominins (ranging from locomotor adaptation to phylogenetic affiliation) including the ardipithecines (White et al., 2014) and australopithecines (Ward, 2013) would also benefit from a refined look at diaphyseal shape, given the similar mosaic nature between their fore- and hindlimbs.

6.3 Additional considerations for future research

Because forces generated by muscles typically constitute the greatest diaphyseal loads (Frost and Schönau, 2000; Rittweger, 2008; but see Judex and Carlson, 2009 for an investigation of other contributing factors), accounting for muscle size as well as the relative locations of ligament and tendon entheses are important considerations for future research on limb cross-sectional growth and adaptation. While studies centred on long bone morphology are effective at linking form to function, a closer look at musculoskeletal dynamics can better explain 'how' and 'why' skeletal form varies among taxa in ways that this thesis cannot. Studies on primate muscle and tendon materials and mechanics offered insight into the skeletal adaptations of the taxa studied here (Thorpe et al., 1999; Payne et al., 2006a,b; Channon et al., 2010a,b; Vereecke and Channon, 2013; Diogo et al., 2015, 2017) but without a combined analysis of soft and hard tissues, it becomes easy to develop "just-so" stories to explain complex biological relationships between the skeleton and its loading environment. Though difficult to procure, cadaveric tensile tests for the purpose of collecting load-displacement data, combined with CT and micro-CT analysis of weight-bearing bones, would more accurately demonstrate how different regions along the shaft respond to the muscular forces acting on them.

Another consideration for future research interested in building upon the methodology of all three studies here, is histological control. While surface scans are a fast, affordable and accurate way to extrapolate geometric properties from the periosteal contour, a clear depiction of a section's endosteal structure is invaluable to understanding its function, especially when comparing intra-elemental dimensions. In addition to the different growth processes that govern immature and mature bone (Pearson and Lieberman, 2004; Robling et al., 2006), the material properties along the diaphyses are also fundamentally different (White et al., 2012), dictating their ability to resist mechanical loads and thus, their function. Supplementing the three main methods undertaken in this thesis with cortical, trabecular and medullary data would grant an additional level of examination. Cortical area, volume, and density are closely tied to activity and behaviour in intraspecific samples (Adami et al., 1999; Hsieh et al., 2001; Heinonen et al., 2002; Daly et al., 2004; Ireland et al., 2011, 2015; Shaw et al., 2014) and can be used to discriminate mature primate taxa (Shaw and Ryan, 2012). Moreover, increases in bone mineral content resulting from habitual loading are not always confined to the mid-diaphysis but the metaphyses (Hamrick et al., 2006).

Cancellous tissue is particularly relevant when comparing structural proportions in an ontogenetic context as well, as immature elements possess more trabecular bone their mature counterparts (Gosman and Ketcham, 2009). Comparing developmental differences in bone structure among the sample used in this thesis could therefore clarify the relationship between form and function. For instance, the suspensory apes exhibited a similar humeral shape pattern to one another compared to the habitually quadrupedal gorillas and macaques; could signals of suspension or quadrupedalism then be identifiable by studying the density and distribution of cortical or trabecular bone between developmental stages? Furthermore, studies on skeletally mature and immature tetrapods generally agree that repetitive loading results in decreased medullary and increased endosteal area at the mid-diaphysis (Matsuda et al., 1986; Plochocki et al., 2008), but can these observations be extended to the distal and proximal diaphyses among phylogenetically similar, locomotor variable taxa like primates?

Bone growth and adaptation studies often control for variation using a sedentary sample or an unloaded limb (Hsieh et al., 2001; Lieberman et al., 2003; Daly et al., 2004). Controls are valuable determinants of the proximate causes of shape or structural change along a diaphysis but are difficult to implement in studies focused on wild-caught specimens with limited life history information available. While at least one study has attempted to control for load-induced bone adaptation in captive and wild primates (Morimoto et al., 2011), no habitat regulation was established for the captive zoo sample – including enclosure size or sub- and superstrate availability – which hailed from several different locales (Canington et al., 2017, considered these limitations in greater detail). Moreover, diaphyseal adaptation is understood to be more responsive to dynamic rather than average loads (Frost, 1997; Demes et al., 2001), suggesting that the suspensory and climbing behaviours performed by the captive chimpanzees studied by Morimoto et al. (2011) should have been capable of stimulating bone deposition to the same capacity as their wild counterparts. Unlike humans, whose behaviour is often sedentary by choice, it is difficult to control for mobility rate or frequency in non-human primates. Ultimately, a longitudinal study where bone form is monitored at set intervals of time would be ideal, but difficult to fund and perform. Therefore, future research interested in limb and locomotor ontogeny with an emphasis on plastic adaptation may benefit looking to other mammals such as rats and mice for interspecific

comparisons, or other small vertebrates with relatively short life cycles, where induced loading behaviour can be controlled with fewer ethical concerns.

Along with accounting for microstructural and behavioural differences between taxa, the introduction of phylogenetic control has the potential to clarify how much geometric variation is attributable to phylogenetic inertia or constraint. Some long bone cross-sectional studies actively elect not to incorporate phylogenetic comparative methods, citing that hyper-plastic nature of diaphyses during an individual's life makes it difficult to separate the effects of heritability from the loading environment (Ruff, 2002; Shaw and Ryan, 2012). While it has been established that adult long bone lengths emit a clear phylogenetic signal, it is indeed difficult to verify the effects of phylogeny on cross-sectional geometric properties (O'Neill and Dobson, 2008). That said, a study on interspecific trabecular bone variation incorporated phylogenetic corrections with some success (Tsegai et al., 2013). With a larger interspecific sample that incorporates species differences, a similar phylogenetic generalised least squares approach could be implemented on the specimens here. Moreover, to moderate the conflation of environmental with phylogenetic effects, distal diaphyseal sections or epiphyses could be the central focus of such a study.

6.4 Concluding remarks

As new ground is made studying the relationship between bone form and function, novel approaches will continue to be innovated, supplying researchers with an ever-growing analytical toolkit. While pioneering techniques can address questions otherwise out of their precursors' reach, this thesis serves as a reminder not to throw the baby out with the bathwater. Augmenting conventional beam modelling methods, or simply applying them in new ways, can inform about long bone development and adaptation without invoking advanced technical analyses. A similar approach to geometric morphometrics showed that simple 2D cross-sectional images can describe contour shape with great clarity using semilandmarks alone. The findings presented from these techniques have direct implications to prior research on primate skeletal adaptation, and offer new suggestions for studying extant and fossil primate ecology looking forward. Given the plastic/constrained duality of long bone adaptation, information on distal and proximal aspects add context to midshaft form, acting as static markers by which signals of habitual loading can be

compared. Even in interspecific comparisons when proximal and distal aspects vary, midshaft form is often congruent between locomotor-similar taxa, grouping them on a behavioural basis. Developmental comparisons add further context to this dynamic, demonstrating how different diaphyseal sections correspond to the ecological demands placed on them. Ultimately, accounting for form along an element's length adds a crucial component to investigations of primate behavioural ecology.

Along with the information that studies of long bone form can contribute to our knowledge of primate ecology, it is equally important to appreciate what it cannot. Despite increased interest in long bone cross-sectional research over the past four decades though, investigators continue to limit their analyses, usually to single bone sections (e.g., midshafts for their load adaptive-responsiveness) or deficient methods altogether (e.g., defining section shape exclusively with a single area ratio), inadvertently overlooking answers that their research questions aim to address. The relationship between mechanical loading and cross-sectional form is complex and multi-faceted, yet is frequently viewed monolithically in this sense. In reality, the primary mechanisms that govern bone form could be related to different locomotor patterns during ontogeny (Sparacello et al., 2010), the sensitivity of separate limb elements to different mechanical forces (Marchi and Shaw, 2011), an individual's stature, physique or body shape (Ruff, 1995; Ruff et al., 2006) (and the subsequent effects of gravity on them) (Judex and Carlson, 2009), the role of systemic and localised factors attributed to the phenotype (Lovejoy et al., 2003; Judex et al., 2007), likely some combination of all of these factors, and possibly, other entirely different phenomena. To paraphrase the Harvard Law of Biology, "under the most rigorously controlled conditions, biological material will do whatever it damn well pleases". Making matters more complex, it follows that these mechanisms act on human and non-human primate taxa in markedly different ways, dependent on the length, bowing and curvature of their diaphyses (Macintosh et al., 2015; Hunt, 2016), size of the moment arms acting on a region (Payne et al., 2006b; Holowka and O'Neill, 2013) and bone linear dimensions (Ruff, 2003b; Marchi, 2015b), as well as the region's adjacent characters (e.g., retroflexed shaft, brachioradialis flange). Thus, searching for a "silver-bullet" interpretation of behaviour using cross-sectional geometry alone is likely impossible in the absence of more complex biomechanical models that incorporate these different components together. That said, the findings presented here contribute to the broader paradigm of skeletal

development in several important ways, by exploring patterns along the diaphysis, across development and between taxa. Studying three diaphyseal locations among the five ontogenetic series provided new insights into long bone function, including how each element adapts to facilitate each taxon's biology and behaviour with growth. Some examples include the locomotor signals emitted by the mid-humerus and adult body mass signals identified at the distal femur, while allometry along the ulna and tibia revealed how diaphyseal strength is modified dependent on a taxon's ecological and developmental demands. It was also possible to corroborate the present findings with those of several prior studies (specifically those that focused on either a single bone section, single developmental group or a single taxon). Looking forward, the next task will be to expand upon the information discussed here, by improving methodology (CT technology for exploring endosteal data), incorporating larger and more diverse samples (including suborder Strepsirrhini and parvorder Platyrrhini) and applying the methods in new areas (fossil primate specimens). It is an exciting time to be an anthropologist, and with the advancement of analytical techniques and regular emergence of important fossil discoveries, it is little wonder the field is growing at the rate it is. With its rapid growth though, it is important to thoroughly understand the data and methods available to us before chasing the next big wave. Doing so will better inform future research by placing it into a finer developmental, behavioural and evolutionary framework.

APPENDIX

TABLE A2.1. Technical error of measurement and reliability data of adult femoral midshafts

Specimen	**Taxon**	I_x **Correct**	I_x **Augmented**	I_x **Difference**	I_x **Difference^2**
M696	Gorilla	23223.25198	24392.29701	1116.04503	13466.44899
ZVI30	Gorilla	42610.89451	47650.39293	5039.49842	253510.6589
167335	Gorilla	43217.34178	45124.31806	190.97628	36471.93952
38326	Gorilla	18002.04186	18056.41567	54.37381	2956.511214
112720	Hylobates	434.89624	439.57642	46.8018	2190.408483
119601	Hylobates	602.62867	595.61633	70.01234	4901.727752
AS907	Hylobates	300.46875	297.46711	30.00164	900.0984027
AS1538	Hylobates	524.69576	522.78383	191.91193	36830.18888
30620	Macaca	99.23465	127.57336	283.33871	80280.82458
103649	Macaca	329.38941	331.28215	189.274	35824.64708
537258	Macaca	441.521	447.58376	60.6276	3675.705882
537253	Macaca	1326.83372	1361.05094	34.21722	1170.818145
38020	Pan	12064.06622	12368.21698	304.15076	92507.68481
22063	Pan	11128.72383	11587.93214	459.20831	210872.272
23163	Pan	12703.91566	12913.22291	209.30725	43809.5249
51202	Pan	11770.62908	11619.33894	151.29014	22888.70646
37365	Pongo	7284.28069	7604.49231	320.21162	102535.4816
50958	Pongo	2815.20805	2826.95834	117.5029	13806.93151
145306	Pongo	5442.06253	5687.25774	245.19521	60120.69101
153805	Pongo	4052.76802	4186.756	133.98798	17952.77878

All A–P bending rigidity (I_x) values given in mm^2.

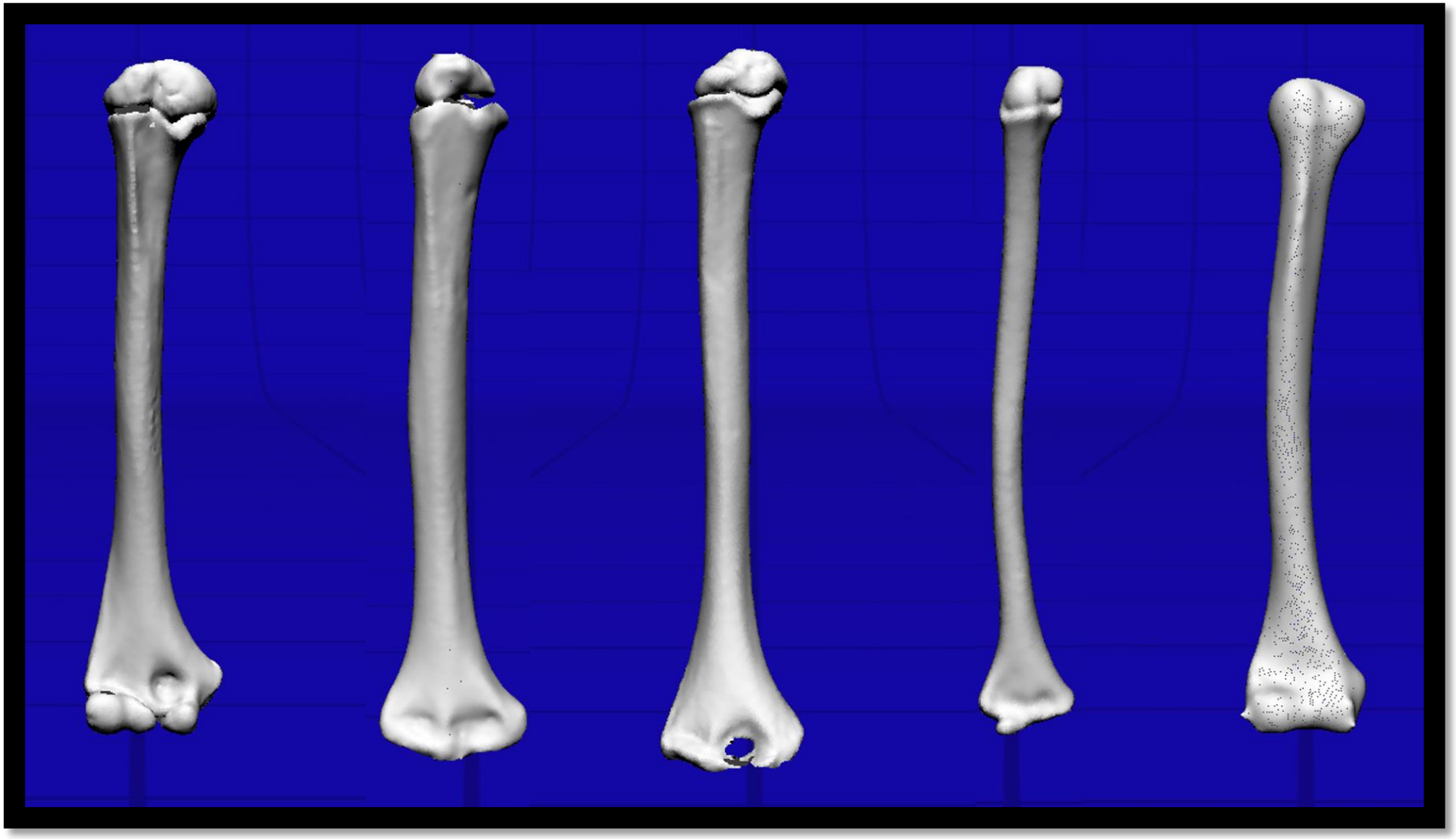

Fig. A2.1a. An example of five infant humeral models generated from each of the catarrhine taxa (mixed sexes). All models oriented anteriorly. From left to right: *Pan. troglodytes schweinfurthii*, *G. g. gorilla*, *P. pygmaeus* spp., *Hylobates lar* spp., *Macaca mulatta*. Models not to scale.

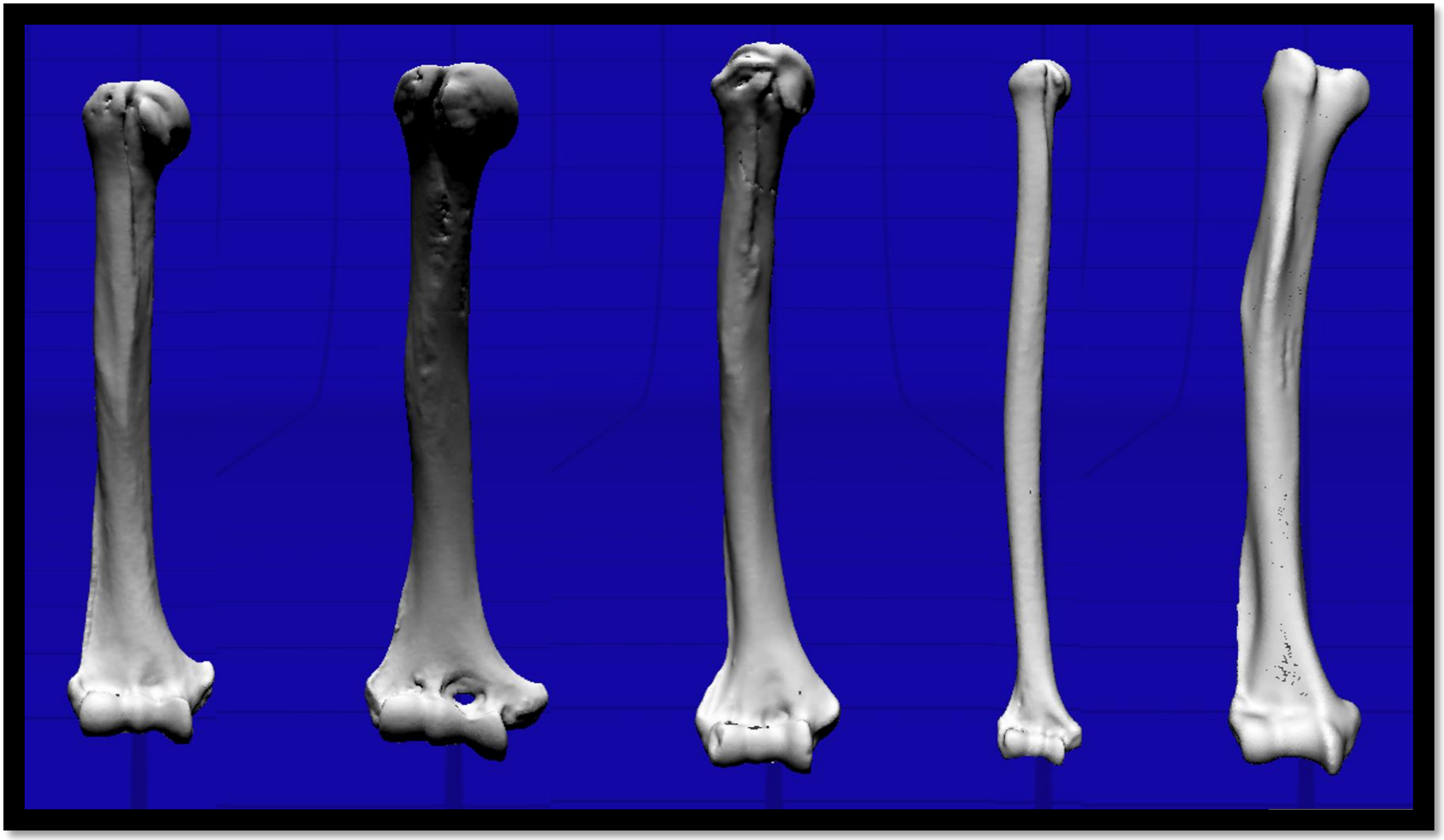

Fig. A2.1b. An example of five adult humeral 3D models generated from each of the catarrhine taxa (all male specimens). All models oriented anteriorly. From left to right: Pan. troglodytes schweinfurthii, G. g. gorilla, P. pygmaeus spp., Hylobates lar spp., Macaca mulatta. Models not to scale.

Fig. A2.2a. An example of five infant ulnar 3D models generated from each of the catarrhine taxa (mixed sexes). All models oriented anteriorly. From left to right: *Pan. troglodytes schweinfurthii*, *G. g. gorilla*, *P. pygmaeus* spp., *Hylobates lar* spp., *Macaca mulatta*. Models not to scale.

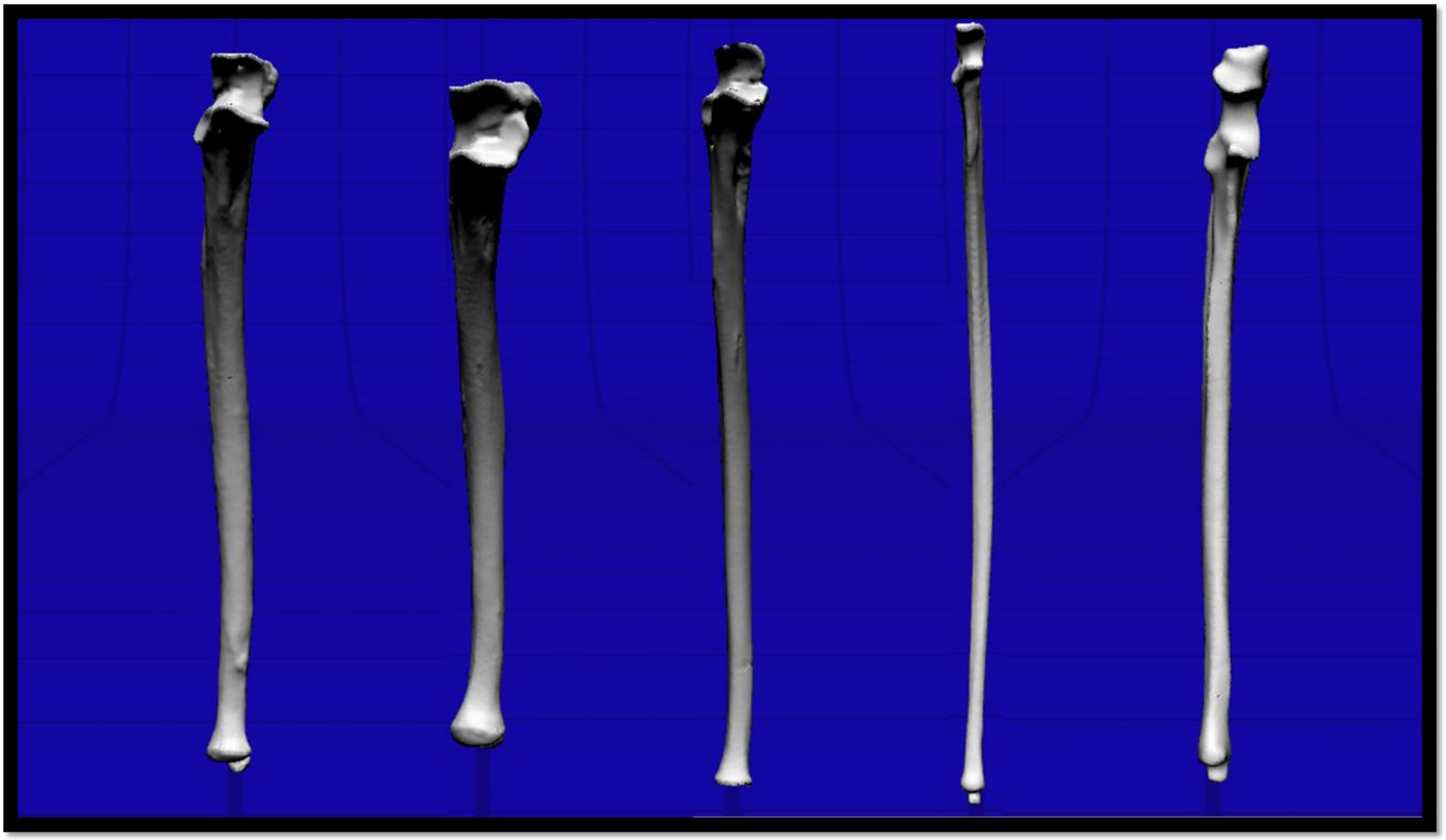

Fig. A2.2b. An example of five adult ulnar 3D models generated from each of the catarrhine taxa (all male specimens). All models oriented anteriorly. From left to right: *Pan. troglodytes schweinfurthii*, *G. g. gorilla*, *P. pygmaeus* spp., *Hylobates lar* spp., *Macaca mulatta*. Models not to scale.

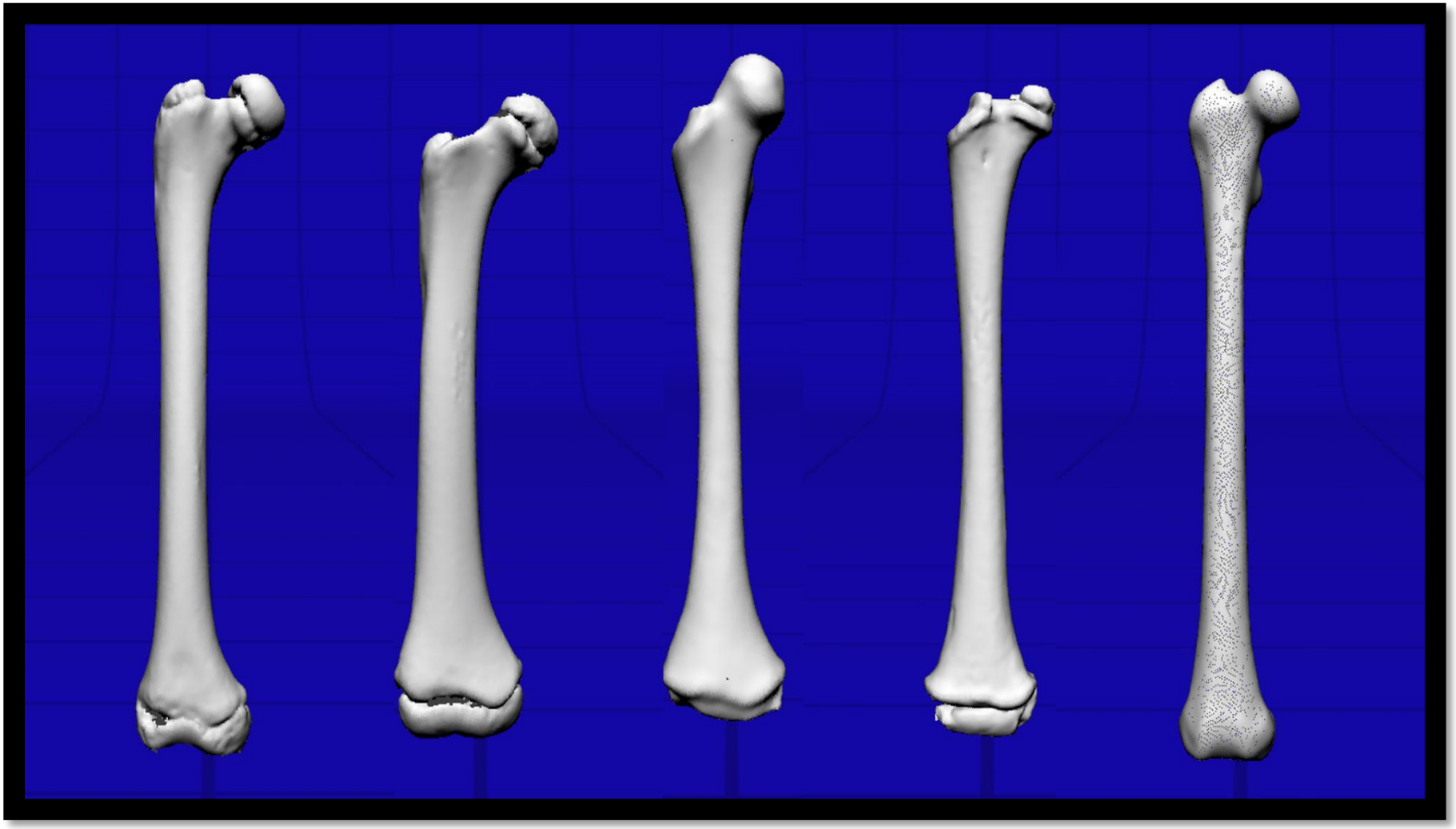

Fig. A2.3a. An example of five infant femoral 3D models generated from each of the catarrhine taxa (mixed sexes). All models oriented anteriorly. From left to right: *Pan. troglodytes schweinfurthii*, *G. g. gorilla*, *P. pygmaeus* spp., *Hylobates lar* spp., *Macaca mulatta*. Models not to scale.

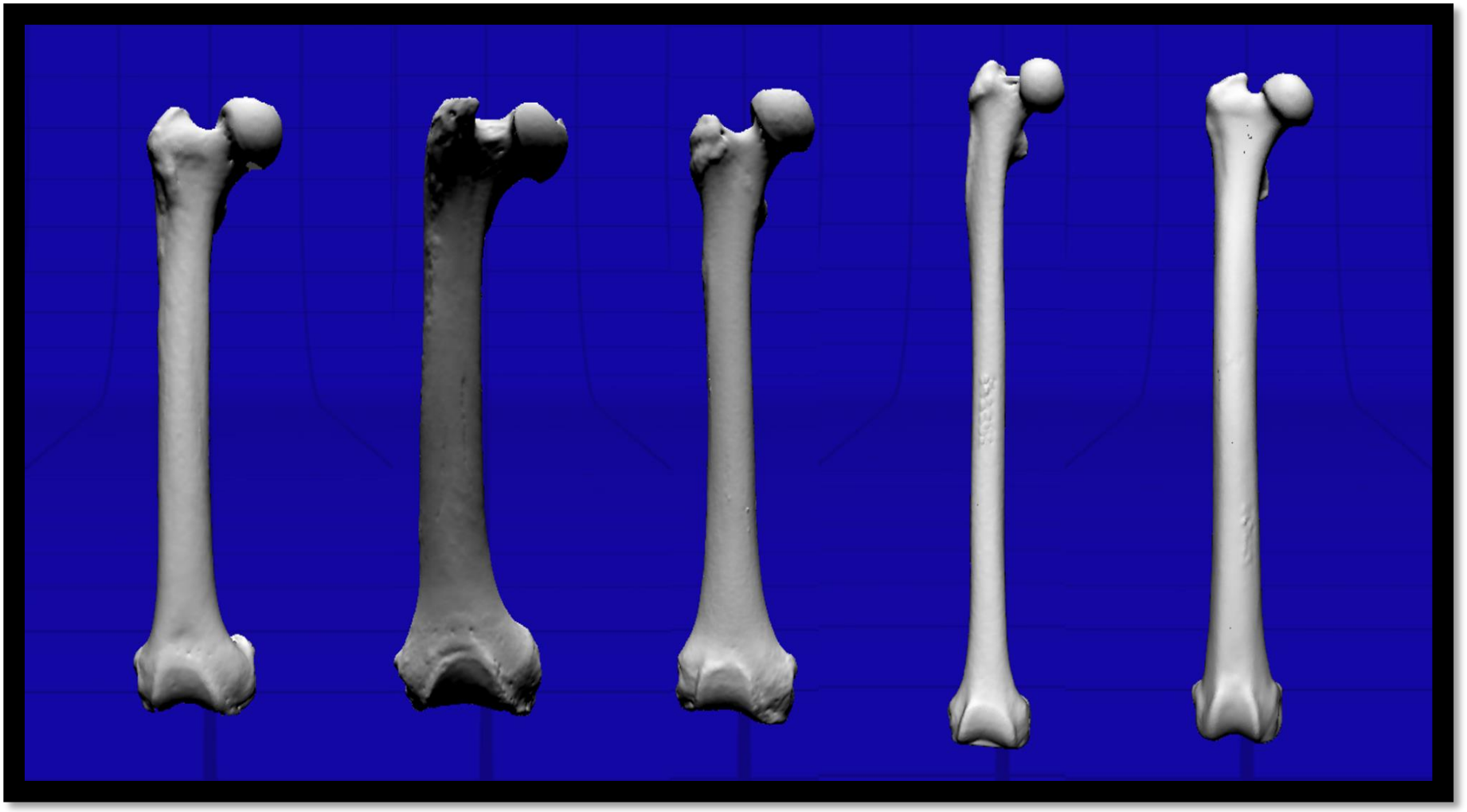

Fig. A2.3b. An example of five adult femoral 3D models generated from each of the catarrhine taxa (all male specimens). All models oriented anteriorly. From left to right: *Pan. troglodytes schweinfurthii*, *G. g. gorilla*, *P. pygmaeus* spp., *Hylobates lar* spp., *Macaca mulatta*. Models not to scale.

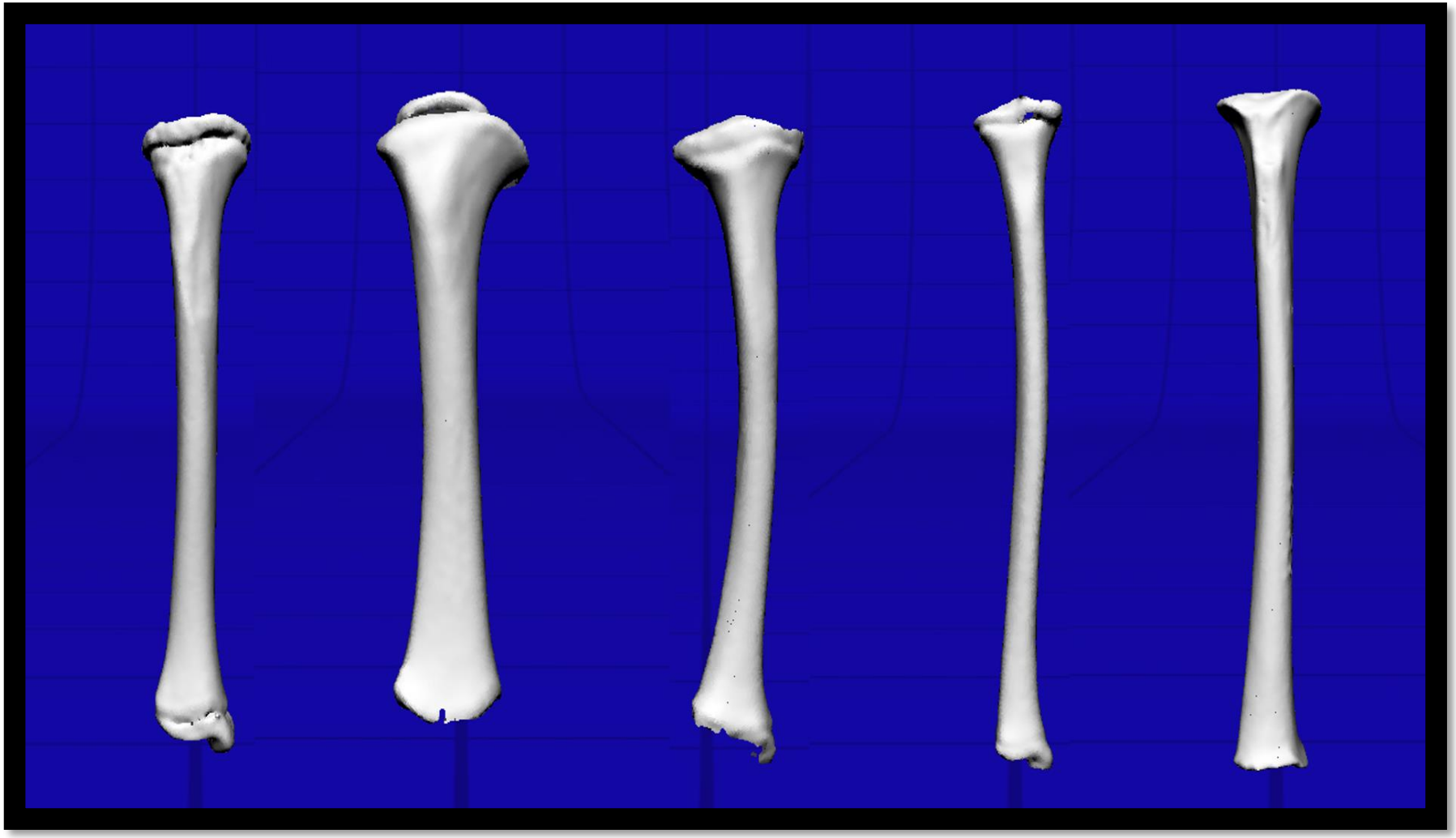

Fig. A2.4a. An example of five infant tibial 3D models generated from each of the catarrhine taxa (mixed sexes). All models oriented anteriorly. From left to right: *Pan. troglodytes schweinfurthii*, *G. g. gorilla*, *P. pygmaeus* spp., *Hylobates lar* spp., *Macaca mulatta*. Models not to scale.

Fig. A2.4b. An example of five adult tibial 3D models generated from each of the catarrhine taxa (all male specimens). All models oriented anteriorly. From left to right: *Pan. troglodytes schweinfurthii*, *G. g. gorilla*, *P. pygmaeus* spp., *Hylobates lar* spp., *Macaca mulatta*. Models not to scale

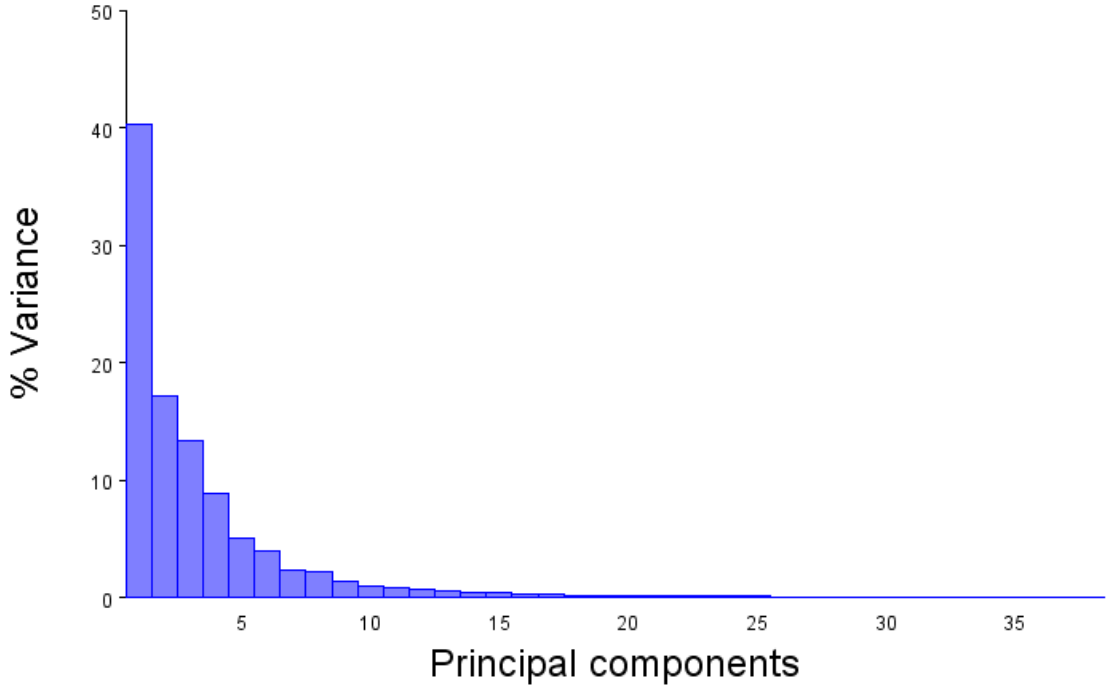

Fig. A5.1a. Scree plot illustrating the percentage of chimpanzee humeral midshaft variance by PC.

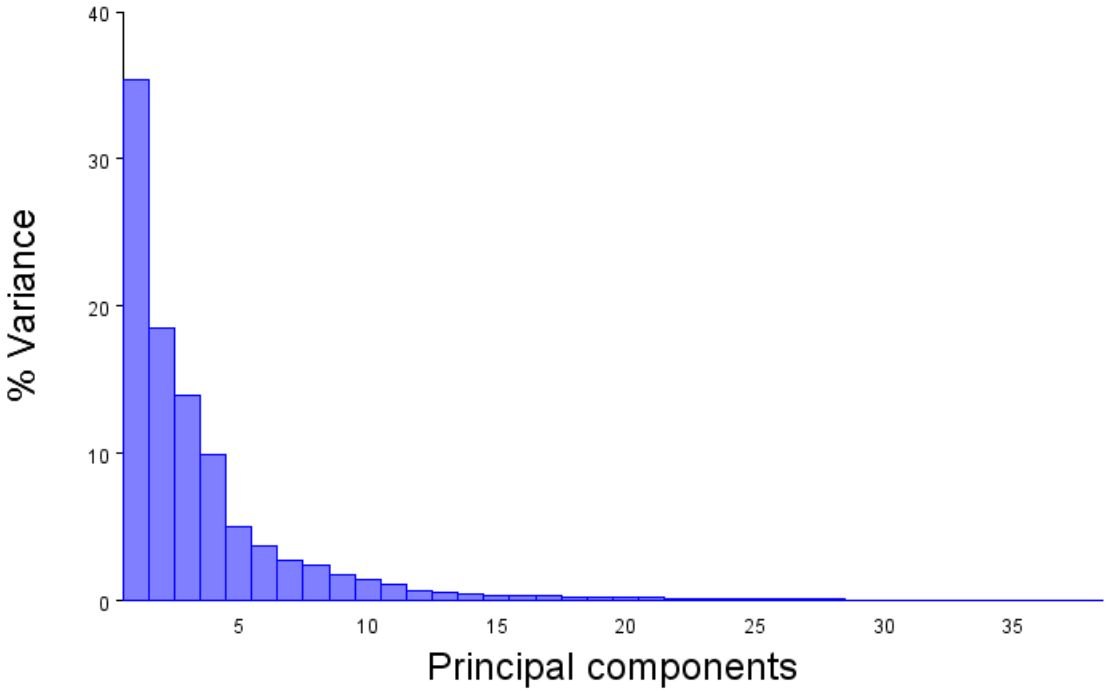

Fig. A5.1b. Scree plot illustrating the percentage of gorilla humeral midshaft variance by PC.

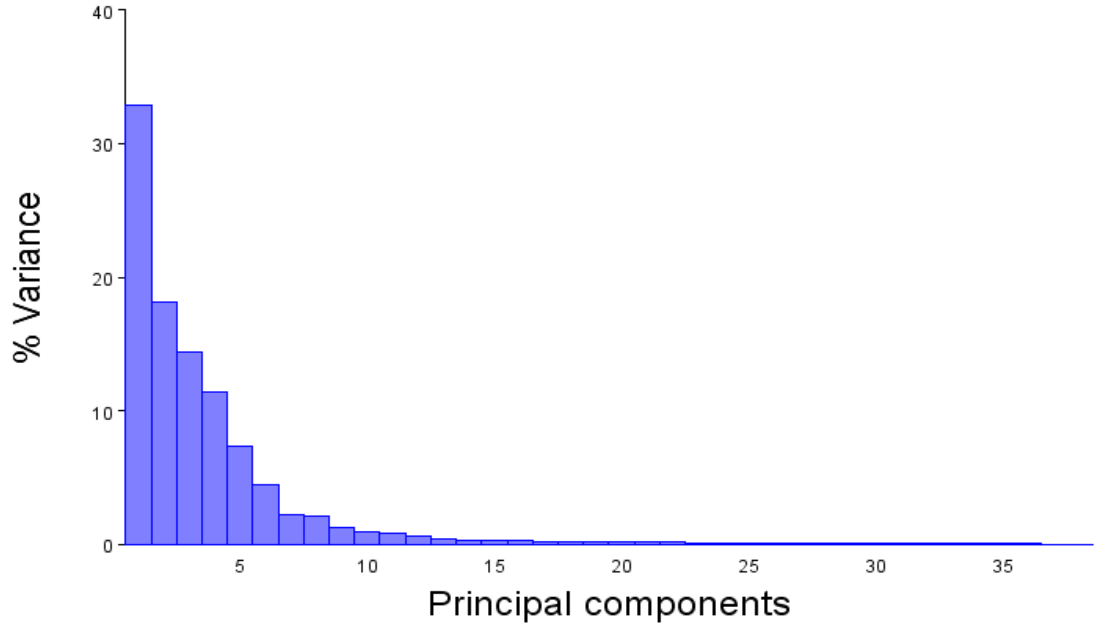

Fig. A5.1c. Scree plot illustrating the percentage of orangutan humeral midshaft shape variance by PC.

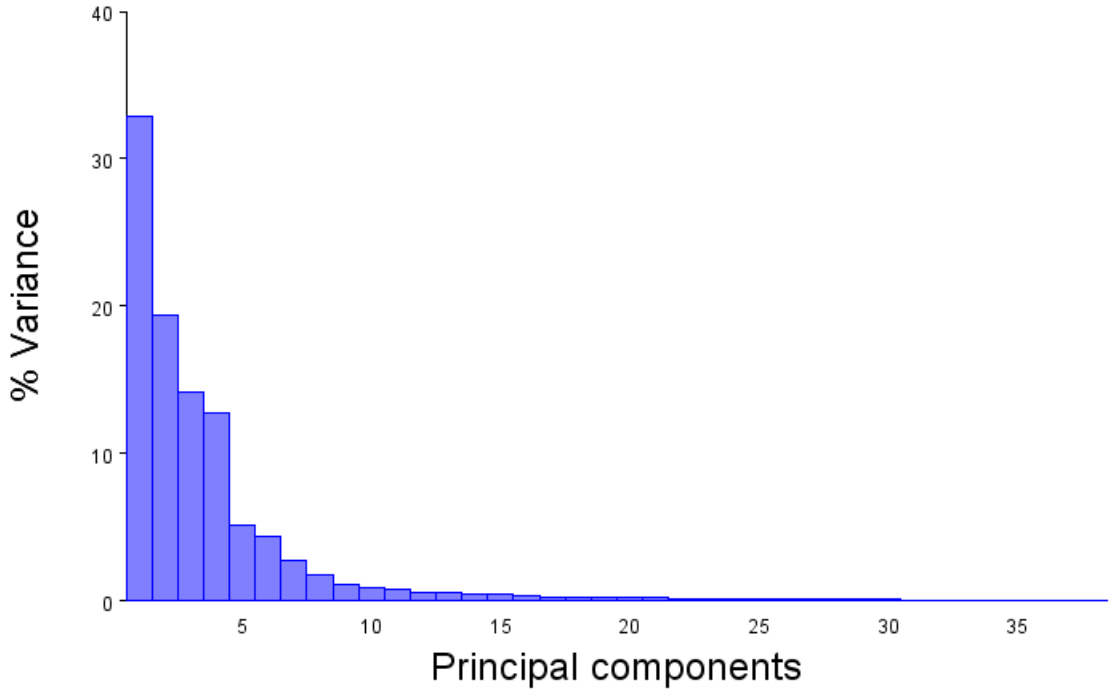

Fig. A5.1d. Scree plot illustrating the percentage of hylobatid humeral midshaft shape variance by PC.

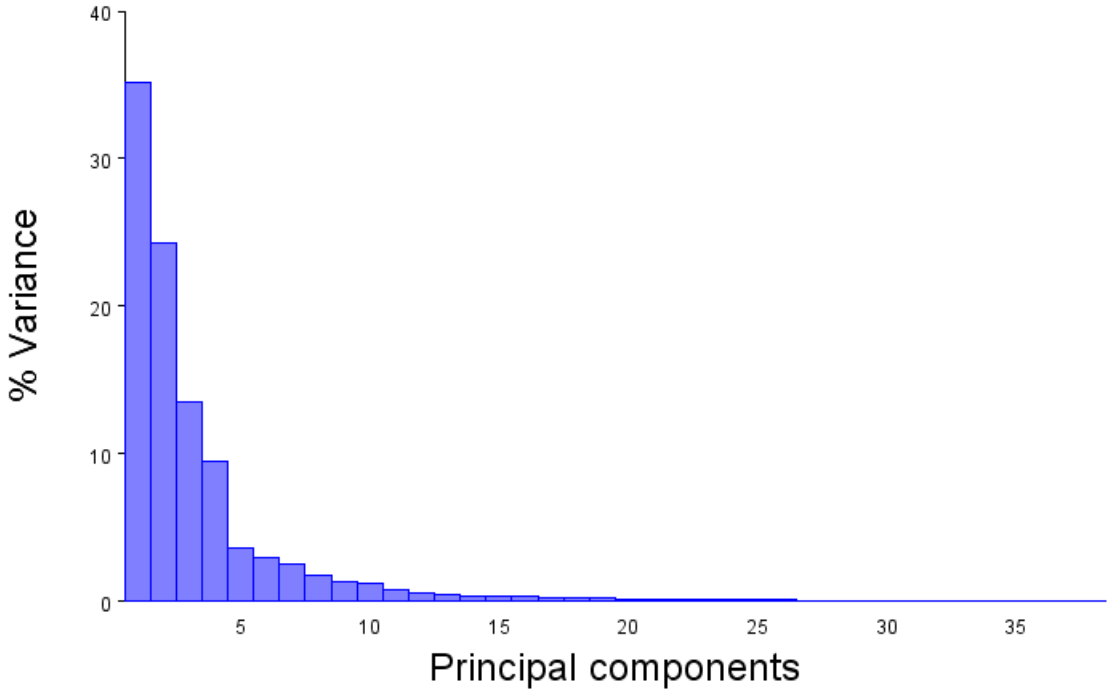

Fig. A5.1e. Scree plot illustrating the percentage of macaque humeral midshaft shape variance by PC.

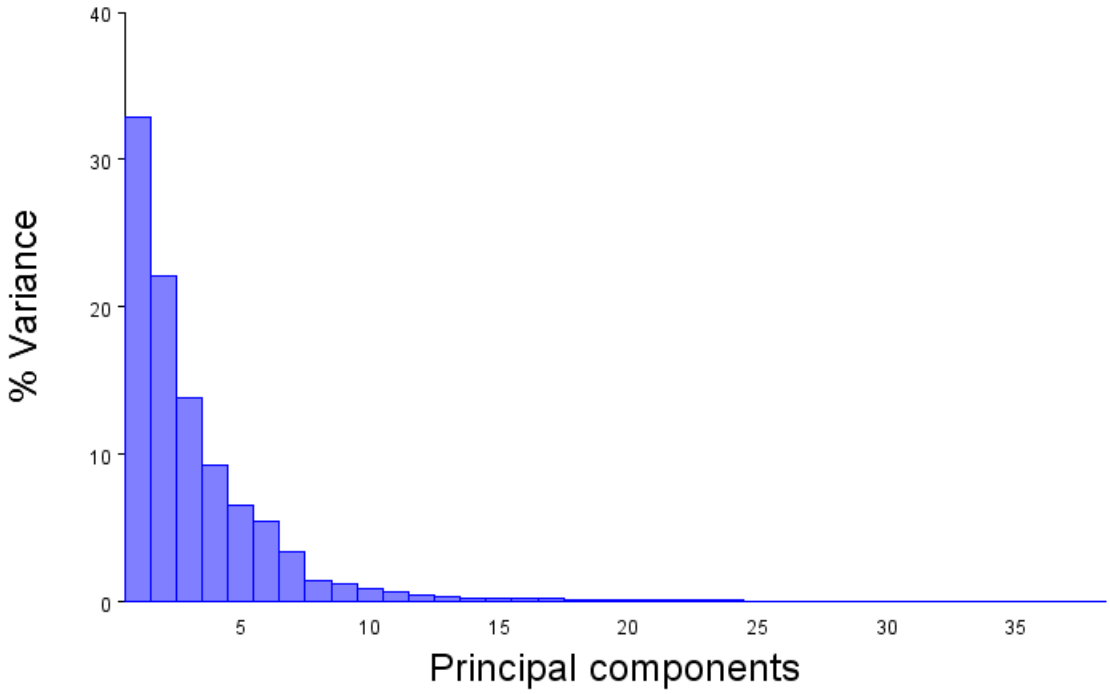

Fig. A5.2a. Scree plot illustrating the percentage of chimpanzee ulnar midshaft shape variance by PC.

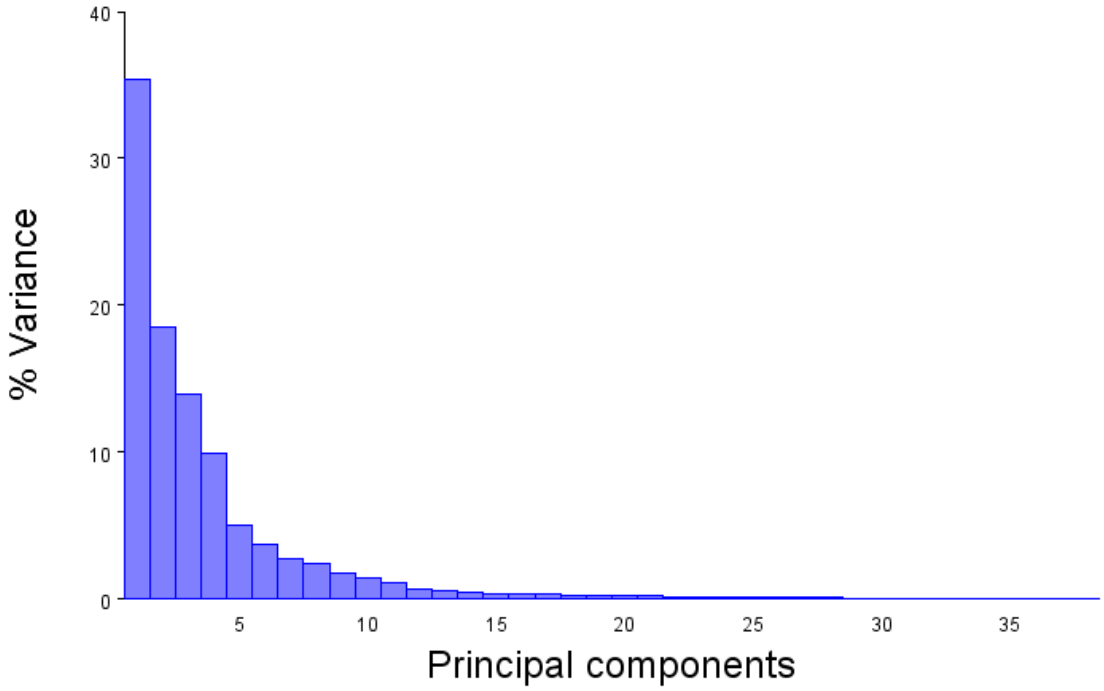

Fig. 5.2b. Scree plot illustrating the percentage of gorilla ulnar midshaft shape variance by PC.

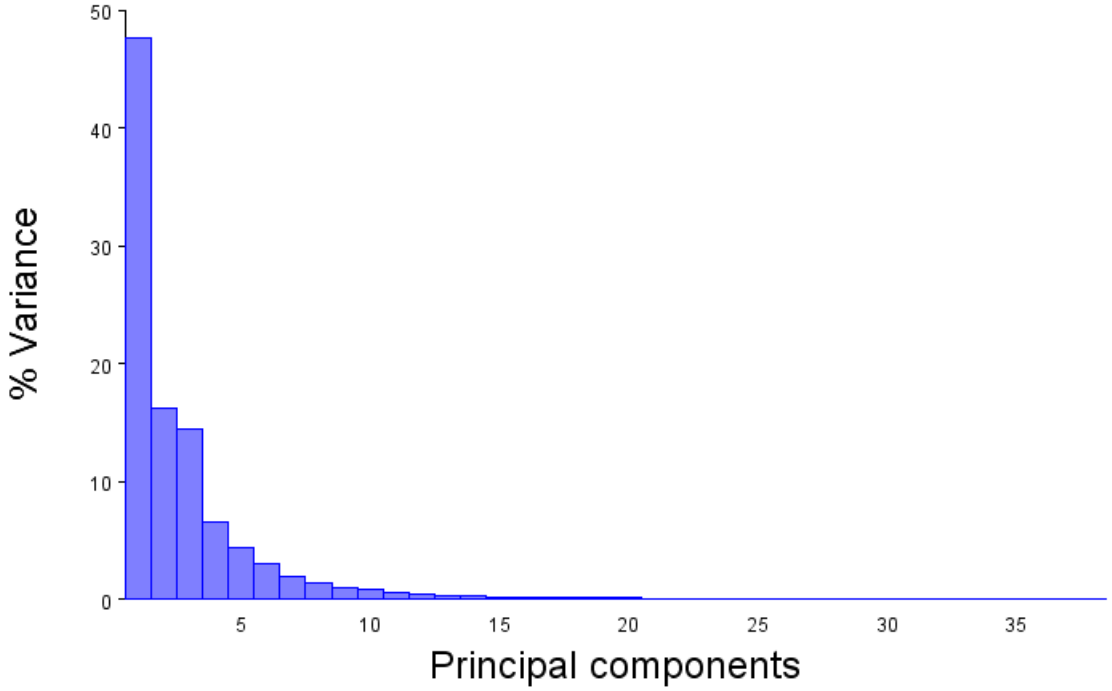

Fig. A5.2c. Scree plot illustrating the percentage of orangutan ulnar midshaft shape variance by PC.

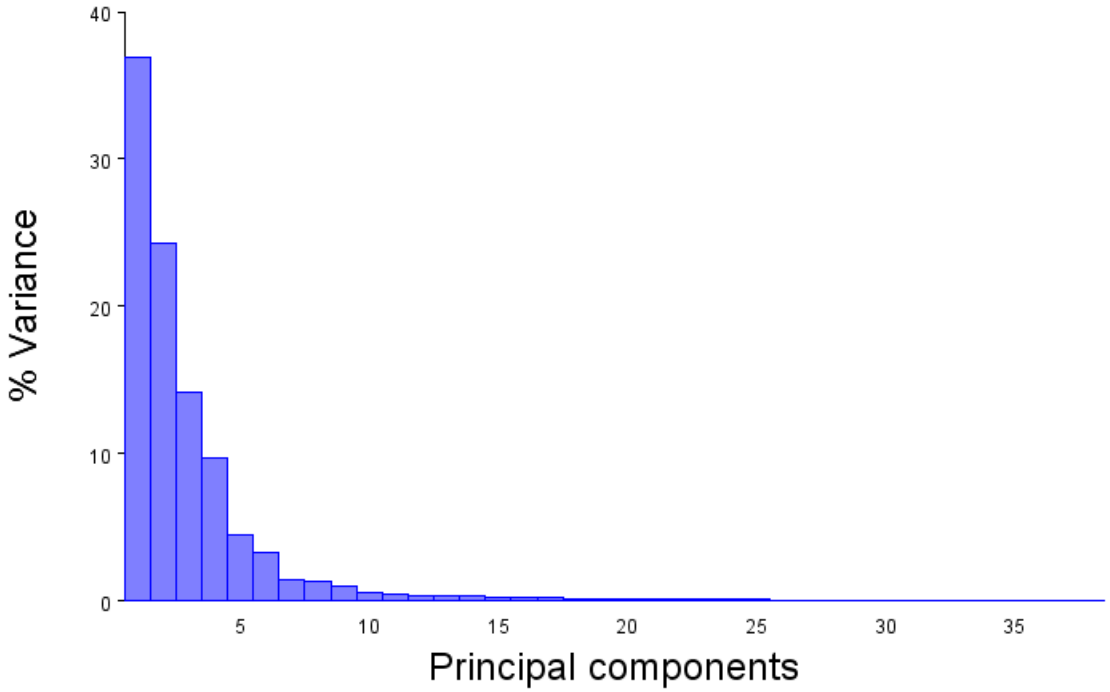

Fig. A5.2d. Scree plot illustrating the percentage of hylobatid ulnar midshaft shape variance by PC.

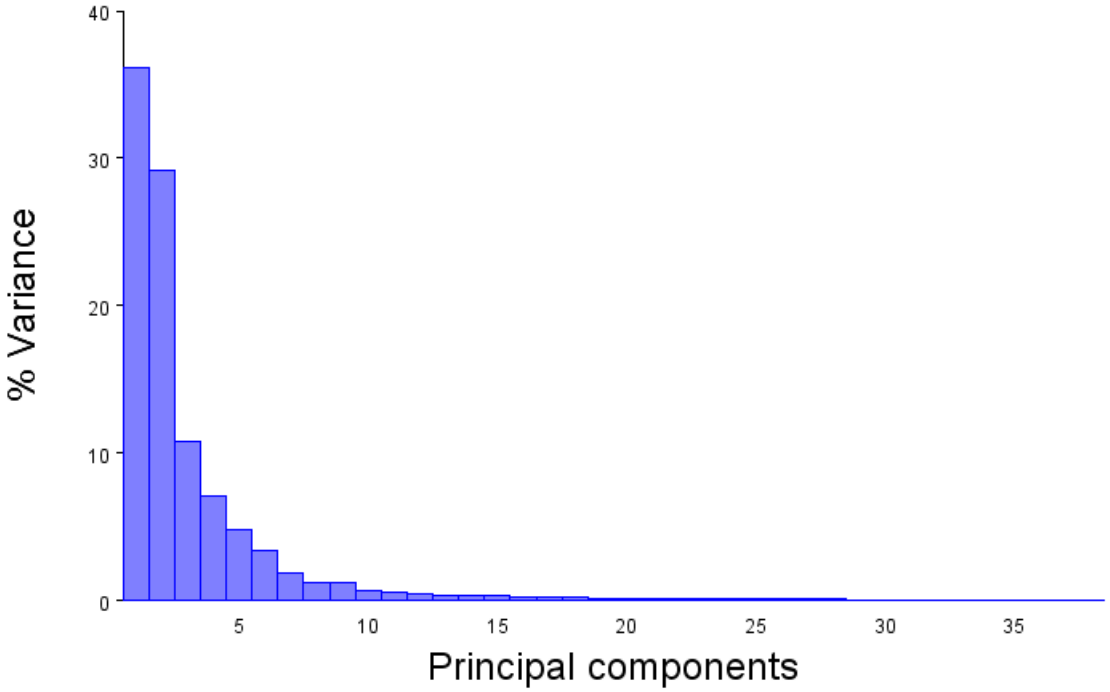

Fig. A5.2e. Scree plot illustrating the percentage of macaque ulnar midshaft shape variance by PC.

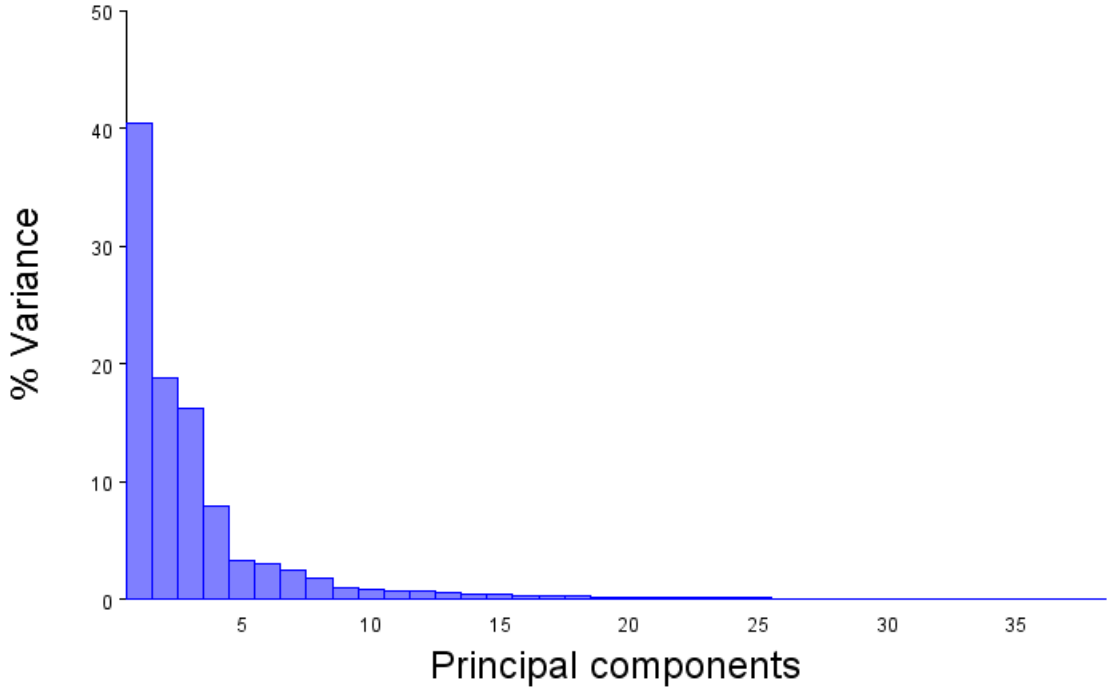

Fig. A5.3a. Scree plot illustrating the percentage of chimpanzee femoral midshaft shape variance by PC.

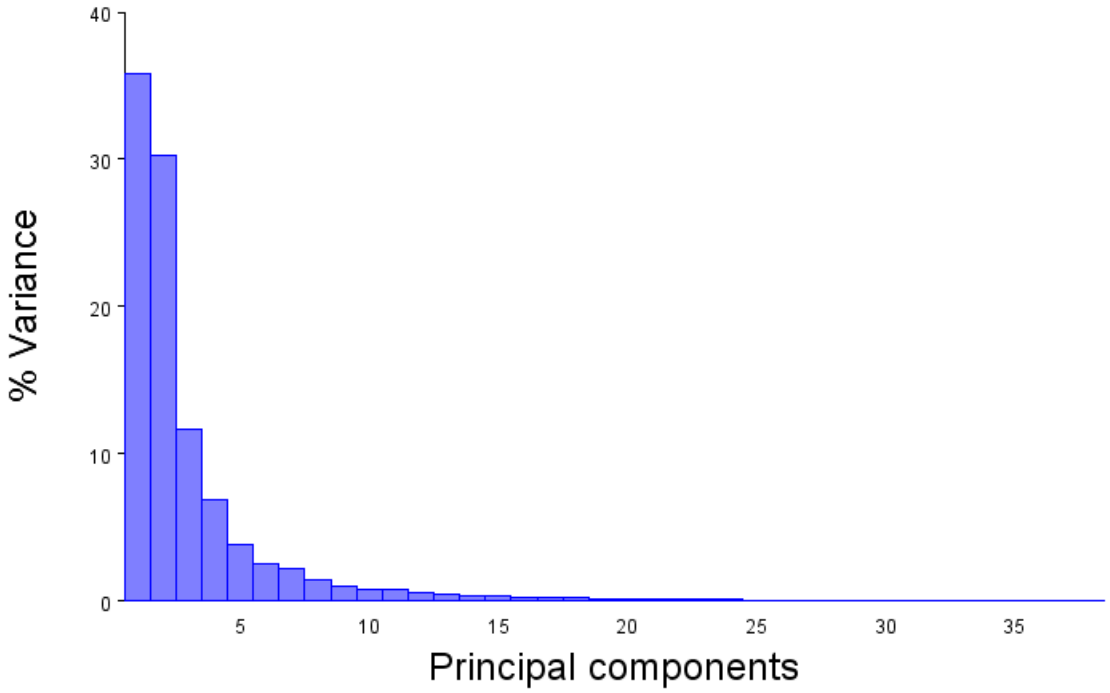

Fig. A5.3b. Scree plot illustrating the percentage gorilla femoral midshaft shape variance by PC.

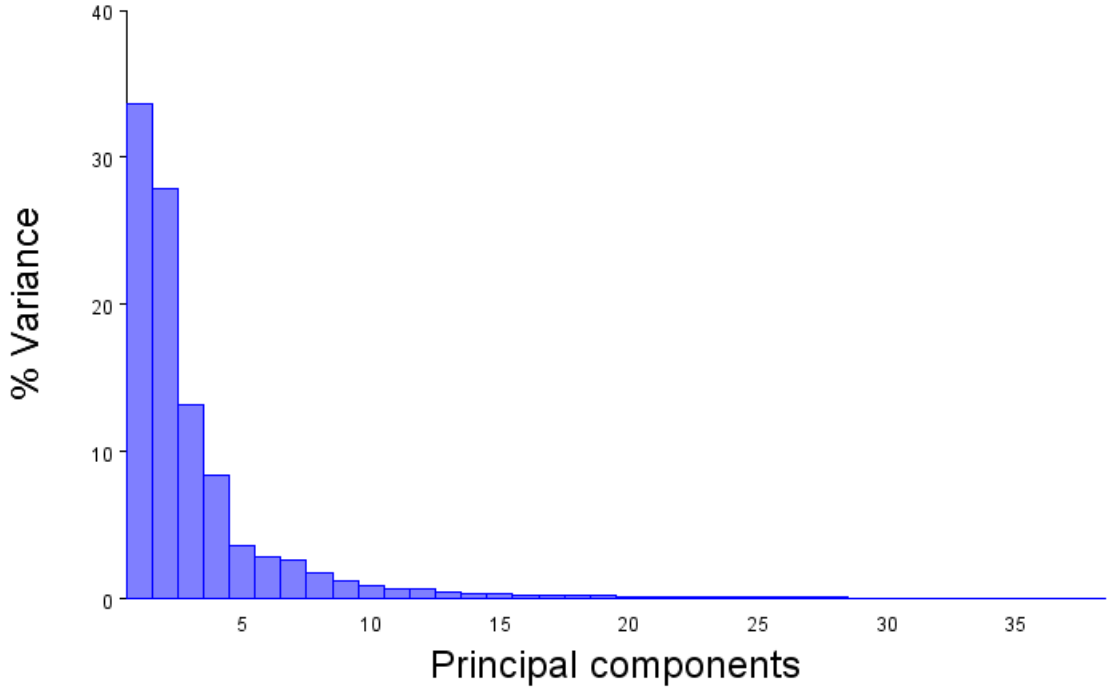

Fig. A5.3c. Scree plot illustrating the percentage of orangutan femoral midshaft shape variance by PC.

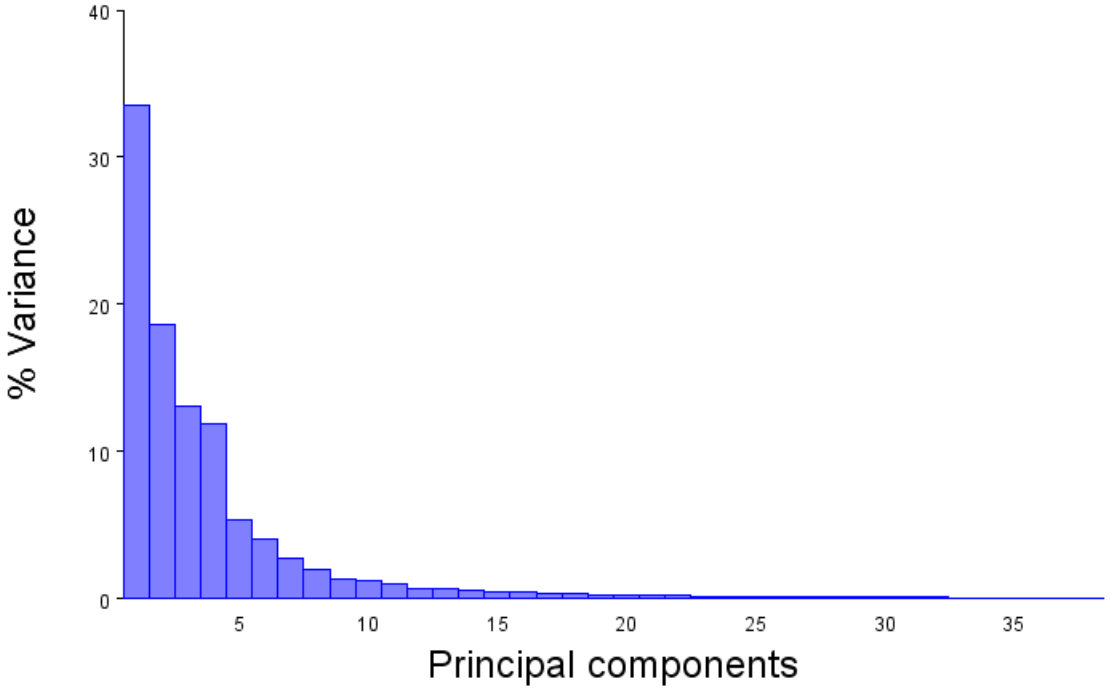

Fig. A5.3d. Scree plot illustrating the percentage of hylobatid femoral midshaft shape variance by PC.

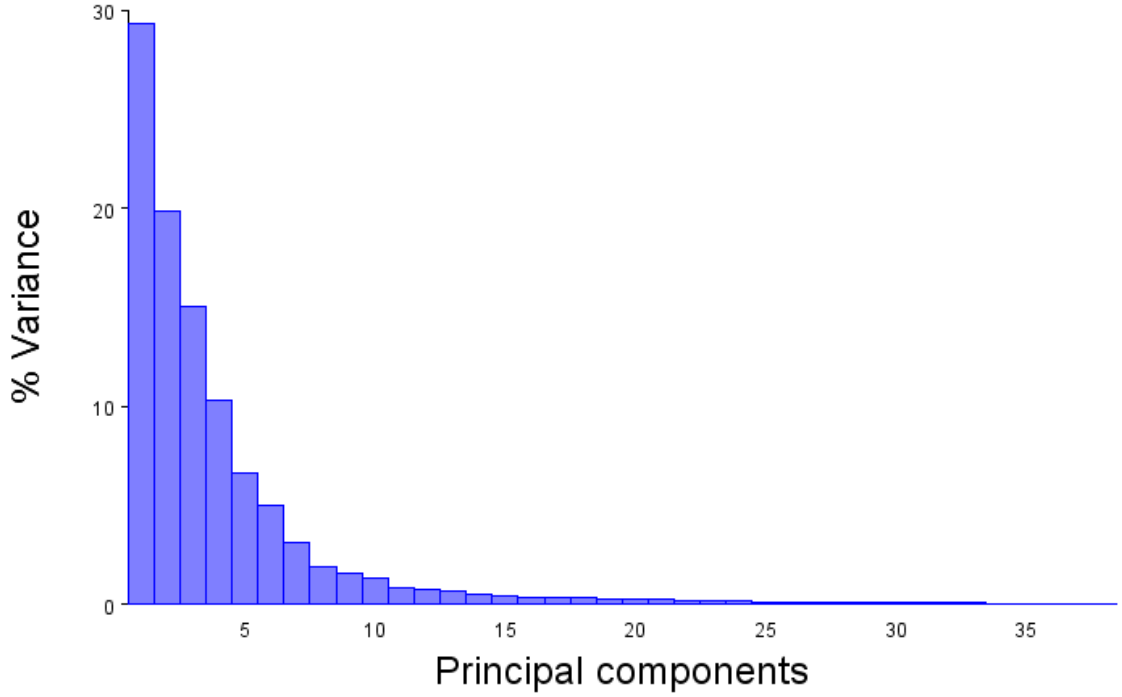

Fig. A5.3e. Scree plot illustrating the percentage of macaque femoral midshaft shape variance by PC.

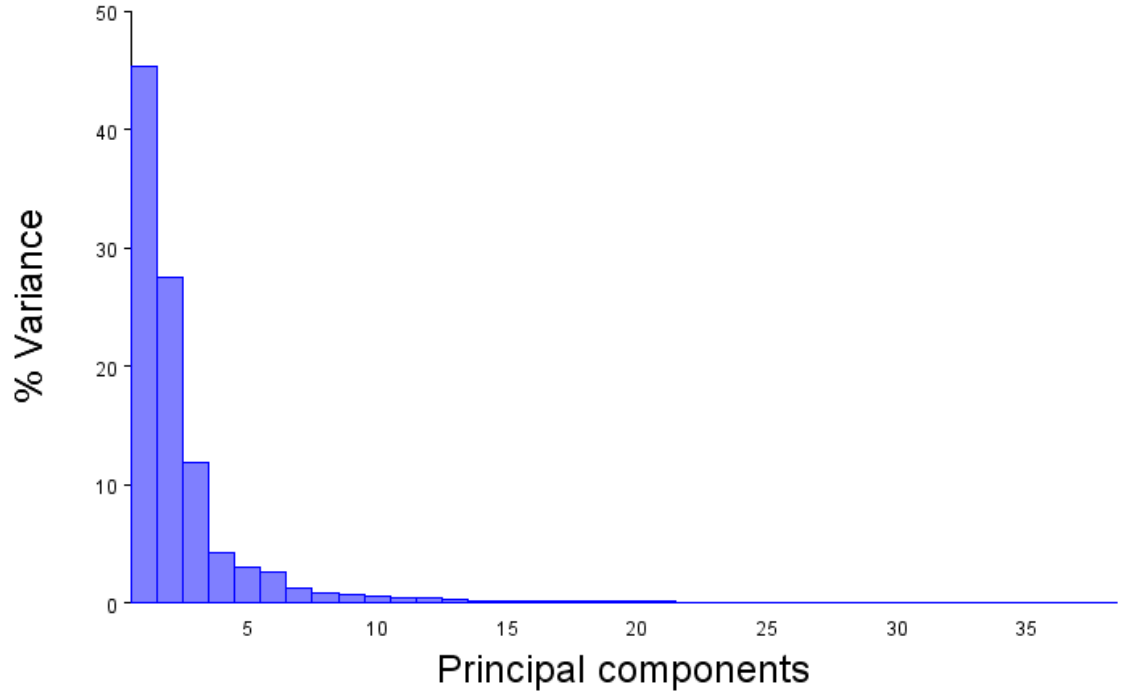

Fig. A5.4a. Scree plot illustrating the percentage of chimpanzee tibial midshaft shape variance by PC.

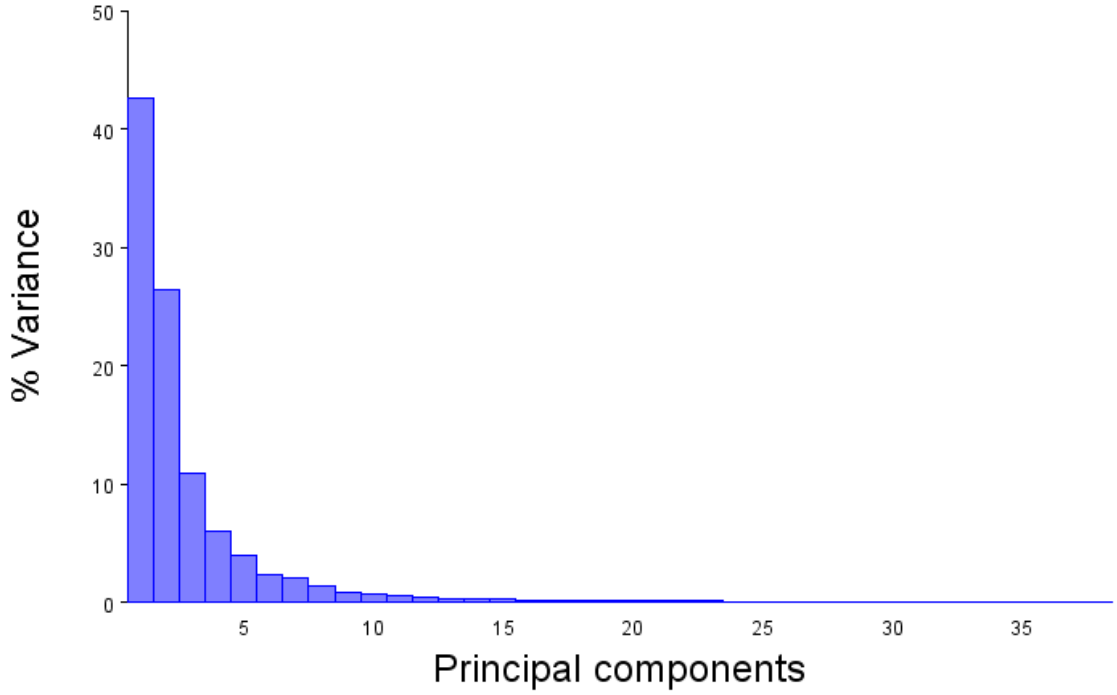

Fig. A5.4b. Scree plot illustrating the percentage of gorilla tibial midshaft shape variance by PC.

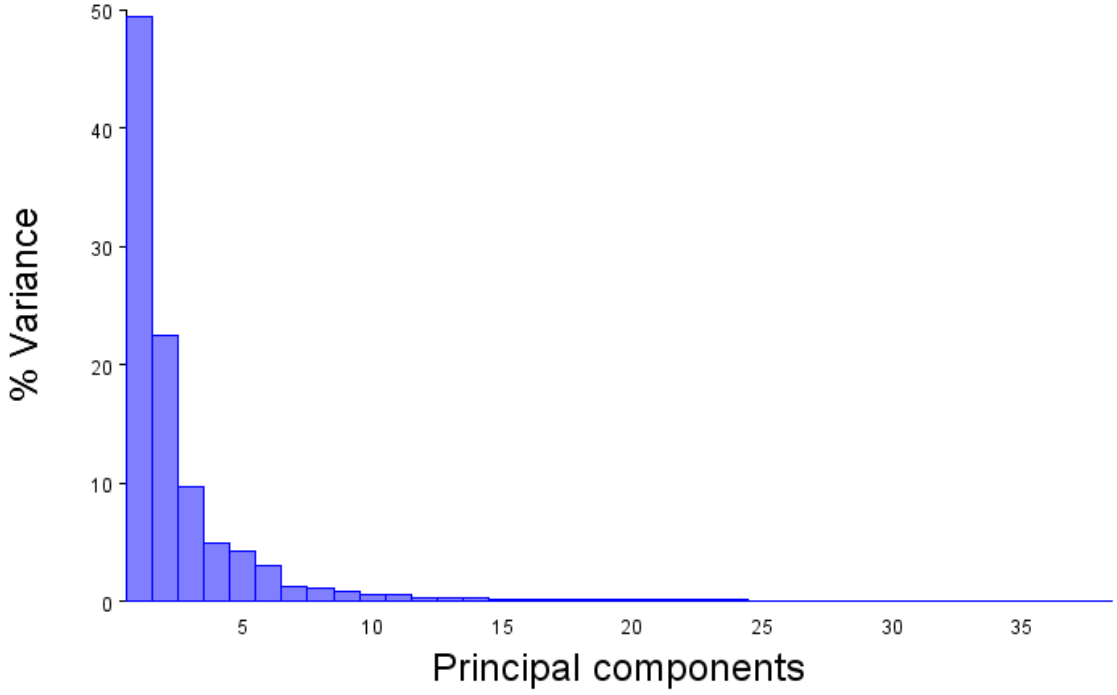

Fig. A5.4c. Scree plot illustrating the percentage of orangutan tibial midshaft shape variance by PC.

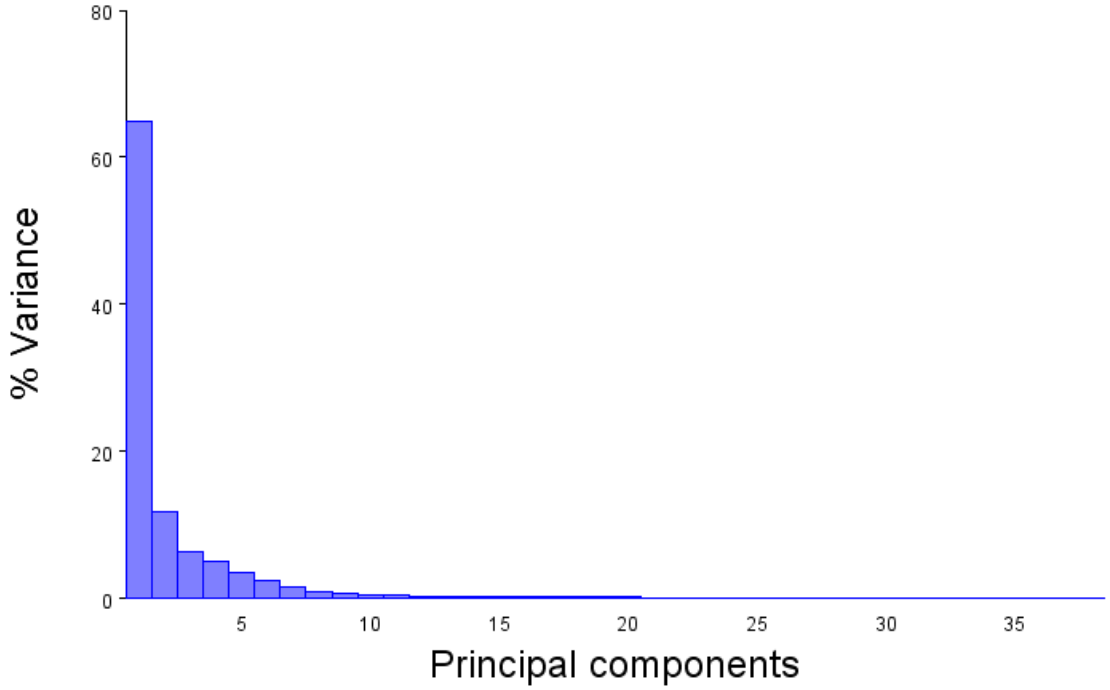

Fig. A5.4d. Scree plot illustrating the percentage of hylobatid tibial midshaft shape variance by PC.

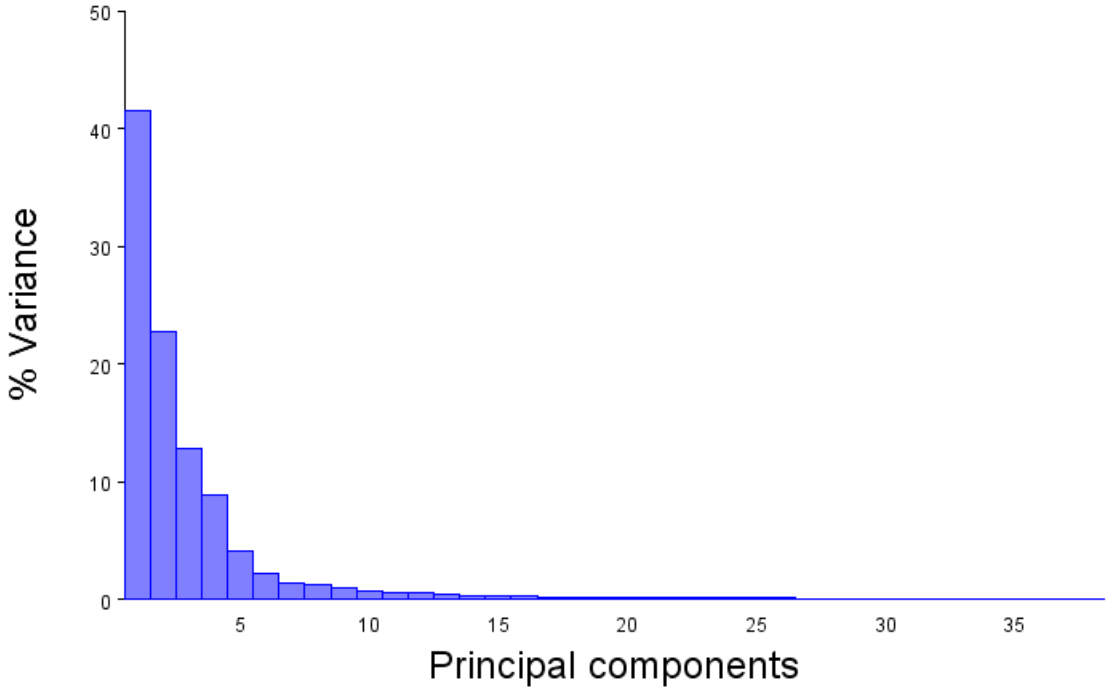

Fig. A5.4e. Scree plot illustrating the percentage of macaque tibial midshaft shape variance by PC.

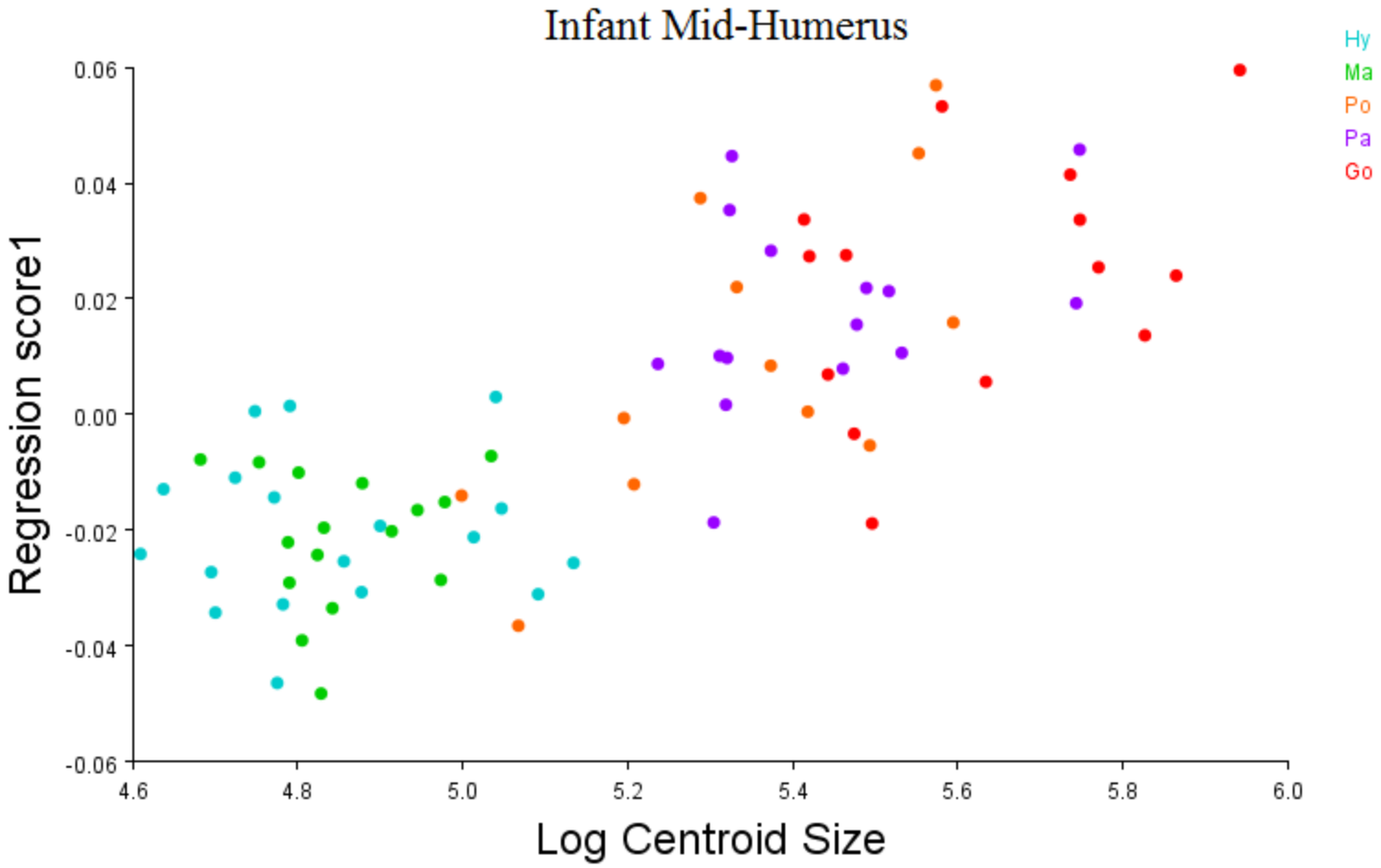

Fig. A5.5a. Log centroid size plotted against shape (procrustes coordinate data) of the pooled infant humeral midshaft.

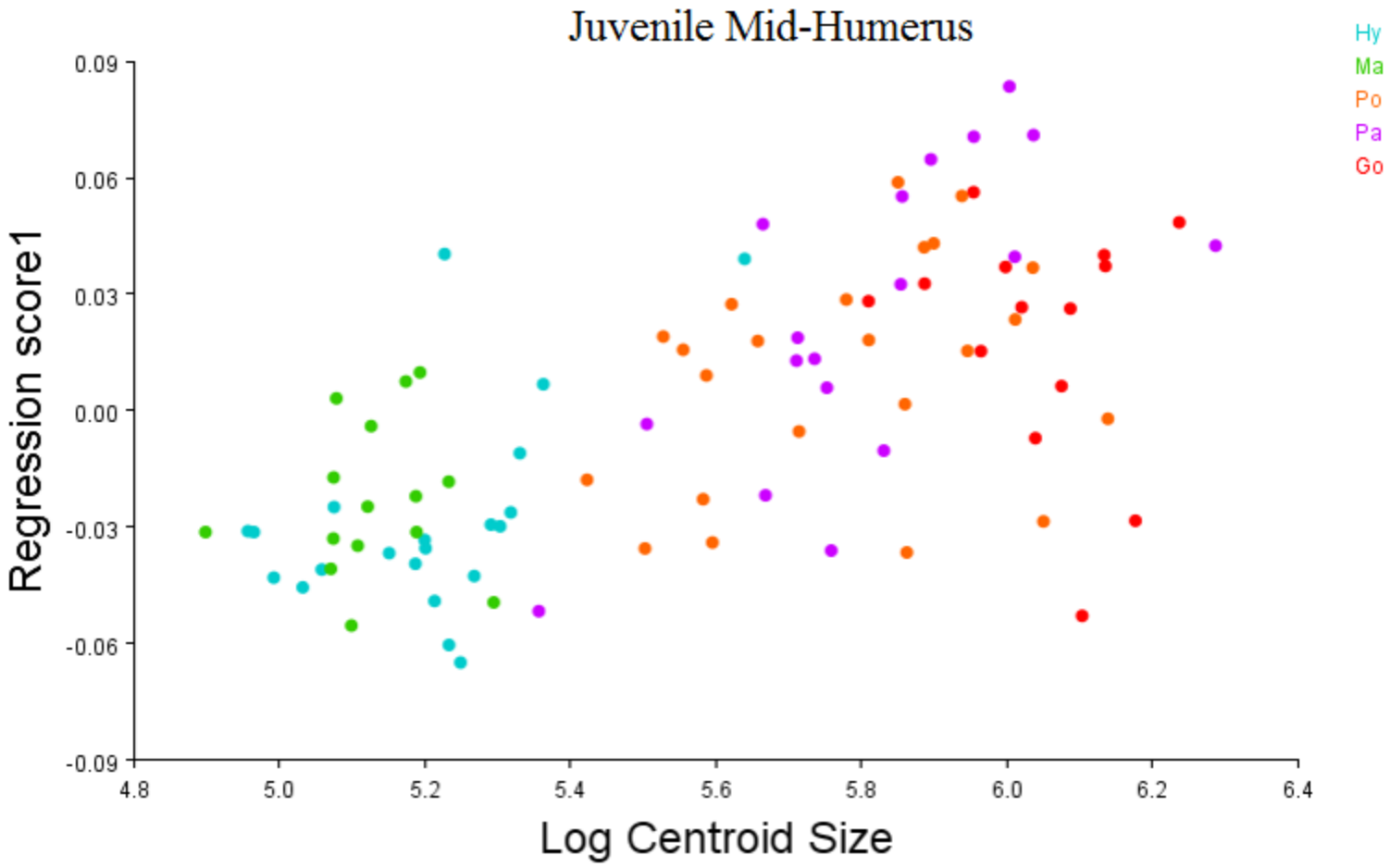

Fig. A5.5b. Log centroid size plotted against shape (procrustes coordinate data) of the pooled juvenile humeral midshaft.

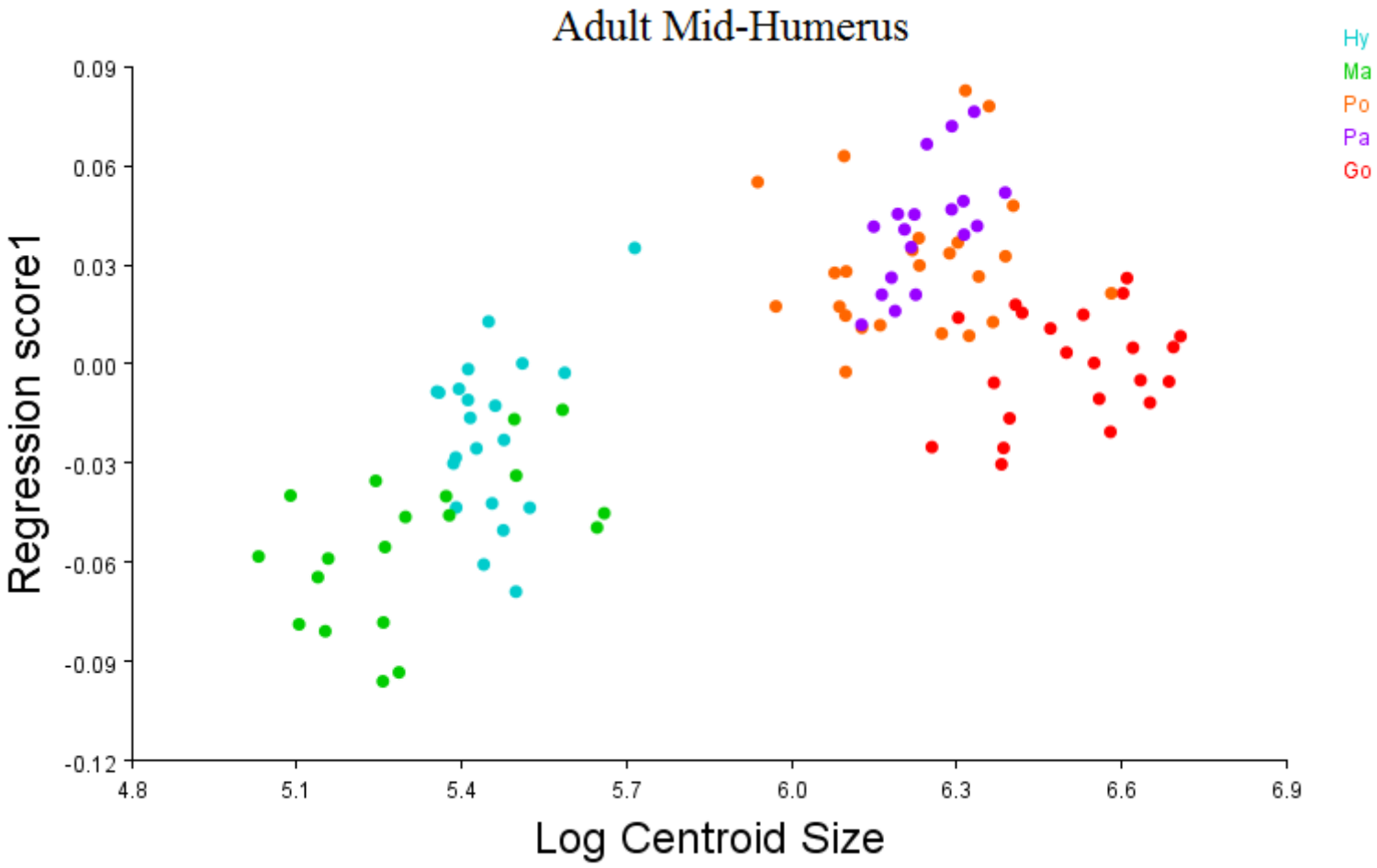

Fig. A5.5c. Log centroid size plotted against shape (procrustes coordinate data) of the pooled adult humeral midshaft.

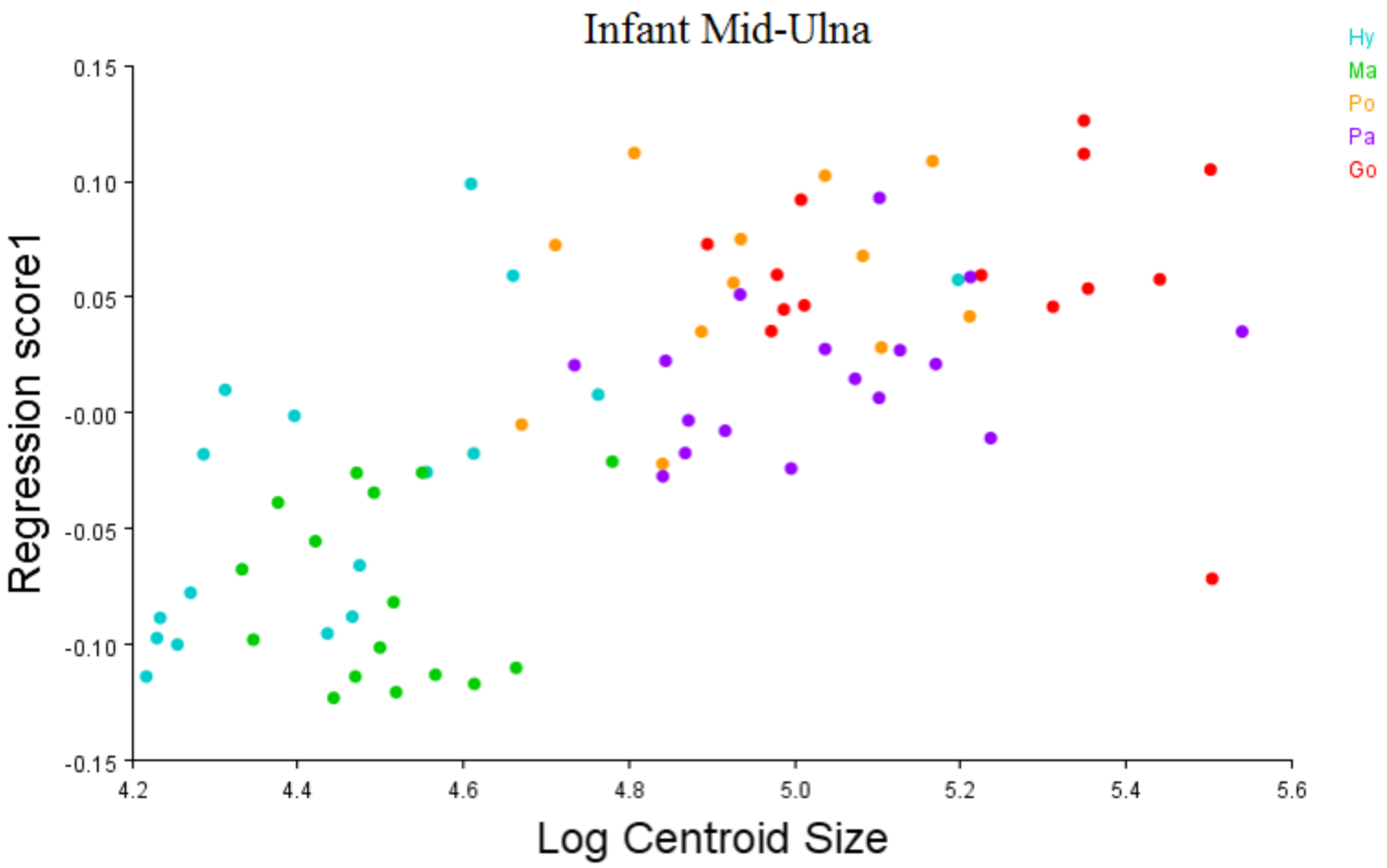

Fig. A5.6a. Log centroid size plotted against shape (procrustes coordinate data) of the pooled infant ulnar midshaft.

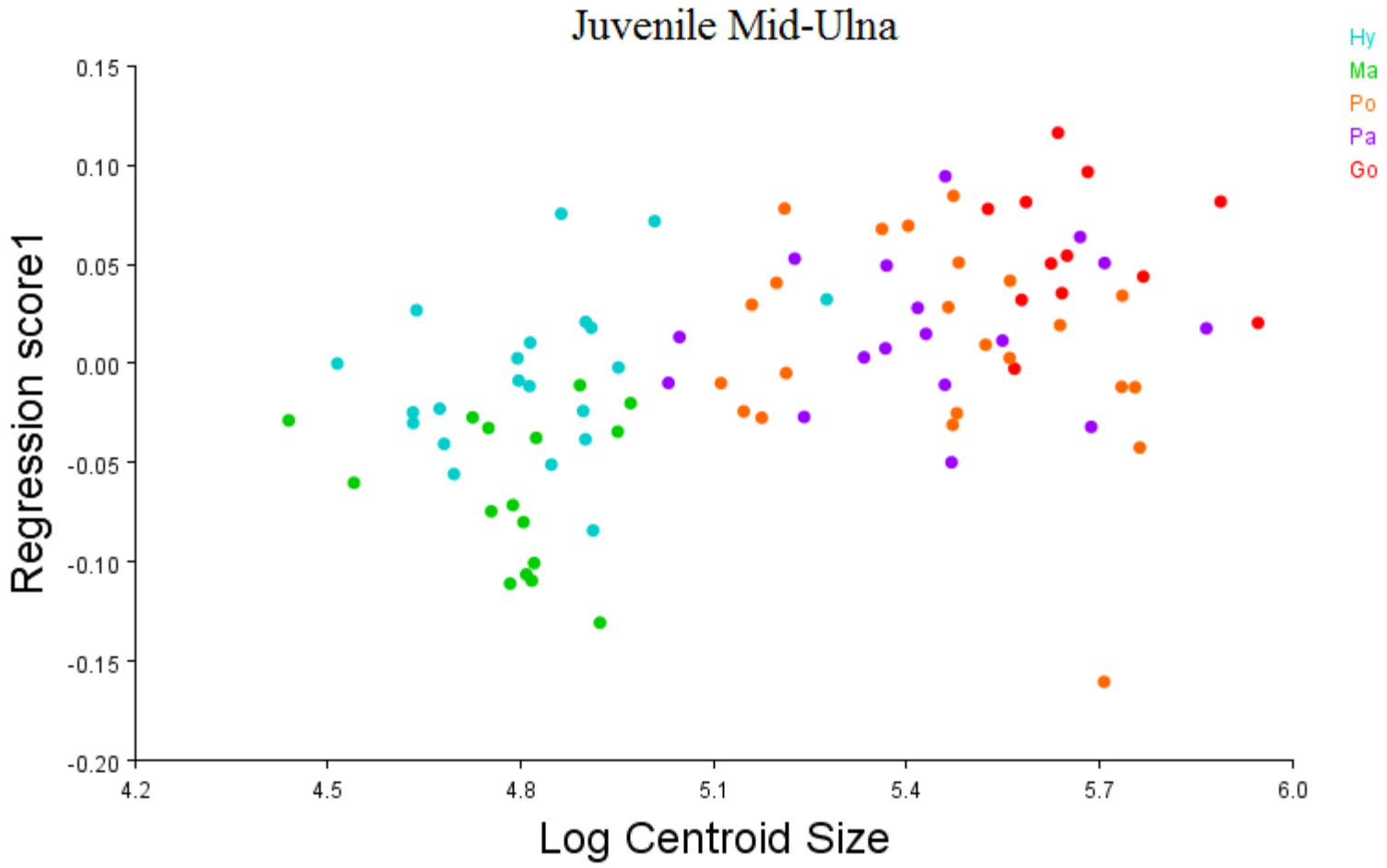

Fig. A5.6b. Log centroid size plotted against shape (procrustes coordinate data) of the pooled juvenile ulnar midshaft.

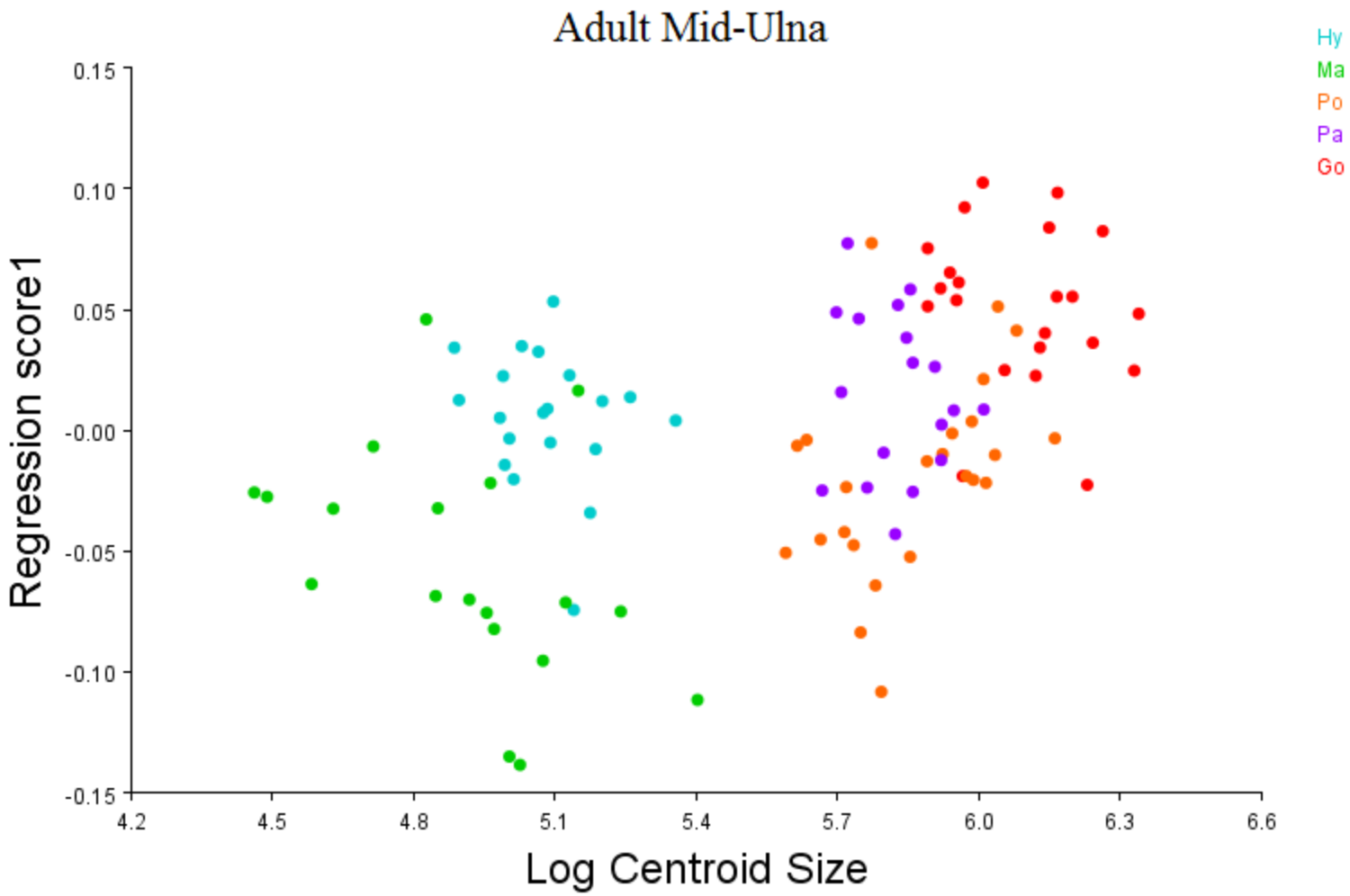

Fig. A5.6c. Log centroid size plotted against shape (procrustes coordinate data) of the pooled adult ulnar midshaft.

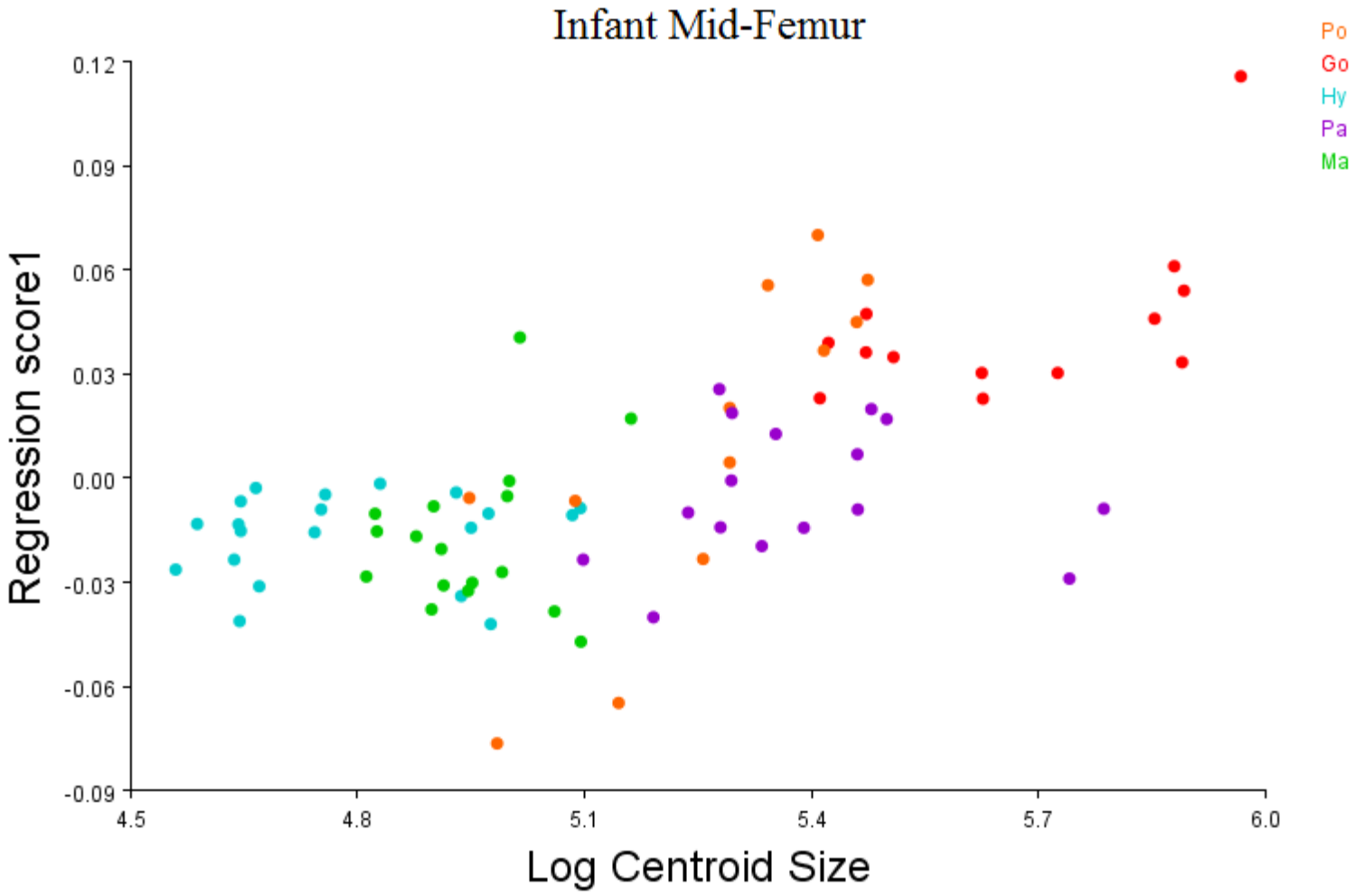

Fig. A5.7a. Log centroid size plotted against shape (procrustes coordinate data) of the pooled infant femoral midshaft.

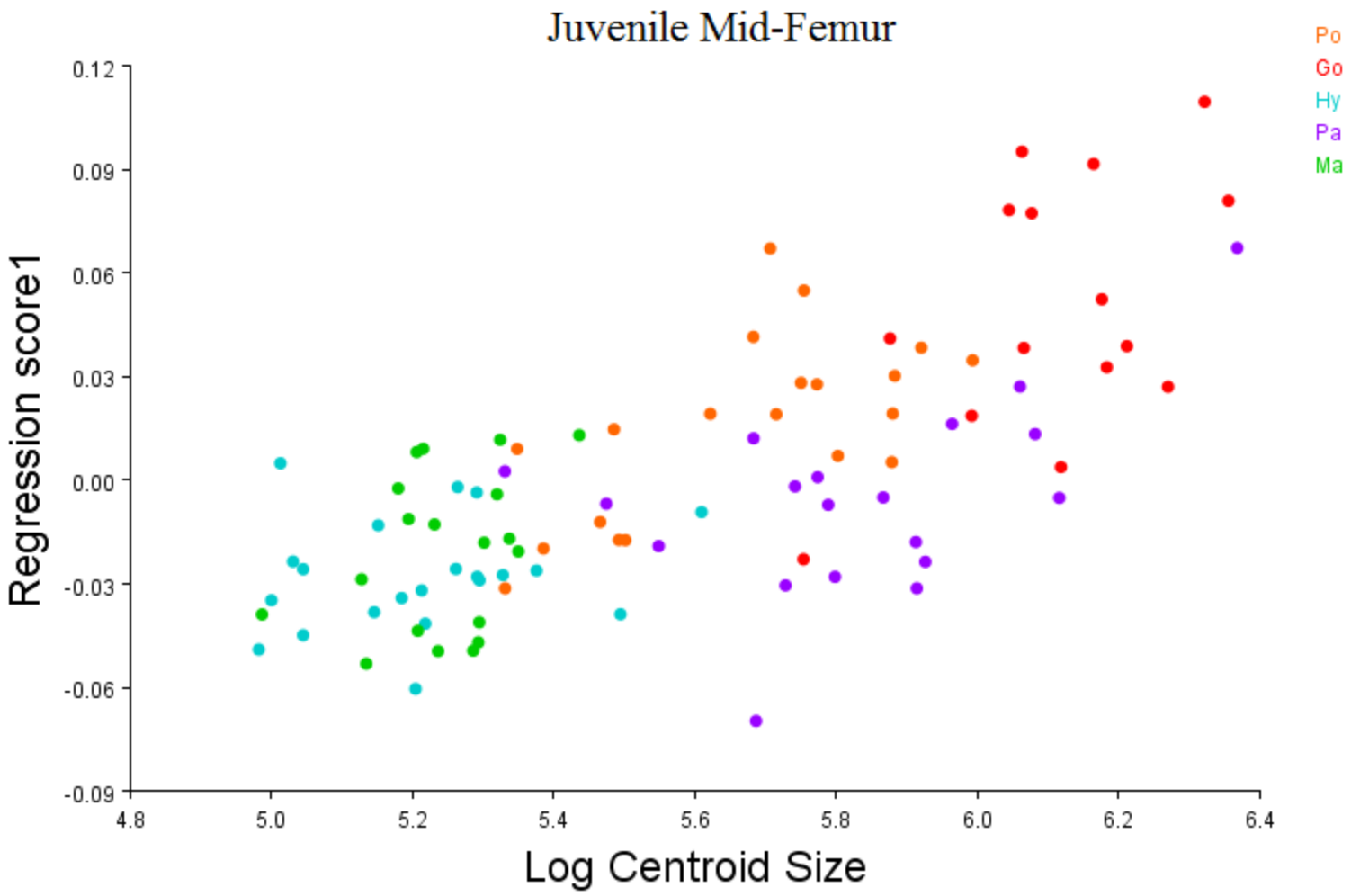

Fig. A5.7b. Log centroid size plotted against shape (procrustes coordinate data) of the pooled juvenile femoral midshaft.

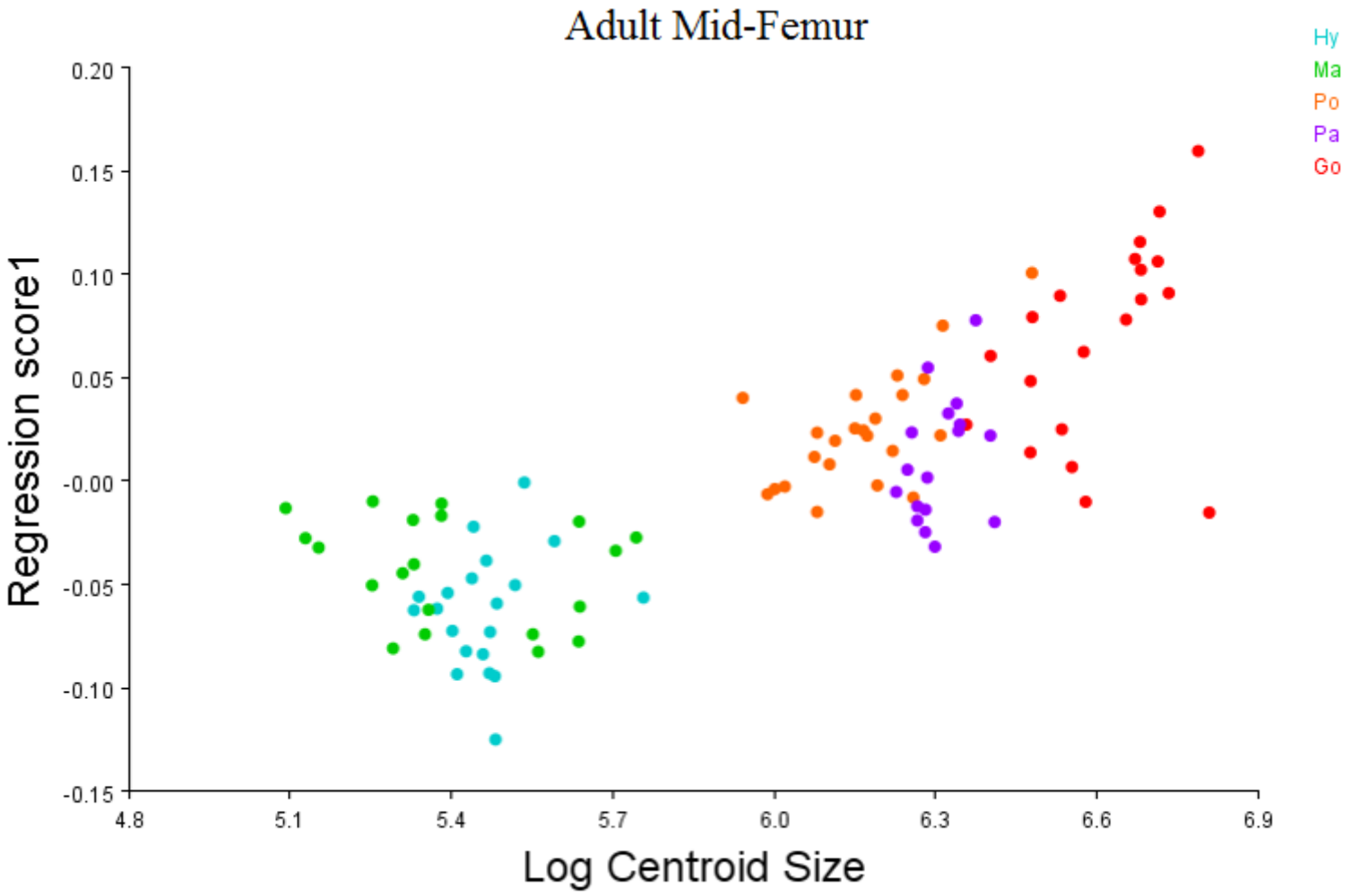

Fig. A5.7c. Log centroid size plotted against shape (procrustes coordinate data) of the pooled adult femoral midshaft.

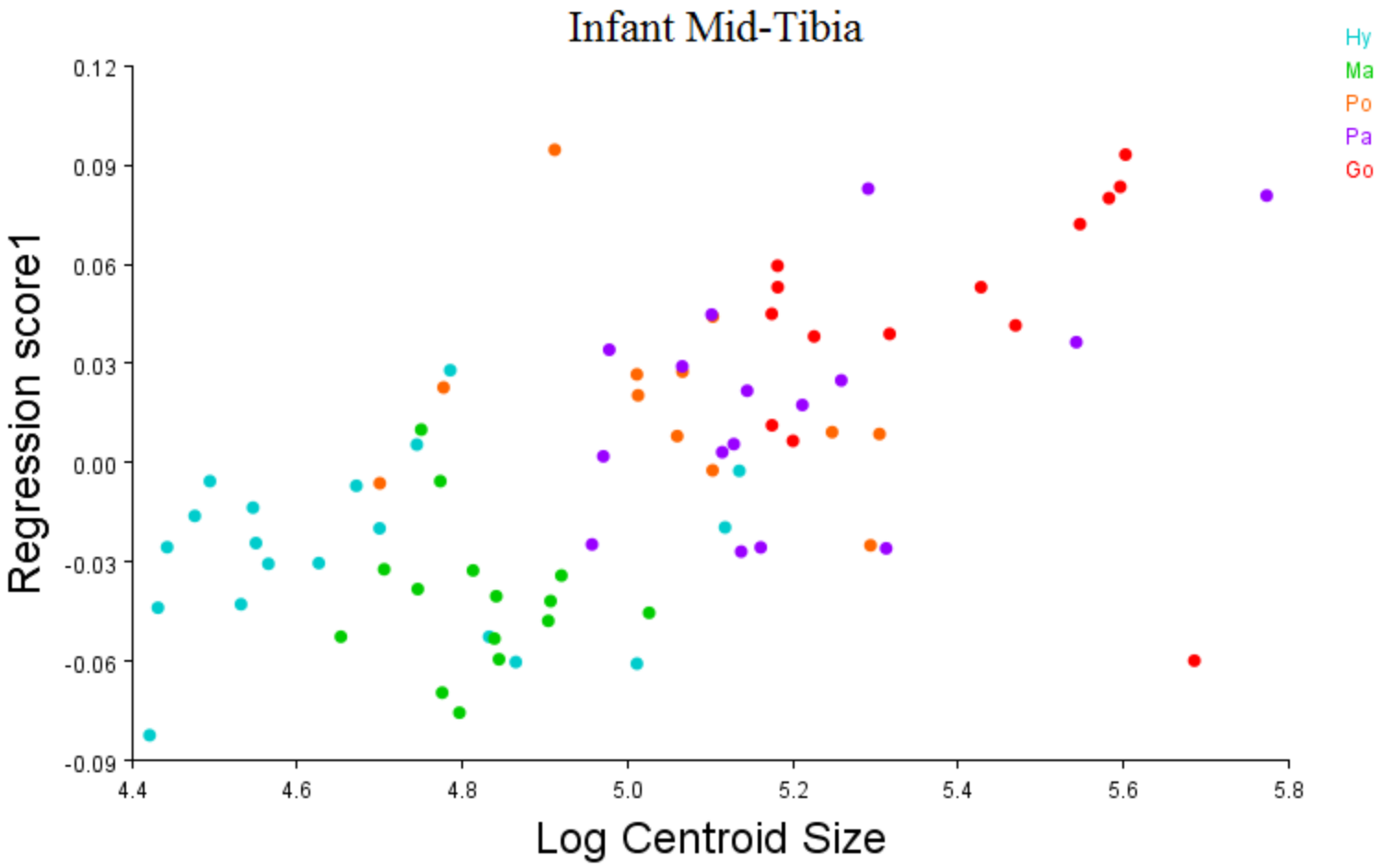

Fig. A5.8a. Log centroid size plotted against shape (procrustes coordinate data) of the pooled infant tibial midshaft.

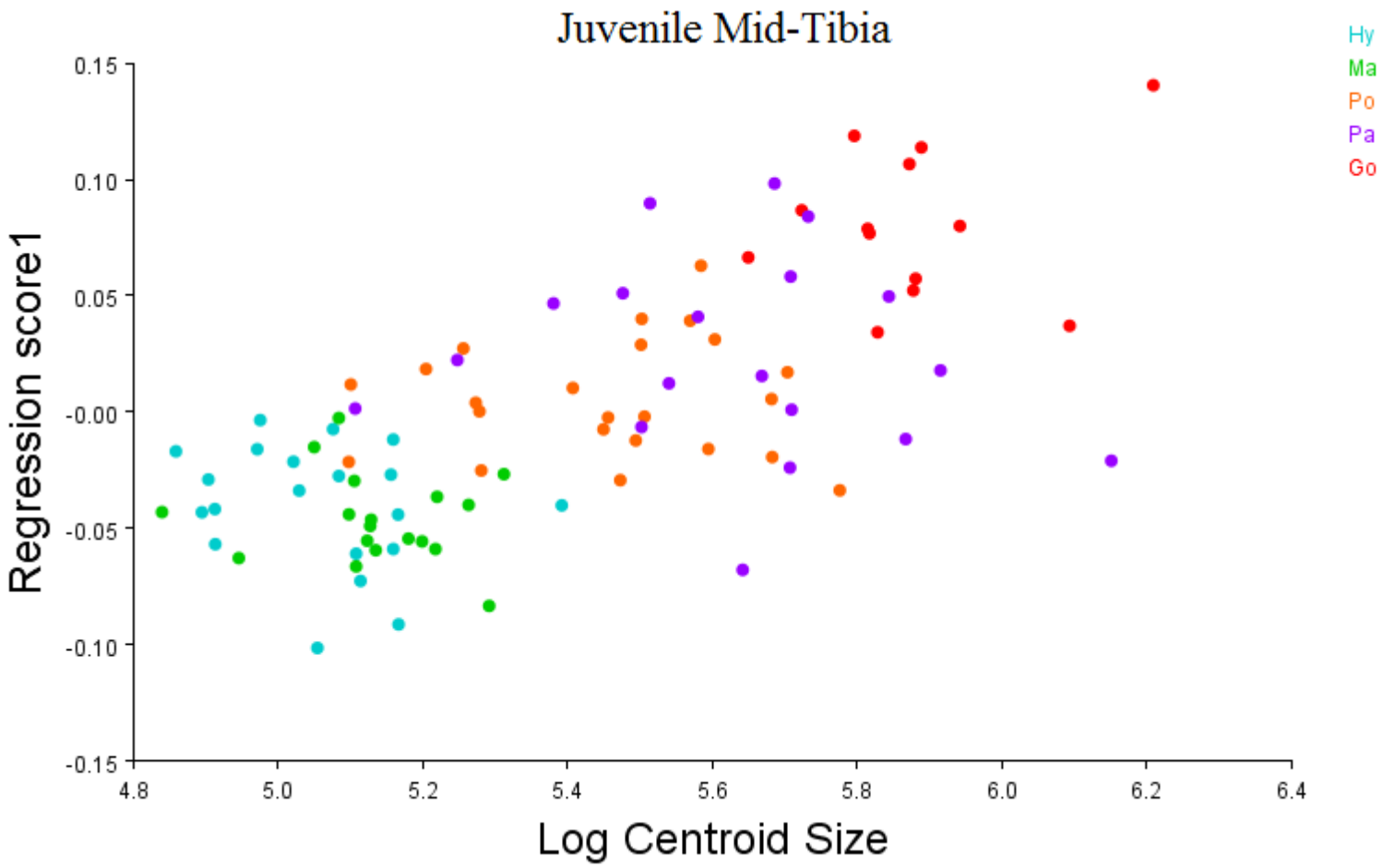

Fig. A5.8b. Log centroid size plotted against shape (procrustes coordinate data) of the pooled juvenile tibial midshaft.

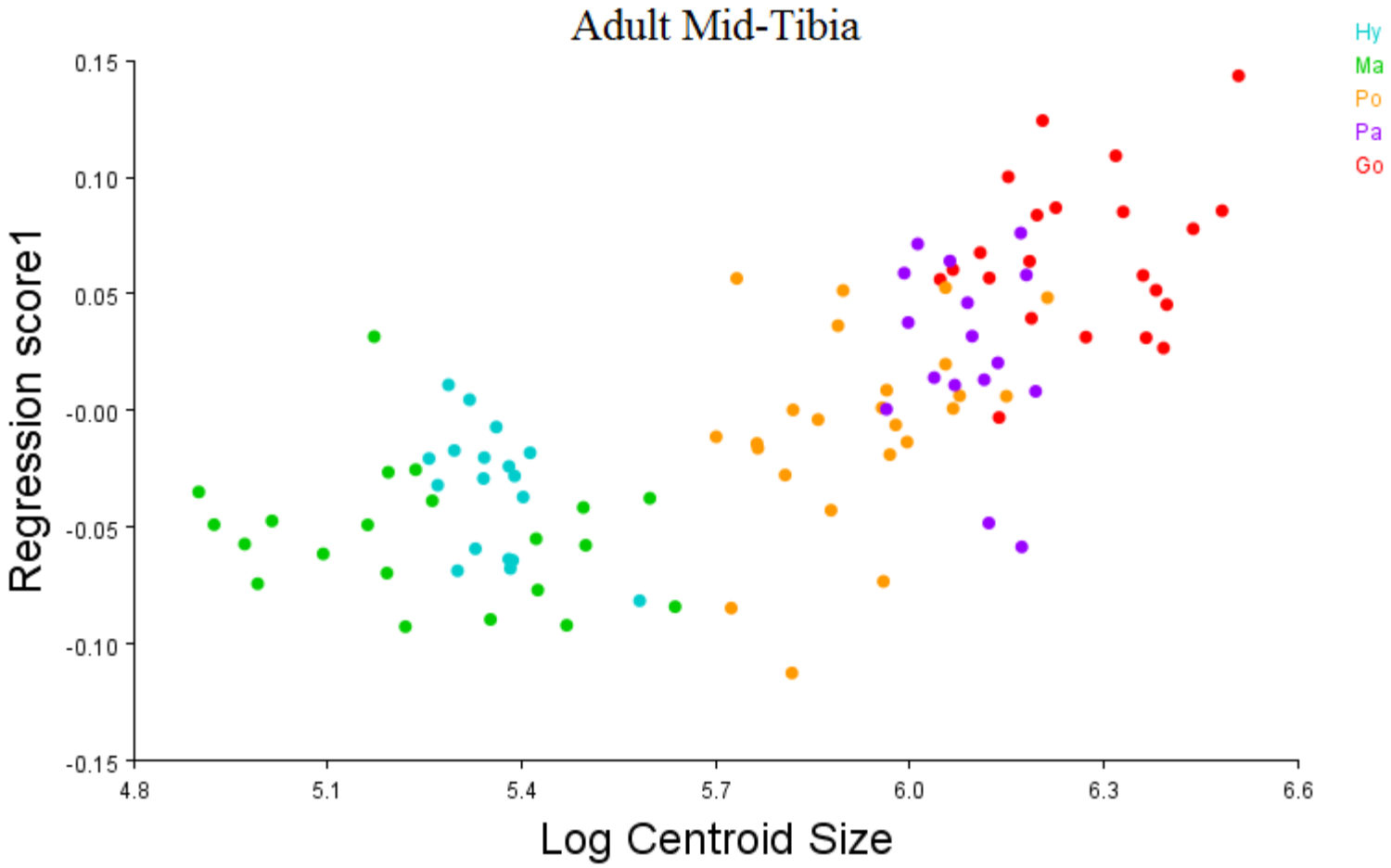

Fig. A5.8c. Log centroid size plotted against shape (procrustes coordinate data) of the pooled adult tibial midshaft.

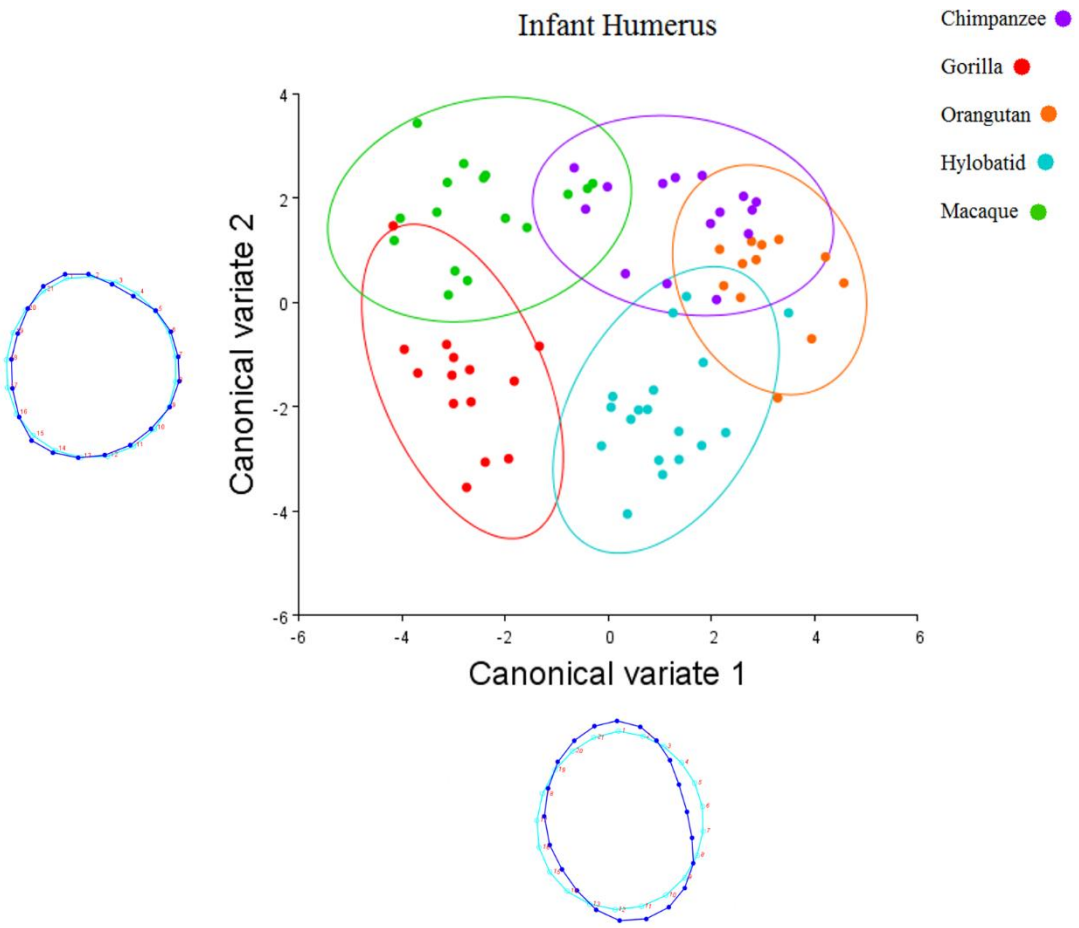

Fig. A5.9a. Scatter plot of infant humeral shape variation of taxonomic group means, plotted onto CV1 and CV2. Wireframes along the axes represent midshaft shape variation; the light blue outlines depict the low ends of their respective axes and the dark blue outlines depict the high ends. Between-group distances and axes are scaled to Mahalanobis distance. Confidence ellipses are drawn at 95% probability.

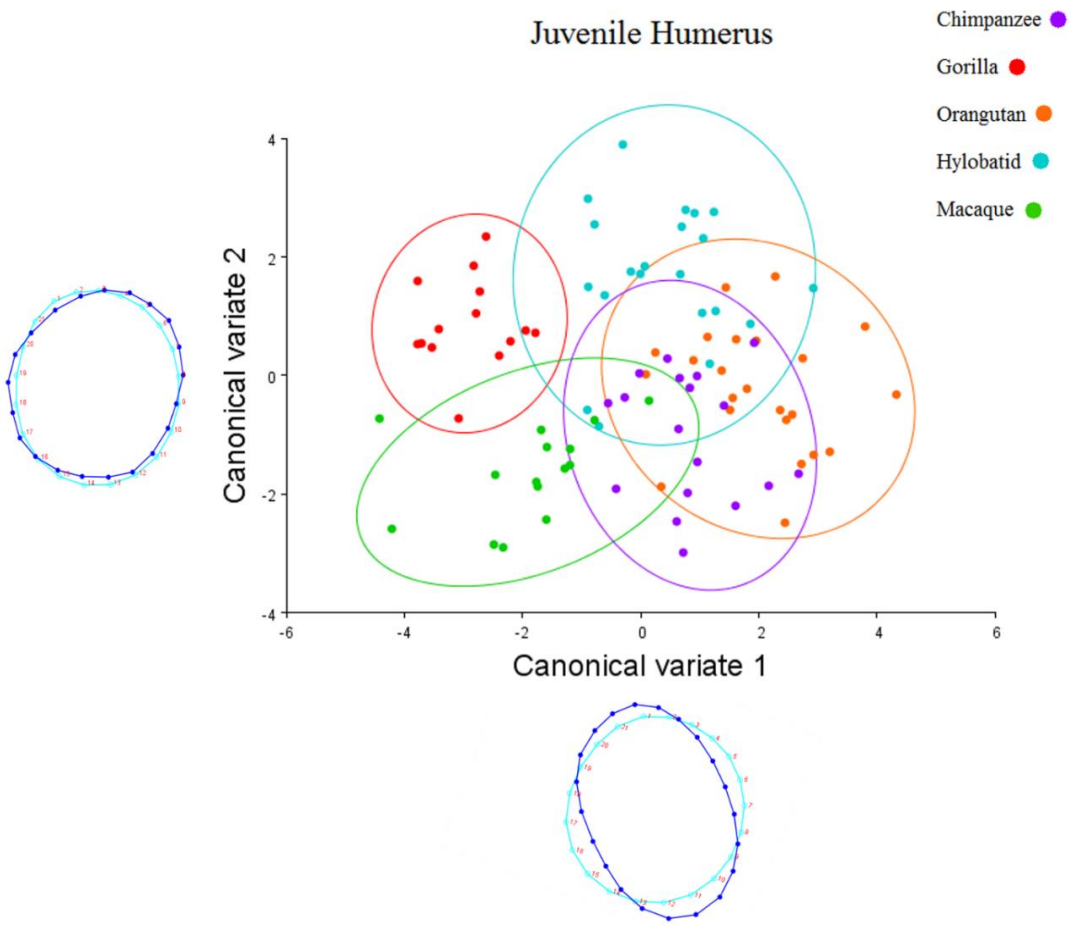

Fig. A5.9b. Scatter plot of juvenile humeral shape variation of taxonomic group means, plotted onto CV1 and CV2. Wireframes along the axes represent midshaft shape variation; the light blue outlines depict the low ends of their respective axes and the dark blue outlines depict the high ends. Between-group distances and axes are scaled to Mahalanobis distance. Confidence ellipses are drawn at 95% probability.

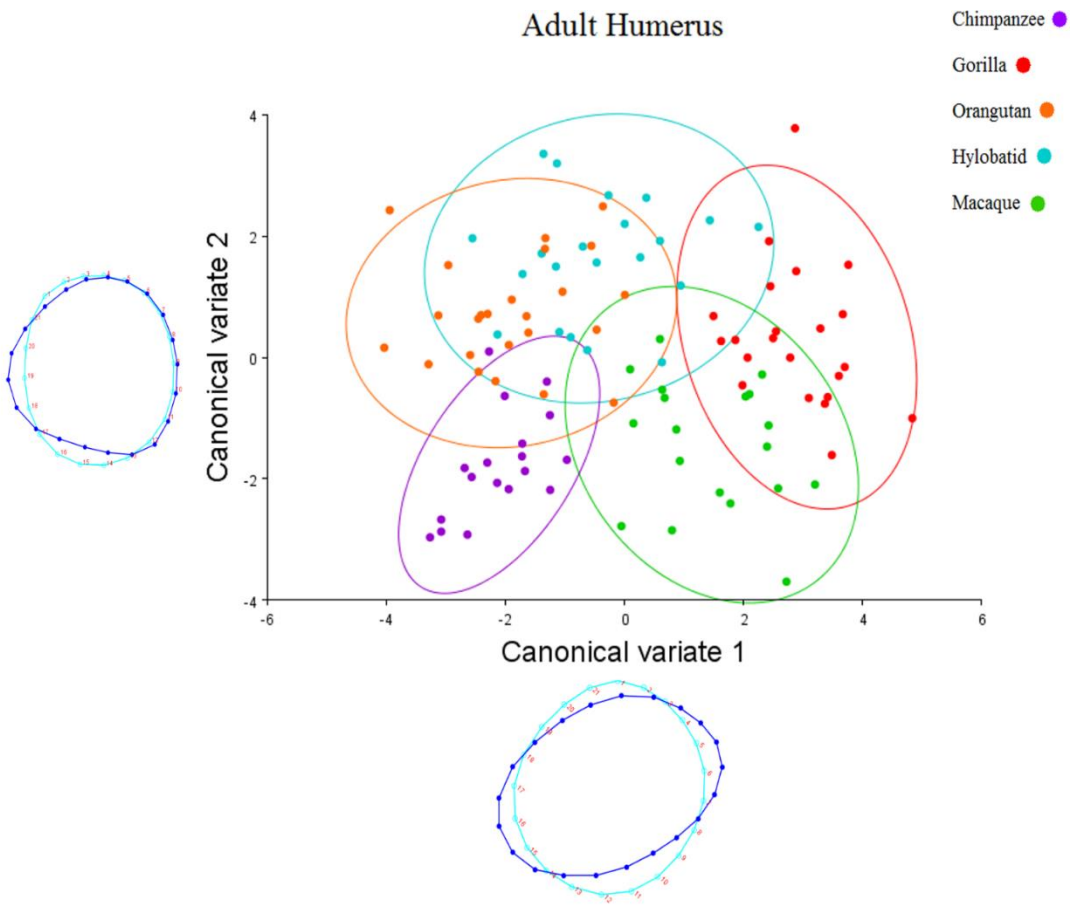

Fig. A5.9c. Scatter plot of adult humeral shape variation of taxonomic group means, plotted onto CV1 and CV2. Wireframes along the axes represent midshaft shape variation; the light blue outlines depict the low ends of their respective axes and the dark blue outlines depict the high ends. Between-group distances and axes are scaled to Mahalanobis distance. Confidence ellipses are drawn at 95% probability.

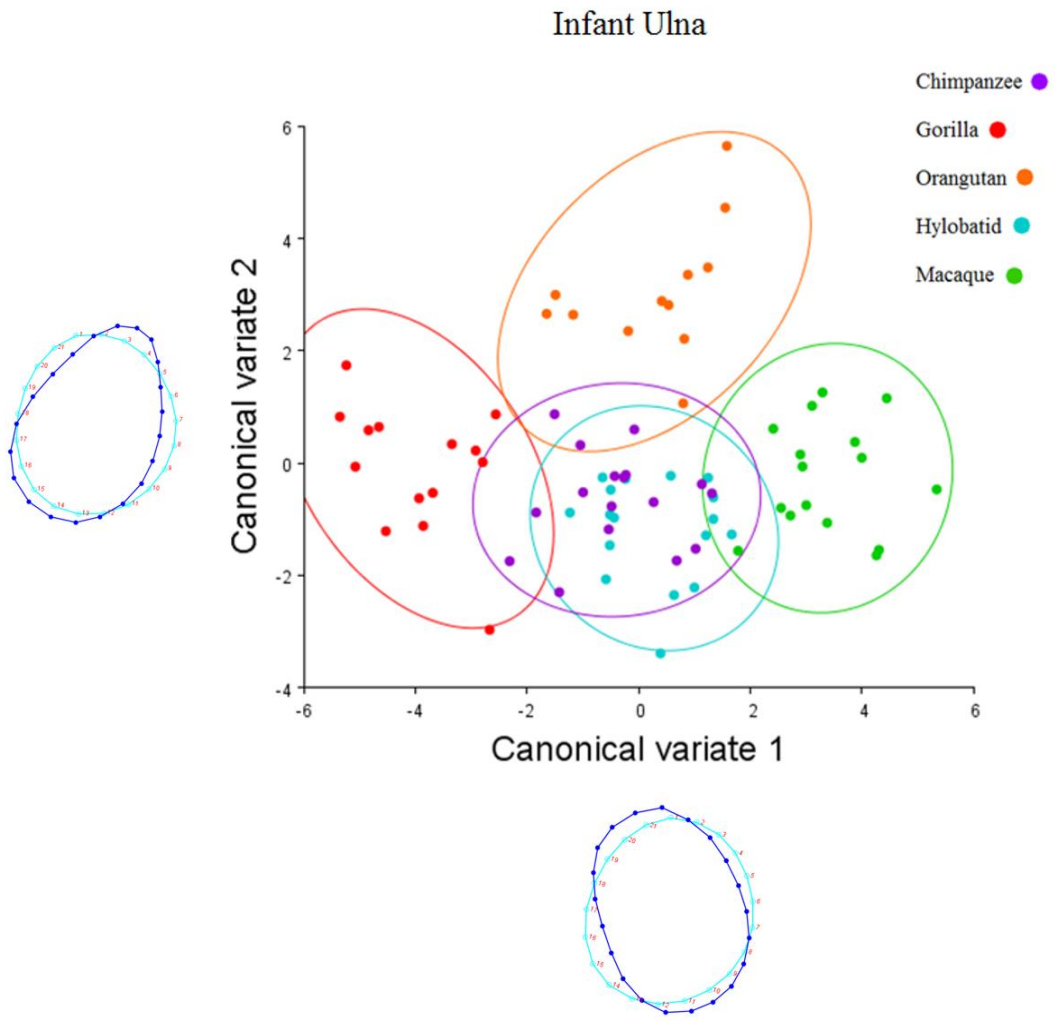

Fig. A5.10a. Scatter plot of infant ulnar shape variation of taxonomic group means, plotted onto CV1 and CV2. Wireframes along the axes represent midshaft shape variation; the light blue outlines depict the low ends of their respective axes and the dark blue outlines depict the high ends. Between-group distances and axes are scaled to Mahalanobis distance. Confidence ellipses are drawn at 95% probability.

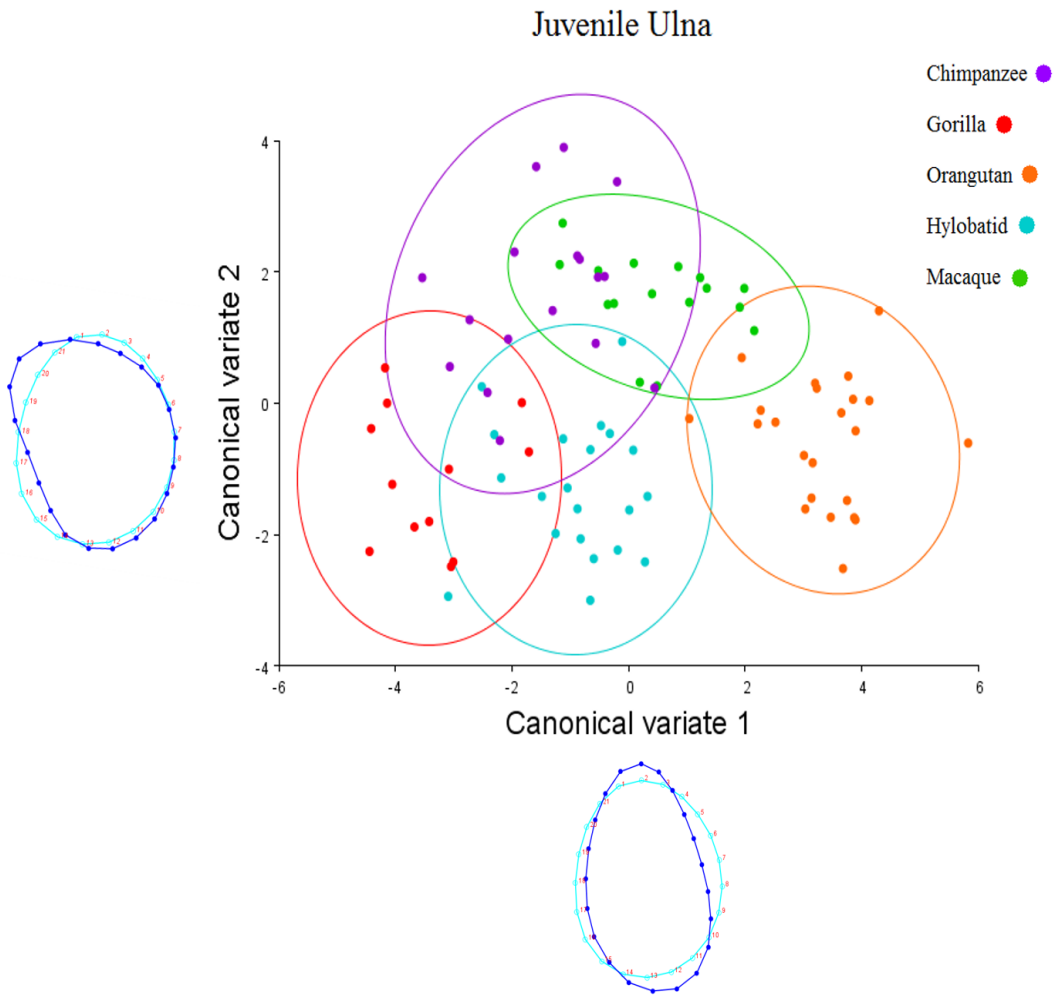

Fig. A5.10b. Scatter plot of juvenile ulnar shape variation of taxonomic group means, plotted onto CV1 and CV2. Wireframes along the axes represent midshaft shape variation; the light blue outlines depict the low ends of their respective axes and the dark blue outlines depict the high ends. Between-group distances and axes are scaled to Mahalanobis distance. Confidence ellipses are drawn at 95% probability.

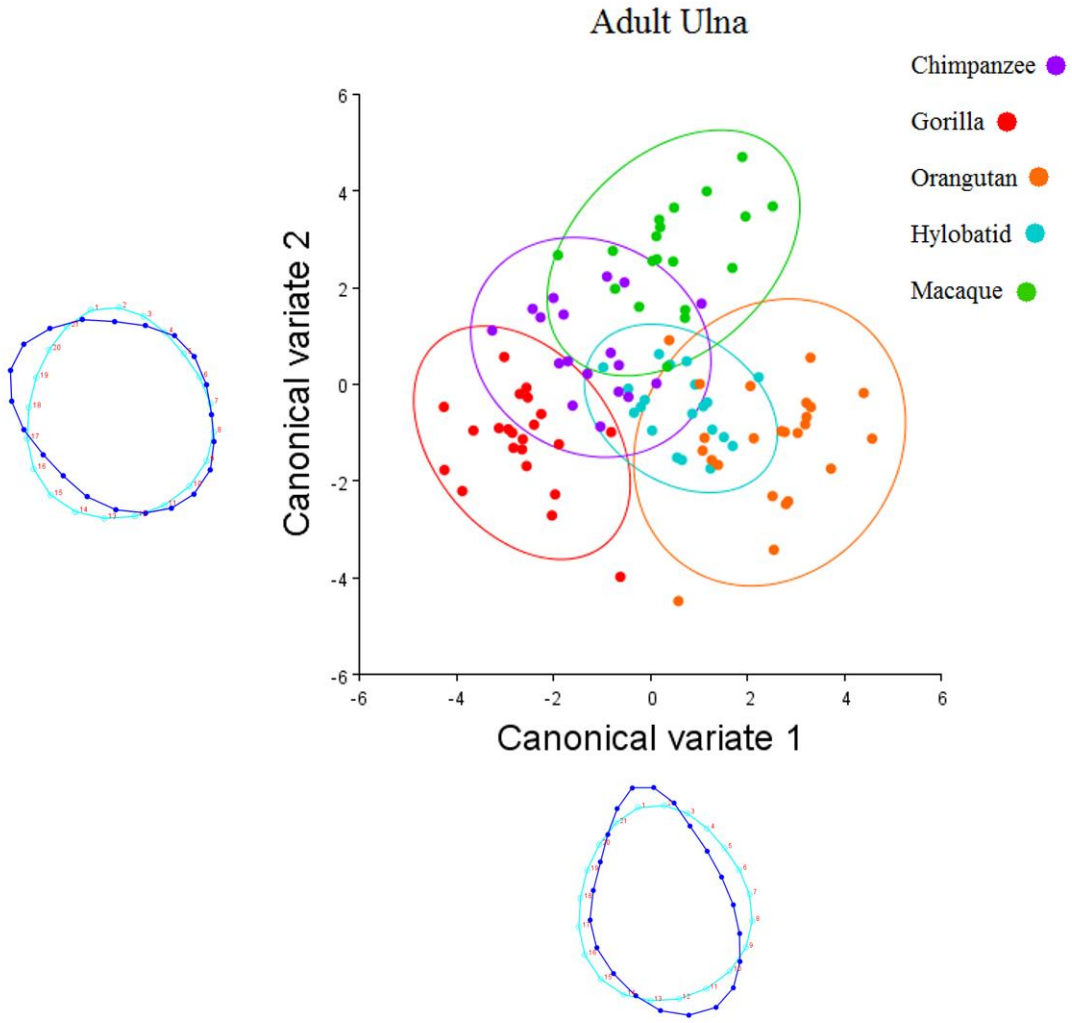

Fig. A5.10c. Scatter plot of adult ulnar shape variation of taxonomic group means, plotted onto CV1 and CV2. Wireframes along the axes represent midshaft shape variation; the light blue outlines depict the low ends of their respective axes and the dark blue outlines depict the high ends. Between-group distances and axes are scaled to Mahalanobis distance. Confidence ellipses are drawn at 95% probability.

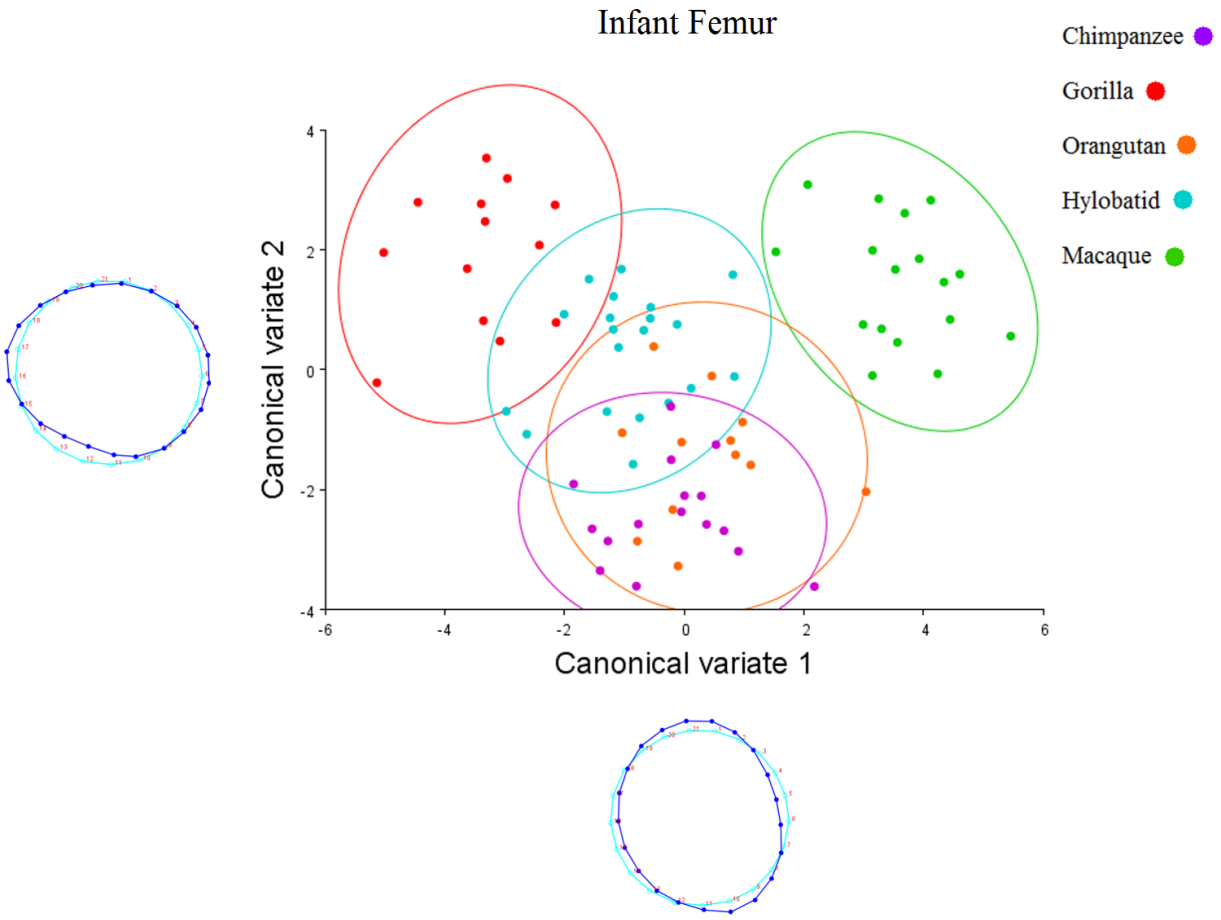

Fig. A5.11a. Scatter plot of infant femoral shape variation of taxonomic group means, plotted onto CV1 and CV2. Wireframes along the axes represent midshaft shape variation; the light blue outlines depict the low ends of their respective axes and the dark blue outlines depict the high ends. Between-group distances and axes are scaled to Mahalanobis distance. Confidence ellipses are drawn at 95% probability.

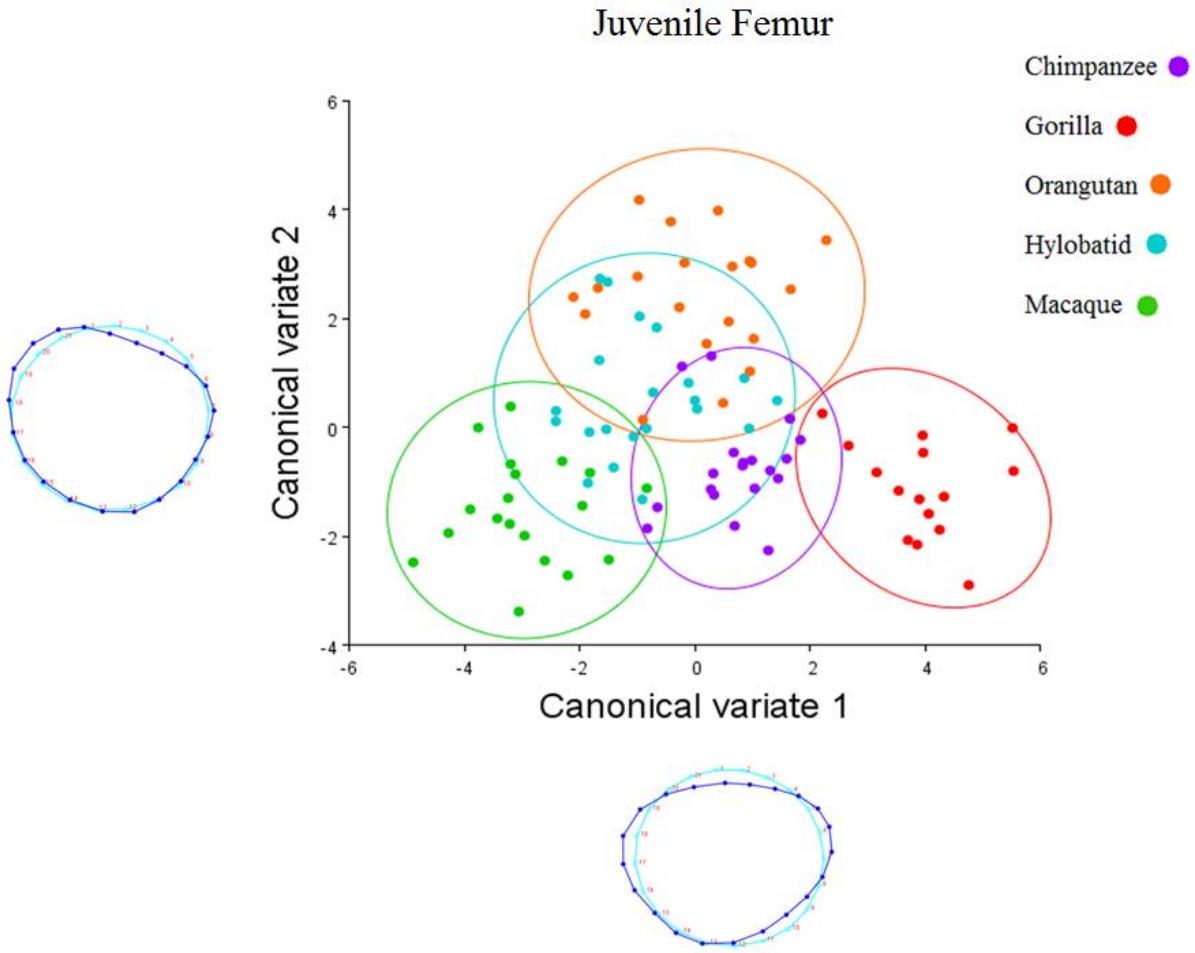

Fig. A5.11b. Scatter plot of juvenile femoral shape variation of taxonomic group means, plotted onto CV1 and CV2. Wireframes along the axes represent midshaft shape variation; the light blue outlines depict the low ends of their respective axes and the dark blue outlines depict the high ends. Between-group distances and axes are scaled to Mahalanobis distance. Confidence ellipses are drawn at 95% probability.

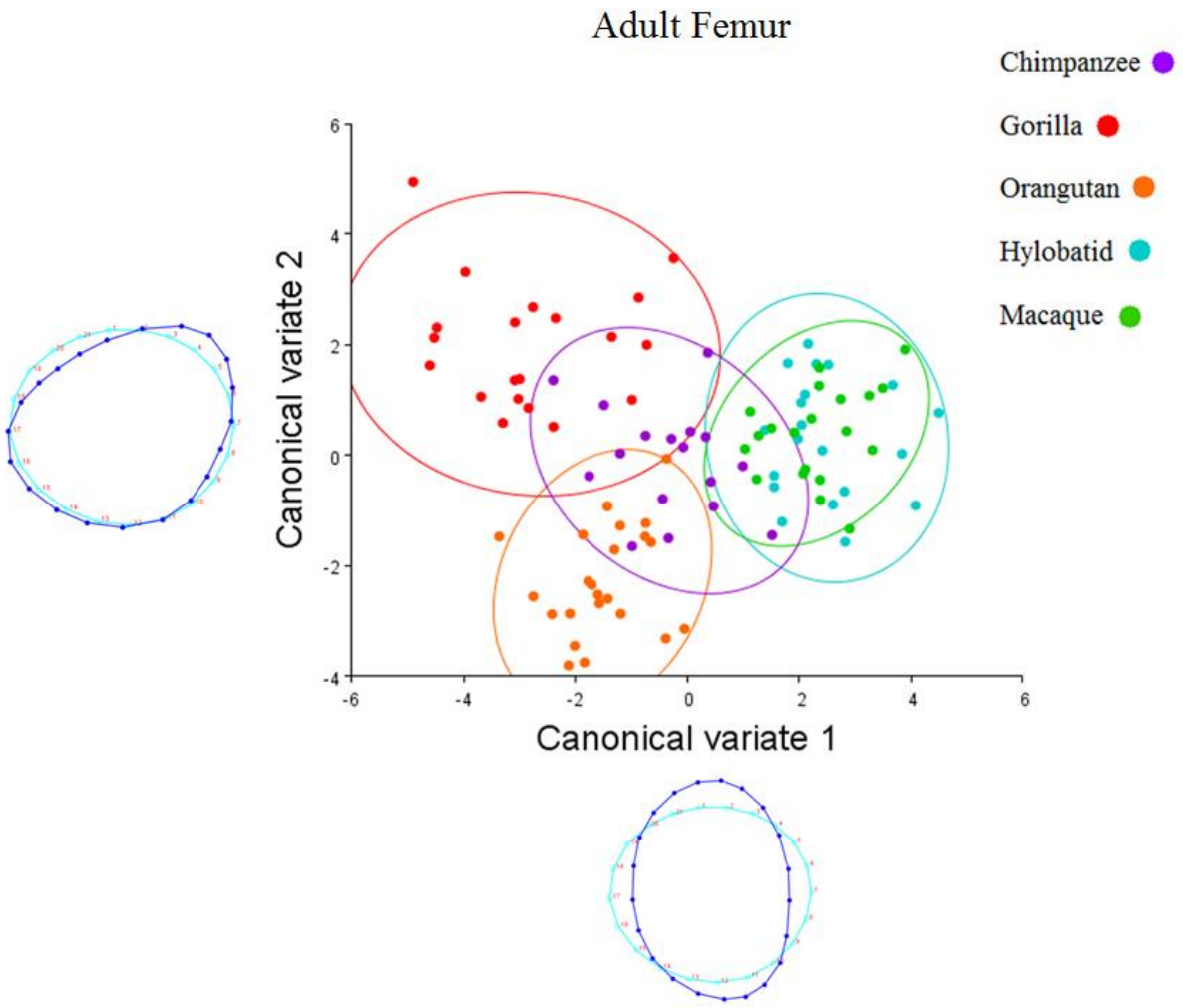

Fig. A5.11c. Scatter plot of adult femoral shape variation of taxonomic group means, plotted onto CV1 and CV2. Wireframes along the axes represent midshaft shape variation; the light blue outlines depict the low ends of their respective axes and the dark blue outlines depict the high ends. Between-group distances and axes are scaled to Mahalanobis distance. Confidence ellipses are drawn at 95% probability.

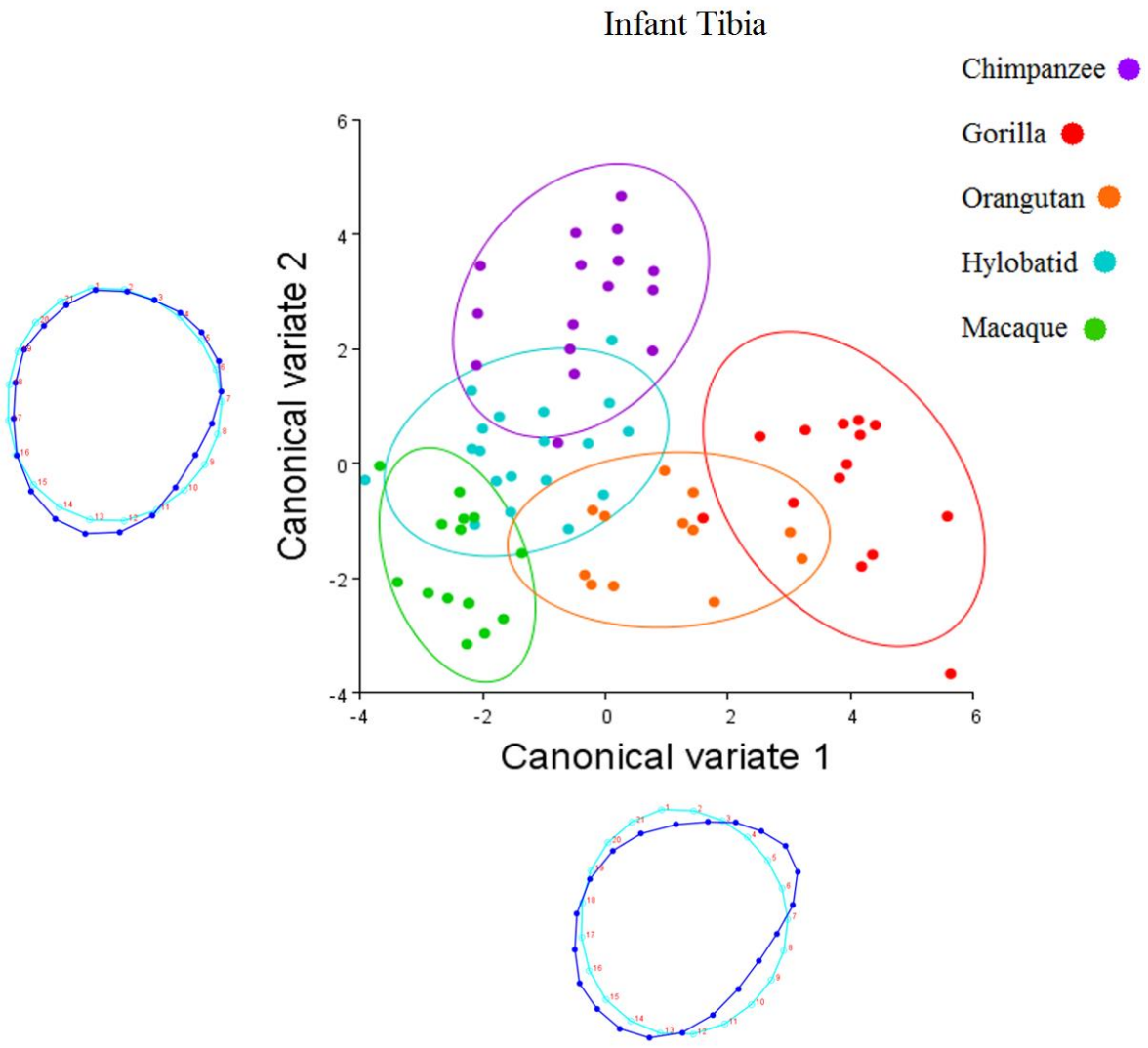

Fig. A5.12a. Scatter plot of infant tibia shape variation of taxonomic group means, plotted onto CV1 and CV2. Wireframes along the axes represent midshaft shape variation; the light blue outlines depict the low ends of their respective axes and the dark blue outlines depict the high ends. Between-group distances and axes are scaled to Mahalanobis distance. Confidence ellipses are drawn at 95% probability.

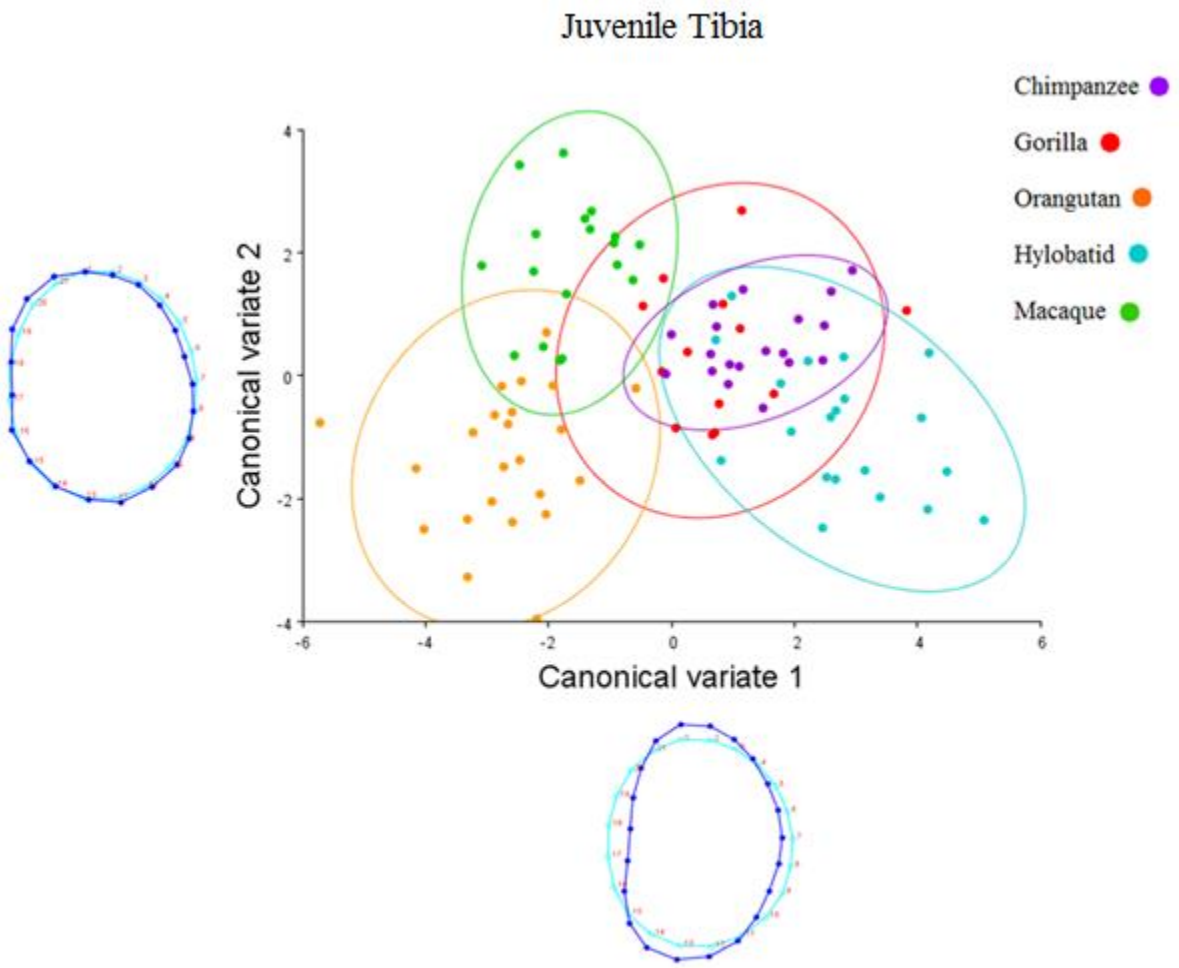

Fig. A5.12b. Scatter plot of juvenile tibia shape variation of taxonomic group means, plotted onto CV1 and CV2. Wireframes along the axes represent midshaft shape variation; the light blue outlines depict the low ends of their respective axes and the dark blue outlines depict the high ends. Between-group distances and axes are scaled to Mahalanobis distance. Confidence ellipses are drawn at 95% probability.

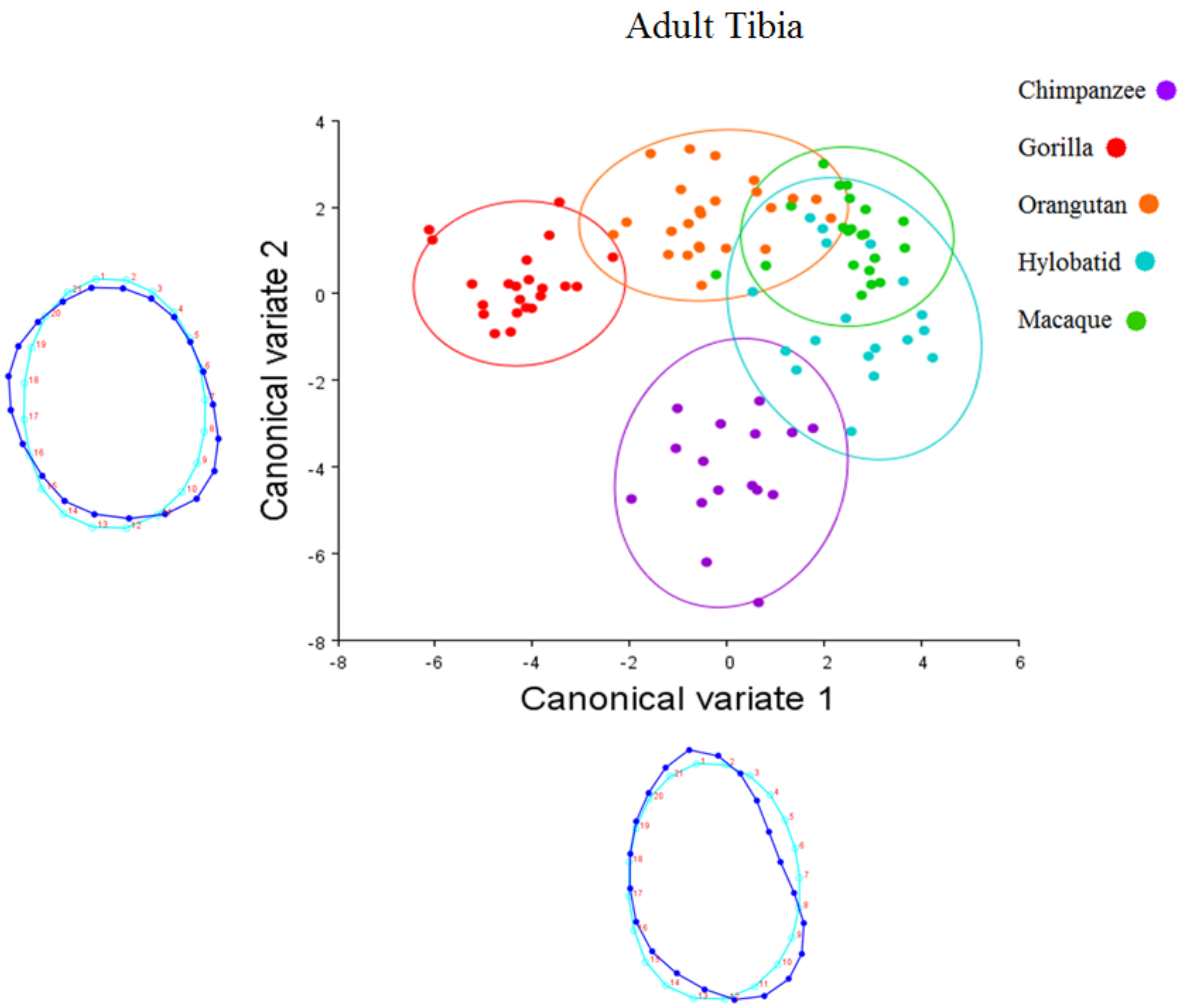

Fig. A5.12c. Scatter plot of adult tibia shape variation of taxonomic group means, plotted onto CV1 and CV2. Wireframes along the axes represent midshaft shape variation; the light blue outlines depict the low ends of their respective axes and the dark blue outlines depict the high ends. Between-group distances and axes are scaled to Mahalanobis distance. Confidence ellipses are drawn at 95% probability.

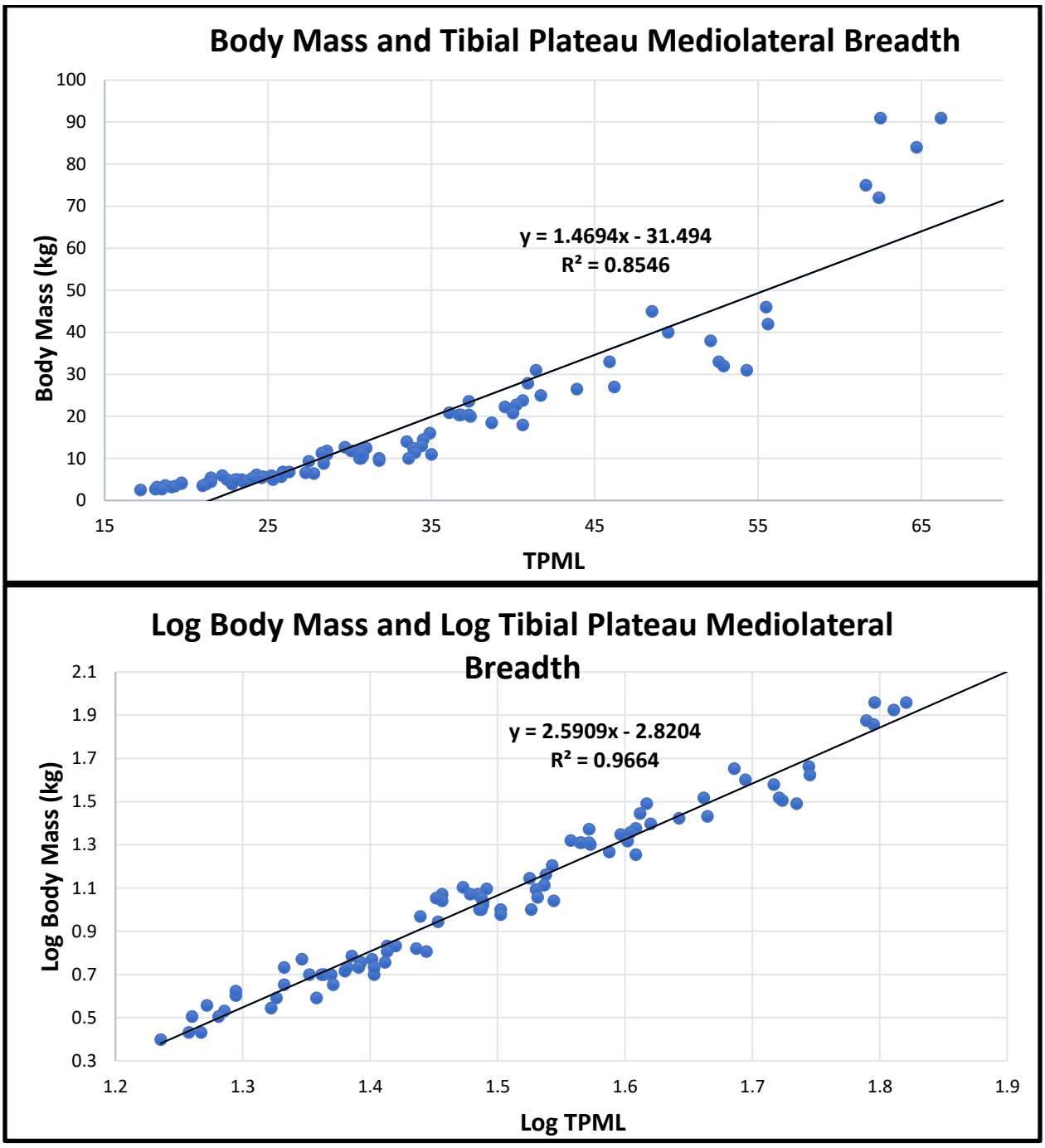

Fig. A6.1. Body mass estimation equation of tibial plateau mediolateral breadth (TPML) applied to a mixed sample of primate taxa with known body masses from Ruff (2003b) and this study. The top regression gives the raw values of body mass and TPML while the bottom graph gives the natural log-transformed (ln) values to fit the curve.

Bibliography

Adami S, Gatti D, Braga V, Bianchini D, Rossini M. 1999. Site-specific effects of strength training on bone structure and geometry of ultradistal radius in postmenopausal women. J Bone Miner Res 14:120–124.

van Adrichem GGJ, Utami SS, Wich SA, van Hooff JARAM, Sterck EHM. 2006. The development of wild immature sumatran orangutans (*Pongo abelii*) at Ketambe. Primates 47:300–309.

Aerts P. 1998. Vertical jumping in Galago senegalensis: the quest for a hidden power amplifier. Phil Trans R Soc Lond 353, 1607–1620.

Aiello LC. 1981. The allometry of primate body proportions. Symp. Zool. Soc. Lond. 48:331–358

Alba DM, Moyà-Solà S, Almécija S. 2011. A partial hominoid humerus from the middle miocene of Castell de Barberà (Vallès-Penedès Basin, Catalonia, Spain). Am J Phys Anthropol 144:365–381.

Alexander, R.McN. 1974. The mechanics of jumping by a dog (*Canis familiaris*). J. ZooL, Lond.

Alexander R McN. 1977. Terrestrial locomotion. In: R. M. Alexander and G. Goldspink (eds.) Mechanics and Energetics of Animal Locomotion, pp. 168–203. London: Chapman & Hall.

Alexander R McN., Jayes, AS., Maloiy, GMO. and Wathuta, EM. 1979. Allometry of the limb bones of mammals from shrews (Sorex) to elephant (Loxodonta). J. Zool. (Lond.) 194, 539–552.

Alexander R. McN, Jayes AS, Maloiy GMO, Wathuta EM. 1981. Allometry of the leg muscles of mammals. J. Zool., London 194, 539–552.

Alexander R.M. 1996. Optima for Animals, second ed. Princeton University Press, Princeton.

Alexander RM. 1998. Symmorphosis and safety factors. In: Weibel ER, Taylor CR, Bolis L (eds). Principles of animal design: the optimization and symmorphosis debate. Cambridge: Cambridge University Press. pp. 28–35.

Almécija S, Tallman M, Alba DM, et al. 2013. The femur of Orrorin tugenensis exhibits morphometric affinities with both Miocene apes and later hominins. Nat Comm 4, 2888. Andrews P, Groves CP. 1975. Gibbons And Brachiation. Gibbon and Siamang. 4:167–218.

Anemone RL. 1990. The VCL hypothesis revisited: patterns of femoral morphology among quadrupedal and saltatorial prosimian primates. Am J Phys Anthropol 83:373–393.

Anemone, R.L., Nachman, B.A., 2003. Morphometrics, functional anatomy, and the biomechanics of locomotion among tarsiers. In: Wright, P.C., Simons, E.L., Gursky, S. (eds.), Tarsiers: Past, Present and Future. Rutgers University Press, New Brunswick, pp. 97–120.

Arias-Martorell J, Alba DM, Potau JM, Bello-Hellegouarch G, Pérez-Pérez A. 2015. Morphological affinities of the proximal humerus of *Epipliopithecus vindobonensis* and *Pliopithecus antiquus*: Suspensory inferences based on a 3D geometric morphometrics approach. J Hum Evol 80:83–95.

Arlegi M, Gomez-Olivencia A, Albessard L, Martinez I, Balzeau A, Arsuaga JL, Been E. 2017. The role of allometry and posture in the evolution of the hominin subaxial cervical spine. J Hum Evol 104:80–99.

Asensio N, José-Domínguez JM, Kongrit C, Brockelman WY. 2017. The ecology of white-handed and pileated gibbons in a zone of overlap and hybridization in Thailand. Am J Phys Anthropol:716–728.

Ashton EH, Oxnard CE. 1964. Function adaptations in the primate shoulder girdle. Proc. Zool. Soc. Lond. 142, 49–66.

Auerbach BM, Ruff CB. 2004. Human body mass estimation: a colkmparison of "morphometric" and "mechanical" methods. Am J Phys Anthropol 125:331–342.

Auerbach BM, Gooding AF, Shaw CN, Sylvester AD. 2017. The relative position of the human fibula to the tibia influences cross-sectional properties of the tibia. Am J Phys Anthropol:148–157.

Baab KL. 2008. The taxonomic implications of cranial shape variation in Homo erectus. J Hum Evol 54:827–47.

Baab KL, McNulty KP. 2009. Size, shape, and asymmetry in fossil hominins: the status of the LB1 cranium based on 3D morphometric analyses. J Hum Evol. 57:608–22.

Barak MM, Lieberman DE, Hublin J-J. 2011. A Wolff in sheep's clothing: Trabecular bone adaptation in response to changes in joint loading orientation. Bone 49:1141–1151.

Bartlett TQ. 2007. The Hylobatidae: small apes of Asia. In CJ Campbell, A. Fuentes, K. C. MacKinnon, M. Panger & S. K. Bearder (eds.) Primates in perspective, pp. 274–289. Oxford: Oxford University Press.

Bass S, Pearce G, Bradney M, Hendrich E, Delmas PD, Harding A, Seeman E. 1998. Exercise before puberty may confer resid- ual benefits in bone density in adulthood: studies in active prepubertal and retired female gymnasts. J Bone Miner Res 13:500–507.

Bass SL, Saxon L, Daly RM, Turner CH, and Robling AG, Seeman E, Stuckey S. 2002. The effect of mechanical loading on the size and shape of bone in pre-, peri, and postpubertal girls: a study in tennis players. J Bone Miner Res 17:2274–2280.

Begun DR. 1992. Phyletic diversity and locomotion in primitive European hominids. Am J Phys Anthropol 87:311–340.

Begun DR. 2004a. The three "Cs" of behavioral reconstruction in fossil primates. J Hum Evol. 46:497–505.

Begun DR. 2004b. Enhanced cognitive capacity as a contingent fact of hominid phylogeny. Evol Thought Evol Orig Gt Ape Intell:15–27.

Begun DR. 2007. How to identify (as opposed to define) a homoplasy: examples from fossil and living great apes. J Hum Evol 52:559–72.

Begun DR, Nargolwalla MC, Kordos L. 2012. European Miocene hominids and the origin of the African ape and human clade. Evol Anthropol 21:10–23.

Behringer V, Stevens JMG, Kivell TL, Neufuss J, Boesch C, Hohmann G. 2016. Within arm's reach: Measuring forearm length to assess growth patterns in captive bonobos and chimpanzees. Am J Phys Anthropol 161:37–43.

Berger LR. 1994. Functional Morphology of the Hominoid Shoulder, Past and Present. Volume 1.

Bertram JE, Swartz SM. 1991. The "law of bone transformation": a case of crying Wolff? Biol Rev Camb Philos Soc 66:245–273.

Biewener AA. 1982. Bone Strength In Small Mammals And Bipedal Birds: Do Safety Factors Change With Body Size? J Exp Biol 98:289–301.

Biewener A. 1989. Scaling body support in mammals: limb posture and muscle mechanics. Science 245:45–48.

Biewener AA. 1990. Biomechanics of mammalian terrestrial locomotion. Science 250: I 097–11 03

Biewener AA, Taylor CR. 1986. Bone strain: a determinant of gait and speed? J Exp Biol 123:383–400.

Biewener AA, Bertram JE. 1994. Structural response of growing bone to exercise and disuse. J Appl Physiol 76:946–955.

Birkbeck DP, Failla JM, Hoshaw SJ, Fyhrie DP, Schaffler M. 1997. The interosseous membrane affects load distribution in the forearm. J Hand Surg Am 22:975–980.

Bishop LC, Plummer TW, Hertel F, Kovarovic K. 2011. Paleoenvironments of Laetoli , Tanzania as Determined by Antelope Habitat Preferences. In: TH (ed.) Paleontology and Geology of Laetoli: Human Evolution in Context. Vol. 1. Dordrecht, Heidelberg, London, New York: Springer Science+Business Media. p 355–366.

Boesch C, & Boesch-Achermann H. 2000. The Chimpanzees of the Taï Forest: Behavioural Ecology and Evolution (Vol. 321). Oxford: Oxford University Press.

Bogin B, Rios L. 2003. Rapid morphological change in living humans: implications for modern human origins. Comp Biochem Physiol A Mol Integr Physiol 136:71–84.

Bookstein FL. 1989. Principal Warps: Thin-Plates Splines and the decompostion of deformations. IEEE Trans Pattern Anal Mach Intell 11:567–585.

Bookstein FL. 1991. Morphometric Tools for Landmark Data: Geometry and Biology. Cambridge University Press.

Bookstein FL. 1997. Landmark methods for forms without landmarks: morphometrics of group differences in outline shape. Med Image Anal 1:225–243.

Boyer DM, Yapuncich GS, Butler JE, Dunn RH, Seiffert ER. 2015. Evolution of postural diversity in primates as reflected by the size and shape of the medial tibial facet of the talus. Am J Phys Anthropol 157:134–177.

Breuer T, Breuer-Ndoundou Hockemba M, Olejniczak C, Parnell RJ, Stokes EJ. 2009. Physical maturation, life-history classes and age estimates of free-ranging western gorillas — insights from Mbeli Bai, Republic of Congo. Am J Primatol 71:106–119

Buck LT, Stock JT, Foley RA. 2010. Levels of Intraspecific Variation Within the Catarrhine Skeleton. Int J Primatol 31:779–795.

Burdi AR, Silvey RG. 1969. The relation of sex-associated facial profile reversal and stages of human palatal closure. *Teratology*, *2*(4), 297–303.

Burdi AR. 1969. Cephalometric growth analyses of the human upper face region during the last two trimesters of gestation. *Developmental Dynamics*, *125*(1), 113–122.

Burgess ML, Schmitt D, Zeininger A, McFarlin SC, Zihlman AL, Polk JD, Ruff CB. 2016. Ontogenetic scaling of fore limb and hind limb joint posture and limb bone cross-sectional geometry in vervets and baboons. Am J Phys Anthropol.

Burns BL, Judge DS. 2016. The varied path to adulthood: Plasticity in developmental timing in hylobatids. Am J Primatol 78:610–625.

Burr DB. 1997. Muscle Strength, Bone Mass, and Age • Related Bone Loss. J Bone Miner Res. 12:1547–1551.

Burr DB, Ruff CB, Johnson C. 1989. Structural Adaptations of the Femur and Humerus to Arboreal and Terrestrial Environments in Three Species of Macaque. Am J Phys Anthropol 367:357–367.

Calow LJ, RM Alexander. 1973. A mechanical analysis of a hing leg of a frog (*Rana temporaria*). J. Zool., London 171:293-321.

Cameron N, Bogin B, Bolter D, Berger LR. 2017. The postcranial skeletal maturation of Australopithecus sediba. Am J Phys Anthropol. 1–8.

Cannington SL, Sylvester AD, Burgess ML, Ruff CB. 2017. Long bone cross-sectional diaphyseal shape follows different ontogenetic trajectories in captive and wild gorillas. Conference paper, American Association of Physical Anthropologists, April 2017.

Cannon CH, Leighton M. 1994. Comparative locomotor ecology of gibbons and macaques: selection of canopy elements for crossing gaps. Am J Phys Anthropol 93:505–524.

Cant JGH. 1987. Effects of sexual dimorphism in body size on feeding postural behavior of Sumatran orangutans (Pongo pygmaeus). Am J Phys Anthropol 74:143–148.

Cant JG. 1988. Positional behavior of long-tailed macaques (Macaca fascicularis) in northern Sumatra. Am J Phys Anthropol 76:29–37.

Cant JGH. 1992. Positional behavior and body size of arboreal pri- mates: a theoretical framework for field studies and an illustra- tion of its application. AmJ Phys Anthropol 88:273–283.

Carrier D, Leon LR. 1990. Skeletal growth and function in the California gull (Larus californicus). J. Zool. 222, 375–389.

Cardini A, Elton S. 2007. Sample size and sampling error in geometric morphometric studies of size and shape. Zoomorphology 126:121–134.

Cardini A, Elton S. 2008a. Variation in guenon skulls (I): species divergence, ecological and genetic differences. J Hum Evol 54:615–37.

Cardini A, Elton S. 2008b. Variation in guenon skulls (II): sexual dimorphism. Journal of Human Evolution, 54, 638–647.

Cardini A, Elton S. 2009. Geographical and taxonomic influences on cranial variation in red colobus monkeys (Primates, Colobinae): introducing a new approach to “morph” monkeys. Glob Ecol Biogeogr 18:248–263.

Carlson KJ. 2002. Shape and material properties of African pongid femora and humeri: their relationship to observed positional behaviors. Ph.D. dissertation, Indiana University, Bloomington.

Carlson KJ. 2005. Investigating the form-function interface in African apes: Relationships between principal moments of area and positional behaviors in femoral and humeral diaphyses. Am J Phys Anthropol 127:312–34.

Carlson KJ, Demes B, Franz TM. 2005. Mediolateral forces associated with quadrupedal gaits of lemurids. J Zool 266:261–273.

Carlson KJ, Judex S. 2007. Increased non-linear locomotion alters diaphyseal bone shape. J Exp Biol 210:3117–3125.

Carpenter CR. 1964. A field study in Siam of the behavior and social relations of the gibbon (*Hylobates lar*). In: Carpenter CR. (ed.) Naturalistic Behavior of Nonhuman Primates. The Pennsylvania State University Press, University Park, pp. 145-271.

Carr, S. 2005. Allometric Coefficient Text Material. https://www.mun.ca/biology/scarr/Allomteric_Equation.html

Cartmill M. 1985. Climbing. In M Hildebrand, DM Bramble, KF Liem, DB Wake (eds.) Functional Vertebrate Morphology, pp. 73–88.

Carter DR, Beaupré GS, 2007. Skeletal function and form: mechanobiology of skeletal development, aging, and regeneration. Cambridge University Press.

Chan LK. 2007. Scapular position in primates. Folia Primatol 78:19–35.

Chan LK. 2008. The range of passive arm circumduction in primates: do hominoids really have more mobile shoulders? Am J Phys Anthropol 136, 265–277.

Channon AJ, Cunther MM, Crompton RH, et al. 2009. Mechanical constraints on the functional morphology of the gibbon hind limb. J Anat 215, 383–400.

Channon AJ, Crompton RH, Günther MM, D'Août K, Vereecke EE. 2010a. The biomechanics of leaping in gibbons. Am J Phys Anthropol 143:403–416.

Channon AJ, Crompton RH, Günther MM, Vereecke EE. 2010b. Muscle moment arms of the gibbon hind limb: Implications for hylobatid locomotion. J Anat 216:446–462.

Chappell J, Phillips AC, Van Noordwijk MA, Setia TM, Thorpe SKS. 2015. The ontogeny of gap crossing behaviour in bornean orangutans (*Pongo pygmaeus wurmbii*). PLoS One 10:1–15.

Charnov EL, Berrigan D. 1993. Why do female primates have such long lifespans and so few babies? or life in the slow lane. Evol. Anthropol. 1, 191–194.

Chatani K. 2003. Positional behavior of free-ranging Japanese macaques (*Macaca fuscata*). Primates 44:13–23.

Chatterjee HJ. 2006. Phylogeny and biogeography of gibbons: A dispersal-vicariance analysis. International Journal of Primatology. 27, 699–712.

Chatterjee HJ, Ho SY, Barnes I, Groves C. 2009. Estimating the phylogeny and divergence times of primates using a supermatrix approach. BMC Evol Biol 9:259.

Chirchir H, Kivell TL, Ruff CB, Hublin, J-J, Carlson KJ, Zipfel B, Richmond BG. 2015. Recent origin of low trabecular bone density in modern humans. Proceedings of the National Academy of Sciences of the United States of America, 112, 366–371.

Cheng EJ, Scott SH. 2000. Morphometry of Macaca mulatta forelimb. I. Shoulder and elbow muscles and segment inertial parameters. J Morphol 245:206–224.

Cheverud JM. 1981. Epiphyseal union and dental eruption in *Macaca mulatta*. Am J. Phys. Anthropol. 56(2):157–167.

Cheverud JM. 1982. Phenotypic, genetic, and environmental morphological integration in the cranium. Evolution 47:1138– 1151.

Ciani A. 1986. Intertroop agonistic behavior of a feral rhesus macaque troop ranging in town and forest areas in India. Aggress Behav 12:433–439.

Clutton-Brock TH, Harvey P. 1977. Primate ecology and social organization. J. Zool., Lond. 183(1):1-39.

Clutton-Brock TH, Harvey PH. 1980. Primates, brains and ecology. J Zool Lond 190:309–323.

Cobb SN, O'Higgins P. 2004. Hominins do not share a common postnatal facial ontogenetic shape trajectory. J Exp Zool Part B, Mol Dev Evol 302:302–321.

Cobb SN, O'Higgins P. 2007. The ontogeny of sexual dimorphism in the facial skeleton of the African apes. J Hum Evol 53:176–90.

Cock AG. 1966. Genetical aspects of metrical growth and form in animals. Q Rev Biol 41:131–190.

Collis A, Harding J, Bricknell S. 1999. Gibbon research: the study of wild populations. Australas Primatol 13, 2–10.

Connour JR, Glander K, Vincent F. 2000. Postcranial adaptations for leaping in primates. J. Zool., 79–103.

Cowgill LW, Warrener A, Pontzer H, Ocobock C. 2010. Waddling and toddling: the biomechanical effects of an immature gait. Am J Phys Anthropol 143:52–61.

Crompton RH, Li Y, Alexander RM, et al. 1996. Segment inertial properties of primates: new techniques for laboratory and field studies of locomotion. Am J Phys Anthropol 99, 547–570.

Crompton RH, Sellers WI. 2007. A consideration of leaping locomotion as a means of predator avoidance in prosimian primates.In: Gursky S, Nekaris K (eds.). Primate anti-predator strategies. Berlin: Springer. pp. 127–145.

Crompton RH, Vereecke EE, Thorpe SKS. 2008. Locomotion and posture from the common hominoid ancestor to fully modern hominins, with special reference to the last common panin/hominin ancestor. J Anat 212:501–43.

Crompton RH, Blanchard ML, Coward S, Alexander RM, Thorpe SK. 2010. Vertical clinging and leaping revisited: locomotion and habitat use in the western tarsier, *Tarsius bancanus* explored via loglinear modeling. Int J Primatol 31:958–979.

Cunha E, Umbelino C. 1995. What can bones tell about labour and occupation: the analysis of skeletal markers of occupational stress in the identified skeletal collection of the Anthropological Museum of the University of Coimbra (preliminary results). Antropol Portuguesa 13:49–68.

Currey J. 1984. The Mechanical Adaptations of Bones. Princeton: Princeton University Press.

Currey JD. 2002. Bones: Structure and Mechanics. Princeton Univ Press, Princeton. pp. 28-79.

Currey JD, Alexander RM. 1985. The thickness of the walls of tubular bones. J Zool Lond A 206:453–468.

Daegling DJ. 2002. Estimation of torsional rigidity in primate long bones. J Hum Evol 43:229–239.

Dagosto M. 1986. The joints of the tarsus in the strepsirrhine primates: functional, adaptive, and evolutionary implications. Ph.D. thesis. City University of New York.

Dagosto M, Terranova C. 1992. Estimating the body size of Eocene primates: a comparison of results from dental and postcranial variables. Int J Primatol 13:307–344

Daly RM, Saxon L, Turner CH, Robling AG, Bass SL. 2004. The relationship between muscle size and bone geometry during growth and in response to exercise. Bone 34:281–287.

Damuth J., MacFadden BJ. 1990. Body Size in Mammalian Paleobiology. In: Damuth, John., MacFadden BJ, editor. Body Size in Mammalian Paleobiology. Cambridge: Cambridge University Press. p 1–10.

Davies TG, Shaw CN, Stock JT. 2012. A test of a new method and software for the rapid estimation of cross-sectional geometric properties of long bone diaphyses from 3D laser surface scans. Archaeol Anthropol Sci 4:277–290.

de Beer GR. 1958. Embryos and Ancestors, third ed. Oxford University Press, Oxford.

Debat V, Alibert P, David P, Paradis E, Auffray J-C. 2000. Independence between developmental stability and canalization in the skull of the house mouse. Proc R Soc B Biol Sci 267:423–430.

Dellanini L, Hawkins D, Martin RB, Stover S. 2003. An investigation of the interactions between lower-limb bone morphology, limb inertial properties and limb dynamics. J Biomech 36:913–919.

Delson E, Terranova CJ, Jungers WL, Sargis EJ, Jablonski NG. 2000. Body Mass In Cercopithecidae (Primates, Mammalia): Estimation and Scaling in Extinct and Extant Taxa. New York: American Museum of Natural History, Anthropological Papers, Number 83.

Demes B, Jungers WL. 1993. Long-bone cross-sectional dimensions, locomotor adaptations and body-size in prosimian primates. J. Hum. Evol. 25, 57–74.

Demes B, Jungers W, Nieschalk U, Stack M., Niemetz C. 1990. Size- and speed- related aspects of quadrupedal walking in slender and slow lorises. In: Jouffroy F (ed.) Gravity, Posture and Locomotion in Primates. Il Sedicesimo, Firenze, pp. 175–197

Demes B, Jungers WL, Selpien K. 1991. Body size, locomotion, and long bone cross-sectional geometry in indriid primates. Am J Phys Anthropol 86:537–47.

Demes B, Larson SG, Stern JT, Jungers WL, Biknevicius AR, Schmitt D. 1994. The kinetics of primate quadrupedalism: "hindlimb drive" reconsidered. J Hum Evol 26:353–374.

Demes B, Qin YX, Stern JT, Larson SG, Rubin CT. 2001. Patterns of strain in the macaque tibia during functional activity. Am J Phys Anthropol 116:257–65.

Demes B, Gunther MM. 1989. Biomechanics and allometric scaling in primate locomotion and morphology. Folia Primatol 52:58–69.

Demes B, Stern JT, Hausman MR, Larson SG, McLeod KJ, Rubin CT. 1998. Patterns of strain in the macaque ulna during functional activity. Am J Phys Anthropol 106:87–100.

DeRousseau CJ, Rawlins RG, Denlinger JL. 1983. Aging in the musculoskeletal system of rhesus monkeys: I. Passive joint excursion. Am J Phys Anthropol. 61(4), 483-494.

DeSilva JM. 2008. Vertical climbing adaptations in the ape ankle and midfoot. Impli- cations for locomotion in Miocene catarrhines and Plio-Pleistocene hominins. PhD dissertation (Univ of Michigan, Ann Arbor, MI).

DeSilva JM. 2009. Functional morphology of the ankle and the likelihood of climbing in early hominins. Proc Natl Acad Sci U S A 106:6567–6572.

Diogo R, Wood B. 2011. Soft-tissue anatomy of the primates: Phylogenetic analyses based on the muscles of the head, neck, pectoral region and upper limb, with notes on the evolution of these muscles. J Anat 219:273–359.

Diogo R, Molnar J. 2014. Comparative Anatomy, Evolution, and Homologies of Tetrapod Hindlimb Muscles, Comparison with Forelimb Muscles, and Deconstruction of the Forelimb-Hindlimb Serial Homology Hypothesis. Anat Rec 297:1047–1075.

Diogo R, Muchlinski MN, Hartstone-Rose A, Carolina S. 2015. Comparative anatomy of primates. Basics Hum Evol:43–55.

Diogo R, Molnar JL, Wood B. 2017. Bonobo anatomy reveals stasis and mosaicism in chimpanzee evolution, and supports bonobos as the most appropriate extant model for the common ancestor of chimpanzees and humans. Sci Rep 7:608.

Dirks W, Bowman JE. 2007. Life history theory and dental development in four species of catarrhine primates. J Hum Evol 53:309–20.

Doran DM. 1992a. The ontogeny of chimpanzee and pygmy chimpanzee locomotor behavior: a case study of paedomorphism and its behavioral correlates. Journal of Human Evolution 23:139–157.

Doran DM. 1992b. Comparison of instantaneous and locomotor bout sampling methods: a case study of adult male chimpanzee locomotor behavior and substrate use. American Journal of Physical Anthropology 89:85–99.

Doran DM. 1993. Sex differences in adult chimpanzee positional behavior: The influence of body size on locomotion and posture. Am J Phys Anthropol 91:99–115.

Doran DM. 1996. Comparative positional behavior of the African apes. In: McGrew W, Marchant L, Nishida T (eds.), Great ape societies, pp. 213–224. Cambridge: Cambridge University Press.

Doran DM. 1997. Ontogeny of locomotion in mountain gorillas and chimpanzees. J Hum Evol 32:323–344.

Doran DM, Hunt KD. 1994. Comparative locomotor behavior of chimpanzees and bonobos: Species and habitat differences. In: Wrangham RW, McGrew WC, de Waal FBM, Heltne PG (eds.), Chimpanzee cultures pp. 93–106. Cambridge, MA: Harvard University Press.

Doran DM, Mcneilage A. 1998. Gorilla ecology and behavior. Evol Anthropol Issues, News Rev 6:120–131

Doran-Sheehy D, Andrianady M, Lodwick J. 2009. Sex differences in western gorilla arboreality. Am. J. Phys. Anthropol. Vol 48 S, 120.

Drapeau MS, Streeter MA. 2006. Modeling and remodeling responses to normal loading in the human lower limb. Am J Phys Anthropol 129:403–409.

Dryden IL, Mardia KV. 1998. Statistical Shape Analysis. Wiley, Chichester.

Dunbar DC. 1989. Locomotor behavior of rhesus macaques (*Macaca mulatta*) on Cayo Santiago, PR. Health Sci J 8:79– 85.

Dunbar DC. 1994. The influence of segmental movements and design on whole-body rotations during the airborne phase of primate leaps. Zeitschrift fur Morphologie und Anthropologie 80:109–124.

Dunbar DC, Badam GL. 1998. Development of posture and locomotion in free-ranging primates. Neurosci Biobehav Rev 22:541–6.

Enlow DH. 1963. Principles of Bone Remodeling: An Account of Postnatal Growth and Remodeling Processes in Long Bones and the Mandible. Springfield: Charles C Thomas.

Fabre A-C, Marigó J, Granatosky MC, Schmitt D. 2017. Functional associations between support use and forelimb shape in strepsirrhines and their relevance to inferring locomotor behavior in early primates. J Hum Evol 108:11–30.

Faccia K, Buie H, Weber A, Bazaliiskii VI, Goriunova OI, Boyd S, Hallgrímsson B, Katzenberg MA. 2014. Bone quality in prehistoric, cis-baikal forager femora: A micro-CT analysis of cortical canal microstructure. Am J Phys Anthropol 154:486–97.

Fajardo RJ, Muller R, Ketcham RA, Colbert M. 2007. Nonhuman anthropoid primate femoral neck trabecular architecture and its relationship to locomotor mode. Anat Rec 290: 422–436.

Fan P, Scott MB, Fei H, Ma C. 2013. Locomotion behavior of cao vit gibbon (*Nomascus nasutus*) living in karst forest in Bangliang Nature Reserve, Guangxi, China. Integr Zool 8:356–364.

Feldesman MR, Fountain RL. 1996. ‘‘Race’’ specificity and the femur/stature ratio. Am J Phys Anthropol 100:207–244.

Fleagle JG. 1974. Dynamics of a brachiating siamang [Hylobates (*Symphalangus*) syndactylus]. Nature 248:259–260.

Fleagle JG. 1976. Locomotion and Posture of the Malayan Siamang and Implications for Hominoid Evolution. Folia Primatol 26:245–269.

Fleagle JG. 1980. Locomotion and posture. In: Chivers, DJ (ed.) Malayan Forest Primates: Ten Years' Study in Tropical Rain Forests. Plenum Press, New York, pp. 191-209.

Fleagle JG. 1999. Primate Adaptation and Evolution (Academic Press, New York). 15.

Fleagle JG. 2013. Primate Adaptation and Evolution, third ed. Academic Press, San Diego.

Fleagle JG, Lieberman DE. 2015. Major Transformations in the Evolution of Primate Locomotion. In: Great Transformations in Vertebrate Evolution. 1st ed. London: University of Chicago Press. p 257–282.

Flück M. 2006. Functional, structural and molecular plasticity of mammalian skeletal muscle in response to exercise stimuli. J Exp Biol 209:2239–48.

Frelat MA, Mittereocker P. 2011. Postnatal ontogeny of tibia and femur form in two human populations: a multivariate morphometric analysis. Am J Hum Biol 23:796–804.

Frost HM. 1997. Why Do Marathon Runners Have Less Bone Than Weight Lifters? A Vital Biomechanical View and Explanation. Bone 20:183–189.

Frost HM. 2003. Bone's Mechanostat: A 2003 Update. Anat Rec Part A A275:1081–1101.

Frost HM. Schönau E. 2000. The “muscle-bone unit” in children and adolescents: A 2000 overview. J Pediatr Endocrinol Metab 13:571–590.

Galilei G. 1638. Dialogues concerning two new sciences. Leiden: Elzevir. Crew H, de Salvio A, translators. 1914. New York: Macmillan.

Gebo DL. 1992. Locomotor and postural behavior in Alouatta palliata and Cebus capucinus. Am J Primatol 26:277–290.

Gebo DL. 1993. The Functional Morphology of the Foot in Primates. In: DL Gebo (ed.) Postcranial Adaptation in Nonhuman Primates. Dekalb: Northern Illinois University Press, pp. 175-196.

Gebo DL. 1996. Climbing, brachiation, and terrestrial quadrupedalism: Historical precursors of hominid bipedalism. Am J Phys Anthropol 101:55–92

Gebo DL. 2011. Vertical clinging and leaping revisited: vertical support use as the ancestral condition of strepsirrhine primates. Am J Phys Anthropol 146:323–345.

Gebo DL, Smith T, Dagosto M. 2012. New postcranial elements for the earliest Eocene fossil primate Teilhardina belgica. J Hum Evol 63:205–218.

Gibbs RA, Rogers J, Katze MG, et al. 2007. Evolutionary and Biomedical Insights from the Rhesus Macaque Genome. Science. 316:222–234.

Gibson AR, Baker AJ, Moeed A. 1984. Morphometric Variation In Introduced Populations Of The Common Myna (*Acridotheres tristis*): An Application Of The Jackknife To principal Component Analysis. Syst Biol 33(4):408-421.

Gingerich PD, Schoeninger M. 1977. The fossil record and primate phylogeny. J Hum Evol 6:483–505.

Gittins SP. 1983. Use of the forest canopy by the agile gibbon. Folia Primatol. (Basel) 40:134-144.

Godfrey L, Sutherland M, Boy D, Gomberg N. 1991. Scaling of limb joint surface areas in anthropoid primates and other mammals. J Zool Lond 223:603–625.

Good P. 2013. Permutation tests: A practical guide to resampling methods for testing hypotheses. New York: Springer Science & Business Media.

Goodall J. 1963. Feeding behavior of wild chimpanzees. Symp. Zool. Soc. London 10:39-48.

Gordon AD, Marcus E, Wood B. 2013. Great ape skeletal collections: making the most of scarce and irreplaceable resources in the digital age. Am J Phys Anthropol 152 Suppl:2–32.

Gosman JH, Ketcham RA. 2009. Patterns in ontogeny of human trabecular bone from SunWatch Village in the Prehistoric Ohio Valley: General features of microarchitectural change. Am J Phys Anthropol 138, 318–332.

Gould SJ. 1966. Allometry and size in ontogeny and phylogeny. Biol. Rev. 41, 587–640.

Gould SJ. 1975. Allometry in primates, with emphasis on scaling and the evolution of the brain. In: F. Szalay (ed.) Approaches to Primate Paleobiology, Contributions to Primatology, vol. 5, pp. 244–292. New York: Karger, Basel.

Gould SJ. 1977. Ontogeny and Phylogeny. Cambridge, Mass.: Harvard University Press.

Gould SJ. 1989. Wonderful Life. W. W. Norton, New York.

Gower JC. 1975. Generalised Procrustes analysis. Psychme- trika 40:33–50.

Grabowski M, Hatala KG, Jungers WL, Richmond BG. 2015. Body mass estimates of hominin fossils and the evolution of human body size. J Hum Evol 85:75–93.

Granatosky MC, Tripp CH, Fabre A-C, Schmitt D. 2016. Patterns of quadrupedal locomotion in a vertical clinging and leaping primate (*Propithecus coquereli*) with implications for understanding the functional demands of primate quadrupedal locomotion. Am J Phys Anthropol 160(4), 644-652.

Grand TI. 1983. Motion economy within the canopy. Four strategies for mobility. In: Rodman PS, Cant JGH, editors. Adaptations for foraging in nonhuman primates. Contributions to an organismal biology of prosimians, monkeys and apes. New York: Columbia University Press.

Green DJ, Serrins JD, Seitelman B, Martiny AR, Gunz P. 2015. Geometric Morphometrics of Hominoid Infraspinous Fossa Shape. Anat Rec 298:180–194.

Gunz P, Neubauer S, Maureille B, Hublin J-J. 2010. Brain development after birth differs between Neanderthals and modern humans. Curr Biol 20:R921–R922.

Gunz P, Mitteroecker P. 2013. Semilandmarks: A method for quantifying curves and surfaces. Hystrix 24:103–109.

Haapasalo H, Sievanen H, Kannus P, Heinonen A, Oja P, Vuori I. 1996. Dimensions and estimated mechanical characteristics of the humerus after long-term tennis loading. J Bone Miner Res 11:864–872.

Hagihara Y, Takashi N. 2017. The characteristic mid-shaft cross-sectional shape of the ulna in Jomon hunter-gatherers. Am J Phys Anthropol:1–11.

Hallgrimsson B, Swartz S. 1995. Biomechanical Adaptation of Ulnar Cross-Sectional Morphology in Brachiating Primates. J Morphol 224:111–123.

Hamada Y, San AM, Malaivijitnond S. 2016. Assessment of the hybridization between rhesus (*Macaca mulatta*) and long-tailed macaques (*M . fascicularis*) based on morphological characters. Am J Phys Anthropol 159(2), 189-198.

Hamrick MW, Skedros JG, Pennington C, McNeil PL. 2006. Increased osteogenic response to exercise in metaphyseal versus diaphyseal cortical bone. J Musculoskelet Neuronal Interact 6:258–63.

Harmon EH. 2007. The shape of the hominoid proximal femur: A geometric morphometric analysis. J Anat 210:170–185.

Harrison T. 2005. The Zoogeographic and Phylogenetic Relationships of Early Catarrhine Primates in Asia . Anthropological Science 113 : 43 – 51 .

Harrison T. 2013. Catarrhine Origins. In: Begun DR, editor. A Companion to Paleoanthropology. 1st ed.. pp. 376–396.

Harvey PH, Clutton-Brock TH. 1985. Life History Variation in Primates. Soc Study Evol 39:559–581.

Hayssen V, Lacy RC. 1985. Basal Metabolic Rates in Mammals: Taxonomic Differences in the Allometry of BMR and Body Mass. Comp Biochem Physiol 81A:741–754.

Hebert PL, Bard K. 2000. Orangutan use of vertical space in an innovative habitat. Zoo Biol 19:369–382.

Heinonen A, Sievänen H, Kannus P, Oja P, Vuori I. 2002. Site-specific skeletal response to long-term weight training seems to be attributable to principal loading modality: a pQCT study of female weightlifters. Calcif Tissue Int 70:469–74.

Hildebrand M. 1985. Walking and running. In Functional Vertebrate Morphology. In: M. Hildebrand, D. M. Bramble, K. F. Liem and D. B. Wake (eds.) p. 38-57. Cambridge: Harvard University Press.

Hildebrand M, Hurley J. 1985. Energy of the oscillating legs of a fast-moving cheetah, pronghorn, jackrabbit, and elephant. J. Morphol. 184, 23-31.

Holowka NB, O'Neill MC. 2013. Three-dimensional moment arms and architecture of chimpanzee (*Pan troglodytes*) leg musculature. J Anat 223:610–628.

Holt BM. 2003. Mobility in Upper Paleolithic and Mesolithic Europe: Evidence From the Lower Limb. Am J Phys Anthropol 122:200–215.

Horvat JR, Kraemer HC. 1982. Behavioral changes during weaning in captive chimpanzees. Primates 23: 488–499.

Hotchkiss RN, An KN, Sowa DT, Basta S, Weiland AJ. An anatomic and mechanical study of the interosseous membrane of the forearm: pathomechanics of proximal migration of the radius. J Hand Surg 1989; 14A:256-261.

Hsieh Y, Robling AG, Ambrosius WT, Burr DB, Turner CH. 2001. Mechanical Loading of Diaphyseal Bone In Vivo : The Strain Threshold for an Osteogenic Response Varies with Location. J Bone Miner Res 16:2291–2297.

Huang Z, Huang C, Wei H, et al. 2015. Factors influencing positional behavior and habitat use of sympatric macaques in the limestone habitat of Nonggang, China. International Journal of Primatology 36:95–112.

Huiskes R. 1982. On the modeling of long bones in structural analyses. J Biomech 15:65–69.

Hunt KD. 1991. Positional behavior in the Hominoidea. Int J Primatol 12, 95–118.

Hunt KD. 1992. Positional Behavior of Pan Troglodytes in the Mahale Mountains and Gombe Stream National Parks, Tanzania. Am J Phys Anthropol 87:83–105.

Hunt KD. 2004. The special demands of great ape locomotion and posture. In: Russon AE, Begun DR, editors. The evolution of thought: evolutionary origins of great ape intelligence. Cambridge: Cambridge University Press. p 172–189.

Hunt KD. 2016. Why are there apes? Evidence for the co-evolution of ape and monkey ecomorphology. J Anat 228:630–685.

Hunt KD, Cant JGH, Rico P. 1996. Standardized Descriptions of Primate Locomotor and Postural Modes. J Hum Evol 37:363–387.

Hürzeler J. 1949. Neubeschreibung von Oreopithecus bambolii Gervais. Schweiz. Palaeont. Abh. 66, 1–20.

Huxley J. 1932. Problems in Relative Growth. London: Methuen.

Huxley JS, Teissier G. 1936. Terminology of relative growth. Nature 137:780–781.

Ibáñez-Gimeno P, De Esteban-Trivigno S, Jordana X, Manyosa J, Malgosa A, Galtés I. 2013. Functional plasticity of the human humerus: Shape, rigidity, and muscular entheses. Am J Phys Anthropol 150:609–617.

Inouye SE. 1994. Ontogeny of knucle-walking hand postures in African apes. J Hum Evol 26:459–485.

Ireland A, Korhonen M, Heinonen A, Suominen H, Baur C, Stevens S, Degens H, Rittweger J. 2011. Side-to-side differences in bone strength in master jumpers and sprinters. J Musculoskelet Neuronal Interact 11:298–305.

Ireland A, Sayers A, Deere KS, Emond A, Tobias JH. 2015. Motor Competence in Early Childhood Is Positively Associated with Bone Strength in Late Adolescence. J Bone Miner Res 1–10.

Ireland A, Capozza RF, Cointry GR, Nocciolino L, Ferretti JL RJ. 2016. Meagre effects of disuse on the human fibula are not explained by bone size or geometry. Osteoporos Int IN PRESS:0–28.

Ito T, Nishimura TD, Hamada Y, Takai M. 2014. Contribution of the maxillary sinus to the modularity and variability of nasal cavity shape in Japanese macaques. Primates 56:11–19.

Jackson DA. 1993. Stopping Rules in Principal Components Analysis : A Comparison of Heuristical and Statistical Approaches Stable. Stat Approaches 74:2204–2214.

Janson CH, van Schaik CP. 1993. Ecological risk aversion in juvenile primates: slow and steady wins the race. In: Pereira ME, Fairbanks LA, editors. Juvenile primates. New York: Oxford University Press. pp. 57–74.

Jenkins FA. 1973. The functional anatomy and evolution of the mammalian humero-ulnar articulation. Am. J. Anat. 137, 281-298.

Jenkins FA, Camazine SM. 1977. Hip structure and locomotion in ambulatory and cursorial carnivores. J Zool Lond 181:351–370.

Jolicoeur P. 1963. The Multivariate Generalization of the Allometry Equation. Biometrics 19:497–499.

Judex S, Carlson KJ. 2009. Is Bone's Response to Mechanical Signals Dominated by Gravitational Loading? Med Sci Sport Exerc. 41:2037–2043.

Judex S, Gross TS, Zernicke RF. 1997. Strain gradients correlate with sites of exercise-induced bone-forming surfaces in the adult skeleton. J Bone Miner Res 12: 1737–1745.

Judex S, Lei X, Han D, Rubin C. 2007. Low-magnitude mechan- ical signals that stimulate bone formation in the ovariectomized rat are dependent on the applied frequency but not on the strain magnitude. J Biomech 40:1333–1339.

Jungers WL. 1984. Aspects of size and scaling in primate biology with special reference to the locomotor skeleton. Am J Phys Anthropol 27:73–97.

Jungers WL. 1985. Body size and scaling of limb proportions in primates.In: Jungers WL (ed.) Size and scaling in primate biology. New York: Plenum. pp. 345–381.

Jungers WL. 1987. Body size and morphometric affinities of the appendicular skeleton in *Oreopithecus bambolii* (IGF 11778). J Hum Evol 16:445–456.

Jungers WL, Susman RL. 1984. Body size and skeletal anatomy in the African apes. In: RL Susman (ed.) The Pygmy Chimpanzee: Evolutionary Biology and Behavior. New York: Plenum Press.

Jungers WL. 1985. Body size and scaling of limb proportions in primates. In: WL Jungers (ed.) Size and Scaling in Primate Biology. New York: Plenum, pp. 345-381.

Jungers WL, Hartmann SE. 1988. Relative growth of the locomotor skeleton in orang-utans and other large-bodied hominoids. In: Schwartz JH (ed.) Orang-utan Biology, pp. 347–359.

Jungers WL, Godfrey LR, Simons EL, Wunderlich RE, Richmond BG, Chatrath PS. 2002. Ecomorphology and behavior of giant extinct lemurs from Madagascar. In: Plavcan JM, Kay RF, Jungers WL, van Schaik CP (eds.) Reconstructing Behavior in the Primate Fossil Record. Kluwer Academic/Plenum Publishers, New York, pp. 371-411.

Kanthaswamy S, Satkoski J, George D, Erickson BJ-A, Smith DG. 2008. Hybridization and stratification of nuclear genetic variation in *Macaca mulatta* and *M. fascicularis*. Int J Primatol 29:1295–1311.

Kay RF. 1975. The functional adaptations of primate molar teeth. Am J Phys Anthropol 43:195–216.

Kelley J, Schwartz GT. 2010. Dental development and life history in living African and Asian apes. Proc Natl Acad Sci 107:1035–1040.

Khan KM, Bennell KL, Hopper JL, Flicker L, Nowson CA, Sherwin AJ, Crichton KJ, Harcourt PR, Wark JD. 1998. Self-reported ballet classes undertaken at age 10–12 years and hip bone Mineral density in later life. Osteoporosis International 8, 165–173.

Khan SN, Bostrom MP, Lane JM. 2000. Bone growth factors. Orthop Clin North Am 31:375–388.

Kimura T. 1992. Hindlimb dominance during primate high-speed locomotion. Primates 33: 465–476.

Kimura T. 2000. Development of quadrupedal locomotion on level surfaces in Japanese macaques. Folia Primatol. 71, 323–333.

Kimura T, Okada M, Ishida H. 1979. Kinesiological characteristics of primate walking: its significance in human walking. In: Morbeck ME, Preuschoft H, Gomberg N (eds.) Environment, Behaviour and Morphology: Dynamic Interactions in Primates. pp. 297–311. New York, NY: Gustav Fischer.

Kivell TL. 2016a. A review of trabecular bone functional adaptation: what have we learned from trabecular analyses in extant hominoids and what can we apply to fossils? J Anat: 228(4), 569-594.

Kivell TL. 2016b. The Primate Wrist. In: Kivel TL, Lemelin P, Richmond BG, Schmitt D. The Evolution of the Primate Hand (pp. 17–54). Springer, New York.

Kivell TL, Schmitt D. 2009. Independent evolution of knuckle-walking in African apes shows that humans did not evolve from a knuckle-walking ancestor. Proc Natl Acad Sci U S A 106:14241–6.

Kivell TL, Skinner MM, Lazenby R, Hublin J-J. 2011. Methodological considerations for analyzing trabecular architecture: an example from the primate hand. J. Anat. 218, 209–225.

Kivell TL, Barros AP, Smaers JB. 2013. Different evolutionary pathways underlie the morphology of wrist bones in hominoids. BMCEvol Biol. 13: 229.

Klegarth AR, Sanders SA, Gloss AD, Lane-deGraaf KE, Jones-Engel L, Fuentes A, Hollocher H. 2017. Investigating biogeographic boundaries of the Sunda shelf: A phylogenetic analysis of two island populations of *Macaca fascicularis*. Am J Phys Anthropol:658–670.

Klingenberg CP. 1996. Multivariate Allometry. In: Marcus LF (ed.) Advances in Morphometrics. New York: Plenum Press. pp. 23–49.

Klingenberg CP. 2009. Morphometric integration and modularity in configurations of landmarks: Tools for evaluating a priori hypotheses. Evol Dev 11:405–421.

Klingenberg CP. 2011. MorphoJ: an integrated software package for geometric morphometrics. Mol. Ecol. Resour. 11, 353–357.

Klingenberg CP. 2016. Size, shape, and form: concepts of allometry in geometric morphometrics. Dev Genes Evol 226:113–137.

Klingenberg CP, Spence JR. 1993. Heterochrony and allometry: lessons from the water strider genus *Limnoporus*. Evolution (NY) 47:1834–1853.

Klingenberg CP, Monteiro LR. 2005. Distances and directions in multidimensional shape spaces: implications for morphometric applications. Syst Biol 54:678–688.

Klingenberg CP, Marugán-Lobón J. 2013. Evolutionary covariation in geometric morphometric data: Analyzing integration, modularity, and allometry in a phylogenetic context. Syst Biol 62:591–610.

Knott CD. 2005. Energetic responses to food availability in the great apes: implications for hominin evolution. In: DK Brockman, CP van Schaik (eds.) Seasonality in primates, pp. 351–378. Cambridge, UK: Cambridge University Press.

Knott CD, Thompson ME, Wich SA. 2009. The ecology of female reproduction in wild orangutans. In: Wich SA, Atmoko SSU, Setia TM, Van Schaik CP (eds.) Orangutans: Geographic variation in behavioral ecology and conservation. Oxford. pp. 171–188.

Köhler M, Moyà-Solà S. 1997. Ape-like or hominid-like? The positional behavior of Oreopithecus bambolii reconsidered. Proc Natl Acad Sci USA 94:11747–50.

Kovarovic K, Slepkov R, Mcnulty KP. 2013. Ecological continuity between Lower and Upper Bed II, Olduvai Gorge, Tanzania. J Hum Evol 64:538–555.

Kraemer HC, Horvat JR, Doering C, McGinnis PR. 1982. Male chimpanzee development focusing on adolescence: Integra- tion of behavioral with physiological changes. Primates 23:393–405.

Kurki HK, Ginter JK, Stock JT, Pfeiffer S. 2010. Body size estimation of small-bodied humans: Applicability of current methods. Am J Phys Anthropol 141:169–80.

Kuroda S. 1992. Ecological interspecies relationships between gorillas and chimpanzees in the Ndoki-Nouabale Reserve, Northern Congo. In Itoigawa N, Sugiyama Y, Sackett G, Thompson RKR (eds.), Topics in Primatology. vol. 2: Behavior, Ecology and Conservation, pp 385–394. Tokyo: University of Tokyo Press.

Lague M, Jungers W. 1996. Morphometric variation in Plio- Pleistocene hominid distal humeri. Am J Phys Anthropol 101:401–427.

Lande R. 2013. Genetic and Evolutionary Aspects of Allometry. In: Jungers WJ (ed.) Size and Scaling in Primate Biology, pp. 21–31. Springer Science and Business Media.

Langergraber KE, Prüfer K, Rowney C, Boesch C, Crockford, C. 2012. Generation times in wild chimpanzees and gorillas suggest earlier divergence times in great ape and human evolution. Proc Nat Acad Sci USA 109: 15716–15721.

Langsrud O. 2003. ANOVA for unbalanced data; Use Type II instead of Type III sums of squares. Stat Comput 13:163–167.

Lanyon LE, Rubin CT. 1985. Functional adaptation in skeletal structures. In: Hildebrand M, Bramble DM, Liem KF, Wake BD, editors. Functional vertebrate morphology.Cambridge, MA: Belknap Press. pp. 1–25.

Lanyon LE, Goodship AE, Pye CJ, MacFie JH. 1982. Mechanically adaptive bone remodelling. J Biomech 15, 141–154.

Lanyon L. 1987. Functional Strain In Bone Tissue As An Objective And Controlling Stimulus For Adaptive Bone Remodelling. J Biomech 20:1083–1093.

Lappan S. 2008. Male care of infants in a siamang (*Symphalangus syndactylus*) population including socially monogamous and polyandrous groups. Behavioral Ecology and Sociobiology, 62, 1307–1317.

Lappan S. 2009. The effects of lactation and infant care on adult energy budgets in wild siamangs (*Symphalangus syndactylus*). American Journal of Physical Anthropology, 140, 290–301.

Larson SG. 1998. Unique aspects of quadrupedal locomotion in nonhuman primates. In: Strasser E, Fleagle JG, Rosenberger AL, McHenry HM (eds.) Primate Locomotion: Recent Advances, pp. 157–173. Plenum Press, New York.

Larson SG. 2013. Shoulder morphology in early hominin evolution. In: Reed, K.E., Fleagle, J.G., Leakey, R.E. (eds.) The Paleobiology of Australopithecus. Vertebrate Paleobiology and Paleoanthropology Series, pp. 247–261, Springer, New York.

Larson SG. 2015. Humeral torsion and throwing proficiency in early human evolution. J Hum Evol 85, 198–205.

Larson SG, Stern Jr. J. 1987. EMG of chimpanzee shoulder muscles during knuckle-walking: problems of terrestrial locomotion in a suspensory adapted primate. J. Zool. 212, 629-655.

van Lawick-Goodall J. 1967. Mother-offspring relationships in free-ranging chimpanzees. In: D. Morris (ed.) Primate ethology, pp. 287–346. London, UK: Weidenfield.

Latimer B, Ohman JC, Lovejoy CO, 1987. Talocrural joint in African hominoids: implications for Australopithecus afarensis. Am. J. Phys. Anthropol. 74, 155–175.

Leigh SR. 1992. Patterns of variation in the ontogeny of primate body size dimorphism. J Hum Evol 23:27–50.

Leigh SR. 1993. Ontogeny and body size dimorphism in extant hominoid primates. Am J Phys Anthropol Suppl. 16:133.

Leigh SR, Setchell JM, Buchanan LS. 2005. Ontogenetic bases of canine dimorphism in anthropoid primates. Am J Phys Anthropol 127:296–311.

Leigh SR, Shea BT. 1995. Ontogeny and the evolution of adult body size dimorphism in apes. Am J Primatol 36:37–60.

Leigh SR, Shea BT. 1996. Ontogeny of body size variation in African apes. Am J Phys Anthropol 99:43–65.

Leigh SR, Blomquist GE. 2011. Life history. In CJ Campbell, A Fuentes, KC MacKinnon, SK Bearder, RM Stumpf (eds.) Primates in perspective, pp. 418–428, New York: Oxford University Press.

Levin NE, Haile-selassie Y, Frost SR, Saylor BZ. 2015. Dietary change among hominins and cercopithecids in Ethiopia during the early Pliocene. PNAS - Proc Natl Acad Sci 112:12304–12309.

Lewis SJ. 1999. University of Chester Digital Repository Quantifying measurement error. In: Anderson S (ed.) Current and Recent Research in osteoarchaeology 2: proceedings of the 4th, 5th and 6th meetings of the Osteoarchaeological Research Group, pp. 54–55. Oxford: Oxbow Books.

Lewton KL. 2015. Allometric scaling and locomotor function in the primate pelvis. Am J Phys Anthropol 156(4), 511–530.

Li Y, Crompton RH, Alexander R.McN, Gunther MM, Wang WJ. 1996. Characteristics of ground reaction forces in normal and chimpanzee-like bipedal walking by humans. Folia Primatol. 66, 137–159.

Lieberman DE, Pearson OM, Polk JD, Demes B, Crompton AW. 2003. Optimization of bone growth and remodeling in response to loading in tapered mammalian limbs. J Exp Biol 206:3125–3138.

Lieberman DE. 1996. How and why humans grow thin skulls: experimental evidence for systemic cortical robusticity. Am J Phys Anthropol 101:217–36.

Lieberman DE, Crompton AW. 1998. Responses of bone to stress: constraints on symmorphosis. In: Webel ER, Taylor CR, Bolis L (ed.) Principles of animal design: the optimization and symmorphosis debate. Cambridge: Cambridge University Press. pp. 78–86.

Lieberman DE, Carlo J, Ponce de León M, Zollikofer CPE. 2007. A geometric morphometric analysis of heterochrony in the cranium of chimpanzees and bonobos. J Hum Evol 52:647–662.

Lieberman DE, Polk JD, Demes B. 2004. Predicting Long Bone Loading from Cross-Sectional Geometry. Am J Phys Anthropol 123:156–171.

Lieverse AR, Stock JT, Katzenberg MA, Haverkort CM. 2011. In: Pinhasi R, Stock JT (eds.) The Bioarchaeology of Habitual Activity and Dietary Change in the Siberian Middle Holocene, pp. 265–291. Wiley-Blackwell, Hoboken, NJ.

Lockwood CA, Lynch JM, Kimbel W. 2002. Quantifying temporal bone morphology of great apes and humans: an approach using geometric morphometrics. J Anat 201:447–464.

Lordkipanidze D, Ponce de Leon MS, Margvelashvili A, Rak Y, Rightmire GP, Vekua A, Zollikofer CPE. 2013. A Complete Skull from Dmanisi, Georgia, and the Evolutionary Biology of Early Homo. Science 342(6156), 326–331.

Lovejoy CO, Burstein a H, Heiple KG. 1976. The biomechanical analysis of bone strength: a method and its application to platycnemia. Am J Phys Anthropol 44:489–505.

Lovejoy CO, McCollum M a., Reno PL, Rosenman B a. 2003. Developmental Biology and Human Evolution. Annu Rev Anthropol 32:85–109.

Lumer H. 1939. Relative growth of the limb bones in the anthropoid apes. Hum. Biol. 11, 379–392.

Macdonald HM, Cooper DML, McKay HA. 2009. Anterior-posterior bending strength at the tibial shaft increases with physical activity in boys: evidence for non-uniform geometric adaptation. Osteoporos Int 20:61–70.

Macintosh AA, Davies TG, Ryan TM, Shaw CN, Stock JT. 2013. Periosteal versus true cross-sectional geometry: a comparison along humeral, femoral, and tibial diaphyses. Am J Phys Anthropol 150:442–452.

Macintosh AA, Davies TG, Pinhasi R, Stock JT. 2015. Declining tibial curvature parallels ~6150 years of decreasing mobility in central european agriculturalists. Am J Phys Anthropol 157(2), 260–275.

MacKinnon J, MacKinnon K. 1978. Comparative feeding ecology of six sympatric primates in West Malaysia. In: D. Chivers and J. Herbert, (eds.) Recent Advances in Primatology. Vol. 1, pp. 305–321. Academic Press, London.

Main RP. 2007. Ontogenetic relationships between in vivo strain environment, bone histomorphometry and growth in the goat radius. J Anat 210: 272.

Main RP, Biewener AA. 2004. Ontogenetic patterns of limb loading, in vivo strains and growth in the goat radius. J Exp Biol 207:2577–2588.

Main RP, Biewener AA. 2007. Skeletal strain patterns and growth in the emu hindlimb during ontogeny. J Exp Biol 210: 2676–2690.

Manduell KL, Harrison ME, Thorpe SKS. 2012. Forest structure and support availability influence orangutan locomotion in Sumatra and Borneo. Am J Primatol 74:1128–1142.

Mann A, Weiss M. 1996. Hominoid phylogeny and taxonomy: a consideration of the molecular and fossil evidence in a historical perspective. Mol. Phylogenet. Evol. 5, 169–181.

Marchi D, Patel BA. 2015. Post-cranial suspensory adaptations of the subfossil lemur Babakotia radofilai. In: 13th Annual Meeting of the European Association of Vertebrate Palaeontologists, pp. 159.

Marchi D. 2007. Relative strength of the tibia and fibula and locomotor behavior in hominoids. J Hum Evol 53:647–655.

Marchi D. 2015a. Variation in tibia and fibula diaphyseal strength and its relationship with arboreal and terrestrial locomotion: Extending the investigation to non-hominoid primates. J Anthropol Sci 93:153–156.

Marchi D. 2015b. Using the morphology of the hominoid distal fibula to interpret arboreality in Australopithecus afarensis. J Hum Evol 85:136–148.

Marchi D, Shaw CN. 2011. Variation in fibular robusticity reflects variation in mobility patterns. J Hum Evol 61:609–16.

Mariotti V, Facchini F, Belcastro MG. 2004. Enthesopathies — proposal of a standardized scoring method and applications. Coll Anthropol 28:145–159.

Martin R, Saller K. 1957. Lehrbuch der anthropologie. Stuttgart: Fischer.

Martín-Serra A, Figueirido B, Palmqvist P. 2014. A three-dimensional analysis of morphological evolution and locomotor performance of the carnivoran forelimb. PLoS ONE 9(1), e85574

Masi S. 2004. Tree use by a western gorilla group (*Gorilla gorilla gorilla*) in the Dzanga-Ndoki National Park, Central African Republic. Folia Primatol. 75, 385–414.

Matsuda JJ, Zernicke RF, Vailas AC, Pedrini VA, Pedrini-Mille A, Maynard JA. 1986. Structural and mechanical adaptation of immature bone to strenuous exercise. J Appl Physiol 60: 2028–2034.

Mayr E. 1956. Geographical character gradients and climatic adaptation. Evolution, 10, 105–108.

Mcfarlin SC, Terranova CJ, Zihlman AL, Enlow DH, Bromage TG. 2008. Regional variability in secondary remodeling within long bone cortices of catarrhine primates: The influence of bone growth history. J Anat 213:308–324.

McMahon TA. 1975. Using body size to understand the structural design of animals: quadrupedal locomotion. 1. Appl. Physiol. 39:619-627.

van der Meulen MC, Beaupre´ GS, Carter DR. 1993. Mechanobiologic influences in long bone cross-sectional growth. Bone 14: 635–42.

van der Meulen MCH, Ashford Jr MW, Kiratli BJ, Bachrach LK, Carter DR. 1996. Determinants of femoral geometry and structure during adolescent growth. J Orthop Res 14:22–29.

Michilsens F, Vereecke EE, D'Août K, Aerts P. 2009. Functional anatomy of the gibbon forelimb: Adaptations to a brachiating lifestyle. J Anat 215:335–354.

Miller B, Spevak L, Lukashova L, Javaheri B, Pitsillides AA, Boskey A, Bou-Gharios G, Carriero A. 2017. Altered Bone Mechanics, Architecture and Composition in the Skeleton of TIMP-3-Deficient Mice. Calcif Tissue Int :1–10.

Mitteroecker P, Gunz P. 2009. Advances in Geometric morphometrics. Evol Biol 36:235–247.

Mitteroecker P, Gunz P, Bernhard M, Schaefer K, Bookstein FL. 2004. Comparison of cranial ontogenetic trajectories among great apes and humans. J Hum Evol 46:679–698.

Mitteroecker P, Gunz P, Windhager S, Schaeffer K. 2013. A brief review of shape, form, and allometry in geometric morphometrics, with applications to human facial morphology. Hystrix, Ital J Mammal 24:59–66.

Monteiro LR. 1999. Multivariate Regression Models and Geometric Morphometrics: The Search for Causal Factors in the Analysis of Shape. Soc Syst Biol 48:192–199.

Morimoto N, De León MSP, Zollikofer CPE. 2011. Exploring Femoral Diaphyseal Shape Variation in Wild and Captive Chimpanzees by Means of Morphometric Mapping: A Test of Wolff's Law. Anat Rec 294:589–609.

Morino L, Borries C. 2016. Offspring loss after male change in wild siamangs: The importance of abrupt weaning and male care. Am J Phys Anthropol:180–185.

Morland HS. 1990. Parental behavior and infant development in ruffed lemurs (*Varecia variegata*) in a northeast Madagascar rain forest. Am. J. Primatol. 20, 253–265.

Moyà-Solà S, Kohler M. 1996. A Dryopithecus Skeleton and origins of great-ape locomotion. Lett To Nat 379:156–159.

Moyà-Solà S, Kohler M, Alba DM, Casanovas-Vilar I, Galindo J. 2004. Pierolapithecus catalaunicus, a New Middle Miocene Great Ape from Spain. Science. 306:1339–1344.

Murta-Fonseca RA, Fernandes DS. 2016. The skull of *Hydrodynastes gigas* (Duméril, Bibron & Duméril, 1854) (Serpentes: Dipsadidae) as a model of snake ontogenetic allometry inferred by geometric morphometrics. Zoomorphol (Berl).

Myers MJ, Steudel K. 1985. Effect of limb mass and its distribution on the energetic cost of running. J Exp Biol 116:363–73.

Nadell JA, Shaw CN. 2016. Phenotypic plasticity and constraint along the upper and lower limb diaphyses of Homo sapiens. Am J Phys Anthropol 422:410–422.

Napier JR, Walker AC. 1967. Vertical clinging and leaping, a newly recognized category of locomotory behavior among primates. Folia Primatol 6:180–203.

Nakatsukasa M, Almécija S, Begun DR. 2016. The Hands of Miocene Hominoids. In: Kivell TL (ed.). The Evolution of the Primate Hand. New York: Springer Science+Business Media. pp. 485–514.

Neufuss J, Robbins MM, Baeumer J, Humle T, Kivell TL. 2017. Comparison of hand use and forelimb posture during vertical climbing in mountain gorillas (*Gorilla beringei beringei*) and chimpanzees (*Pan troglodytes*). Am J Phys Anthropol.164:651–664.

Newman MC. 1993. Regression Analysis of Log-Transformed Data -Statistical Bias and Its Correction (Short Communication). Environ Toxicol Chem 12:1129–1133.

Nicholson CL, Firth EC. 2010. Assessment of bone response to conditioning exercise in the radius and tibia of young thoroughbred horses using pQCT. J Musculoskelet Neuronal Interact 10:199–206.

van Noordwijk MA, van Schaik CP. 2005. Development of ecological competence in Sumatran orangutans. Am J Phys Anthropol 127:79–94.

Nowell AA, Fletcher AW. 2007. Development of independence from the mother in Gorilla gorilla gorilla. Int J Primatol. 28(2):441–455.

O'Connor BL, Rarey KE. 1979. Normal amplitudes of radioulnar pronation and supination in several genera of anthropoid primates. Am J Phys Anthropol 51:39–44.

O'Higgins P. 2000. The study of morphological variation in the hominid fossil record: biology, landmarks and geometry. J. Anat. 197, 103–120.

O'Higgins P, Nicholas M. 2013. Applying geometric morphometrics to compare changes in size and shape arising from finite elements analyses. Hystrix:1–7.

O'Neill MC, Ruff CB. 2004. Estimating human long bone cross- sectional geometric properties: A comparison of noninvasive methods. J Hum Evol 47:221–235.

O'Neill MC, Dobson SD. 2008. The degree and pattern of phylogenetic signal in primate long-bone structure. J Hum Evol 54:309–22.

Ohman JC. 1993. Computer software for estimating cross-sectional geometric properties of long bones with concentric and eccentric elliptical models. J Hum Evol 25:217–227.

Oishi M, Ogihara N, Endo H, Asari M. 2008. Muscle architecture of the upper limb in the orangutan. Primates 49:204–209.

Oishi M, Ogihara N, Endo H, et al. 2009. Dimensions of forelimb muscles in orangutans and chimpanzees. J Anat 215, 373–382.

Osada N, Hashimoto K, Kameoka Y, Hirata M, Tanuma R, Uno Y, Inoue I, Hida M, Suzuki Y, Sugano S, Terao K, Kusuda J, Takahashi I. 2008. Large-scale analysis of *Macaca fascicularis* transcripts and inference of genetic divergence between *M. fascicularis* and *M. mulatta*. BMC Genom 9:90.

Osada N, Uno Y, Mineta K, Kameoka Y, Takahashi I, Terao K. 2010. Ancient genome-wide admixture beyond the current hybrid zone between *Macaca fascicularis* and *M. mulatta*. Mol Ecol 19:2884–2895.

Owen R. 1849. On the nature of limbs. London: John Van Voorst.

Palombit RA. 1994. Dynamic pair bonds in hylobatids: Implications regarding monogamous social systems. Behaviour 128:65–101.

Panagiotopoulou O. 2009. Finite element analysis (FEA): Applying an engineering method to functional morphology in anthropology and human biology. 36:609–624.

Parkin TDH, Clegg PD, French NP, Proudman CJ, Riggs CM, Singer ER, Morgan KL. 2004. Race-and course-level risk factors for fatal distal limb fracture in racing Thoroughbreds. Equine Vet J 36:521–526.

Patel BA. 2009. Not so fast: Speed effects on forelimb kinematics in cercopithecine monkeys and implications for digitigrade postures in primates. Am J Phys Anthropol 140:92–112.

Patel BA, Polk JD. 2010. Distal forelimb kinematics in *Erythrocebus patas* and *Papio anubis* during walking and galloping. International Journal of Primatology, 31, 191–207.

Patel BA, Ruff CB, Simons ELR, Organ JM. 2013. Humeral cross-sectional shape in suspensory primates and sloths. Anat Rec 296:545–56.

Pauwels F. 1976. Biomechanics of the Normal and Diseased Hip. Berlin: Springer-Verlag.

Payne RC, Crompton RH, Isler K, Savage R, Vereecke EE, Günther MM, Thorpe SKS, Août KD. 2006a. Morphological analysis of the hindlimb in apes and humans. I. Muscle architecture. J Anat 208:725–742.

Payne RC, Crompton RH, Isler K, Savage R, Vereecke EE, Günther MM, Thorpe SKS, D'Août K. 2006b. Morphological analysis of the hindlimb in apes and humans. II. Moment arms. J Anat 208:725–742.

Pearson OM, Petersen TR, Sparacello VS, Daneshvari SR, Grine FG. 2014. Activity, "Body Shape," and Cross-Sectional Geometry of the Femur and Tibia. In: Carlson KJ, Marchi D (eds.) Reconstructing Mobility: Environmental, Behavioral, and Morphological Determinants. Vol. 9781489974. 1st ed. New York: Springer Science+Business Media. pp. 1–295.

Pearson OM, Lieberman DE. 2004. The aging of Wolff's "law": ontogeny and responses to mechanical loading in cortical bone. Am J Phys Anthropol Suppl 39:63–99.

Pereira ME, Altmann J. 1985. Development of social behavior in free-living nonhuman primates. In: ES. Watts (ed.) Nonhuman primate models for human growth and development, pp. 217–309. New York: Alan R Liss.

Piziali RL, Hight, TK, Nagel DA. 1976. An extended structural analysis of long bones–application to the human tibia. J. Biomech. 9, 695-701.

Plant TM., Barker-Gibb ML. 2004. Neurobiological mechanisms of puberty in higher primates. Hum Reprod Update 10:67–77.

Plochocki JH, Rivera JP, Zhang C, Ebba SA. 2008. Bone modeling response to voluntary exercise in the hindlimb of mice. J Morphol 318:313–318.

Polk JD, Demes B, Jungers WL, Biknevicius AR, Heinrich RE, Runestad JA. 2000. A comparison of primate, carnivoran and rodent limb bone cross-sectional properties: are primates really unique? J Hum Evol 39:297–325.

Ponce de León MS, Zollikofer CP. 2001. Neanderthal cranial ontogeny and its implications for late hominid diversity. Nature 412:534–538.

Ponssa ML, Candioti MFV. 2012. Patterns of skull development in an- urans: size and shape relationship during postmetamorphic cranial ontogeny in five species of the Leptodactylus fuscus group (Anura: Leptodactylidae). Zoomorphol (Berl) 131:349–362.

Pontzer H, Wrangham RW. 2004. Climbing and the daily energy cost of locomotion in wild chimpanzees: implications for hominoid locomotor evolution. J Hum Evol.

Prado-Martinez J, Sudmant PH, Kidd JM (74 co-authors). 2014. Great ape genetic diversity and population history. Nature 499:471–475.

Preuschoft H, Tardieu C. 1996. Biomechanical reasons for the divergent morphology of the knee joint and the distal epiphyseal suture in hominoids. Folia Primatol. 66, 82–92.

Preuschoft H, Gunther MM, Christian A. 1998. Size dependence in prosimian locomotion and its implications for the distribution of body mass. Folia primatol. 69(S1)60–81.

Püschel TA, Sellers WI. 2016. Standing on the shoulders of apes: Analyzing the form and function of the hominoid scapula using geometric morphometrics and finite element analysis. Am J Phys Anthropol 159:325–341.

Raaum RL, Sterner KN, Novielleo CM. 2005. Catarrhine primate divergence dates estimated from complete mitochondrial genomes: Concordance with fossil and nuclear DNA evidence. Journal of Human Evolution, 48, 237–257.

Rabinowitz RS, Light TR, Havey RM, Gourineni P, Patwardhan AG, Sartori MJ, Vrbos L. 1994. The role of the interosseous membrane and triangular fibrocartilage complex in forearm stability. J Hand Surg 1994;19A:385–393.

Radin E, Orr R, Kelman J, Paul I, Rose R. 1982. Effect of prolonged walking on concrete on the knees of sheep. J Biomech 15:487–492.

Raichlen DA. 2005a. Effects of limb mass distribution on the ontogeny of quadrupedalism in infant baboons (*Papio cynocephalus*) and implications for the evolution of primate quadrupedalism. J Hum Evol 49:415–431.

Raichlen DA. 2005b. Ontogeny of limb mass distribution in infant baboons (*Papio cynocephalus*). J Hum Evol 49:452–467.

Raichlen DA. 2006. Effects of limb mass distribution on mechanical power outputs during quadrupedalism. J Exp Biol209:633–44.

Raichlen DA, Gordon AD, Foster AD, Webber JT, Sukhdeo SM, Scott RS, Gosman JH, Ryan TM. 2015. An ontogenetic framework linking locomotion and trabecular bone architecture with applications for reconstructing hominin life history. J Hum Evol 81:1–12.

Rafferty KL., Walker, A., Ruff, C.B., Rose, M.D., Andrews, P.J., 1995. Postcranial es- timates of body weight in Proconsul, with a note on a distal tibia of P. major from Napak, Uganda. Am. J. Phys. Anthropol. 97, 391-402.

Rauwerdink GP. 1991. Muscle fiber and tendon lengths in the distal limb segments of primates. Z Morphol Anthropol 78:331–340.

Rawlins RG. 1976. Locomotor ontogeny of Macaca mulatta:I. Behavioral strategies and tactics. Am J Phys Anthropol 44: 201.

Rawlins RG. 1993. Locomotor and manipulative use of the hand in Cayo Santiago macaques (*Macaca mulatta*). In: H. Preuschoft & D. J. Chivers (eds.) Hands of primates pp. 21–30. New York: Springer-Ulag.

Rawlinson CF, Mosley JR, Suswillo RFL, Pitsillides AA, and Lanyeon LE. 1995. Calvarial and limb bone cells in organ and monolayer culture do not show the same early responses to dynamic mechanical strain. J. Bone Miner. Res. 10:1225-1232.

Reichard UH, Barelli C. 2008. Life history and reproductive strategies of Khao Yai *Hylobates lar:* Implications for social evolution in apes. Int J Primatol 29:823–844.

Reichard UH., Ganpanakngan M, Barelli C. 2012. White-handed gibbons of Khao Yai: Social flexibility, complex reproductive strategies, and a slow life history. In: PM Kappeler, DP Watts (eds.) Long-term field studies of primates, pp. 237–258. Berlin: Springer.

Remis M. 1994. Feeding ecology and positional behavior of western lowland gorillas (*Gorilla gorilla gorilla*) in the Central African Republic. Ph.D. Dissertation, Yale University.

Remis MJ. 1995. The effects of body size and social context on the arboreal activities of lowland gorillas in the Central African Republic. Amer. J. Phys. Anthropol., 97: 413-433.

Remis M. 1998. The Gorilla Paradox: The Effects of Body Size and Habitat on the Positional Behavior of Lowland and Mountain Gorillas. In: Strasser E, Fleagle JG, McHenry HM, Rosenberger A (eds.) *Primate Locomotion: Recent Advances*. pp. 95-105. New York, NY: Plenum Press.

Remis M. 1999. Tree structure and sex differences in arboreality among western lowland gorillas (Gorilla gorilla gorilla) at Bai Hokou, Central African Republic. Primates 40:383–396.

Reno PL, Meindl RS, McCollum MA, Lovejoy CO. 2003. Sexual dimorphism in Australopithecus afarensis was similar to that of modern humans. Proc Natl Acad Sci USA 100:9404–9409.

Reynolds, TR. 1981. Mechanics of interlimb weight re- distribution in primates. PhD Dissertation, Department of Anthropology, Rutgers University, New Brunswick, New Jersey.

Reynolds TR. 1985a. Stresses on the limbs of quadrupedal primates. Am J Phys Anthropol 67:351–362.

Reynolds TR. 1985b. Mechanics of increased support of weight by the hindlimbs in primates. Am J Phys Anthropol 67:335–349.

Rilling, JK. 2006. Primate Brain Evolution: Integrating Comparative, Neurophysiological, and Ethological Data. Evol Anthropol 15:224–236.

Rilling JK. 2014. Comparative primate neuroimaging: Insights into human brain evolution. Trends Cogn Sci 18:46–55.

Rittweger J. 2008. Ten years muscle-bone hypothesis : What have we learned so far ? -Almost a Festschrift-. J Musculoskelet Neuronal Interact 8:174–178.

Roark RJ, Young WC. 1976. Formulas for Stress and Strain, 5th Edition. Auckland: McGraw-Hill.

Robling AG, Castillo AB, Turner CH. 2006. Biomechanical and Molecular Regulation of Bone Remodeling. Annu Rev Biomed Eng 8:455–498.

Rodman PS. 1979. Skeletal differentiation of *Macaca fascicularis* and *Macaca nemestrina* in relation to arboreal and terrestrial quadrupedalism. Am. J. Phys. Anthropol. 51, 51–62.

Rodman PS, McHenry HM. 1980. Bioenergetics and the origin of hominid bipedalism. Am. J. Phys. Anthropol. 52, 103–106.

Rohlf JF, Marcus LF. 1993. A Revolution in Morphometrics. Trends Ecol Evol 8:129–132.

Rohlf FJ. 2015. The tps series of software. Hystrix, Ital J Mammal 26:9–12.

Rohlf FJ, Slice D. 1990. Extensions of the Procrustes Method for the Optimal Superimposition of Landmarks. Syst ZoolZool 39:40–59.

Rohlf FJ, Marcus LF. 1993. Arevolution morphometrics. Trends in Ecology & Evolution 8:129–132.

Rook L, Bondioli L, Köhler M, Moyà-Solà S, Macchiarelli R. 1999. Oreopithecus was a bipedal ape after all: evidence from the iliac cancellous architecture. Proc Natl Acad Sci U S A 96:8795–9.

Rook L, Bondioli L, Casali F, Rossi M, Köhler M, Moyá Solá S, Macchiarelli R, 2004. The bony labyrinth of Oreopithecus bambolii. J. Hum. Evol. 46, 349–356.

Rose CP. 1981. Injuries in women's field hockey: a four year study. Phys Sports Med 9:97–98. 100.

Rose MD. 1973a. Quadrupedalism in new and old world monkeys. London: University of London.

Rose MD. 1973b. Quadrupedalism in primates. Primates 14:337–357.

Rose MD. 1983. Miocene Hominoid Postcranial Morphology; Monkey-like, Ape-like, Neither, or Both? In: Ciochon, RL, Corruccini RS (ed.). New Interpretations of Ape and Human Ancestry. 1st Edition, pp. 405–413. New York: Springer.

Rose MD. 1988. Another look at the anthropoid elbow. J. Hum. Evol. 17:193–224.

Rose MD. 1991. The process of bipedalization in hominids. In: Senut B, Coppens Y (eds.) Origines de la bipedie chez les Hominides. pp. 37–48. Paris: CNRS.

Rose MD. 1993. Locomotor anatomy of Miocene hominoids. In: Gebo DL (ed.) Postcranial Adaptation in Nonhuman Primates, pp. 252–272. DeKalb, IL: Northern Illinois University Press.

Rubin CT, Lanyon LE. 1982. Limb mechanics as a function of speed and gait: a study of functional strains in the radius and tibia of horse and dog. J Exp Biol 101:187–211.

Rubin CT, Lanyon LE. 1984. Regulation of bone formation by applied dynamic loads. J Bone Jt Surg 66:397–402.

Ruff CB. 1988. Hindlimb articular surface allometry in Hominoidea and Macaca, with comparisons to diaphyseal scaling. J. Hum. Evol. 17:687–714.

Ruff CB. 1990. Body mass and hindlimb bone cross-sectional and articular dimensions in anthropoid primates. In Body Size in Mammalian Paleobiology (ed.) J. Damuth, B. J. McFadden, ed. pp. 119–149. Cambridge: Cambridge Univ Press.

Ruff CB. 1995. Biomechanics of the hip at birth in early Homo. Am. J. Phys. Anthropol. 98, 527-574.

Ruff CB. 2002. Long bone articular and diaphyseal structure in old world monkeys and apes. I: locomotor effects. Am J Phys Anthropol 119:305–42.

Ruff C. 2003a. Ontogenetic adaptation to bipedalism: age changes in femoral to humeral length and strength proportions in humans, with a comparison to baboons. J Hum Evol 45:317–349.

Ruff CB. 2003b. Long bone articular and diaphyseal structure in Old World monkeys and apes. II: Estimation of body mass. Am J Phys Anthropol 120:16–37.

Ruff CB. 2008. Biomechanical Analyses Of Archaeological Human Skeletons. In: Biological Anthropology of the Human Skeleton. Wiley, pp. 183–206.

Ruff CB, Runestad JA. 1992. Primate Limb Bone Structural Adaptations. Annu Rev Anthropol 21:407–433.

Ruff CB, Walker A, Trinkaus E. 1994. Postcranial robusticity in Homo. III: Ontogeny. Am J Phys Anthropol 93:35–54.

Ruff CB, Holt BM, Sládek V, Berner M, Murphy WA, zur Nedden D, Seidler H, Recheis W. 2006. Body size, body proportions, and mobility in the Tyrolean "Iceman." J Hum Evol 51:91–101.

Ruff CB, Burgess ML, Bromage TG, Mudakikwa A, McFarlin SC. 2013. Ontogenetic changes in limb bone structural proportions in mountain gorillas (*Gorilla beringei beringei*). J Hum Evol 65:693–703.

Russo GA, Shapiro LJ. 2013. Reevaluation of the lumbosacral region of *Oreopithecus bambolii*. J Hum Evol 65:253–265.

Sabater Pi J. 1979. Feeding behavior and diet of chimpanzees (*Pan troglodytes troglodytes*) in the Okorobiko Mountains of Rio Muni (West Africa). Z Tierpsychol 50, 265–281.

San Millán M, Kaliontzopoulou A, Rissech C, Turbon D. 2015. A geometric morphometric analysis of acetabular shape of the primate hip joint in relation to locomotor behaviour. J Hum Evol 83:15–27.

Sarmiento EE. 1988. Anatomy of the hominoid wrist joint: its evolutionary functional implications. Int. J. Primatol. 9, 281e345.

Sarringhaus LA, Stock JT, Marchant LF, McGrew WC. 2005. Bilateral asymmetry in the limb bones of the chimpanzee (*Pan troglodytes*). Am J Phys Anthropol 128:840–845.

Sarringhaus LA, Maclatchy LM, Mitani JC. 2014. Locomotor and postural development of wild chimpanzees. J Hum Evol. 66, 29–38.

Sarringhaus LA, MacLatchy LM, Mitani JC. 2016. Long bone cross-sectional properties reflect changes in locomotor behavior in developing chimpanzees. Am J Phys Anthropol 60(1), 16-29.

Sati JP, Alfred JRB. 2002. Locomotion and posture in Hoolock gibbon. Annal Forest. 10, 298-306.

Scally A, Dutheil JY, Hillier LW, (68 co-authors). 2012. Insights into hominid evolution from the gorilla genome sequence. Nature 483, 169-175.

Schaffler MB, Burr DB, Jungers WL, Ruff CB. 1985. Structural and mechanical indicators of limb specialization in primates. Folia Primatol (Basel) 45:61–75.

Schaefer K, Mitteroecker P, Gunz P, Bernhard M, Bookstein FL. 2004. Craniofacial Sexual Dimorphism Patterns and Allometry Among Extant Hominids. Ann Anat 186:471–478.

Schilling A-M, Tofanelli S, Hublin J-J, Kivell TL. 2014. Trabecular bone structure in the primate wrist. J Morphol.

Schmidt M, Voges D, Fischer MS. 2002. Shoulder movement during quadrupedal locomotion in arboreal primates. Z. Morph. Anthropol. 83, 235–242.

Schmidt M, Krause C. 2011. Scapula movements and their contribution to three-dimensional forelimb excursions in quadrupedal primates. In: D'Aout K, Vereecke E (ed.). Primate locomotion: linking field and laboratory research. New York: Springer.

Schmidt-Nielsen K. 1992. Scaling. Why is Animal Size So Important? New York: Cambridge University Press.

Schmitt D. 1994. Forelimb mechanics as a function of substrate type during quadrupedalism in two anthropoid primates. J Hum Evol 26:441–457.

Schmitt D. 1999. Compliant walking in primates. J. Zool. London. 248, 149–160.

Schmitt D. 2003. Mediolateral reaction forces and forelimb anatomy in quadrupedal primates: Implications for interpreting locomotor behavior in fossil primates. J Hum Evol 44:47–58.

Schmitt D, Larson SG.1995. Heel contact as a function of substrate type and speed in primates. Am. J. Phys. Anthropol. 96, 39–50.

Schneider K, Zernicke RF. 1992. Mass, center of mass, and moment of inertia estimate for infant limb segments. J Biomech 25:145–148.

Scholz MN, D'Aouˆt K, Bobbert MF, et al. 2006. Vertical jumping performance of bonobo (*Pan paniscus*) suggests superior muscle properties. Proc R Soc B: Biol Sci 273, 2177–2184.

Schrago CG, Russo CA. 2003. Timing the origin of New World monkeys. Molecular Biology and Evolution, 20(10), 1620-1625.

Schultz AH. 1924. Growth studies on primates bearing upon man's evolution. Am. J. Phys. Anthrop. 7, 149–164.

Schultz AH. 1926. Foetal growth of man and other primates. Q Rev Biol 1:463–521. Schwabe

Schultz AH. 1937. Proportions, Variability and Asymmetries of the Long Bones of the Limbs and the Clavicles in Man and Apes. Hum Biol 9:281–328.

Schultz AH. 1960. Einige Beobachtungen und Maße am Skelett von Oreopithecus: im Vergleich mit anderen catarrhinen Primaten. Z. Morphol. Anthropol. 50, 136–149.

Schuppli C, Forss SIF, Meulman EJM, Zweifel N, Lee KC, Rukmana E, Vogel ER, van Noordwijk MA, van Schaik CP. 2016. Development of foraging skills in two orangutan populations: needing to learn or needing to grow? Front Zool 13:43.

Sellers WI. 1992. A study of leaping prosimian primates. Ph.D. thesis, Liverpool: University of Liverpool.

Shaw CN, Ryan TM. 2012. Does skeletal anatomy reflect adaptation to locomotor patterns? Cortical and trabecular architecture in human and nonhuman anthropoids. Am J Phys Anthropol 147(2), 187-200.

Shaw CN, Stock JT. 2009a. Habitual throwing and swimming correspond with upper limb diaphyseal strength and shape in modern human athletes. Am J Phys Anthropol 140:160–72.

Shaw CN, Stock JT. 2009b. Intensity, repetitiveness, and directionality of habitual adolescent mobility patterns influence the tibial diaphysis morphology of athletes. Am J Phys Anthropol 140:149–59.

Shaw CN., Stock JT., Davies TG., M. RT. 2014. Does the Distribution and Variation in Cortical Bone Along Lower Limb Diaphyses Reflect Selection for Locomotor Economy? In: Marchi D, Carlson K (ed.). Reconstructing Mobility. Springer. pp. 49–66.

Shea BT. 1983. Allometry and heterochrony in the African apes. Am J Phys Anthropol 62:275–89.

Shea BT. 1985. The ontogeny of sexual dimorphism in the African Apes. American Journal of Primatology, 8, 183–188.

Shea BT. 1986. Scapula form and locomotion in chimpanzee evolution. Am. J. Phys. Anthropol. 70, 475–488.

Siegal ML, Bergman A. 2002. Waddington's canalization revisited: developmental stability and evolution. Proc Natl Acad Sci USA 99:10528–10532.

Simmen B, Darlu P, Hladik CM, Pasquet P. 2015. Scaling of free-ranging primate energetics with body mass predicts low energy expenditure in humans. Physiol. Behav. 138:193–99

Skedros JG, Sybrowsky CL, Parry TR, Bloebaum RD. 2003. Regional differences in cortical bone organization and microdamage prevalence in Rocky Mountain mule deer. Anat Rec A Discov Mol Cell Evol Biol 274:837–50.

Skinner MM, Stephens NB, Tsegai ZJ, Foote AC, Nguyen NH, Gross T, Pahr DH, Hublin J-J, Kivell TL. 2015. Human-like hand use in Australopithecus africanus. Science 347(6220), 395-399.

Smith JM, Savage RJG. 1956. Some locomotory adaptations in mammals. Zool J Linn Soc 42:603–622.

Smith AL, Benazzi S, Ledogar JA, Tamvada K, Leslie C, Smith P, Weber GW, Spencer MA, Dechow PC, Grosse IR, Ross CF, Richmond BG, Wright BW, Wang Q. 2015. Biomechanical implications of intraspecific shape variation in chimpanzee crania: moving towards an integration of geometric morphometrics and finite element analysis. Anat Rec 298:122–144.

Smith RJ, Jungers WL. 1997. Body mass in comparative primatology. J Hum Evol 32:523–59.

Smith BH, Boesch C. 2011. Mortality and the magnitude of the "wild effect" in chimpanzee tooth emergence. J Hum E 60:34–46.

Smith Holly B, Crummett TL, Brandt KL. 1994. Ages of Eruption of Primate Teeth: A Compendium for Aging Individuals and Comparing Life Histories. Yearb Phys Anthropol 37:177–231.

Sokal RR, Rohlf FJ. 1995. Biometry. New York: W.H. Freeman and Company.

Sparacello VS, Pearson OM. 2010. The importance of accounting for the area of the medullary cavity in cross-sectional geometry: A test based on the femoral midshaft. Am J Phys Anthropol 143:612–624.

Speakman JR. 2005. Body size, energy metabolism and lifespan. J Exp Biol 208(Pt 9): 1717–1730.

Sponheimer M, Alemseged Z, Cerling TE, Grine FE, Kimbel WH. 2013. Isotopic evidence of early hominin diets. PNAS - Proc Natl Acad Sci 110:10513–10518.

Stearns SC. 2000. Life history evolution: successes, limitations, and prospects. Naturwissenschaften 87:476–486.

Steiper ME, Young NM. 2006. Primate Molecular Divergence Dates. Mol Phyl Evol 41:384–394

Stern JJT, Susman RL. 1983. The locomotor anatomy of Australopithecus afarensis. Am J Phys Anthropol 60:279–317.

Stewart TD. 1983. Adolph Hans Schultz, 1891–1976. Biographical Memoir. J Med Primatol 6:325–349.

Stock JT. 2006. Hunter-gatherer postcranial robusticity relative to patterns of mobility, climatic adaptation, and selection for tissue economy. Am J Phys Anthropol 131:194–204.

Stock J, Pfeiffer S. 2001. Linking structural variability in long bone diaphyses to habitual behaviors: foragers from the southern African Later Stone Age and the Andaman Islands. Am J Phys Anthropol 115:337–48.

Stock JT, Pfeiffer SK. 2004. Long bone robusticity and subsistence behaviour among Later StoneAge foragersofthe forest andfynbosbiomes of South Africa. JArch Sci 31(7):999–1013.

Stock JT, Shaw CN. 2007. Which Measures of Diaphyseal Robusticity Are Robust ? A Comparison of External Methods of Quantifying the Strength of Long Bone Diaphyses to Cross-Sectional Geometric Properties. Am J Phys Anthropol 423:412–423.

Stock JT, Macintosh AA. 2016. Lower limb biomechanics and habitual mobility among mid-Holocene populations of the Cis-Baikal. Quat Int 405:200–209.

Strand Vidarsdottir U, O'Higgins P, Stringer CB. 2002. A geometric morphometric study of regional differences in the growth of the modern human facial skeleton. Journal of Anatomy 201:211–229.

Strasser E. 1992. Hindlimb proportions, allometry, and biomechanics in Old World monkeys (Primates, Cercopithecidae). Am J Phys Anthropol 87, 187–213.

Straus W. 1962. Fossil evidence of the evolution of the erect, bipedal posture. Clin. Orthop. 259-19.

Sugardjito J, van Hooff J. 1986. Sex–age class differences in positional behavior of Sumatran orangutan (*Pongo pygmaeus abelii*) in Gunung Leuser National Park, Indonesia. Folia Primatol 47, 14–25.

Swartz SM, Bertram JEA, and Biewener AA. 1989. Telemetered in vivo strain analysis of locomotor mechanics of brachiating gibbons. Nature 342:270– 272.

Szalay FS, Dagosto M. 1980. Locomotor adaptations as reflected on the humerus of Paleogene primates. Folia Primatol (Basel) 34:1–45.

Tallman M. 2012. Morphology of the distal radius in extant hominoids and fossil hominins: implications for the evolution of bipedalism. Anat Rec (Hoboken) 295:454–64.

Tallman M, Almécija S, Reber SL, Alba DM, Moyà-Solà S. 2013. The distal tibia of *Hispanopithecus laietanus*: More evidence for mosaic evolution in Miocene apes. J Hum Evol 64:319–27.

Taylor AB. 1995. Effects of ontogeny and sexual dimorphism on scapula morphology in the mountain gorilla (*Gorilla gorilla beringei*). Am. J. Phys. Anthropol. 98, 431–445.

Taylor AB. 1997. Scapula form and biomechanics in gorillas. J Hum Evol 33:529–553.

Taylor AB, Yuan T, Ross CF, Vinyard CJ. 2015. Jaw-muscle force and excursion scale with negative allometry in platyrrhine primates. Am J Phys Anthropol 158:242–256.

Terhune CE, Robinson CA, Ritzman TB. 2014. Ontogenetic variation in the mandibular ramus of great apes and humans. J Morphol 275:661–77.

Thorpe SK, Crompton RH, Günther MM, Ker RF, McNeill Alexander R. 1999. Dimensions and moment arms of the hind- and forelimb muscles of common chimpanzees (*Pan troglodytes*). Am J Phys Anthropol 110:179–99.

Thorpe SKS, Crompton RH. 2006. Orangutan Positional Behavior and the Nature of Arboreal Locomotion in Hominoidea. Am J Phys Anthropol 0.

Thorpe SKS, Holder RL, Crompton RH. 2007. Origin of human bipedalism as an adaptation for locomotion on flexible branches. Science 316:1328–31.

Tilkens MJ, Wall-Scheffler C, Weaver TD, Steudel-Numbers KL. 2007. The effects of body proportions on thermoregulation: an experimental assessment of Allen's rule. J Hum Evol 53:286–291.

Tosi AJ, Morales JC, Melnick DJ. 2002. Y-chromosomal and mitochondrial markers in *Macaca fascicularis* indicate introgression with Indochinese *M. mulatta* and a biogeographic barrier in the Isthmus of Kra. International Journal of Primatology, 23, 161–178.

Tosi AJ, Morales JC, Melnick DJ. 2003. Paternal, maternal, and biparental molecular markers provide unique windows onto the evolutionary history of macaque monkeys. Evolution 57:1419–1435.

Tosi AJ, Coke CS. 2007. Comparative phylogenetics offer new insights into the biogeographic history of *Macaca fascicularis* and the origin of the Mauritian macaques. Molecular Phylogenetics and Evolution, 42, 498–504.

Trinkaus E, Churchill SE, Ruff CB. 1994. Postcranial Robusticity in Homo. II: Humeral Bilateral Asymmetry and Bone Plasticity. Am J Phys Anthropol 93:1–34.

Trinkaus E, Ruff CB. 1999. Diaphyseal cross-sectional geometry of Near Eastern Middle Paleolithic hominids: the femur. J Archaeol Sci 26:409–424.

Trinkaus E, Ruff CB. 2012. Femoral and Tibial Diaphyseal Cross-Sectional Geometry in Pleistocene Homo. PaleoAnthropology:13–62.

Trotter M, Hixon BB, Deaton SS. 1975. Sequential changes in weight of the skeleton and in length of long limb bones of *Macaca mulatta*. Am J Phys Anthropol 43:79–93.

Tsegai ZJ, Kivell TL, Gross T, Huynh Nguyen N, Pahr DH, Smaers JB, Skinner MM. 2013. Trabecular bone structure correlates with hand posture and use in hominoids. PLoS One *8*(11), e78781.

Tsegai ZJ, Skinner MM, Gee AH, Pahr DH, Treece GM, Hublin J-J, Kivell TL. 2017. Trabecular and cortical bone structure of the talus and distal tibia in *Pan* and *Homo*. Am J Phys Anthropol:1–22.

Turley K, Frost SR. 2014. The ontogeny of talo-crural appositional articular morphology among catarrhine taxa: Adult shape reflects substrate use. Am J Phys Anthropol 154:447–58.

Turner CH, Pavalko FM. 1998. Mechanotransduction and functional response of the skeleton to physical stress: The mechanisms and mechanics of bone adaptation. J Orthop Sci 3:346–355.

Turnquist JE, Kessler MJ. 1989. Free-ranging Cayo Santiago rhesus monkeys (*Macaca mulatta*): I. Body size, proportion, and allometry. Am. J. Primatol. 19, 1–13.

Turnquist JE, Wells JP. 1994. Ontogeny of Locomotion in Rhesus Macaques (*Macaca mulatta*): I. Early Postnatal Ontogeny of the Musculoskeletal System. J Hum Evol 26:487–499.

Tutin CEG, Fernandez M. 1985. Foods consumed by sympatric populations of *Gorilla gorilla gorilla* and *Pan troglodytes troglodytes* in Gabon: Some preliminary data. Int. J. Primatol. 6:27-43.

Tutin, C.E.G., Fernandez, M., Rogers, M.E., Williamson, E.A., McGrew, W.C., Altmann, S.A., Southgate, D.A.T., Crowe, I., Whiten, A., 1991. Foraging profiles of sympatric lowland gorillas and chimpanzees in the Lope Reserve, Gabon [and discussion]. Philosophical Transac- tions of the Royal Society of London Series B: Biological Sciences 334, 179.

Tuttle RH. 1972. Functional and evolutionary biology of hylobatid hands and feet. Gibbon and Siamang 1, 136–206.

Tuttle RH, Watts DP. 1985. The positional behavior and adaptive complexes of *Pan gorilla*. In: Kondo S (ed.) Primate Morphophysiology, Locomotor Analysis and Humanism, pp. 261–288. Tokyo: University of Tokyo Press.

Umemura Y, Ishiko T, Yamauchi T, Kurono M, Mashiko S. 1997. Five jumps per day increase bone mass and breaking force in rats. J Bone Miner Res 12:1480–1485.

Usherwood JR, Bertram JEA. 2003. Understanding brachiation: insight from a collisional perspective. J. Exp. Biol. 206, 1631–1642.

Venkataraman VV, Kraft TS, DeSilva JM. 2013. Phenotypic Plasticity of Climbing-Related Traits in the Ankle Joint of Great Apes and Rainforest Hunter-Gatherers. Hum Biol 85:309–328

Vereecke EE, Channon AJ. 2013. The role of hind limb tendons in gibbon locomotion: springs or strings? J Exp Biol 216:3971–3980.

Vereecke EE, D'Août K, Aerts P. 2006. Locomotor versatility in the white-handed gibbon (*Hylobates lar*): A spatiotemporal analysis of the bipedal, tripedal, and quadrupedal gaits. J Hum Evol 50:552–567.

Verheyen K, Price J, Lanyon L, Wood J. 2006. Exercise distance and speed affect the risk of fracture in racehorses. Bone 39: 1322–1330.

Vidarsdóttir US, O'Higgins P, Stringer C. 2002. A geometric morphometric study of regional differences in the ontogeny of the modern human facial skeleton. J Anat 201:211–29.

Waddington CH. 1942. Canalisation of development and the inheritance of acquired characters. Nature, 150(3811), 563–565.

Wallace IJ, Demes B, Mongle C, Pearson OM, Polk JD, Lieberman DE. 2014. Exercise-induced bone formation is poorly linked to local strain magnitude in the sheep tibia. PLoS ONE 9, 99108.

Ward CV. 2007. Postcranial and locomotor adaptations of hominoids. In: Henke W, Tattersall I. (eds.) Handbook of Paleoanthropology. Springer, Berlin, pp. 1011-1030.

Ward CV, Flinn M, Begun DR. 2004. Body size and intelligence in hominoid evolution. In: Russon A, Begun DR (ed.) The evolution of thought: Evolutionary origins of great ape intelligence, pp. 335–345. Cambridge: Cambridge University Press.

Watts DP. 1991. Mountain gorilla reproduction and sexual behavior. Am J Primatol 24, 211–226.

Watts D, Pusey A. 1993. Behavior of juvenile and adolescent great apes. In: Pereira, M.E., Fairbanks, L.A. (eds.) Juvenile Primates: Life History, Development, and Behavior. Oxford University Press, Oxford, pp. 148-167.

Weatherholt AM, Warden SJ. 2017. Tibial bone strength is enhanced in the jump leg of collegiate-level jump athletes: a within-subject controleld cross-sectional study. Calcif Tissue Int 98:129–139.

Wells JP, Turnquist JE. 2001. Ontogeny of locomotion in rhesus macaques (*Macaca mulatta*): II. Postural and locomotor behavior and habitat use in a free-ranging colony. Am J Phys Anthropol 115:80–94.

Western D. 1979. Size, life-history and ecology in mammals. Afr. J. Ecol. 17:185–204.

Wheatley BP. 1980. Feeding and ranging of east Bornean *Macaca fascicularis*. In DG Lindburg (ed.) The Macaques: Studies in Ecology, Behavior and Evolution. Princeton, NJ Van Nostrand Reinhold, pp. 215–246.

White TD, Asfaw B, Beyene Y, Haile-Selassie Y, Owen Lovejoy C, Suwa G, WoldeGabriel GC. 2009. *Ardipithecus ramidus* and the Paleobiology of Early Hominids. Science 326:75–86.

White TD, Black MT, Folkens PA. 2012. Human Osteology. Academic Press.

Whitmoor TC. 1975. Tropical Rain Forests of the Far East. Oxford: Clarendon Press.

Wich SA, Utami-Atmoko SS, Setia TM, Rijksen HD, Schürmann C, van Hooff, J.A.R.A.M., et al. 2004. Life history of wild Sumatran orangutans (*Pongo abelii*). J. Hum Evol., 47(6), 385–398.

Will M, Stock JT. 2015. Spatial and temporal variation of body size among early Homo. J Hum Evol 2015.

Wilson LAB, Humphrey LT. 2015. A Virtual geometric morphometric approach to the quantification of long bone bilateral asymmetry and cross-sectional shape. Am J Phys Anthropol 158(4), 541-556.

Wintheiser J, Clauser D, Tappen N. 1977. Sequence of eruption of permanent teeth and epiphyseal union in three species of African monkeys. Folia Primatol 27:178–197.

Wolff J. 1892. Das Gesetz der Transformation der Knochen. Berlin: A. Hirchwild.

Won YJ, Hey J. 2005. Divergence population genetics of chimpanzees. Mol Biol Evol 22:297–307.

Woo SLY, Kuei SC, Amiel D, Gomez MA, Hayes WC, White FC, Akeson WH. 1981. The effect of prolonged physical training on the properties of long bone: A study of Wolff's law. J. Bone Joint Surg. 635, 80–787.

Wood BA, Li Y, Willoughby C. 1991. Intraspecific variation and sexual dimorphism in cranial and dental variables among higher primates and their bearing on the hominid fossil record. J Anat, 174(2), 185–208.

Young NM. 2003. A reassessment of living hominoid postcranial variability: implications for ape evolution. J Hum Evol 45:441–464.

Young NM. 2006. Function, ontogeny and canalization of shape variance in the primate scapula. J Anat 209:623–36.

Young NM, MacLatchy L. 2004. The phylogenetic position of Morotopithecus. J Hum Evol 46, 163.

Young JW, Ferna D, Fleagle JG. 2010a. Ontogeny of long bone geometry in capuchin monkeys (*Cebus albifrons* and *Cebus apella*): implications for locomotor development and life history. Biol Lett 6:197–200.

Young NM, Wagner GP, Hallgrimsson B. 2010b. Development and the evolvability of human limbs. Proc Natl Acad Sci. 107:3400–3405.

Young NM, Wagner GP, Hallgrimsson B. 2010b. Supplementary Info. Proc Natl Acad Sci.

Zelditch ML, Swiderski DL, Sheets H.D. 2012. Geometric Morphometrics for Biologists: a primer (Second Edition). Academic Press.

Zihlman AL. 1992. Locomotion as a life history character: the contribution of anatomy. J. Hum. Evol. 22, 315–325.